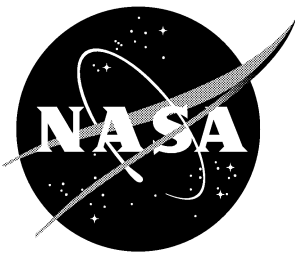


NASA Technical Memorandum 4611

Measurements of Store Forces and Moments and Cavity Pressures for a Generic Store In and Near a Box Cavity at Subsonic and Transonic Speeds

Robert L. Stallings, Jr., E. B. Plentovich, M. B. Tracy, and Michael J. Hensch

May 1995



Measurements of Store Forces and Moments and Cavity Pressures for a Generic Store In and Near a Box Cavity at Subsonic and Transonic Speeds

Robert L. Stallings, Jr.

Lockheed Engineering & Sciences Company • Hampton, Virginia

E. B. Plentovich and M. B. Tracy

Langley Research Center • Hampton, Virginia

Michael J. Hemsch

Lockheed Engineering & Sciences Company • Hampton, Virginia

Available electronically at the following URL address: <http://techreports.larc.nasa.gov/ltrs/ltrs.html>

Printed copies available from the following:

NASA Center for AeroSpace Information
800 Elkridge Landing Road
Linthicum Heights, MD 21090-2934
(301) 621-0390

National Technical Information Service (NTIS)
5285 Port Royal Road
Springfield, VA 22161-2171
(703) 487-4650

Summary

An experimental study has been conducted in the Langley 8-Foot Transonic Pressure Tunnel to measure the forces and moments on a generic store in and near rectangular box cavities in a flat-plate configuration at subsonic and transonic speeds. Surface pressure measurements were obtained inside the cavities and on the flat plate. The measurements were obtained for the store near a flat-plate surface, and inside and near two shallow cavities and two deep cavities. The shallow cavities had a depth h of 2.40 in. and lengths l of 26.00 in. and 30.00 in. with corresponding values of l/h of 10.83 and 12.50. The deep cavities had a depth of 4.80 in., lengths of 26.00 in. and 30.00 in., and corresponding values of l/h of 5.42 and 6.25. All cavities had a width of 9.60 in. Measurements were obtained with the store located in a plane perpendicular to the cavity floor that contained the cavity longitudinal centerline (centerline plane) and in a parallel plane 2.50 in. to the right of the centerline plane (off-centerline plane). The tests were conducted over a free-stream Mach number M_∞ range of 0.20 to 0.95.

For these tests, surface pressure measurements inside the cavities indicated that, through the test range of M_∞ , the flow fields for the shallow cavities were either closed or transitional near the transitional/closed boundary, and the flow fields for the deep cavities were either open or transitional near the open/transitional boundary. The installations of the store assembly inside the cavity and the position of the store after installation did not change the type of cavity flow field and had only small effects on the cavity and flat-plate pressure distributions. The effects of M_∞ on the store forces and moments were primarily results of the effect of M_∞ on the type of cavity flow field rather than a direct effect of M_∞ on the store loads. For the shallow cavities with closed cavity flow fields, varying M_∞ had only small effects on the cavity and flat-plate pressure distributions and on the store forces and moments. When the flow fields for the shallow cavities were transitional near the transitional/closed boundary, increasing M_∞ resulted in large reductions in pitching-moment coefficient C_m . Varying the length of the shallow cavities from 26.00 in. to 30.00 in. (≈ 15 percent) had a large effect on C_m , normal-force coefficient C_N , and axial-force coefficient C_A . Lateral positioning of the store in the cavity had only small effects on the cavity and flat-plate pressure distributions and on the store forces and moments. Cavity depth had large effects on C_m and C_N for all cavity configurations and on C_A for the longer cavities ($l = 30.00$ in.). These large effects resulted from the effect of cav-

ity depth on the type of cavity flow field. Values of C_m were always much greater for the shallow cavities with closed cavity flow than for the deep cavities with open flow. This result is similar to trends previously observed at supersonic speeds.

Introduction

The internal carriage of stores on an aircraft, compared with external store carriage, results in reduced drag and lower radar cross section for the parent aircraft at all flight speeds. There are, however, some undesirable features of internal carriage, such as increased aircraft volume requirements, more constraints on store geometry and size, and large dynamic loadings on weapons-bay components when the bay is open. Also, it has been established (e.g., refs. 1 to 4) that adverse store-separation characteristics can exist for certain weapons-bay geometries at supersonic speeds. The main purpose of the investigation reported in this paper was to determine whether adverse store-separation characteristics also occurred at subsonic and transonic speeds for similar weapons-bay geometries. An additional purpose was to investigate the effects of varying the cavity length on the store forces and moments from a typical length that accommodates just the store to a typical length that would accommodate the store with a conventional offset sting arrangement. Store forces and moments for the shorter cavity length could be obtained in the present tests, since the store model was supported by a blade-strut assembly that extended from the cavity floor.

The investigation reported in this paper was part of an overall program that was conducted at NASA Langley to investigate cavity flow fields at subsonic and transonic flight speeds. Tests were conducted over a wide range of cavity parameters. Results from a test conducted to investigate the effects of cavity geometry on cavity flow fields are given in reference 5. The different types of flow fields that occur in the subsonic and transonic speed range are catalogued in reference 5, and the range of cavity variables associated with the different types of cavity flow fields is defined. A brief review of these findings is included in the present paper. A test was also conducted to investigate the effects of Reynolds number and yaw angle on the steady (ref. 6) and unsteady (refs. 7 and 8) pressure distributions inside cavities at transonic speeds. Results from tests to investigate the effects of passive venting on cavity flow fields at subsonic and transonic speeds are presented in reference 9. These tests were also conducted as part of the Langley cavity program.

Cavity models in the present investigation consisted of both deep (cavity length-to-height ratio, $l/h = 5.42$ and 6.25) and shallow cavities ($l/h = 10.83$ and 12.50) that were installed in a flat-plate configuration. The store model consisted of a body of revolution with an ogive nose and cylindrical afterbody that had a length-to-diameter ratio of 20.10. The store model was attached to a remote-controlled, blade-strut assembly that could be used to position the store from inside the cavity to approximately 2 store diameters outside the cavity. The strut assembly protruded through the cavity floor. Static pressure measurements on the cavity and flat-plate surfaces and force and moment measurements from a six-component balance inside the store model were obtained at Mach numbers from 0.20 to 0.95.

Symbols

The store moment reference center was located 13.27 in. aft of the nose.

A	cross-sectional area of store body, 1.131 in ²	d	store diameter, 1.20 in.
C_A	axial-force coefficient of store, $\frac{\text{Axial force}}{q_\infty A}$	FPL	fluctuating pressure level, $20 \log \frac{p'}{q_\infty}$, dB
C_{AB}	axial-force coefficient of store base, $-C_{PB}$	h	cavity depth or height, in.
C_m	pitching-moment coefficient of store, $\frac{\text{Pitching moment}}{q_\infty A d}$	h_{sh}	height of strut housing above cavity floor, in. (see fig. 4(c))
C_N	normal-force coefficient of store, $\frac{\text{Normal force}}{q_\infty A}$	l	cavity length, in.
C_n	yawing-moment coefficient of store, $\frac{\text{Yawing moment}}{q_\infty A d}$	M_∞	free-stream Mach number
C_p	pressure coefficient, $\frac{p - p_\infty}{q_\infty}$	p	measured surface static pressure, psi
C_{PB}	pressure coefficient of store base, $\frac{p_B - p_\infty}{q_\infty}$	p'	fluctuating pressure, psi
$(C_p)_{crit}$	critical pressure coefficient	p_B	measured pressure on store base, psi
CPxxx	pressure coefficients for orifice number xxx (see tables 2-30)	$p_{t,\infty}$	free-stream total pressure, psi
C_Y	side-force coefficient of store, $\frac{\text{Side force}}{q_\infty A}$	p_∞	free-stream static pressure, psi
		q_∞	free-stream dynamic pressure, psi
		R_∞	free-stream unit Reynolds number, per foot
		r_n	store model nose radius, 0.032 in.
		$T_{t,\infty}$	free-stream total temperature, °F
		U	velocity, ft/sec
		U_∞	free-stream velocity, ft/sec
		w	cavity width, 9.60 in. for present test
		x	distance in streamwise direction relative to cavity leading edge, in. (see fig. 3)
		Y_s	lateral or spanwise distance from longitudinal centerline of cavity to centerline of store, in. (positive direction to right of cavity centerline looking upstream, see fig. 4(b))
		y	distance in lateral or spanwise direction relative to cavity centerline, in. (positive direction to left of cavity centerline looking upstream, see fig. 3)
		Z_s	vertical distance from flat-plate surface to centerline of store, in. (positive direction away from cavity, see fig. 4(b))
		z	distance normal to flat plate relative to plate surface, in. (positive direction into cavity, see fig. 3)
		δ	boundary-layer thickness ($U/U_\infty = 0.99$), in.

Experimental Methods

Models

Figure 1 is a photograph of the cavity-plate assembly installed in the test section of the wind tunnel. The flat-plate surface was located approximately on the longitudinal centerline of the test section. Vertical loads on the plate assembly were carried by six legs that were attached to the tunnel floor structure, and lateral loads were carried by four cables that were attached to the tunnel sidewall. The forward and middle pairs of legs were swept forward to improve the longitudinal cross-sectional area distribution of the plate assembly for blockage considerations. Fairings were mounted around the cavity on the lower side of the flat plate.

Photographs of the store model attached to the remotely controlled blade-strut assembly and installed in the cavity are shown in figure 2. The cavity configuration shown in these photographs is a shallow cavity with a depth of 2.40 in., a length of 26.00 in., and a width of 9.60 in. Both photographs show the store assembly installed 2.40 in. to the right of the cavity longitudinal centerline. The store is shown at two vertical positions in the photographs. Figure 2(a) shows the store in a retracted position inside the cavity with the store centerline located 0.90 in. below the flat-plate surface. Figure 2(b) shows the store in an extended position with the store centerline located 2.37 in. above the plate surface.

Sketches that show the basic dimensions of the cavity-plate assembly are presented in figure 3. The flat plate had a length of 111.00 in., a width of 48.00 in., and a nominal thickness of 1.00 in. The leading-edge cross section of the flat plate was half of a 12:1 ellipse. Tests were conducted with and without the store model installed in the cavity for cavity lengths of 26.00 in. and 30.00 in. and depths of 2.40 in. and 4.80 in. Limited tests were also conducted with the cavity floor positioned flush with the flat plate ($h = 0.00$ in.). Cavity length was varied by installing block inserts in the rear of the cavity, and cavity depth was varied by changing the length of the cavity-floor-assembly support struts (fig. 3). The cavity leading edge for all cavity configurations was located 36.00 in. downstream of the plate leading edge. The origin of the coordinate system that was used to define the locations of the pressure orifices in the cavity and on the flat plate was located on the longitudinal centerline of the flat-plate surface and at the cavity leading edge. (See fig. 3.) A turbulent boundary layer on the plate surface ahead of the cavity was obtained by installing a 0.10-in-wide

strip of No. 60 carborundum grit 1.00 in. downstream from the plate leading edge. The size and location of the grit were determined from references 10 and 11. Boundary-layer profiles measured during the tests of reference 5 with a similar cavity-plate assembly and at test conditions similar to the present test indicated that the boundary layer was turbulent at the cavity entrance for all Mach numbers.

Sketches of the assembly and basic dimensions of the store model and the blade-strut assembly are shown in figure 4. The store model is representative of a generic missile model with an ogive nose and a cylindrical afterbody. The installation of the store model and strut assembly in a typical shallow-cavity configuration is shown in figure 4(a). The store model was attached to an aft-facing six-component force-and-moment balance, which in turn was attached to the movable strut. The strut passed through a slot on the cavity side of the store model with a clearance between the strut and store model shell of 0.060 in. Vertical travel of the strut was provided by an internal strut-drive screw that was powered by an externally mounted strut-drive motor. The maximum vertical travel of the strut was 3.30 in. An encoder was mounted on the end of the strut-drive screw and was used to determine the strut position. The strut moved inside and was supported by a strut housing that was secured by the strut-housing support. The strut housing could be positioned at two vertical locations in the strut-housing support such that the height of the strut housing above the cavity floor h_{sh} was either 0.450 in. or 2.850 in. For all the shallow-cavity configurations and the flat-plate configuration, only the lower position was used, and it provided a range of Z_s from -0.90 in. to 2.36 in. for the shallow-cavity configurations and from 1.75 in. to 4.98 in. for the flat-plate configuration. For the deep-cavity configurations, both the upper and lower positions were used and provided a range of Z_s from -3.00 in. to 2.31 in. When the movable strut was fully extended, the blunt section of the strut extended 0.47 in. into the flow.

The arrangement of the store model in the cavity is shown in figure 4(b). The store model was tested on the cavity centerline ($Y_s = 0.00$ in.) and 2.40 in. to the right of the cavity centerline ($Y_s = 2.40$ in.). For both lateral positions, the store nose was located 1.20 in. downstream of the cavity leading edge. As shown in the side view of the model, the store vertical position Z_s was measured relative to the flat-plate surface. The moment reference center for the balance data was located 13.27 in. aft of the model nose, or 55 percent of the store model length. Basic

dimensions of the store model and strut assembly are given in figure 4(c). A 0.10-in-wide transition strip of No. 80 carborundum grit was applied to the nose of the store model 1.00 in. downstream of the nose tip, measured along the store surface. The size and location of the grit were determined from references 10 and 11.

A summary of descriptive information for all configurations tested is given in table 1.

Wind-Tunnel and Test Conditions

The tests were conducted in the Langley 8-Foot Transonic Pressure Tunnel. This facility is a continuous-flow, transonic wind tunnel capable of operating over a Mach number range from 0.2 to 1.3. The tunnel can obtain Reynolds numbers from 0.5×10^6 to 6×10^6 ft⁻¹ and stagnation pressures from 3.7 to 29.5 psia. A description of the facility is given in reference 12.

Tests were conducted with the flat-plate surface at an angle of attack of 0° relative to the test-section centerline for the nominal test conditions shown in the following table. The second set of test conditions, for $M_\infty \geq 0.60$, are for the configurations that included the store model installed in the deep cavities ($h = 4.80$ in.). For these deep-cavity configurations at $M_\infty \geq 0.60$, excessive lateral vibrations of the store model occurred and required the tunnel to be operated at reduced pressures to prevent overloading the balance side-force beam. At these reduced pressures, the boundary-layer trips should still be effective in inducing turbulent flow based on the estimates of references 10 and 11. Also, these reductions in pressure should result in less than a 10-percent increase in the boundary-layer thickness at the cavity leading edge, based on estimates from equation (27.66a) of reference 13. Therefore, these reductions in pressure did not have any significant effects on the trends shown by the results of this investigation. Values of boundary-layer thickness presented in this table are from reference 5 and were 36.00 in. from the plate leading edge. Forward of $x = 42$ in., the plate in reference 5 was a duplicate of the plate used in this investigation. Values of δ were obtained at approximately the same free-stream conditions as the present tests.

Instrumentation and Measurements

Pressures

The cavity floor and sidewalls and the flat-plate surface were instrumented with a total of 121 pressure orifices. Not all the pressure orifices in the cavities were used for all configurations; some of the floor

Configuration	M_∞	$p_{t,\infty}$, lb/in ²	$T_{t,\infty}$, °F	R_∞ , ft ⁻¹	δ , in.	q_∞ , lb/in ²
1-18	0.20	23.61	100	2.0×10^6	0.45	0.65
1-18	.40	22.22	↓	3.6	.48	2.23
1-10	.60	20.83		4.7	.47	4.12
11-18	.60	12.50		2.8		2.47
1-10	.80	14.18		3.8	.50	4.17
11-18	.80	9.44		2.5		2.78
1-10	.90	12.47		3.5	.52	4.18
11-18	.90	8.34		2.3		2.80
1-10	.95	11.81		3.4	.55	4.17
11-18	.95	8.34		2.4		2.94

and sidewall orifices were covered by the rear-block insert for the shorter cavities, and some of the sidewall orifices were covered for the shallow cavities. The orifices had inside diameters of 0.020 in. Detailed information on the locations of all the orifices in the cavity and on the flat plate are given in figure 5. A base pressure orifice was located at the center of the base of the store model.

All the surface pressure measurements on the models were obtained by using electronically scanned pressure (ESP) transducers referenced to tunnel static pressure. The pressure measurements are the average values of 10 data samples taken over a time period of 1 sec. The transducers had a range of ± 5 psid and a quoted accuracy of ± 0.01 psi. This increment in pressure corresponds to the following increments in pressure coefficient:

M_∞	$p_{t,\infty}$, lb/in ²	ΔC_p
0.20	23.61	± 0.015
.40	22.22	$\pm .004$
.60	20.83	$\pm .002$
.60	12.50	$\pm .004$
.80	14.18	$\pm .002$
.80	9.44	$\pm .004$
.90	12.47	$\pm .002$
.90	8.34	$\pm .004$
.95	11.81	$\pm .002$
.95	8.34	$\pm .003$

As discussed in reference 5, local Mach numbers on the flat-plate surface ($h = 0.00$ in.) in the region of the cavity installation could vary by as much as 0.03 from the nominal free-stream values shown in the table above as a result of a large ratio of model to tunnel blockage. However, because of the relative insensitivity of the cavity pressure distributions

to a Mach number variation of this magnitude at subsonic and transonic speeds, nominal free-stream values were used for reducing and reporting all data. Tunnel free-stream static and stagnation pressures were measured with sonar-sensed mercury manometers, which have an accuracy of ± 0.0035 psi.

Forces and Moments

Aerodynamic forces and moments on the store were measured with a six-component strain-gage balance. Store base pressures were measured with a single static pressure orifice located at the center of the store base. The force and moment measurements were not corrected by the base pressure measurements because the base of the model was not distorted as would normally be required for a conventional sting installation. Therefore, the uncorrected measurements are believed to be representative of the actual drag of the store during an unpowered separation. However, the base pressures were used to compute a base axial-force coefficient ($C_{AB} = -C_{PB}$), which is presented for all test conditions. Positive directions of the store forces and moments are shown in figure 4(b). The quoted accuracy of the strain-gage balance used is 0.5 percent of full-scale values. The full-scale values are as follows: Normal force = 150 lb, Axial force = 30 lb, Pitching moment = 200 in-lb, Side force = 75 lb, and Yawing moment = 100 in-lb. The accuracies correspond to the following increments in the force and moment coefficients.

M_∞	$P_{t,\infty}$, lb/in ²	ΔC_N	ΔC_A	ΔC_m	ΔC_Y	ΔC_n
0.20	23.61	± 1.02	± 0.204	± 1.13	± 0.510	± 0.567
.40	22.22	$\pm .30$	$\pm .059$	$\pm .33$	$\pm .149$	$\pm .165$
.60	20.83	$\pm .16$	$\pm .032$	$\pm .18$	$\pm .080$	$\pm .089$
.60	12.50	$\pm .27$	$\pm .054$	$\pm .30$	$\pm .134$	$\pm .149$
.80	14.18	$\pm .16$	$\pm .032$	$\pm .18$	$\pm .080$	$\pm .088$
.80	9.44	$\pm .24$	$\pm .048$	$\pm .27$	$\pm .119$	$\pm .133$
.90	12.47	$\pm .16$	$\pm .032$	$\pm .18$	$\pm .079$	$\pm .088$
.90	8.34	$\pm .24$	$\pm .047$	$\pm .26$	$\pm .118$	$\pm .132$
.95	11.81	$\pm .16$	$\pm .032$	$\pm .18$	$\pm .080$	$\pm .088$
.95	8.34	$\pm .23$	$\pm .045$	$\pm .25$	$\pm .113$	$\pm .125$

The store model did not have any canards, wings, or fins, so the rolling-moment measurements were near zero. Therefore, rolling-moment data are not presented.

Presentation of Data

Selected pressure data are tabulated in tables 2-18, and a complete set of force and moment data

from the store model is tabulated in tables 19-30. Figures 6, 7, and 8, which are discussed subsequently, present previously published information on cavity flow fields. Selected pressure data and force and moment data from the present test are presented graphically in the following figures.

Cavity Pressure Distributions

	Figure
Shallow-cavity configurations ($h = 2.40$ in.):	
Effect of Mach number on cavity floor pressure distributions	9
Effect of store vertical position on cavity floor pressure distributions	10
Effect of cavity length on cavity floor pressure distributions	11
Deep-cavity configurations ($h = 4.80$ in.):	
Effect of Mach number on cavity floor pressure distributions	12
Effect of store vertical position on cavity floor pressure distributions	13
Effect of cavity length on cavity floor pressure distributions	14

Flat-Plate Pressure Distributions

Shallow-cavity configurations ($h = 2.40$ in.):	
Effect of empty shallow cavities on flat-plate pressure distributions	15
Effect of store vertical position on flat-plate pressure distributions	16
Deep-cavity configurations ($h = 4.80$ in.):	
Effect of empty deep cavities on flat-plate pressure distributions	17
Effect of store vertical position on flat-plate pressure distributions	18

Store Forces and Moments

Shallow-cavity configurations ($h = 2.40$ in.):	
Effect of Mach number on store load characteristics	19
Effect of cavity length on store load characteristics	20
Effect of lateral position on store load characteristics	21
Deep-cavity configurations ($h = 4.80$ in.):	
Effect of Mach number on store load characteristics	22
Effect of cavity length on store load characteristics	23
Effect of lateral position on store load characteristics	24

Deep- and shallow-cavity configurations ($h = 4.80$ in. and 2.40 in.):	
Effect of cavity depth on store load characteristics, $M_\infty = 0.40$	25
Effect of cavity depth on store load characteristics, $M_\infty = 0.95$	26
Flat-plate configuration ($h = 0.00$ in.):	
Effect of Mach number on store load characteristics	27

Results and Discussion

A Review of Cavity Flow Fields

Only limited experimental data are available in the literature detailing cavity flow fields at subsonic and transonic speeds. However, at supersonic speeds numerous studies have been conducted that provide considerable insight into the structure of such flow fields, partly because at supersonic speeds the shock-wave structure associated with a change in flow direction is readily apparent from schlieren photographs. At subsonic and transonic speeds, however, schlieren and vapor-screen flow-visualization techniques have not revealed any useful information on the type of flow field.

A comparison of measured cavity pressure distributions obtained at subsonic and transonic speeds with data obtained at supersonic speeds indicates that for many cavity configurations the cavity flow fields over these speed ranges are similar (ref. 5). Therefore, in the present review of cavity flow fields, flow-field models are presented from the literature that are representative of supersonic speeds as well as subsonic and transonic speeds.

Cavity Flow Fields at Supersonic Speeds

At supersonic speeds, four types of cavity flow were defined in references 2, 3, and 14. The four flow types—open, closed, transitional-closed, and transitional-open, are briefly discussed. The first flow type generally occurs when the cavity is “deep,” as found in bomb bays, and is termed open cavity flow. Sketches of a hypothetical two-dimensional open cavity flow field and typical pressure distributions are shown in figure 6(a). Open cavity flow generally occurs for $l/h \lesssim 10$ at supersonic speeds, and for this case, the flow essentially bridges the cavity with a shear layer forming over the cavity. When the cavity flow is open, a nearly uniform longitudinal static pressure distribution is produced, which is desirable for safe store separation; however, high-intensity acoustic tones can develop, as indicated in

figure 6(a). These tones can induce vibrations in the surrounding structure, including the store, and can lead to structural fatigue.

The second type of cavity flow is for “shallow” cavities and is termed closed cavity flow. The cavity configurations typical of missile bays on fighter aircraft are likely to be shallow cavities. Figure 6(a) also provides a sketch of a hypothetical two-dimensional flow field and typical pressure distributions for closed cavity flow. At supersonic speeds, closed cavity flow generally occurs for $l/h \gtrsim 13$. In closed cavity flow, the flow separates at the forward face of the cavity, reattaches at some point along the cavity floor, and separates again before reaching the rear cavity face. This creates two distinct separation regions—one downstream of the forward face and one upstream of the rear face. For shallow cavities, where the flow is of the closed type, acoustic tones are not present; however, the flow produces an adverse static pressure gradient that can cause the store to experience large nose-into-the-cavity pitching moments.

The third and fourth mean cavity flow types (transitional-closed and transitional-open) occur for cavities that have values of l/h that fall between closed cavity flow and open cavity flow (i.e., l/h between 10 and 13). Transitional-closed cavity flow is the type of flow that occurs at the lower l/h boundary of closed cavity flow. For this case, the impingement shock and exit shock that normally occur for closed cavity flow coincide and produce a single shock, as shown in figure 6(b). As with closed cavity flow, large longitudinal pressure gradients occur in the cavity that can contribute to large nose-into-the-cavity pitching moments of the store.

With a very small reduction in l/h from a value corresponding to transitional-closed cavity flow, the impingement-exit shock wave abruptly changes to a series of compression wavelets, indicating that the shear layer still turns into the cavity; however, it no longer impinges on the cavity floor. This type of flow field is referred to as transitional-open cavity flow. For this type of flow field, as also indicated in figure 6(b), longitudinal pressure gradients in the cavity are not as large as shown for transitional-closed cavity flow; consequently, the problem of store nose-into-the-cavity pitching moment is not as severe as can occur for closed cavity flows (ref. 2).

The determinations of transitional-closed and transitional-open cavity flows, as well as open and closed cavity flows, were made by observation of the static pressure distribution in the cavity and schlieren photographs of the cavity flow field (ref. 15). Figures 6(a) and 6(b) provide typical static pressure

distributions for each flow type, which can be used as guidelines for determining the type of cavity flow. Figure 6(a) also provides typical dynamic pressure distributions for open and closed cavity flows. Typical dynamic pressure distributions for transitional-closed and transitional-open cavity flows have not been determined.

Cavity flow types are generally defined in terms of the length-to-height ratio of the cavity. However, other parameters can affect the exact value of l/h where the flow transitions from closed to open. Some of these other parameters include Mach number (ref. 16), the ratio of cavity width to cavity depth (ref. 15), the ratio of boundary-layer height to cavity depth (ref. 17), and the location of stores inside the cavity (ref. 2). Care should be taken to match cavity parameters and free-stream conditions when making data comparisons.

Cavity Flow Fields at Subsonic and Transonic Speeds

Cavity pressure distributions measured at subsonic and transonic speeds are presented in reference 5 for a wide range of cavity variables and are used to identify the different types of cavity flow fields in this speed range by comparisons with similar supersonic pressure distributions. These results show that in the subsonic-transonic speed range, three general cavity flow types—open, closed, and transitional—can be identified from the cavity floor pressure distributions. Pressure distributions for the open and closed types of flow fields were shown to be similar to the respective open and closed flows at supersonic speeds. The transitional type of flow field for subsonic and transonic speeds occurs over the range of l/h between open flow and closed flow. For subsonic-transonic speeds, sketches of the characteristic pressure distributions for each of the types of cavity flow and flow at the boundaries are shown in figure 7. These characteristic pressure distributions and flow-field types for subsonic-transonic speeds that are illustrated in figure 7 are summarized as follows (from ref. 5):

Open flow (fig. 7(a)):

- Value of pressure ($C_p \approx 0$) for $x/l \lesssim 0.6$ is uniform.
- At $x/l \gtrsim 0.6$, the pressures increase with increasing x/l and the distribution has a concave-up shape.

Open/transitional flow boundary (fig. 7(b)):

- An inflection point occurs in the pressure distribution at $x/l \approx 0.5$; over the rear portion of the cavity floor ($x/l \gtrsim 0.6$), the pressure distribution changes from a concave-up shape to a concave-down shape.
- The pressure coefficients over the forward portion of cavity are close to 0.

Transitional flow (fig. 7(c)):

- Pressure distributions over the rear portion of the cavity floor ($x/l \gtrsim 0.6$) have a concave-down shape.
- As l/h increases, the C_p distribution along the cavity floor gradually varies from the shape at the open/transitional flow boundary to that shown at the transitional/closed flow boundary.

Transitional/closed flow boundary (fig. 7(d)):

- Pressure coefficients increase uniformly from negative values in the vicinity of the front face to large positive values ahead of the rear face. The minimum values in the vicinity of the front face and maximum values ahead of the rear face are approximately of the same magnitudes that are measured for closed cavity flow.

Closed flow (figs. 7(e) and 7(f)):

- The flow becomes closed when the first inflection point moves forward and when a second inflection point occurs in the pressure distribution at $x/l \approx 0.5$ as a result of increasing l/h .
- With a further increase in l/h , a plateaued region occurs in the pressure distribution in the vicinity of the second inflection point.
- A still further increase in l/h causes a decrease in pressure to occur downstream of the plateaued region, followed by an increase in pressure to the maximum value ahead of the rear face.
- The maximum pressure ahead of the rear face remains at approximately the same value that was measured at the boundary with transitional flow.

It should be noted that the boundaries presented in reference 5 (and used in this report) were considered approximate and are not absolute. As at supersonic speeds, other parameters can affect the exact values of l/h at which the flow transitions from one type to the other. Care should be taken to match cavity parameters and free-stream conditions when

making data comparisons. To determine the boundaries of the transitional flow type from the pressure distribution at subsonic and transonic speeds, pressure distributions over the full range of flow types, open to closed, are required.

Shown in figure 8 are l/h boundaries from reference 5 for the three general flow types at subsonic and transonic Mach numbers. These regimes are shown for several cavity width and cavity depth configurations.

Cavity Pressure Distributions

Shallow-Cavity Configurations, $h = 2.40$ in.

Effects of M_∞ . The effects of Mach number on cavity floor pressure distributions for the shallow-cavity configurations are presented in figure 9. Results are presented for cavity lengths of 26.00 and 30.00 in. The store is at various vertical locations in a plane that is perpendicular to the cavity floor and contains the cavity longitudinal centerline (centerline plane, $Y_s = 0.00$ in.) and in a parallel plane 2.40 in. to the right of the centerline plane (off-centerline plane, $Y_s = 2.40$ in.). Data are also presented with the store assembly removed from the cavity (empty-cavity configuration) for comparison purposes. The pressure distributions presented in figure 9(a) are for the store located in the centerline plane of the 26.00-in-long cavity. A comparison of these pressure distributions with the representative cavity floor pressure distributions for the different types of cavity flow fields shown in figure 7 indicates that increasing M_∞ resulted in the cavity flow fields changing from a closed type of flow to a transitional type of flow. The boundary between closed and transitional flow appeared to occur at $M_\infty \approx 0.80$ for the test range of the store vertical locations as well as for the empty cavity. The results also show that when the flow field is closed, a change in M_∞ has only a small effect on the pressure distributions. When the flow field becomes transitional, increasing M_∞ causes the pressure distributions on the cavity floor to change in the direction of the open/transitional flow boundary; however, they remain more representative of the transitional/closed boundary than the open/transitional boundary. A comparison of the results presented in the different plots of figure 9(a) indicates that the cavity floor pressure distributions are not significantly affected by Z_s . Also, these results show that the pressure distributions for the empty cavity are approximately the same as for the cavity with the store assembly installed. This trend is more clearly shown in figure 10, where results from the empty

cavity and the cavity with the store installed at various values of Z_s are presented on the same plot.

Cavity floor pressure distributions obtained with the store located in the centerline plane of the 30-in-long cavity are shown in figure 9(b). As with the results obtained from the shorter cavity presented in figure 9(a), the pressure distributions for the empty cavity and for the cavity with the store installed show that the addition of the store assembly to the cavity had only small effects on the cavity pressure distributions for the test ranges of Z_s and M_∞ . A comparison of data presented in figures 9(a) and 9(b) at $M_\infty \leq 0.60$ shows that for the longer cavity, the cavity l/h has increased sufficiently to cause a reduction in the pressures immediately downstream of the plateau region. As described in the discussion of figure 7(e) in the section "Cavity Flow Fields at Subsonic and Transonic Speeds," this reduction occurs for the larger values of l/h in the closed flow regime. For $M_\infty \leq 0.60$, varying M_∞ had only small effects on the cavity floor pressure distributions. Increasing M_∞ for $M_\infty > 0.60$ resulted in the pressure distribution varying in the direction of the transitional/closed boundary; at the maximum test Mach numbers of 0.90 and 0.95, the pressure distributions are representative of flow at or near this boundary.

Cavity floor pressure distributions are presented in figures 9(c) and 9(d) with the store located in the off-centerline plane ($Z_s = 2.40$ in.) for the 26.00-in-long and 30.00-in-long cavities. The pressure distributions for the empty cavity and the cavity with the store installed show that the addition of an off-centerline store assembly had only small effects on C_p for the range of Z_s and M_∞ tested. A comparison of the results with the data presented in figures 9(a) and 9(b) shows that changing the store lateral position by 2.40 in. off the cavity centerline did not have any significant effect on the cavity floor pressure distribution at the location of the pressure instrumentation.

Effects of Z_s . The effect of adding the store assembly to the cavity and the effect of the store vertical position on the cavity floor pressure distributions are presented in figure 10. These results generally show that for both cavity lengths and both store lateral positions (figs. 10(a)–10(d)), the addition of the store or the position of the store in the cavity had only small effects on the cavity floor pressure distributions if the flow fields were of the closed type. These data also show that for cavity flow fields near the transitional/closed boundary ($M_\infty \geq 0.80$), the addition or position of the store in the cavity only

slightly changed the level of the pressure and did not change the type of flow field.

Effects of l . The effect of cavity length on cavity floor pressure distributions is shown in figure 11 for the shallow-cavity configuration with the store located at $Z_s = 0.00$ in. and $Y_s = 0.00$ in. The trends indicated by these data are applicable for the test range of Z_s and Y_s and for the empty-cavity configurations, since the addition of the store assembly to the cavity or its position in the cavity had only small effects on the cavity floor pressure distributions (fig. 10). For all Mach numbers, the pressure coefficients for the 30.00-in. cavity are less than those for the 26.00-in. cavity in the region downstream of the front face of the cavity, where the flow is expanding into the cavity ($x < 8$ in.). This difference is probably a result of the flow field for the longer cavity being farther away from the transitional/closed flow boundary. For all Mach numbers, the peak pressures at the end of the cavity are greater for the 30.00-in. cavity than for the 26.00-in. cavity. For $M_\infty \leq 0.60$, the pressure distributions for the two cavity lengths in the region of increasing pressure downstream of the flow expansion region ($x > 8$ in.) are essentially the same up to the approximate location of the plateau pressures for the 30-in. cavity ($x \approx 15$ in.). For greater values of x , the pressures for the 26.00-in. cavity are greater than for the 30.00-in. cavity. The greater pressures in this region for the shorter cavity are believed to be associated with the flow exiting the cavity, which occurs at smaller values of x for the shorter cavity. Since the store position in the cavity is fixed at the same location for both cavity lengths ($1.20 \leq x \leq 25.33$), the greater pressures and flow turning angles for the shorter cavity at $x > 15$ in. occur over the approximate 40-percent rear length of the store and would be expected to result in greater pitching moments for the shorter cavity. This trend was shown to be true and is discussed in the section "Store Forces and Moments."

Deep-Cavity Configurations, $h = 4.80$ in.

Effects of M_∞ . The effects of Mach number on cavity floor pressure distributions for the deep-cavity configurations are presented in figure 12. Results are again presented for cavity lengths of 26.00 in. and 30.00 in.; the store is in the centerline plane and in the off-centerline plane (figs. 12(a)-12(d)). Data are also shown in these figures for the empty-cavity configuration. Results are presented in figure 12(a) for the store located in the centerline plane of the 26.00-in. cavity. A comparison of these pressure distributions with the representative distribu-

tions shown in figure 7 suggests that for $M_\infty \leq 0.40$, the cavity flow fields are of the open type for the empty-cavity configuration and for the store-cavity configurations. The pressure orifices for the present data at $x = 25$ in. are closer to the rear face of the cavity than are the data from reference 5 that were used to determine the representative distributions of figure 7. Therefore, the rapid increase in pressure that occurs immediately ahead of the rear face as shown by the present data is not reflected in the distributions of figure 7. The distributions shown in figure 12(a) for $M_\infty \geq 0.60$ are indicative of flow near the open/transitional boundary. Although there are some small effects of Mach number for $M_\infty \geq 0.60$, the flow-field type remains the same. The somewhat flat dip in pressure observed in figure 12(a) for $Z_s = 0.00$ in. and 2.31 in. for $17 \text{ in.} \leq x \leq 23 \text{ in.}$ is unusual compared with the curves for the empty cavity and for the case with $Z_s = -3.00$ in. The pressure distribution shape may be caused by interference of the store model wake with the cavity lip shear layer.

Presented in figure 12(b) are pressure distributions on the cavity floor for the store located in the centerline plane of the 30.00-in. cavity. For this cavity, with or without the store assembly installed, the cavity flow field is of the open type for $M_\infty = 0.20$. At Mach numbers of 0.40 and 0.60, the flow-field type appears to be near the open/transitional boundary for all configurations. At $M_\infty = 0.80$, the increased pressure levels over the rear half of the cavity floor suggest that the flow field is transitional. Further increases in M_∞ result in a decrease in the pressure levels in this region, and the pressure distributions again become representative of flow near the open/transitional boundary. This change in the type of cavity flow field with increasing M_∞ was also observed in reference 5 for cavity configurations similar to those in figure 8 for $w = 9.60$ in. and $h = 2.40$ in.

Pressure distributions are shown in figures 12(c) and 12(d) for the store located in the off-centerline plane of the 24.00-in. and 30.00-in. cavities. These data are similar to the data presented in figures 12(a) and 12(b) for the store located in the centerline plane. Therefore, these results indicate that lateral position of the store for the range of spacing tested had little effect on the cavity floor pressure distributions. As shown in figure 9, this trend was also observed for the shallow cavity.

Effects of Z_s . The effects of the store vertical position on the cavity floor pressure are shown in figure 13 for the deep cavity. These pressure distributions can be directly compared with the empty-cavity pressure distributions that are presented on each plot. Results are presented in figure 13(a)

for the store located in the centerline plane of the 26.00-in. cavity. These data show that, although at some Mach numbers there were small effects of store position, the cavity flow field generally remained of the same type with or without the store in the cavity and for the test range of Z_s . Similar trends were obtained with the store located in the centerline plane of the 30-in. cavity (fig. 13(b)) and with the store located in the off-centerline plane of the 26.00-in. and 30.00-in. cavities (figs. 13(c) and 13(d)).

Effects of l . Presented in figure 14 are the effects of cavity length on the floor pressure distributions of the deep-cavity configurations with the store located at $Z_s = 0.00$ in. and $Y_s = 0.00$ in. Since the presence of the store or its position in the cavity had only small effects on the cavity floor pressure distributions, the trends shown in figure 14 should also be applicable when the store is located at other positions in the deep cavity or for the deep cavity without the store assembly installed (empty cavity). The data presented in figure 14 show that, for $x \leq 24$ in., the pressure distributions for both cavity lengths are approximately the same for most of the test Mach numbers. This agreement would indicate that the effect of cavity length on the store separation characteristics for the deep cavities would not be as great as for the shallow cavities (fig. 11). The effects of cavity length on the store separation characteristics are discussed in more detail in the section "Store Forces and Moments."

Flat-Plate Pressure Distributions

Shallow-Cavity Configurations, $h = 2.40$ in.

Effects of l . Pressure distributions obtained on the flat-plate surface for the empty shallow-cavity configurations are shown in figure 15. Data are also shown for the flat-plate configuration ($h = 0.00$ in.) so that the effects of the cavities can be determined. Results are presented only at Mach numbers of 0.40 and 0.95; however, similar effects of the cavities on the flat-plate pressure distributions were observed at the other test Mach numbers. The pressure orifices ahead of and downstream of the cavity cutout in the plate assembly ($x < 0$ in. and $x > 43$ in.) are located on the flat-plate longitudinal centerline. Pressure orifices for 0 in. $< x \leq 43$ in. are located to the side of the cavity installation at $y = 7.80$ in. (3.00 in. from the side edge of the cavities).

The results presented in figure 15 at $M_\infty = 0.95$ show that the local flow over the plate leading edge became supersonic and that a normal shock occurred at $x \approx -28$ in. The local Mach number ahead of

the normal shock based on the static pressure measurements was approximately 1.17. Because the local Mach number preceding the shock wave was low, the shock wave probably induced a localized separation of the boundary layer. This separation does not have a significant effect on the pressure distributions in the region of the cavity because of the large distance from the location of the shock wave to the cavity (≈ 28 in.). Similar results were obtained at $M_\infty = 0.90$. At $M_\infty \leq 0.80$, the pressure measurements indicate that the local flow on the plate leading edge remained subsonic.

The data in figure 15 show that, in addition to the large effect of the cavity on the plate pressure distributions to the side of the cavity, the cavity affects the pressures upstream and downstream of the cavity. The effect upstream of the cavity is associated with the flow expanding into the cavity and results in a reduction in the plate pressures that extends approximately 10 in. ahead of the cavity at $M_\infty = 0.40$. At $M_\infty = 0.95$, this effect only extends upstream about 5 in. The pressure distributions to the side of the shallow-cavity configurations at $M_\infty = 0.40$ show trends that are similar to those that occur on the floor of a shallow cavity; the low pressure is in the forward region of the cavity, and the maximum pressure is toward the rear face. The exception is a rapid decrease in pressure with increasing x on the plate surface as the value of x that corresponds to the rear face of the cavity is approached. This decrease in pressure on the flat-plate surface is probably associated with the flow exiting the cavity and expanding over the outer edge of the rear face. The low pressure associated with this expansion could propagate on the flat-plate surface to the side and upstream of the outer edge of the cavity rear face as shown by the pressure data. At $M_\infty = 0.95$, the pressures to the side of the cavities are similar to the results obtained at $M_\infty = 0.40$, except that the maximum pressures are greater and the minimum pressures are smaller. With increasing values of x downstream of the rear face of the cavity, the pressures increase and approach the undisturbed plate values at approximately 24 in. aft of the rear face for $M_\infty = 0.40$ and approximately 16 in. downstream of the rear face for $M_\infty = 0.95$. At $M_\infty = 0.95$, the decrease in pressure at $x \gtrsim 45$ in. for all configurations is probably caused by plate blockage.

When the store assembly is installed in the cavity, the base of the store is located at $x = 25.33$ in.; at this station (fig. 15) there is a large difference in the level of pressure for the two cavity lengths. If this trend of the variation of pressures with cavity length also occurs in the flow field over the cavity when the store

assembly is installed, then base drag, and hence the overall drag of the store when it is outside the cavity, will be greater for the shorter cavity. This trend is discussed further in the section "Store Forces and Moments."

Effects of Z_s . Presented in figure 16 are the effects of store vertical position on the flat-plate pressure distributions for the case of the store assembly installed in the shallow cavities. Plate pressure distributions are also shown for the empty-cavity configuration for comparison purposes. Pressure distributions presented in figure 16(a) are for the store located in the centerline plane of the 26.00-in. cavity. Results are shown for Mach numbers of 0.40 and 0.95 and are representative of data for the test Mach number range. The data show that the presence of the store, regardless of the store vertical position, had little effect on the plate pressure distributions. Similar trends are shown for the store located in the centerline plane of the 30-in. cavity in figure 16(b). For both cavity lengths, the maximum effects of the store occur in the elevated pressure regions to the sides of the cavity and the minimum pressure regions immediately downstream of the cavity trailing edge. At both of these locations, the effects were greatest when the store was at $Z_s = 0.00$ in. A comparison of the results presented in figures 16(a) and 16(b) with the results presented in figures 16(c) and 16(d) shows that lateral spacing of the store assembly had little effect on the plate pressure distributions.

Deep-Cavity Configurations, $h = 4.80$ in.

Effects of l . Presented in figure 17 are the effects of the empty deep-cavity configurations on the flat-plate pressure distributions. Results are shown only for $M_\infty = 0.40$ and 0.95; however, similar effects were observed at the other test Mach numbers. The plate pressure distributions for the deep cavities are somewhat similar to the distributions shown for the shallow cavities in figure 15, with the following exceptions: (1) there is no decrease in pressure on the flat plate near the forward wall of the deep cavities, and (2) the pressure coefficient levels on the flat plate immediately downstream of the deep cavities are generally less negative than for the shallow cavities. The pressure for the 26.00-in. deep cavity at the location of the store base ($x = 25.33$ in.) is less than the pressure at this location for the 30.00-in. deep cavity. This difference is somewhat less for the deep cavities than for the shallow cavities, as shown in figure 15.

Effects of Z_s . Shown in figure 18 are pressure distributions on the flat-plate surface with the store

assembly installed in the deep-cavity configurations at $M_\infty = 0.40$ and 0.95. The effects of the store on the flat-plate pressure distributions at these Mach numbers are similar to the results obtained at the other test Mach numbers. Results are presented in figure 18(a) for the store located in the centerline plane of the 26.00-in. cavity. At $M_\infty = 0.95$, the addition of the store to the cavity resulted in a small decrease in the maximum pressures to the side of the cavity and a small increase in the minimum pressures immediately downstream of the cavity rear face. Changing the store vertical position had little effect on the plate pressure distributions. Similar trends are shown in figure 18(b) for the store located in the centerline plane of the 30.00-in. cavity. A comparison of the pressure distributions presented in figures 18(a) and 18(b) with the results presented in figures 18(c) and 18(d) shows that changing the lateral position of the store by 2.50 in. had little effect on the pressure distributions when the store was positioned inside the cavity ($Z_s = -0.90$ in.) or outside the cavity ($Z_s = 2.40$ in.). However, when the store was positioned at $Z_s = 0.00$ in., changing the store lateral position resulted in a slight reduction in the peak pressures to the side of the cavity and a slight increase in the minimum pressure downstream of the cavity.

Store Forces and Moments

Shallow-Cavity Configurations, $h = 2.40$ in.

Effects of M_∞ . Shown in figure 19 are the effects of Mach number on the forces and moments of the store as it separates from the shallow cavities ($h = 2.40$ in.). Data are presented for cavity lengths of 26.00 in. and 30.00 in. with the store located in a plane perpendicular to the cavity floor on the cavity longitudinal centerline (centerline plane, figs. 19(a) and 19(b)), respectively, and with the store located in a parallel plane 2.40 in. to the right of the centerline plane (off-centerline plane, figs. 19(c) and 19(d)), respectively. The axial-force coefficients presented are uncorrected for base pressure; however, the base axial-force coefficients ($C_{AB} = -C_{PB}$) are also shown. The axial-force coefficients are presented uncorrected, because the base of the model was not distorted as would normally be required for a conventional sting installation; therefore, the uncorrected measurements are believed to be more representative of the true missile drag during an unpowered separation than values corrected for base pressure. Also, since the missile model did not have any fins and since the rolling moment was therefore always approximately zero, rolling-moment measurements are

not presented. If fins were present on the model, it is likely that all the moments would be considerably larger in magnitude.

The variations of the store pitching moment C_m with Z_s for the shallow cavity (fig. 19) are similar to the trends previously obtained at supersonic speeds for shallow cavities (e.g., see refs. 1-4). For increasing store distances from the shallow cavity, the pitching moments increase (positive C_m is with the nose into the cavity) as a result of: (1) the flow expanding into the cavity, which forces the store nose into the cavity, and (2) the flow exiting at the rear of the cavity, which forces the rear of the store out of the cavity. This combination of loadings can result in large pitching moments, even though the overall normal force C_N can be near zero. With increasing distance from the cavity, the effects of the cavity flow field on the store forces and moments generally begin to decrease; this decrease results in a reduction in C_m . For example, the results presented in figure 19(a) show that maximum pitching moments occur when the store is approximately one store diameter ($d = 1.20$ in.) away from the cavity.

The results presented in figure 19(a) ($l = 26.00$ in., $Y_s = 0.00$ in.) show that pitching moments are much more sensitive to the variation in M_∞ than the other force and moment measurements. For $0.2 \leq M_\infty \leq 0.6$, increasing M_∞ results in a small decrease in C_m . As previously discussed, the pressure data (fig. 9) indicate that for this range of M_∞ ($0.2 \leq M_\infty \leq 0.6$), the cavity flow field for this configuration was of the closed type. For $0.6 < M_\infty \leq 0.95$, increasing M_∞ results in a large decrease in the level of C_m . The pressure data for this cavity configuration and M_∞ range indicated that the flow field was of the transitional type and that increasing M_∞ caused it to change in the direction of the open/transitional boundary. At supersonic speeds, a change in the cavity flow field toward open cavity flow generally results in a reduction in peak pitching moment (refs. 1-4), and the present results indicate that similar trends occur at subsonic and transonic speeds. Therefore, the effect of M_∞ on C_m shown in figure 19(a) is probably a result of the effect of M_∞ on the type of cavity flow field, rather than a direct effect of M_∞ on the store loads. The present results show that while the flow field remains of the closed flow type, increasing M_∞ results in only a small decrease in C_m .

As shown in figure 19(a), values of C_N for this cavity configuration remained between -1 and 0 for the range of separation distances and Mach numbers. When the flow field was of the closed type, the values of C_N were essentially invariant with M_∞ ; when the

flow field was of the transitional type, C_N shifted toward a value of 0 as Mach number increased. Similar to the previous discussion for C_m , the effect of M_∞ on C_N is probably a result of the effect of M_∞ on the cavity flow field.

Axial-force coefficients for the cavity with $l = 26.00$ in. and $h = 2.40$ in. (fig. 19(a)) vary from negative values (thrust) with the store inside the cavity to peak values ranging from approximately 0.6 to 0.8 with the store outside the cavity. The peak values of C_A tend to decrease with increasing M_∞ and appear to be less sensitive to flow-field type than C_m and C_N . Although these peak values are not very sensitive to flow-field type, they are still influenced by the cavity flow field, because they are considerably greater than C_A measurements obtained with the store near a flat surface ($h = 0.00$, fig. 27). A comparison of C_A and C_{A_B} (fig. 19(a)) shows that for this configuration, essentially all the store drag with the store inside the cavity is base drag, and outside the cavity base drag is roughly 70 percent of the total drag.

Since the results presented in figure 19(a) are for $Y_s = 0.00$ in., the lateral parameters C_Y and C_n are approximately 0.00 throughout the test range of Z_s and M_∞ .

Shown in figure 19(b) are the effects of M_∞ on the forces and moments of the store as it separates in the centerline plane ($Y_s = 0.00$) of the 30.00-in. shallow cavity. A comparison of the C_m data in this figure with the data in figure 19(a) shows that the magnitudes of the pitching moments are lower for the longer cavity. The results presented in figure 19(b) show that the trend of the variation of C_m with M_∞ is similar to that shown in figure 19(a) for the shorter cavity. As determined previously from the cavity pressure distributions, a reduction occurs in the magnitude of C_m with increasing M_∞ at the larger values of M_∞ , where the flow field is of the transitional type. There was little effect of M_∞ on C_m at the lower Mach numbers when the flow field was of the closed flow type. There was essentially no effect of M_∞ on C_N for this configuration throughout the test Mach number range. Increasing M_∞ resulted in a slight reduction in C_A and C_{A_B} . A comparison of the variation of C_A with Z_s shows that for the longer cavity (fig. 19(b)), the increase of C_A with Z_s is much less than for the shorter cavity (fig. 19(a)). A similar trend is shown for C_{A_B} . The effects of l on both C_m and C_A are further discussed in the next section "Effects of l ."

A comparison of the data shown in figures 19(c) and 19(d) with the data in figures 19(a) and 19(b)

shows that the effects of M_∞ on C_m , C_N , C_A , and C_{AB} with the store in the off-centerline plane are nearly the same as with the store in the centerline plane. In fact, the magnitudes of these parameters at similar values of Z_s are essentially the same at the two lateral stations. This trend can be more clearly seen in figure 21, which shows the force and moment measurements at the two lateral stations on the same plot. The effects of Mach number on C_n when the store is located in the off-centerline plane are similar to the effects of M_∞ on C_m ; these effects consist of small reductions in C_n with increasing M_∞ when the flow field is closed and larger reductions in C_n with increasing M_∞ when the flow field becomes transitional. The positive values of C_n indicate that the cavity flow field is trying to rotate the nose of the store toward the cavity centerline (fig. 4(b)) for the test Mach number range.

Effects of l . Presented in figure 20 are the effects of cavity length on the forces and moments of the store in and near the shallow cavities. Results are shown with the store located in the centerline plane and the off-centerline plane at Mach numbers of 0.40 and 0.95. The trends of the variation of the store forces and moments with cavity length at these Mach numbers are representative of the data over the range of M_∞ tested. The data presented in figure 20(a) show that, with the store located in the centerline plane of the shallow cavity at $M_\infty = 0.40$, cavity length has large effects on C_m , C_N , C_A , and C_{AB} . The variation in C_m with l is probably associated with the variation of the location of the flow exiting the cavity relative to the rear half of the store model. As previously noted in the discussion of the pressure data shown in figure 11, the pressure measurements for the shorter cavity ($l = 26.00$ in.) at $M_\infty = 0.40$ indicate that the cavity flow field is of the closed flow type and that approximately 40 percent of the rear length of the store is exposed to flow exiting the cavity. For the 30.00-in. cavity, the pressure data of figure 11 also indicate that the flow field is of the closed flow type but that only about 20 percent of the rear length of the store is exposed to flow exiting the cavity. Also, the flow angularity that is present over the aft portion of the store for this case is likely to have a smaller average value. Since the flow in this region tends to force the rear of the store from the cavity, a decrease in the extent of the store, aft of the moment center, that is exposed to this (perhaps weaker) flow would be expected to result in a decrease in pitching moment, which is the trend shown in figure 20(a). Similarly, it would be expected that C_N would be less negative for the longer cavity. This trend is also shown by the data in figure 20(a).

Values of C_A presented in figure 20(a) are much less for the 30.00-in. cavity than for the 26.00-in. cavity after the store leaves the cavity. Most of this difference is a result of the difference in base pressure, as shown by the variation of C_{AB} with Z_s in figure 20(a). Although flow-field pressure measurements are not available that could explain the difference in base pressure measurements for the two cavity lengths, a possible explanation may be obtained by examining the flat-plate pressures shown in figure 15. The rapid decrease in pressure that occurs to the side of the cavities immediately upstream of the x -location of the cavity rear face could, as previously discussed, be caused by the decrease in pressure that results from propagation of the flow expansion over the outer edge of the cavity rear face to the side and upstream of the rear face. If this pressure decrease also propagates upstream over the cavity, then it would be expected to have a greater effect on the base of the store when the store is outside the shorter cavity than when outside the longer cavity because of the closer proximity of the cavity rear face to the store base.

Because the force and moment measurements shown in figure 20(a) are with the store located in the centerline plane, C_Y and C_n are near zero and are invariant with cavity length.

Results presented in figure 20(b) with the store located in the off-centerline plane of the shallow cavity at $M_\infty = 0.40$ show variations in C_m , C_N , C_A , and C_{AB} with l that are similar to those shown in figure 20(a) with the store located in centerline plane. These data show that increasing l results in a reduction in C_n and a slight increase in C_Y .

The effects of cavity length on the forces and moments of the store in the centerline plane of the shallow cavity at $M_\infty = 0.95$ are shown in figure 20(c). At this Mach number, the pressure data presented in figure 11 indicate that the cavity flow fields for both cavity lengths are transitional. The data presented in figure 20(c) show that increasing cavity length resulted in a reduction in C_m , even though the cavity floor pressure distributions for the two cavity lengths as shown in figure 11 are similar at this Mach number. The values of C_m are larger for the shorter cavity than for the longer cavity because the rear of the store is closer to the cavity rear face and is therefore in a region of larger flow angles. The larger flow angles over the rear of the store in the shorter cavity would also cause the values of C_N to be more negative as indicated by the data. The effects of cavity length on C_A and C_{AB} at $M_\infty = 0.95$ (fig. 20(c)) are similar to the effects shown in figure 20(a) for $M_\infty = 0.40$ and consist of large

reductions in drag with increasing values of l . Since the pressure distributions to the side of the cavities shown in figure 15 for these cavity configurations at $M_\infty = 0.95$ show the same trends that are shown at $M_\infty = 0.40$, the reasoning that is used to explain the variation of C_A and C_{AB} with l in figure 20(a) would also apply for the $M_\infty = 0.95$ data in figure 20(c).

Results presented in figure 20(d) with the store located in the off-centerline plane of the shallow cavity at $M_\infty = 0.95$ show effects of l on the store force and moment coefficients that are similar to those shown in figure 20(c) for the store located in the centerline plane.

The data in figure 20 clearly show the importance of simulating the length of shallow cavities, for the range of l/h of the present investigation, to obtain realistic store-separation measurements in wind-tunnel experiments. These data show that differences in cavity length of only about 15 percent can result in significant differences in the force and moment data. Therefore, results from models with rear-mounted sting support assemblies that require extended cavity lengths should be used with great caution since the results are likely to be nonconservative.

Effects of Y_s . Presented in figure 21 are the effects of lateral position on the forces and moments of the store in and near the shallow cavities. Results are shown for both cavity lengths at Mach numbers of 0.40 and 0.95 and are representative of data for the test range of Mach number. The data presented in figure 21(a) show that lateral position had little effect on C_m , C_N , C_A , and C_{AB} with the store in and near the 26.00-in. cavity at $M_\infty = 0.40$. Lateral position did have an effect on C_n and C_Y ; the data show that, with the store in the centerline plane, the values of these parameters were approximately zero. With the store in the off-centerline plane, positive values of C_n and negative values of C_Y were measured. This trend could possibly result from the flow exiting toward the rear and side of the cavity with a velocity component directed toward the side of the cavity. When impacting the rear of the store, this component would create negative values of C_Y and positive values of C_n . (See fig. 4(b).) The velocity component near the shear layer as it enters the cavity at the front lip may also contribute to this trend.

Results presented in figure 21(b) also show that, similar to the results shown in figure 22(a), store lateral position had little effect on values of C_m , C_N , C_A , and C_{AB} for the store in and near the 30.00-in. cavity. The data presented in figure 21(b) show that positive values of C_n were measured with the store in the off-centerline plane; however, the magnitude

was less than for the store in the off-centerline plane of the shorter cavity shown in figure 21(a). Also, the results presented in figure 21(b) show that lateral position had little effect on C_Y . The values of C_n and C_Y for the longer cavity could be smaller because the position of the rear of the store is farther from the cavity rear face and could therefore be exposed to reduced values of the velocity component that is directed toward the side of the cavity that was hypothesized in the preceding paragraph.

The effects of lateral position on the store in the shallow cavity at $M_\infty = 0.95$ are shown in figures 21(c) and 21(d) for the 26.00-in. and 30.00-in. cavities, respectively. The trend of the effects of lateral position on the store forces and moments at this Mach number is similar to the trends that were shown at the lower Mach numbers for the respective cavities, but the magnitude of the effects at the higher Mach number was smaller.

Deep-Cavity Configurations, $h = 4.80$ in.

As discussed in the section "Wind-Tunnel and Test Conditions," large lateral vibrations of the store model occurred inside the deep-cavity configurations. Because of these large vibrations, the tunnel was operated at reduced pressures for $M_\infty \geq 0.60$ to prevent overloading the balance side-force beam. At these reduced pressures, the boundary-layer trips should still be effective based on the estimates of references 10 and 11. Also, these reductions in pressure should result in less than a 10-percent increase in the boundary-layer thickness at the cavity leading edge based on estimates from equation (27.66a) of reference 13. Therefore, these reductions in pressure did not have any significant effects on the trends shown by the results of this investigation. The balance dynamic measurements were not recorded in this investigation; therefore, only static measurements are presented.

Because of the limited vertical travel of the strut component of the store separation assembly, it was necessary to conduct tests with the strut housing in two different positions (figs. 4(a) and 4(c)) to obtain the desired range of Z_s for the deep-cavity configurations. With the strut housing in the lower position ($h_{sh} = 0.45$ in.), Z_s was varied from -3.0 in. to 0.0 in.; with the strut housing in the upper position ($h_{sh} = 2.85$ in.), Z_s was varied from -0.9 in. to 2.4 in. This variation results in an overlap region of 0.9 in. for the two strut-housing positions. Since there is a slight difference in the geometry of the separation assembly for the two strut-housing positions, data are presented for both positions in the overlap regions to determine whether the differences in geometry had

any significant effects on the force and moment data. As can be seen in figures 22–26, the data in the overlap regions for the two strut-housing positions are generally in good agreement; this agreement indicates that the differences in the strut-housing geometry did not significantly affect the data.

Effects of M_∞ . Shown in figure 22 are the effects of M_∞ on the forces and moments of the store in and near the deep-cavity configurations. As discussed previously, the pressure data for these deep-cavity configurations indicate that the cavity flow fields were either open or near the open/transitional boundary through the test Mach number range. Results are presented in figures 22(a) and 22(b) for the store in the centerline plane of the 26.00-in. and 30.00-in. cavities; results are presented in figures 22(c) and 22(d) for the store in the off-centerline plane of the 26.00-in. and 30.00-in. cavities. The results presented in figure 22(a) for the store in the centerline plane of the 26.00-in. cavity show that M_∞ has only small effects on all the force and moment measurements except C_m . At the lower test Mach numbers of 0.20 and 0.40, the pressure data indicate that the cavity flow fields were open, and figure 22(a) shows negative or near-zero values of C_m for the test range of Z_s at these Mach numbers. At greater Mach numbers, the pressure data indicate that the cavity flow field was near the open/transitional boundary; the results presented in figure 22(a) show that for this case, negative values of C_m still occur when the store is inside the cavity, but they become positive when the store is outside the cavity. The maximum values of C_m are much less than those obtained for the shallow cavities with closed or transitional/closed flow, which is consistent with results obtained at supersonic speeds.

Mach number had only small effects on the force and moment measurements obtained with the store in the center plane of the 30.00-in. deep cavity. (See fig. 22(b).) The pressure data for this cavity configuration indicated that the cavity flow field was open at $M_\infty = 0.2$, was transitional/open at $M_\infty = 0.40$ and 0.60, was transitional at $M_\infty = 0.80$, and was transitional/open at $M_\infty = 0.90$ and 0.95. Even with the range of flow-field types that occurred with varying Mach numbers, only small variations occurred in the force and moment measurements, including C_m . For this cavity configuration, C_m was relatively insensitive to Z_s and to M_∞ . The smaller variations in C_m with both M_∞ and Z_s for the 30-in. cavity are probably due in part to the greater distance from the rear of the store to the cavity rear face.

The effects of M_∞ on C_m , C_N , C_A , and C_{AB} with the store in the off-centerline plane of the 26.00-

in-long deep cavity (fig. 22(c)) are similar to the effects shown in figure 22(a) with the store in the centerline plane. The results presented in figure 22(c) show that M_∞ had only small effects on C_Y with the store in the off-centerline plane. There was an effect of M_∞ on C_n , however, with the store in the off-centerline plane when the store was inside the cavity. The greatest effects occurred with the store located at $Z_s = -3.0$ in. For $0.20 \leq M_\infty \leq 0.80$, C_n increased with increasing M_∞ . A slight reduction in C_n occurred for $M_\infty > 0.80$. At $Z_s = -3.0$ in., minimum values of C_n were measured when the flow field was open, and maximum values were measured when the flow field was transitional. When the flow field was at or near the open/transitional boundary, intermediate levels of C_n were measured. When the store was located outside the cavity, the effects of M_∞ on C_n were minimal.

The effects of M_∞ on the force and moment measurements with the store in the off-centerline plane of the 30.00-in. cavity (fig. 22(d)) are similar to those shown in figure 22(c) for the 26.00-in. cavity except for C_n . For the 30.00-in. cavity, the effects of M_∞ on C_n are greatest at intermediate values of Z_s , $-2.0 \leq Z_s \leq 0.5$, and consist of a decrease in C_n with increasing M_∞ . This effect of M_∞ is opposite to the effect of M_∞ on C_n inside the cavity that was observed for the shorter cavity (fig. 22(c)).

Effects of l . Presented in figure 23 are the effects of l on the forces and moments of the store in the centerline and off-centerline planes at $M_\infty = 0.40$ and 0.95. These data are representative of the test range of M_∞ . Results are presented in figure 23(a) for the store in the centerline plane of the deep cavities at $M_\infty = 0.40$. These data show that C_N , C_Y , and C_n were approximately zero through the range of Z_s for both cavity lengths. Although the variations of C_m , C_A , and C_{AB} with Z_s were affected by cavity length, the magnitudes of these parameters for the two cavity lengths were not greatly different from the shallow-cavity data shown in figure 20. With the exception of C_n , the trends shown for the store in the off-centerline plane of the deep cavity are similar to those shown in figure 23(b). The values of C_n were either positive or near zero for the range of Z_s for the 26.00-in. cavity; for the 30-in. cavity, values of C_n were negative for most of the range of Z_s .

The effects of l shown in figures 23(c) and 23(d) for the store in the centerline and off-centerline planes of the deep cavity at $M_\infty = 0.95$ are similar to the results shown in figures 23(a) and 23(b) at $M_\infty = 0.40$. The major difference is that at the higher Mach number, the effect of l on C_n is greater

with the store in the off-centerline plane (fig. 23(d)) than at $M_\infty = 0.40$ (fig. 23(b)).

Effects of Y_s . Presented in figure 24 are the effects of the lateral position of the store-separation plane on the forces and moments of the store in and near the deep cavities at Mach numbers of 0.40 and 0.95. These data are representative of the test Mach number range. Results are presented in figures 24(a) and 24(b) for the 26.00-in. and 30.00-in. cavities at $M_\infty = 0.40$ and in figures 24(c) and 24(d) for the same two cavity lengths at $M_\infty = 0.95$. These data show that in general, the greatest effect of Y_s is on C_n , and this effect is the greatest for the 30.00-in. cavity at $M_\infty = 0.95$. The values of C_Y and C_n for the store in the off-centerline plane of the 30.00-in. cavity at $M_\infty = 0.95$ (fig. 24(d)) show that the side force is positive and is therefore directed toward the centerline of the cavity. Since C_n is negative, the resultant side force is acting through a point located aft of the moment-center location. Also, the peak side forces and yawing moments occur near the cavity opening ($Z_s = 0.0$ in.), which suggests that flow is directed into the cavity in the region of the rear half of the store. This flow direction is opposite to what is generally assumed to occur in this region over closed cavity flow and over shallow cavities. Comparison of figure 21 ($h = 2.40$ in.) with figure 24 ($h = 4.80$ in.) shows that for the shallow cavity (fig. 21), C_n is always positive; this shows that the flow is directed out of the cavity in the region over the rear half of the store. For the deep cavity (fig. 24), the flow appears to be directed only into the cavity over the rear portion of the store (negative value of C_n) for $l = 30.00$ in. ($l/h = 6.25$). (See figs. 24(b) and 24(d).) In reference 5, it is shown that for subsonic-transonic flows, it would be possible for a cavity with $l/h = 6.25$ to be in the transitional cavity flow regime. Unpublished colored-water flow-visualization photographs of surface flow patterns show that a transitional cavity flow would have some flow directed into the rear portion of the cavity, which could result in a negative value of C_n . An open cavity flow would span the length of the cavity, and the value of C_n would be near zero; a closed cavity flow would exit from the rear corners of the cavity and would result in a positive value of C_n . The cavity with $l/h = 5.42$, which would be expected to be in an open flow regime, shows a positive value of C_n when the store is positioned in the cavity and off the centerline (figs. 24(a) and 24(c)); the reason for the positive value is unknown.

Effects of h . Shown in figures 25 and 26 are the effects of cavity depth on the forces and moments of the store in the centerline and off-centerline planes

of the 26.00-in. and 30.00-in. cavities at $M_\infty = 0.40$ and 0.95, respectively. These data are representative of the test range of M_∞ . As previously discussed, the pressure data from the present test indicate that for the shallow cavities ($h = 2.40$ in.), the cavity flow fields are either closed or near the transitional/closed boundary; for the deep cavities ($h = 4.80$ in.), the cavity flow fields are either open or near the open/transitional boundary. Therefore, for the present tests, the effects of varying cavity depth from 2.40 in. to 4.80 in. would be expected to have a large effect on some of the forces and moments, especially C_m . The data presented in figure 25 clearly show the expected large effects of h on C_m for the range of l and Y_s at $M_\infty = 0.40$. The effects of h on C_m are greater when $l = 26.00$ in. than when $l = 30.00$ in., probably because the aft section of the store is closer to the rear face of the cavities for the shorter cavities than for the longer cavities. The results presented in figure 25 also show that negative values of C_N occur for the shallow cavities through most of the range of variables; for the deep cavity, C_N remains approximately zero. The effects of h on C_A and C_{AB} were greater for the cavity with $l = 30.00$ in. than for the cavity with $l = 26.00$ in.; for the cavity with $l = 30.00$ in., the drag level was consistently greater for the cavity with $h = 4.80$ in. With the store in the off-centerline plane, C_n was always positive for the shallow cavity; however, for the deep cavity, C_n was either negative or near zero for most of the range of Z_s .

Shown in figure 26 are the effects of cavity depth on the forces and moments of the store in the centerline and off-centerline planes of the 26.00-in. and 30.00-in. cavities at $M_\infty = 0.95$. The trends of the effects of h on the store forces and moments at $M_\infty = 0.95$ are similar to the results shown in figure 25 at $M_\infty = 0.40$.

The results presented in figures 25 and 26 show that the most significant difference between the forces and moments of the store in and near the shallow and deep cavities is that the store pitching moment is much greater for the shallow cavities. If the store has insufficient aerodynamic control to neutralize these pitching moments, the store angle of attack (nose into the cavity) tends to increase as distance from the cavity increases. This increase in angle of attack results in an increase in normal force in the direction back into the cavity.

Flat-Plate Configuration, $h = 0.00$ in.

Presented in figure 27 are the effects of M_∞ on the forces and moments of the store near the flat-plate surface. These data show that for the

range of test variables, all the forces and moments presented, with the exception of C_m , are essentially invariant with both M_∞ and Z_s . Values of C_m vary slightly with Z_s for $Z_s < 2.5$ in.; this variation may be partly caused by the strut housing. For $Z_s \geq 2.5$ in., C_m remains approximately constant with Z_s and decreases slightly with increasing M_∞ . Because of the small variations of the force and moment parameters with Z_s , and because the magnitudes of C_N and C_m were small, the strut support assembly used in the present tests did not have any significant effect on the force and moment data.

Conclusions

An experimental study has been conducted to measure the force and moment characteristics of a generic store in and near rectangular box cavities installed in a flat-plate configuration at subsonic and transonic speeds. Surface pressure measurements were also obtained inside the cavity and on the flat plate. The measurements were obtained for the store near a flat-plate surface, and in and near two shallow cavities and two deep cavities. The shallow cavities had a depth h of 2.40 in. and lengths l of 26.00 in. and 30.00 in. with corresponding values of l/h of 10.83 and 12.50. The deep cavities had depths of 4.80 in., lengths of 26.00 in. and 30.00 in., and corresponding values of l/h of 5.42 and 6.25. All cavities had a width of 9.60 in. Measurements were obtained with the store in a plane perpendicular to the cavity floor and containing the cavity longitudinal centerline (centerline plane) and in a parallel plane 2.50 in. to the right of the centerline plane (off-centerline plane). The tests were conducted over a free-stream Mach number M_∞ range of 0.20 to 0.95. Results from these tests lead to the following conclusions:

1. Surface pressure measurements inside the cavities indicated that through the test range of M_∞ , the flow fields for the shallow cavities were either closed or transitional near the transitional/closed boundary, and the flow fields for the deep cavities were either open or near the open/transitional boundary.
2. The installations of the store assembly inside the cavity and the position of the store after installation did not change the type of cavity flow field and had only small effects on the cavity and flat-plate pressure distributions.
3. The effects of M_∞ on the store forces and moments were primarily results of the effect of M_∞ on the type of cavity flow field, rather than a direct effect of M_∞ on the store loads.
4. For the shallow cavities with closed cavity flow fields, varying M_∞ had only small effects on the cavity and flat-plate pressure distributions and on the store forces and moments. When the flow fields for the shallow cavities were transitional near the transitional/closed boundary, increasing M_∞ resulted in large reductions in pitching-moment coefficient C_m .
5. Varying the length of the shallow cavities from 26.00 in. to 30.00 in. (≈ 15 percent) had a large effect on C_m , normal-force coefficient (C_N), and axial force coefficient (C_A). Therefore, results from models with rear-mounted sting support assemblies that require extended cavity lengths should be used with great caution since the results are likely to be nonconservative.
6. Lateral positioning of the store in the cavity had only small effects on the cavity and flat-plate pressure distributions and on C_m , C_N , and C_A .
7. Cavity depth had large effects on C_m and C_N for all cavity configurations and on C_A for the longer cavities ($l = 30.00$ in.). These large effects resulted from the effect of cavity depth on the type of cavity flow field. Values of C_m were always much greater for the shallow cavities with closed cavity flow than for the deep cavities with open flow. This result is similar to trends previously observed at supersonic speeds.

NASA Langley Research Center
Hampton, VA 23681-0001
February 14, 1995

References

1. Stallings, Robert L., Jr.: Store Separation From Cavities at Supersonic Flight Speeds. *J. Spacecr. & Rockets*, vol. 20, no. 2, Mar.-Apr 1983, pp. 129-132.
2. Stallings, Robert L., Jr.; and Forrest, Dana K: *Separation Characteristics of Internally Carried Stores at Supersonic Speeds*. NASA TP-2993, 1990.
3. Wilcox, Floyd J., Jr.: Experimental Measurements of Internal Store Separation Characteristics at Supersonic Speeds. *Store Carriage, Integration and Release*, R. Aeronaut. Soc., 1990, pp. 5.1-5.16.
4. Blair, A. B., Jr.; and Stallings, R. L., Jr.: Cavity Door Effects on Aerodynamic Loads of Stores Separating From Cavities. *J. Aircr.*, vol. 26, July 1989, pp. 615-620.
5. Plentovich, E. B.; Stallings, Robert L., Jr.; and Tracy, M. B.: *Experimental Cavity Pressure Measurements at Subsonic and Transonic Speeds—Static Pressure Results*. NASA TP-3358, 1993.

6. Plentovich, E. B.; Chu, Julio; and Tracy, M. B.: *Effects of Yaw Angle and Reynolds Number on Rectangular-Box Cavities at Subsonic and Transonic Speeds*. NASA TP-3099, 1991.
7. Tracy, M. B.; Plentovich, E. B.; and Chu, Julio: *Measurements of Fluctuating Pressure in a Rectangular Cavity in Transonic Flow at High Reynolds Numbers*. NASA TM-4363, 1992.
8. Tracy, M. B.; and Plentovich, E. B.: *Characterization of Cavity Flow Fields Using Pressure Data Obtained in the Langley 0.3-Meter Transonic Cryogenic Tunnel*. NASA TM-4436, 1993.
9. Stallings, Robert L., Jr.; Plentovich, Elizabeth B.; Tracy, Maureen B.; and Hensch, Michael J.: *Effect of Passive Venting on Static Pressure Distributions in Cavities at Subsonic and Transonic Speeds*. NASA TM-4549, June 1994.
10. Braslow, Albert L.; Hicks, Raymond M.; and Harris, Roy V., Jr.: *Use of Grit-Type Boundary-Layer Transition Trips on Wind-Tunnel Models*. NASA TN D-3579, 1966.
11. Braslow, Albert L.; and Knox, Eugene C.: *Simplified Method for Determination of Critical Height of Distributed Roughness Particles for Boundary-Layer Transition at Mach Numbers From 0.5*. NACA TN 4363, 1958.
12. Peñaranda, Frank E.; and Freda, M. Shannon, eds.: *Aeronautical Facilities Catalogue. Volume 1—Wind Tunnels*. NASA RP-1132, 1985.
13. Shapiro, Ascher H.: *The Dynamics and Thermodynamics of Compressible Fluid Flow*, Volume II. Ronald Press Co., 1954.
14. Wilcox, Floyd J., Jr.: *Experimental Investigation of Porous-Floor Effects on Cavity Flow Fields at Supersonic Speeds*. NASA TP-3032, 1990.
15. Stallings, Robert L., Jr.; and Wilcox, Floyd J., Jr.: *Experimental Cavity Pressure Distributions at Supersonic Speeds*. NASA TP-2683, 1987.
16. Rossiter, J. E.: *Wind-Tunnel Experiments on the Flow Over Rectangular Cavities at Subsonic and Transonic Speeds*. R. & M. 3438, British ARC, 1966.
17. Charwat, A. F.; Roos, J. N.; Dewey, F. C., Jr.; and Hitz, J. A.: An Investigation of Separated Flows—Part I: The Pressure Field. *J. Aerosp. Sci.*, vol. 28, no. 6, June 1961, pp. 457–470.

Table 1. Configuration Identification

[Pressure data not presented for all values of Z_s]

Configuration	h , in.	h_{sh} , in.	l , in.	Y_s , in.	Store	Z_s , in.	Type test (a)	Pressure table	Force table
1	0.00				No		P	2	
2	2.40		26.00		↓		P	3	
3	2.40		30.00		↓		P	4	
4	4.80		26.00		↓		P	5	
5	4.80		30.00		↓		P	6	
6	.00	0.70		0.00	Yes	1.75 to 4.98	P, F		
7	2.40	↓	26.00	.00	↓	-.90 to 2.36	P, F	7	19
8	↓	↓	26.00	2.40	↓	-.90 to 2.37	P, F	8	20
9	↓	↓	30.00	.00	↓	-.90 to 2.37	P, F	9	21
10	↓	↓	30.00	2.40	↓	-.90 to 2.37	P, F	10	22
11	4.80	↓	26.00	.00	↓	-3.00 to 0.00	P, F	11	23
12	↓	3.10	↓	.00	↓	-.90 to 2.31	P, F	12	24
13	↓	.70	↓	2.40	↓	-3.00 to 0.00	P, F	13	25
14	↓	3.10	↓	2.40	↓	-.90 to 2.31	P, F	14	26
15	↓	.70	30.00	.00	↓	-3.00 to 0.00	P, F	15	27
16	↓	3.10	↓	.00	↓	-.90 to 2.31	P, F	16	28
17	↓	.70	↓	2.40	↓	-3.00 to 0.00	P, F	17	29
18	↓	3.10	↓	2.40	↓	-.90 to 2.31	P, F	18	30

^aP indicates pressure tests; F indicates force and moment tests.

Table 2. Pressure Coefficients for Configuration 1 With $h = 0.00$ in.

Run Point	M_∞	$R_\infty \times 10^{-6}$	p_∞ , psi	$P_{t,\infty}$, psi	q_∞ , psi	$T_{t,\infty}$, °F	CP01	CP02	CP03	CP04	CP05	CP06	CP07	CP08	CP09	CP10	CP11
23. 899.	0.20	2.04	22.97	23.63	0.65	101.2	0.8705	-0.2476	-0.2023	-0.1851	-0.1630	-0.1351	-0.1088	-0.0891	-0.0778	-0.0588	-0.0581
23. 898.	0.40	3.64	19.92	22.24	2.23	99.9	0.9100	-0.2597	-0.2065	-0.1898	-0.1637	-0.1400	-0.1029	-0.0873	-0.0733	-0.0619	-0.0541
23. 897.	0.60	4.69	16.30	20.82	4.14	101.2	0.9939	-0.2869	-0.2292	-0.2095	-0.1843	-0.1552	-0.1115	-0.0971	-0.0785	-0.0624	-0.0585
23. 896.	0.80	3.80	9.28	14.17	4.18	100.8	1.1294	-0.3032	-0.2768	-0.2508	-0.2218	-0.1826	-0.1260	-0.1007	-0.0777	-0.0603	-0.0524
23. 895.	0.90	3.53	7.35	12.48	4.20	100.5	1.2081	-0.3275	-0.3211	-0.3588	-0.3587	-0.3141	-0.0826	-0.0606	-0.0424	-0.0291	-0.0219
23. 894.	0.95	3.40	6.61	11.82	4.18	100.2	1.2376	-0.2378	-0.2703	-0.2997	-0.3239	-0.3564	-0.3654	-0.3614	-0.0248	0.0451	0.0492
Run Point	CP12	CP13	CP14	CP15	CP16	CP17	CP18	CP19	CP20	CP21	CP22	CP23	CP24	CP25	CP26	CP27	CP28
23. 899.	-0.0519	-0.0467	-0.0360	-0.0323	-0.0311	-0.0378	-0.0270	-0.0219	-0.0208	-0.0165	-0.0125	-0.0161	-0.0187	-0.0162	-0.0181	-0.0133	-0.0229
23. 898.	-0.0476	-0.0439	-0.0342	-0.0299	-0.0276	-0.0259	-0.0228	-0.0211	-0.0196	-0.0196	-0.0179	-0.0170	-0.0173	-0.0197	-0.0178	-0.0186	-0.0202
23. 897.	-0.0517	-0.0435	-0.0360	-0.0311	-0.0261	-0.0255	-0.0219	-0.0205	-0.0215	-0.0147	-0.0126	-0.0145	-0.0173	-0.0147	-0.0216	-0.0196	-0.0277
23. 896.	-0.0442	-0.0366	-0.0286	-0.0234	-0.0184	-0.0169	-0.0140	-0.0136	-0.0149	-0.0109	-0.0104	-0.0121	-0.0151	-0.0140	-0.0213	-0.0236	-0.0326
23. 895.	-0.0145	-0.0092	-0.0024	0.0023	0.0066	0.0074	0.0084	0.0072	0.0056	0.0072	0.0057	0.0049	0.0035	0.0023	-0.0028	-0.0033	-0.0076
23. 894.	0.0443	0.0374	0.0299	0.0270	0.0267	0.0245	0.0222	0.0176	0.0141	0.0111	0.0072	0.0049	0.0041	0.0005	-0.0049	-0.0030	-0.0048
Run Point	CP29	CP30	CP31	CP32	CP33	CP34	CP35	CP36	CP37	CP38	CP39	CP40	CP41	CP42	CP43	CP44	CP45
23. 899.	-0.0190	-0.0211	-0.0178	-0.0176	-0.0185	-0.0196	-0.0177	-0.0216	-0.0239	-0.0255	-0.0298	-0.0394	-0.0281	-0.0286	-0.0210	-0.0237	-0.0256
23. 898.	-0.0204	-0.0217	-0.0223	-0.0233	-0.0225	-0.0247	-0.0237	-0.0235	-0.0250	-0.0268	-0.0312	-0.0365	-0.0316	-0.0314	-0.0325	-0.0335	-0.0351
23. 897.	-0.0254	-0.0262	-0.0252	-0.0257	-0.0291	-0.0284	-0.0325	-0.0356	-0.0392	-0.0364	-0.0451	-0.0514	-0.0447	-0.0466	-0.0490	-0.0520	-0.0567
23. 896.	-0.0341	-0.0398	-0.0425	-0.0462	-0.0509	-0.0552	-0.0630	-0.0687	-0.0771	-0.0833	-0.1007	-0.1034	-0.1087	-0.1210	-0.1343	-0.1532	-0.1747
23. 895.	-0.0018	0.0038	0.0041	0.0035	0.0037	0.0027	-0.0013	-0.0020	-0.0057	-0.0083	-0.0204	-0.0269	-0.0296	-0.0372	-0.0488	-0.0644	-0.0829
23. 894.	0.0068	0.0218	0.0233	0.0245	0.0277	0.0274	0.0259	0.0281	0.0276	0.0267	0.0185	0.0108	0.0089	0.0038	-0.0059	-0.0180	-0.0341
Run Point	CP46	CP47	CP48	CP49	CP50	CP52	CP82	CP84	CP85	CP86	CP87	CP88	CP89	CP90	CP91	CP92	CP93
23. 899.	-0.0115	-0.0184	-0.0194	-0.0212	-0.0197	-0.0176	-0.0196	-0.0097	-0.0146	-0.0068	-0.0138	-0.0157	-0.0128	-0.0117	-0.0132	-0.0140	-0.0152
23. 898.	-0.0176	-0.0197	-0.0209	-0.0243	-0.0290	-0.0201	-0.0196	-0.0174	-0.0158	-0.0157	-0.0184	-0.0170	-0.0167	-0.0170	-0.0175	-0.0170	-0.0168
23. 897.	-0.0144	-0.0235	-0.0299	-0.0312	-0.0390	-0.0193	-0.0175	-0.0146	-0.0187	-0.0115	-0.0173	-0.0187	-0.0184	-0.0159	-0.0168	-0.0175	-0.0200
23. 896.	-0.0134	-0.0276	-0.0378	-0.0512	-0.0962	-0.0211	-0.0198	-0.0184	-0.0209	-0.0157	-0.0210	-0.0230	-0.0235	-0.0222	-0.0231	-0.0237	-0.0284
23. 895.	0.0036	-0.0050	-0.0046	0.0019	-0.0171	-0.0027	-0.0006	0.0007	-0.0005	0.0039	-0.0002	-0.0016	-0.0019	-0.0011	-0.0014	-0.0016	-0.0031
23. 894.	0.0018	-0.0030	0.0046	0.0245	0.0195	-0.0060	-0.0036	-0.0024	-0.0016	0.0012	-0.0012	-0.0021	-0.0019	-0.0022	-0.0019	-0.0013	-0.0016

Table 2. Concluded

Run Point	CP94	CP95	CP96	CP97	CP98	CP99	CP100	CP101	CP102	CP103	CP104	CP105	CP106	CP107	CP108	CP109	CP110
23. 899.	-0.0129	-0.0112	-0.0137	-0.0110	-0.0217	-0.0250	-0.0167	-0.0137	-0.0149	-0.0137	-0.0179	-0.0110	-0.0222	-0.0191	-0.0148	-0.0133	-0.0208
23. 898.	-0.0166	-0.0172	-0.0157	-0.0155	-0.0160	-0.0224	-0.0149	-0.0159	-0.0176	-0.0155	-0.0167	-0.0157	-0.0207	-0.0171	-0.0179	-0.0184	-0.0189
23. 897.	-0.0189	-0.0192	-0.0213	-0.0193	-0.0250	-0.0306	-0.0219	-0.0194	-0.0234	-0.0218	-0.0256	-0.0229	-0.0264	-0.0225	-0.0217	-0.0224	-0.0282
23. 896.	-0.0263	-0.0264	-0.0284	-0.0272	-0.0310	-0.0357	-0.0297	-0.0286	-0.0328	-0.0325	-0.0348	-0.0340	-0.0381	-0.0352	-0.0360	-0.0392	-0.0427
23. 895.	-0.0025	-0.0026	-0.0028	-0.0013	-0.0029	-0.0062	-0.0001	0.0016	-0.0004	0.0014	0.0017	0.0033	0.0020	0.0053	0.0057	0.0053	0.0040
23. 894.	-0.0013	-0.0012	-0.0002	0.0011	0.0024	0.0000	0.0064	0.0084	0.0088	0.0119	0.0139	0.0165	0.0171	0.0208	0.0214	0.0223	0.0236
Run Point	CP111	CP112	CP113	CP114	CP115	CP116	CP117	CP118	CP119	CP120	CP121						
23. 899.	-0.0165	-0.0165	-0.0142	-0.0217	-0.0177	-0.0158	-0.0170	-0.0169	-0.0185	-0.0179	-0.0130						
23. 898.	-0.0178	-0.0183	-0.0182	-0.0208	-0.0202	-0.0200	-0.0212	-0.0214	-0.0208	-0.0213	-0.0227						
23. 897.	-0.0252	-0.0272	-0.0260	-0.0283	-0.0303	-0.0279	-0.0287	-0.0295	-0.0330	-0.0327	-0.0294						
23. 896.	-0.0423	-0.0449	-0.0454	-0.0500	-0.0527	-0.0537	-0.0562	-0.0593	-0.0640	-0.0663	-0.0685						
23. 895.	0.0051	0.0042	0.0053	0.0028	0.0027	0.0027	0.0019	0.0009	-0.0016	-0.0015	-0.0025						
23. 894.	0.0250	0.0255	0.0271	0.0257	0.0274	0.0275	0.0273	0.0272	0.0273	0.0285	0.0266						

Table 3. Pressure Coefficients for Configuration 2 With $h = 2.40$ in. and $l = 26.00$ in.

Run Point	M_∞	$R_\infty \times 10^{-6}$	p_∞ , psi	$p_{t,\infty}$, psi	q_∞ , psi	$T_{t,\infty}$, °F	CP01	CP02	CP03	CP04	CP05	CP06	CP07	CP08	CP09	CP10	CP11
27. 934.	0.20	2.04	22.95	23.60	0.65	101.2	0.8612	-0.2457	-0.2031	-0.1801	-0.1664	-0.1389	-0.1072	-0.0914	-0.0777	-0.0581	-0.0589
27. 933.	0.40	3.65	19.90	22.24	2.25	100.1	0.9092	-0.2609	-0.2059	-0.1888	-0.1651	-0.1406	-0.1023	-0.0884	-0.0735	-0.0617	-0.0547
27. 932.	0.60	4.68	16.30	20.81	4.13	101.7	0.9913	-0.2896	-0.2301	-0.2110	-0.1844	-0.1564	-0.1115	-0.0963	-0.0786	-0.0669	-0.0588
27. 931.	0.80	3.80	9.30	14.19	4.18	101.3	1.1260	-0.3082	-0.2794	-0.2542	-0.2231	-0.1858	-0.1275	-0.1004	-0.0784	-0.0658	-0.0529
27. 930.	0.90	3.53	7.37	12.49	4.20	100.9	1.2049	-0.3219	-0.3343	-0.3616	-0.3609	-0.2227	-0.0896	-0.0657	-0.0458	-0.0349	-0.0226
27. 929.	0.95	3.40	6.59	11.80	4.18	100.2	1.2415	-0.2218	-0.2618	-0.2982	-0.3206	-0.3553	-0.3641	-0.3605	-0.0386	0.0463	0.0570
Run Point	CP12	CP13	CP14	CP15	CP16	CP17	CP18	CP19	CP20	CP21	CP22	CP23	CP24	CP25	CP26	CP27	CP28
27. 934.	-0.0529	-0.0435	-0.0396	-0.0384	-0.0293	-0.0367	-0.0288	-0.0284	-0.0291	-0.0245	-0.0222	-0.0390	-0.0601	-0.0272	-0.0336	0.0125	0.0562
27. 933.	-0.0480	-0.0428	-0.0352	-0.0307	-0.0259	-0.0254	-0.0231	-0.0224	-0.0234	-0.0246	-0.0289	-0.0385	-0.0606	-0.0296	-0.0319	0.0072	0.0661
27. 932.	-0.0514	-0.0458	-0.0370	-0.0313	-0.0276	-0.0260	-0.0249	-0.0235	-0.0244	-0.0252	-0.0292	-0.0381	-0.0591	-0.0323	-0.0377	0.0017	0.0725
27. 931.	-0.0441	-0.0399	-0.0295	-0.0240	-0.0201	-0.0178	-0.0175	-0.0189	-0.0184	-0.0217	-0.0253	-0.0308	-0.0480	-0.0319	-0.0394	-0.0127	0.0723
27. 930.	-0.0148	-0.0118	-0.0024	0.0028	0.0062	0.0087	0.0087	0.0076	0.0070	0.0022	-0.0018	-0.0059	-0.0189	-0.0086	-0.0121	0.0026	0.0757
27. 929.	0.0519	0.0425	0.0355	0.0318	0.0308	0.0292	0.0252	0.0207	0.0178	0.0101	0.0036	-0.0016	-0.0137	-0.0067	-0.0089	0.0045	0.0767
Run Point	CP29	CP30	CP31	CP32	CP33	CP34	CP35	CP36	CP37	CP38	CP39	CP40	CP41	CP42	CP43	CP44	CP45
27. 934.	0.0564	-0.0874	-0.0845	-0.0625	-0.0567	-0.0430	-0.0380	-0.0370	-0.0339	-0.0278	-0.0324	-0.0478	-0.0356	-0.0304	-0.0365	-0.0386	-0.0374
27. 933.	0.0664	-0.1031	-0.0995	-0.0786	-0.0635	-0.0537	-0.0480	-0.0420	-0.0402	-0.0379	-0.0410	-0.0492	-0.0415	-0.0381	-0.0369	-0.0380	-0.0384
27. 932.	0.0792	-0.1358	-0.1312	-0.1037	-0.0824	-0.0688	-0.0605	-0.0543	-0.0520	-0.0503	-0.0543	-0.0650	-0.0592	-0.0571	-0.0578	-0.0581	-0.0588
27. 931.	0.0971	-0.1904	-0.1774	-0.1423	-0.1157	-0.1027	-0.0949	-0.0911	-0.0933	-0.1005	-0.1129	-0.1165	-0.1235	-0.1344	-0.1472	-0.1633	-0.1827
27. 930.	0.1186	-0.1439	-0.1177	-0.0779	-0.0500	-0.0364	-0.0267	-0.0196	-0.0191	-0.0244	-0.0316	-0.0387	-0.0418	-0.0503	-0.0615	-0.0771	-0.0955
27. 929.	0.1294	-0.1320	-0.1054	-0.0506	-0.0177	-0.0028	0.0087	0.0175	0.0200	0.0163	0.0120	0.0038	0.0028	-0.0030	-0.0109	-0.0234	-0.0395
Run Point	CP46	CP47	CP48	CP49	CP50	CP51	CP52	CP53	CP54	CP55	CP56	CP57	CP58	CP59	CP60	CP61	CP62
27. 934.	-0.0221	0.0182	0.0542	-0.0677	-0.0235	-0.0995	-0.0887	-0.1060	-0.1097	-0.1334	-0.1276	-0.0937	-0.0617	-0.0485	-0.0441	0.0211	0.0969
27. 933.	-0.0262	0.0185	0.0638	-0.0757	-0.0357	-0.0979	-0.1027	-0.1074	-0.1036	-0.1017	-0.1018	-0.1047	-0.1068	-0.0766	-0.0129	0.0695	0.0971
27. 932.	-0.0283	0.0151	0.0775	-0.0940	-0.0521	-0.1017	-0.1024	-0.1033	-0.1128	-0.1209	-0.1148	-0.1043	-0.0972	-0.0770	-0.0221	0.0441	0.0930
27. 931.	-0.0292	0.0009	0.0955	-0.1287	-0.1106	-0.0766	-0.0836	-0.0820	-0.0794	-0.0807	-0.0839	-0.0970	-0.0906	-0.0707	-0.0396	0.0041	0.0482
27. 930.	-0.0057	0.0120	0.1191	-0.0655	-0.0329	-0.0290	-0.0368	-0.0332	-0.0319	-0.0339	-0.0343	-0.0397	-0.0362	-0.0333	-0.0189	0.0035	0.0342
27. 929.	-0.0045	0.0144	0.1293	-0.0340	0.0103	-0.0148	-0.0226	-0.0156	-0.0190	-0.0230	-0.0265	-0.0322	-0.0320	-0.0271	-0.0127	0.0094	0.0287

Table 3. Concluded

Run	Point	CP63	CP64	CP65	CP66	CP67	CP68	CP77	CP78	CP79	CP80	CP81	CP82	CP83	CP84	CP85	CP86	CP87
27.	934.	0.1858	0.2253	0.2485	0.3340	0.3974	0.4327	-0.0996	-0.1224	0.0947	0.2808	0.3922	-0.1012	-0.1118	-0.0997	-0.1113	-0.1039	-0.1180
27.	933.	0.1611	0.2123	0.2585	0.3205	0.3997	0.4206	-0.1021	-0.1161	0.0878	0.2656	0.4344	-0.1050	-0.1107	-0.1116	-0.1154	-0.1167	-0.1241
27.	932.	0.1554	0.2066	0.2733	0.3402	0.4151	0.4542	-0.1031	-0.1206	0.0765	0.2788	0.4352	-0.1052	-0.1103	-0.1112	-0.1149	-0.1188	-0.1250
27.	931.	0.1128	0.1823	0.2499	0.3136	0.3777	0.4277	-0.0833	-0.0926	0.0351	0.2481	0.4090	-0.0831	-0.0880	-0.0891	-0.0894	-0.0942	-0.0984
27.	930.	0.0937	0.1517	0.2097	0.2577	0.3021	0.3299	-0.0339	-0.0388	0.0249	0.2099	0.3296	-0.0349	-0.0404	-0.0425	-0.0403	-0.0434	-0.0444
27.	929.	0.0802	0.1396	0.1999	0.2482	0.2833	0.2955	-0.0228	-0.0268	0.0300	0.1931	0.2962	-0.0223	-0.0277	-0.0294	-0.0267	-0.0308	-0.0305
Run	Point	CP88	CP89	CP90	CP91	CP92	CP93	CP94	CP95	CP96	CP97	CP98	CP99	CP100	CP101	CP102	CP103	CP104
27.	934.	-0.1253	-0.1132	-0.0680	-0.0082	0.0753	0.1408	0.1934	0.2327	0.2455	0.2607	0.2656	0.2839	0.3092	0.3422	0.3689	0.4096	0.4322
27.	933.	-0.1250	-0.1090	-0.0718	-0.0140	0.0557	0.1243	0.1824	0.2231	0.2450	0.2626	0.2770	0.2916	0.3136	0.3419	0.3737	0.4126	0.4464
27.	932.	-0.1260	-0.1087	-0.0714	-0.0186	0.0445	0.1085	0.1651	0.2138	0.2445	0.2670	0.2875	0.3042	0.3272	0.3553	0.3875	0.4271	0.4624
27.	931.	-0.1024	-0.0971	-0.0815	-0.0529	-0.0119	0.0369	0.0860	0.1375	0.1822	0.2196	0.2554	0.2830	0.3094	0.3381	0.3669	0.3989	0.4289
27.	930.	-0.0475	-0.0465	-0.0413	-0.0270	-0.0073	0.0197	0.0485	0.0829	0.1186	0.1512	0.1872	0.2167	0.2437	0.2685	0.2914	0.3145	0.3359
27.	929.	-0.0333	-0.0333	-0.0305	-0.0194	-0.0017	0.0198	0.0436	0.0719	0.1035	0.1321	0.1658	0.1917	0.2182	0.2412	0.2643	0.2848	0.3051
Run	Point	CP105	CP106															
27.	934.	0.4560	0.4618															
27.	933.	0.4714	0.4533															
27.	932.	0.4862	0.4702															
27.	931.	0.4529	0.4168															
27.	930.	0.3445	0.3284															
27.	929.	0.3080	0.2996															

Table 4. Pressure Coefficients for Configuration 3 With $h = 2.40$ in. and $l = 30.00$ in.

Run Point	M_∞	$R_\infty \times 10^{-6}$	p_∞ , psi	$P_{t,\infty}$, psi	q_∞ , psi	$T_{t,\infty}$, °F	CP01	CP02	CP03	CP04	CP05	CP06	CP07	CP08	CP09	CP10	CP11
26. 925.	0.20	2.05	23.03	23.69	0.65	100.1	0.8432	-0.2637	-0.2221	-0.2000	-0.1823	-0.1567	-0.1265	-0.1115	-0.0983	-0.0847	-0.0796
26. 924.	0.40	3.60	19.94	22.23	2.21	102.3	0.9038	-0.2664	-0.2116	-0.1942	-0.1699	-0.1456	-0.1075	-0.0933	-0.0791	-0.0675	-0.0599
26. 923.	0.60	4.69	16.31	20.80	4.11	100.3	0.9861	-0.2921	-0.2348	-0.2139	-0.1903	-0.1594	-0.1155	-0.1015	-0.0835	-0.0676	-0.0630
26. 922.	0.80	3.81	9.30	14.17	4.16	98.9	1.1262	-0.3026	-0.2792	-0.2539	-0.2257	-0.1847	-0.1276	-0.1029	-0.0799	-0.0620	-0.0543
26. 921.	0.90	3.52	7.36	12.47	4.19	101.5	1.2054	-0.3205	-0.3326	-0.3613	-0.3644	-0.2267	-0.0881	-0.0654	-0.0454	-0.0287	-0.0231
26. 920.	0.95	3.39	6.58	11.81	4.18	101.5	1.2404	-0.2233	-0.2651	-0.2978	-0.3254	-0.3542	-0.3645	-0.3634	-0.0505	0.0503	0.0549
Run Point	CP12	CP13	CP14	CP15	CP16	CP17	CP18	CP19	CP20	CP21	CP22	CP23	CP24	CP25	CP26	CP27	CP28
26. 925.	-0.0747	-0.0668	-0.0604	-0.0592	-0.0513	-0.0575	-0.0532	-0.0528	-0.0530	-0.0550	-0.0552	-0.0730	-0.0955	-0.0584	-0.0627	-0.0157	0.0275
26. 924.	-0.0535	-0.0492	-0.0410	-0.0358	-0.0319	-0.0303	-0.0288	-0.0277	-0.0296	-0.0318	-0.0372	-0.0483	-0.0729	-0.0377	-0.0408	-0.0009	0.0547
26. 923.	-0.0560	-0.0478	-0.0403	-0.0355	-0.0325	-0.0325	-0.0290	-0.0270	-0.0315	-0.0292	-0.0342	-0.0486	-0.0751	-0.0380	-0.0509	-0.0058	0.0356
26. 922.	-0.0467	-0.0392	-0.0312	-0.0268	-0.0227	-0.0228	-0.0204	-0.0210	-0.0238	-0.0236	-0.0283	-0.0408	-0.0659	-0.0360	-0.0558	-0.0201	0.0597
26. 921.	-0.0164	-0.0097	-0.0028	0.0004	0.0050	0.0045	0.0058	0.0046	0.0002	0.0007	-0.0033	-0.0146	-0.0369	-0.0136	-0.0345	-0.0054	0.0793
26. 920.	0.0483	0.0436	0.0335	0.0282	0.0276	0.0221	0.0203	0.0155	0.0086	0.0080	0.0035	-0.0067	-0.0287	-0.0098	-0.0328	-0.0076	0.0714
Run Point	CP29	CP30	CP31	CP32	CP33	CP34	CP35	CP36	CP37	CP38	CP39	CP40	CP41	CP42	CP43	CP44	CP45
26. 925.	0.0461	-0.0072	-0.0690	-0.1151	-0.1206	-0.1018	-0.0835	-0.0765	-0.0702	-0.0635	-0.0677	-0.0958	-0.0766	-0.0661	-0.0702	-0.0655	-0.0696
26. 924.	0.0731	0.0173	-0.0569	-0.1199	-0.1201	-0.0978	-0.0766	-0.0621	-0.0545	-0.0475	-0.0458	-0.0707	-0.0587	-0.0537	-0.0460	-0.0422	-0.0455
26. 923.	0.0852	0.0250	-0.0711	-0.1615	-0.1611	-0.1255	-0.1001	-0.0835	-0.0752	-0.0658	-0.0687	-0.0968	-0.0811	-0.0708	-0.0684	-0.0684	-0.0700
26. 922.	0.1122	0.0480	-0.0922	-0.2452	-0.2382	-0.1880	-0.1517	-0.1305	-0.1213	-0.1165	-0.1244	-0.1520	-0.1437	-0.1463	-0.1586	-0.1709	-0.1869
26. 921.	0.1555	0.1015	-0.0404	-0.2211	-0.1972	-0.1302	-0.0916	-0.0669	-0.0534	-0.0435	-0.0484	-0.0731	-0.0632	-0.0645	-0.0719	-0.0846	-0.1032
26. 920.	0.1588	0.1174	-0.0129	-0.1867	-0.1821	-0.0867	-0.0436	-0.0205	-0.0089	0.0036	-0.0005	-0.0181	-0.0089	-0.0104	-0.0163	-0.0286	-0.0455
Run Point	CP46	CP47	CP48	CP49	CP50	CP51	CP52	CP53	CP54	CP55	CP56	CP57	CP58	CP59	CP60	CP61	CP62
26. 925.	-0.0526	-0.0076	0.0428	-0.1274	-0.0598	-0.1497	-0.1432	-0.1500	-0.1561	-0.1732	-0.1559	-0.1435	-0.0987	-0.1082	-0.0298	0.0325	0.0627
26. 924.	-0.0343	0.0108	0.0724	-0.1282	-0.0460	-0.1262	-0.1264	-0.1293	-0.1312	-0.1394	-0.1272	-0.1298	-0.1265	-0.1122	-0.0213	0.0397	0.0936
26. 923.	-0.0357	0.0041	0.0818	-0.1721	-0.0616	-0.1319	-0.1282	-0.1348	-0.1438	-0.1475	-0.1385	-0.1343	-0.1064	-0.0843	-0.0257	0.0261	0.0727
26. 922.	-0.0346	-0.0099	0.1103	-0.2564	-0.1199	-0.1162	-0.1159	-0.1226	-0.1207	-0.1213	-0.1164	-0.1234	-0.1215	-0.0951	-0.0604	-0.0244	0.0212
26. 921.	-0.0125	0.0034	0.1529	-0.2343	-0.0438	-0.0766	-0.0769	-0.0820	-0.0820	-0.0841	-0.0782	-0.0856	-0.0768	-0.0625	-0.0461	-0.0249	0.0195
26. 920.	-0.0095	-0.0006	0.1564	-0.2130	0.0042	-0.0599	-0.0588	-0.0667	-0.0647	-0.0674	-0.0616	-0.0707	-0.0698	-0.0545	-0.0420	-0.0210	0.0083

Table 4. Concluded

Run Point	CP63	CP64	CP65	CP66	CP67	CP68	CP69	CP70	CP77	CP78	CP79	CP80	CP81	CP82	CP83	CP84	CP85
26. 925.	0.0933	0.1266	0.1599	0.1977	0.2197	0.2867	0.3630	0.4529	-0.1478	-0.1678	0.0383	0.1686	0.2860	-0.1467	-0.1581	-0.1505	-0.1582
26. 924.	0.1396	0.1666	0.1930	0.2209	0.2507	0.3137	0.4053	0.4831	-0.1289	-0.1472	0.0691	0.1964	0.3145	-0.1328	-0.1374	-0.1372	-0.1410
26. 923.	0.1309	0.1738	0.1959	0.2338	0.2719	0.3460	0.4354	0.4744	-0.1295	-0.1482	0.0726	0.1985	0.3393	-0.1346	-0.1377	-0.1379	-0.1454
26. 922.	0.1004	0.1655	0.2075	0.2582	0.3110	0.3763	0.4462	0.4996	-0.1170	-0.1270	0.0222	0.2097	0.3763	-0.1211	-0.1243	-0.1235	-0.1282
26. 921.	0.0936	0.1646	0.2134	0.2689	0.3268	0.3921	0.4501	0.4773	-0.0739	-0.0821	0.0177	0.2148	0.3895	-0.0801	-0.0838	-0.0833	-0.0864
26. 920.	0.0735	0.1366	0.1925	0.2519	0.3027	0.3531	0.4012	0.4230	-0.0545	-0.0621	0.0067	0.1933	0.3572	-0.0604	-0.0640	-0.0637	-0.0674
Run Point	CP86	CP87	CP88	CP89	CP90	CP91	CP92	CP93	CP94	CP95	CP96	CP97	CP98	CP99	CP100	CP101	CP102
26. 925.	-0.1583	-0.1702	-0.1693	-0.1422	-0.0781	-0.0059	0.0726	0.1333	0.1794	0.1925	0.1941	0.1931	0.1839	0.1820	0.1904	0.2017	0.2147
26. 924.	-0.1479	-0.1563	-0.1568	-0.1322	-0.0781	-0.0023	0.0753	0.1425	0.1903	0.2143	0.2208	0.2199	0.2169	0.2128	0.2187	0.2269	0.2401
26. 923.	-0.1448	-0.1553	-0.1571	-0.1369	-0.0899	-0.0280	0.0496	0.1169	0.1746	0.2109	0.2246	0.2314	0.2255	0.2242	0.2324	0.2454	0.2583
26. 922.	-0.1264	-0.1335	-0.1381	-0.1311	-0.1068	-0.0705	-0.0228	0.0278	0.0849	0.1368	0.1769	0.2120	0.2313	0.2483	0.2639	0.2813	0.2961
26. 921.	-0.0815	-0.0870	-0.0919	-0.0901	-0.0760	-0.0540	-0.0242	0.0101	0.0522	0.0973	0.1376	0.1792	0.2091	0.2409	0.2687	0.2960	0.3166
26. 920.	-0.0606	-0.0651	-0.0700	-0.0706	-0.0603	-0.0454	-0.0238	-0.0006	0.0324	0.0684	0.1001	0.1383	0.1668	0.1998	0.2315	0.2613	0.2838
Run Point	CP103	CP104	CP105	CP106	CP107	CP108	CP109	CP110									
26. 925.	0.2364	0.2566	0.3042	0.3394	0.4010	0.4464	0.4693	0.4522									
26. 924.	0.2627	0.2914	0.3314	0.3769	0.4327	0.4790	0.5003	0.4845									
26. 923.	0.2828	0.3122	0.3559	0.4007	0.4578	0.5023	0.5217	0.5001									
26. 922.	0.3196	0.3464	0.3821	0.4168	0.4594	0.4939	0.5186	0.4929									
26. 921.	0.3404	0.3620	0.3902	0.4141	0.4432	0.4698	0.4911	0.4561									
26. 920.	0.3070	0.3287	0.3516	0.3698	0.3918	0.4144	0.4281	0.3950									

Table 5. Pressure Coefficients for Configuration 4 With $h = 4.80$ in. and $l = 26.00$ in.

Run Point	M_∞	$R_\infty \times 10^{-6}$	p_∞ , psi	$p_{t,\infty}$, psi	q_∞ , psi	$T_{t,\infty}$, °F	CP01	CP02	CP03	CP04	CP05	CP06	CP07	CP08	CP09	CP10	CP11
24. 908.	0.20	2.05	22.96	23.61	0.65	99.1	0.8737	-0.2424	-0.1958	-0.1806	-0.1588	-0.1328	-0.1003	-0.0815	-0.0733	-0.0546	-0.0536
24. 907.	0.40	3.64	19.93	22.25	2.23	100.1	0.9062	-0.2600	-0.2090	-0.1918	-0.1696	-0.1412	-0.1051	-0.0943	-0.0762	-0.0589	-0.0577
24. 906.	0.60	4.68	16.34	20.85	4.13	102.3	0.9951	-0.2847	-0.2278	-0.2081	-0.1820	-0.1523	-0.1091	-0.0944	-0.0748	-0.0599	-0.0539
24. 905.	0.80	3.82	9.30	14.18	4.17	98.6	1.1259	-0.2985	-0.2742	-0.2502	-0.2189	-0.1801	-0.1241	-0.0990	-0.0756	-0.0599	-0.0495
24. 904.	0.90	3.52	7.36	12.47	4.19	100.4	1.2043	-0.3308	-0.3309	-0.3591	-0.3562	-0.2138	-0.0928	-0.0665	-0.0456	-0.0308	-0.0216
24. 903.	0.95	3.40	6.62	11.82	4.18	100.6	1.2367	-0.2383	-0.2717	-0.3032	-0.3274	-0.3575	-0.3676	-0.3551	-0.0100	0.0465	0.0496
Run Point	CP12	CP13	CP14	CP15	CP16	CP17	CP18	CP19	CP20	CP21	CP22	CP23	CP24	CP25	CP26	CP27	CP28
24. 908.	-0.0440	-0.0404	-0.0287	-0.0241	-0.0201	-0.0249	-0.0155	-0.0141	-0.0093	-0.0074	-0.0040	-0.0029	-0.0025	-0.0075	0.0020	0.0010	-0.0116
24. 907.	-0.0529	-0.0451	-0.0376	-0.0332	-0.0286	-0.0280	-0.0220	-0.0203	-0.0214	-0.0142	-0.0092	-0.0130	-0.0219	-0.0105	-0.0122	-0.0077	-0.0027
24. 906.	-0.0479	-0.0423	-0.0343	-0.0287	-0.0224	-0.0204	-0.0167	-0.0155	-0.0161	-0.0125	-0.0098	-0.0114	-0.0150	-0.0105	-0.0084	-0.0042	0.0192
24. 905.	-0.0415	-0.0357	-0.0248	-0.0181	-0.0134	-0.0105	-0.0075	-0.0074	-0.0091	-0.0099	-0.0091	-0.0094	-0.0159	-0.0111	-0.0057	-0.0074	0.0288
24. 904.	-0.0147	-0.0095	-0.0016	0.0045	0.0094	0.0101	0.0109	0.0107	0.0097	0.0117	0.0125	0.0108	0.0073	0.0094	0.0195	0.0181	0.0496
24. 903.	0.0443	0.0377	0.0327	0.0310	0.0301	0.0284	0.0262	0.0242	0.0215	0.0189	0.0164	0.0152	0.0126	0.0121	0.0261	0.0252	0.0570
Run Point	CP29	CP30	CP31	CP32	CP33	CP34	CP35	CP36	CP37	CP38	CP39	CP40	CP41	CP42	CP43	CP44	CP45
24. 908.	-0.0192	-0.0299	-0.0316	-0.0265	-0.0237	-0.0221	-0.0174	-0.0195	-0.0189	-0.0237	-0.0235	-0.0308	-0.0183	-0.0185	-0.0171	-0.0145	-0.0176
24. 907.	-0.0019	-0.0717	-0.0652	-0.0528	-0.0460	-0.0380	-0.0352	-0.0360	-0.0376	-0.0356	-0.0393	-0.0431	-0.0322	-0.0337	-0.0350	-0.0367	-0.0406
24. 906.	0.0243	-0.1143	-0.1045	-0.0835	-0.0665	-0.0550	-0.0489	-0.0463	-0.0474	-0.0461	-0.0505	-0.0542	-0.0447	-0.0463	-0.0488	-0.0491	-0.0531
24. 905.	0.0294	-0.1609	-0.1463	-0.1196	-0.0994	-0.0888	-0.0827	-0.0818	-0.0848	-0.0917	-0.1057	-0.1058	-0.1068	-0.1194	-0.1375	-0.1547	-0.1736
24. 904.	0.0536	-0.1259	-0.1073	-0.0764	-0.0513	-0.0347	-0.0262	-0.0213	-0.0221	-0.0242	-0.0350	-0.0425	-0.0393	-0.0459	-0.0604	-0.0777	-0.0974
24. 903.	0.0684	-0.1153	-0.0943	-0.0573	-0.0277	-0.0088	0.0032	0.0120	0.0138	0.0141	0.0072	-0.0005	0.0048	-0.0012	-0.0129	-0.0267	-0.0444
Run Point	CP46	CP47	CP48	CP49	CP50	CP51	CP52	CP53	CP54	CP55	CP56	CP57	CP58	CP59	CP60	CP61	CP62
24. 908.	-0.0005	-0.0018	-0.0097	-0.0298	-0.0216	0.0071	0.0049	-0.0006	0.0015	-0.0080	-0.0162	-0.0217	-0.0117	-0.0177	-0.0367	-0.0378	-0.0293
24. 907.	-0.0099	-0.0119	-0.0026	-0.0501	-0.0318	-0.0077	-0.0016	-0.0144	-0.0169	-0.0150	-0.0034	-0.0122	-0.0242	-0.0779	-0.0410	0.0106	-0.0219
24. 906.	-0.0078	-0.0016	0.0213	-0.0751	-0.0467	-0.0045	-0.0022	-0.0082	-0.0093	-0.0289	-0.0474	-0.0479	-0.0457	-0.0552	-0.0384	-0.0512	-0.0676
24. 905.	-0.0079	-0.0060	0.0290	-0.1095	-0.1027	0.0054	0.0068	0.0034	-0.0017	-0.0096	-0.0147	-0.0184	-0.0261	-0.0509	-0.0536	-0.0423	-0.0402
24. 904.	0.0110	0.0184	0.0532	-0.0650	-0.0313	0.0289	0.0282	0.0199	0.0185	0.0161	0.0150	0.0071	-0.0038	-0.0224	-0.0247	-0.0229	-0.0177
24. 903.	0.0138	0.0260	0.0684	-0.0428	0.0087	0.0309	0.0255	0.0183	0.0140	0.0114	0.0077	0.0030	-0.0071	-0.0096	-0.0153	-0.0108	0.0027

Table 5. Concluded

Run Point	CP63	CP64	CP65	CP66	CP67	CP68	CP71	CP72	CP73	CP74	CP75	CP76	CP77	CP78	CP79	CP80	CP81
24. 908.	-0.0464	-0.0072	-0.0574	-0.0668	-0.0517	-0.0710	0.0045	-0.0143	-0.0388	0.0115	-0.0105	-0.0511	0.0005	0.0024	-0.0282	-0.1031	0.0484
24. 907.	-0.0509	-0.0413	0.0598	0.0786	0.0377	-0.0074	-0.0047	-0.0194	0.0472	-0.0072	-0.0165	0.0198	-0.0048	-0.0071	-0.0630	0.0445	-0.0030
24. 906.	-0.0247	0.0446	0.1492	0.1527	0.0415	0.0686	0.0009	-0.0484	0.1227	-0.0043	-0.0363	0.0688	-0.0134	-0.0274	-0.0494	0.1061	0.0332
24. 905.	-0.0079	0.0541	0.1069	0.1206	0.0434	0.0522	0.0025	-0.0165	0.0707	0.0035	-0.0090	0.0472	-0.0068	-0.0238	-0.0414	0.1131	0.0317
24. 904.	0.0220	0.0764	0.1179	0.1268	0.0724	0.0559	0.0285	0.0065	0.0887	0.0259	0.0090	0.0750	0.0199	0.0049	-0.0035	0.1064	0.0653
24. 903.	0.0234	0.0772	0.1235	0.1173	0.0818	0.0733	0.0260	0.0112	0.0914	0.0268	0.0118	0.0729	0.0269	0.0114	0.0018	0.1118	0.0673
Run Point	CP82	CP83	CP84	CP85	CP86	CP87	CP88	CP89	CP90	CP91	CP92	CP93	CP94	CP95	CP96	CP97	CP98
24. 908.	0.0138	0.0022	0.0064	0.0042	-0.0013	-0.0068	-0.0058	-0.0130	-0.0168	-0.0257	-0.0216	-0.0270	-0.0289	-0.0306	-0.0411	-0.0438	-0.0477
24. 907.	-0.0055	-0.0106	-0.0098	-0.0176	-0.0145	-0.0205	-0.0228	-0.0286	-0.0286	-0.0347	-0.0381	-0.0412	-0.0392	-0.0373	-0.0322	-0.0255	-0.0232
24. 906.	-0.0134	-0.0187	-0.0198	-0.0231	-0.0225	-0.0268	-0.0307	-0.0371	-0.0426	-0.0495	-0.0515	-0.0487	-0.0385	-0.0199	0.0038	0.0273	0.0411
24. 905.	-0.0091	-0.0144	-0.0152	-0.0173	-0.0210	-0.0246	-0.0302	-0.0364	-0.0422	-0.0456	-0.0451	-0.0390	-0.0299	-0.0126	0.0071	0.0253	0.0435
24. 904.	0.0173	0.0138	0.0125	0.0084	0.0094	0.0051	-0.0006	-0.0054	-0.0086	-0.0128	-0.0137	-0.0116	-0.0039	0.0111	0.0252	0.0419	0.0527
24. 903.	0.0257	0.0218	0.0194	0.0167	0.0164	0.0133	0.0088	0.0040	-0.0002	-0.0032	-0.0025	0.0001	0.0041	0.0150	0.0266	0.0424	0.0551
Run Point	CP99	CP100	CP101	CP102	CP103	CP104	CP105	CP106									
24. 908.	-0.0569	-0.0586	-0.0565	-0.0529	-0.0355	-0.0144	0.0518	0.1948									
24. 907.	-0.0105	0.0011	0.0140	0.0206	0.0362	0.0500	0.1006	0.2228									
24. 906.	0.0540	0.0652	0.0831	0.1033	0.1242	0.1340	0.1657	0.2887									
24. 905.	0.0582	0.0712	0.0899	0.1140	0.1421	0.1509	0.1777	0.3173									
24. 904.	0.0640	0.0763	0.0928	0.1106	0.1344	0.1420	0.1788	0.3068									
24. 903.	0.0665	0.0784	0.0967	0.1194	0.1388	0.1453	0.1814	0.3113									

Table 6. Pressure Coefficients for Configuration 5 With $h = 4.80$ in. and $l = 30.00$ in.

Run Point	M_∞	$R_\infty \times 10^{-6}$	p_∞ , psi	$p_{t,\infty}$, psi	q_∞ , psi	$T_{t,\infty}$, °F	CP01	CP02	CP03	CP04	CP05	CP06	CP07	CP08	CP09	CP10	CP11
25. 917.	0.20	2.06	22.94	23.60	0.66	99.1	0.8701	-0.2443	-0.1988	-0.1820	-0.1597	-0.1348	-0.1033	-0.0869	-0.0757	-0.0614	-0.0541
25. 916.	0.40	3.63	19.92	22.26	2.24	102.4	0.8978	-0.2644	-0.2141	-0.1951	-0.1755	-0.1474	-0.1105	-0.0988	-0.0822	-0.0649	-0.0647
25. 915.	0.60	4.70	16.32	20.82	4.12	99.8	0.9906	-0.2858	-0.2286	-0.2084	-0.1831	-0.1529	-0.1090	-0.0941	-0.0754	-0.0604	-0.0540
25. 914.	0.80	3.82	9.30	14.19	4.18	99.1	1.1250	-0.3004	-0.2761	-0.2504	-0.2210	-0.1798	-0.1235	-0.0991	-0.0758	-0.0594	-0.0508
25. 913.	0.90	3.51	7.36	12.46	4.18	101.3	1.2025	-0.3278	-0.3365	-0.3605	-0.3531	-0.2121	-0.0940	-0.0663	-0.0446	-0.0296	-0.0225
25. 912.	0.95	3.38	6.59	11.79	4.17	102.7	1.2387	-0.2299	-0.2710	-0.3024	-0.3277	-0.3572	-0.3671	-0.3577	-0.0153	0.0488	0.0515
Run Point	CP12	CP13	CP14	CP15	CP16	CP17	CP18	CP19	CP20	CP21	CP22	CP23	CP24	CP25	CP26	CP27	CP28
25. 917.	-0.0494	-0.0437	-0.0356	-0.0294	-0.0262	-0.0292	-0.0209	-0.0183	-0.0170	-0.0146	-0.0097	-0.0097	-0.0117	-0.0150	-0.0072	-0.0082	-0.0162
25. 916.	-0.0580	-0.0500	-0.0438	-0.0394	-0.0338	-0.0352	-0.0302	-0.0276	-0.0299	-0.0231	-0.0204	-0.0254	-0.0326	-0.0218	-0.0253	-0.0159	-0.0104
25. 915.	-0.0463	-0.0385	-0.0299	-0.0251	-0.0255	-0.0244	-0.0211	-0.0171	-0.0165	-0.0133	-0.0118	-0.0154	-0.0269	-0.0131	-0.0133	-0.0109	0.0045
25. 914.	-0.0426	-0.0364	-0.0261	-0.0193	-0.0126	-0.0106	-0.0069	-0.0054	-0.0090	-0.0080	-0.0077	-0.0092	-0.0191	-0.0104	-0.0085	-0.0121	0.0151
25. 913.	-0.0153	-0.0103	-0.0016	0.0043	0.0081	0.0094	0.0128	0.0137	0.0113	0.0122	0.0117	0.0085	0.0027	0.0076	0.0143	0.0121	0.0249
25. 912.	0.0457	0.0393	0.0331	0.0300	0.0291	0.0274	0.0264	0.0246	0.0208	0.0186	0.0152	0.0111	0.0051	0.0085	0.0200	0.0206	0.0333
Run Point	CP29	CP30	CP31	CP32	CP33	CP34	CP35	CP36	CP37	CP38	CP39	CP40	CP41	CP42	CP43	CP44	CP45
25. 917.	-0.0152	-0.0150	-0.0281	-0.0369	-0.0349	-0.0314	-0.0262	-0.0216	-0.0224	-0.0282	-0.0244	-0.0316	-0.0201	-0.0204	-0.0182	-0.0183	-0.0242
25. 916.	0.0316	-0.0308	-0.0856	-0.1108	-0.1065	-0.0833	-0.0691	-0.0638	-0.0567	-0.0495	-0.0552	-0.0513	-0.0436	-0.0452	-0.0437	-0.0442	-0.0469
25. 915.	0.0606	-0.0311	-0.0963	-0.1257	-0.1171	-0.0954	-0.0778	-0.0672	-0.0600	-0.0546	-0.0581	-0.0495	-0.0434	-0.0458	-0.0473	-0.0500	-0.0539
25. 914.	0.0778	-0.0461	-0.1456	-0.1987	-0.1842	-0.1541	-0.1312	-0.1171	-0.1112	-0.1100	-0.1174	-0.1156	-0.1144	-0.1299	-0.1395	-0.1557	-0.1752
25. 913.	0.0933	0.0095	-0.0844	-0.1457	-0.1300	-0.0955	-0.0685	-0.0507	-0.0410	-0.0369	-0.0428	-0.0448	-0.0413	-0.0491	-0.0622	-0.0779	-0.0975
25. 912.	0.1063	0.0274	-0.0639	-0.1268	-0.1092	-0.0690	-0.0372	-0.0160	-0.0036	0.0015	-0.0007	-0.0026	0.0024	-0.0037	-0.0121	-0.0243	-0.0422
Run Point	CP46	CP47	CP48	CP49	CP50	CP51	CP52	CP53	CP54	CP55	CP56	CP57	CP58	CP59	CP60	CP61	CP62
25. 917.	-0.0104	-0.0087	-0.0200	-0.0439	-0.0257	0.0049	0.0084	0.0033	-0.0011	-0.0142	0.0023	0.0103	0.0003	0.0044	-0.0110	-0.0305	-0.0077
25. 916.	-0.0201	-0.0216	0.0309	-0.1095	-0.0450	-0.0214	-0.0181	-0.0348	-0.0356	-0.0335	-0.0168	0.0034	-0.0116	-0.0445	-0.0661	-0.0939	-0.1015
25. 915.	-0.0115	-0.0112	0.0537	-0.1272	-0.0509	-0.0107	-0.0130	-0.0227	-0.0254	-0.0275	-0.0301	-0.0469	-0.0507	-0.0322	-0.0374	-0.0551	-0.0803
25. 914.	-0.0086	-0.0130	0.0751	-0.1967	-0.1150	-0.0151	-0.0176	-0.0238	-0.0274	-0.0233	-0.0262	-0.0269	-0.0382	-0.0749	-0.0878	-0.0789	-0.0743
25. 913.	0.0089	0.0102	0.0935	-0.1453	-0.0404	0.0148	0.0155	0.0096	0.0072	0.0032	-0.0021	-0.0066	-0.0148	-0.0118	-0.0203	-0.0198	-0.0257
25. 912.	0.0102	0.0196	0.1040	-0.1271	0.0025	0.0259	0.0251	0.0235	0.0226	0.0163	0.0091	-0.0019	-0.0086	-0.0010	0.0051	0.0006	-0.0046

Table 6. Concluded

Run Point	CP63	CP64	CP65	CP66	CP67	CP68	CP69	CP70	CP71	CP72	CP73	CP74	CP75	CP76	CP77	CP78	CP79
25. 917.	-0.0213	-0.0354	-0.0289	-0.0015	0.0174	-0.0456	-0.0268	-0.0710	0.0070	-0.0033	-0.0227	0.0082	-0.0024	-0.0193	0.0032	-0.0004	-0.0367
25. 916.	-0.1036	-0.0205	0.0601	0.0839	0.1393	0.1116	0.0272	0.1198	-0.0166	-0.0196	0.0307	-0.0240	-0.0236	0.0340	-0.0258	-0.0398	-0.0697
25. 915.	-0.0634	0.0106	0.0469	0.1119	0.1761	0.1363	0.0834	0.0826	-0.0130	-0.0253	0.0579	-0.0183	-0.0283	0.0657	-0.0179	-0.0366	-0.0641
25. 914.	-0.0591	0.0125	0.0646	0.1213	0.1464	0.1060	0.0480	0.1497	-0.0141	-0.0234	0.0682	-0.0182	-0.0287	0.0598	-0.0206	-0.0308	-0.0561
25. 913.	-0.0191	0.0141	0.0574	0.1089	0.1569	0.1540	0.0913	0.1293	0.0135	-0.0018	0.0476	0.0127	-0.0019	0.0492	0.0131	0.0056	-0.0175
25. 912.	-0.0078	0.0211	0.0638	0.1312	0.1688	0.1588	0.1017	0.1123	0.0236	0.0118	0.0552	0.0231	0.0167	0.0573	0.0212	0.0128	-0.0097
Run Point	CP80	CP81	CP82	CP83	CP84	CP85	CP86	CP87	CP88	CP89	CP90	CP91	CP92	CP93	CP94	CP95	CP96
25. 917.	-0.0010	-0.0037	0.0018	-0.0052	0.0026	0.0002	0.0002	-0.0041	-0.0032	-0.0050	-0.0053	-0.0134	-0.0134	-0.0207	-0.0235	-0.0230	-0.0299
25. 916.	0.0086	0.1273	-0.0288	-0.0319	-0.0302	-0.0375	-0.0309	-0.0387	-0.0440	-0.0462	-0.0475	-0.0557	-0.0594	-0.0688	-0.0653	-0.0625	-0.0548
25. 915.	0.0688	0.1218	-0.0224	-0.0269	-0.0272	-0.0321	-0.0305	-0.0351	-0.0393	-0.0426	-0.0473	-0.0542	-0.0600	-0.0630	-0.0599	-0.0506	-0.0344
25. 914.	0.0711	0.1431	-0.0226	-0.0266	-0.0274	-0.0326	-0.0324	-0.0375	-0.0426	-0.0481	-0.0530	-0.0608	-0.0626	-0.0628	-0.0569	-0.0415	-0.0218
25. 913.	0.0541	0.1289	0.0116	0.0082	0.0074	0.0030	0.0037	0.0001	-0.0046	-0.0087	-0.0128	-0.0193	-0.0226	-0.0278	-0.0268	-0.0196	-0.0084
25. 912.	0.0731	0.1403	0.0205	0.0170	0.0158	0.0129	0.0138	0.0110	0.0072	0.0035	-0.0007	-0.0073	-0.0099	-0.0136	-0.0126	-0.0069	0.0036
Run Point	CP97	CP98	CP99	CP100	CP101	CP102	CP103	CP104	CP105	CP106	CP107	CP108	CP109	CP110			
25. 917.	-0.0331	-0.0384	-0.0364	-0.0363	-0.0350	-0.0339	-0.0351	-0.0323	-0.0241	-0.0380	-0.0093	0.0150	0.0557	0.2051			
25. 916.	-0.0305	-0.0127	0.0145	0.0434	0.0726	0.0842	0.0898	0.1008	0.1237	0.1643	0.1606	0.1548	0.1961	0.2941			
25. 915.	-0.0120	0.0112	0.0409	0.0718	0.0984	0.1177	0.1354	0.1480	0.1664	0.1831	0.1943	0.1844	0.1912	0.3252			
25. 914.	0.0016	0.0257	0.0552	0.0829	0.1090	0.1319	0.1526	0.1704	0.1993	0.2217	0.2507	0.2522	0.2308	0.3653			
25. 913.	0.0075	0.0258	0.0469	0.0724	0.0970	0.1150	0.1324	0.1467	0.1677	0.1846	0.2083	0.2136	0.2238	0.3527			
25. 912.	0.0170	0.0325	0.0543	0.0764	0.0967	0.1089	0.1230	0.1342	0.1513	0.1701	0.1935	0.1948	0.2016	0.3428			

Table 7. Pressure Coefficients for Configuration 7 With $h = 2.40$ in., $l = 26.00$ in., and $Y_g = 0.00$ in.(a) $Z_g = -0.90$ in.

Run Point	M_∞	$R_\infty \times 10^{-6}$	p_∞ , psi	$p_{t,\infty}$, psi	q_∞ , psi	$T_{t,\infty}$, °F	CP01	CP02	CP03	CP04	CP05	CP06	CP07	CP08	CP09	CP10	CP11
5. 103.	0.20	2.04	22.93	23.58	0.64	98.7	0.8835	-0.2179	-0.1898	-0.1748	-0.1558	-0.1159	-0.0970	-0.0860	-0.0652	-0.0319	-0.0391
5. 92.	0.40	3.64	19.93	22.24	2.22	98.6	0.9090	-0.2560	-0.2059	-0.1940	-0.1679	-0.1397	-0.1050	-0.0932	-0.0752	-0.0614	-0.0554
5. 83.	0.60	4.70	16.35	20.87	4.14	100.9	0.9904	-0.2985	-0.2314	-0.2149	-0.1877	-0.1561	-0.1130	-0.0972	-0.0789	-0.0651	-0.0575
5. 74.	0.80	3.80	9.32	14.20	4.17	100.9	1.1277	-0.3563	-0.2775	-0.2547	-0.2224	-0.1809	-0.1249	-0.0988	-0.0759	-0.0604	-0.0489
5. 56.	0.90	3.52	7.35	12.46	4.18	101.0	1.2030	-0.4169	-0.3782	-0.3765	-0.3691	-0.1673	-0.0947	-0.0694	-0.0475	-0.0335	-0.0230
5. 65.	0.95	3.40	6.61	11.83	4.19	101.0	1.2408	-0.3102	-0.2899	-0.3046	-0.3425	-0.3601	-0.3655	-0.3517	-0.0230	0.0480	0.0545
Run Point	CP12	CP13	CP14	CP15	CP16	CP17	CP18	CP19	CP20	CP21	CP22	CP23	CP24	CP25	CP26	CP27	CP28
5. 103.	-0.0473	-0.0356	-0.0274	-0.0230	-0.0255	-0.0352	-0.0212	-0.0103	-0.0185	-0.0116	0.0004	-0.0238	-0.0573	-0.0119	-0.0228	0.0192	0.0629
5. 92.	-0.0535	-0.0475	-0.0385	-0.0327	-0.0303	-0.0304	-0.0258	-0.0220	-0.0260	-0.0266	-0.0275	-0.0385	-0.0624	-0.0309	-0.0336	0.0048	0.0611
5. 83.	-0.0528	-0.0460	-0.0376	-0.0319	-0.0292	-0.0276	-0.0239	-0.0230	-0.0259	-0.0285	-0.0314	-0.0409	-0.0631	-0.0335	-0.0396	-0.0001	0.0676
5. 74.	-0.0422	-0.0368	-0.0259	-0.0199	-0.0179	-0.0153	-0.0133	-0.0131	-0.0139	-0.0164	-0.0185	-0.0261	-0.0444	-0.0253	-0.0337	-0.0109	0.0654
5. 56.	-0.0165	-0.0112	-0.0022	0.0028	0.0055	0.0068	0.0069	0.0068	0.0051	0.0029	0.0009	-0.0049	-0.0188	-0.0059	-0.0118	0.0026	0.0665
5. 65.	0.0475	0.0407	0.0350	0.0320	0.0287	0.0273	0.0255	0.0223	0.0169	0.0121	0.0075	-0.0006	-0.0130	-0.0033	-0.0077	0.0057	0.0668
Run Point	CP29	CP30	CP31	CP32	CP33	CP34	CP35	CP36	CP37	CP38	CP39	CP40	CP41	CP42	CP43	CP44	CP45
5. 103.	0.0665	-0.0858	-0.0702	-0.0421	-0.0485	-0.0223	-0.0139	-0.0333	-0.0292	-0.0170	-0.0204	-0.0445	-0.0279	-0.0213	-0.0096	-0.0212	-0.0294
5. 92.	0.0613	-0.1046	-0.0980	-0.0753	-0.0646	-0.0507	-0.0435	-0.0432	-0.0402	-0.0372	-0.0373	-0.0544	-0.0453	-0.0433	-0.0392	-0.0378	-0.0380
5. 83.	0.0737	-0.1346	-0.1246	-0.0970	-0.0789	-0.0661	-0.0588	-0.0560	-0.0550	-0.0522	-0.0553	-0.0651	-0.0593	-0.0590	-0.0605	-0.0629	-0.0652
5. 74.	0.0902	-0.1759	-0.1582	-0.1263	-0.1044	-0.0920	-0.0866	-0.0858	-0.0897	-0.0955	-0.1061	-0.1142	-0.1171	-0.1264	-0.1412	-0.1577	-0.1769
5. 56.	0.1114	-0.1319	-0.1073	-0.0714	-0.0467	-0.0317	-0.0233	-0.0185	-0.0192	-0.0233	-0.0321	-0.0415	-0.0416	-0.0486	-0.0606	-0.0761	-0.0950
5. 65.	0.1201	-0.1194	-0.0893	-0.0419	-0.0150	0.0024	0.0137	0.0191	0.0206	0.0188	0.0138	0.0030	0.0053	-0.0001	-0.0078	-0.0215	-0.0385
Run Point	CP46	CP47	CP48	CP49	CP50	CP51	CP52	CP53	CP54	CP55	CP56	CP57	CP58	CP59	CP60	CP61	CP62
5. 103.	-0.0081	0.0244	0.0627	-0.0475	-0.0111	-0.1034	-0.0826	-0.1140	-0.1142	-0.1206	-0.0959	-0.0685	-0.0471	-0.0236	0.0052	0.0597	0.0991
5. 92.	-0.0273	0.0157	0.0607	-0.0711	-0.0363	-0.1036	-0.1009	-0.1079	-0.1083	-0.1125	-0.1083	-0.1147	-0.1002	-0.0633	0.0017	0.0478	0.1063
5. 83.	-0.0308	0.0118	0.0727	-0.0878	-0.0521	-0.0990	-0.1001	-0.1033	-0.1080	-0.1160	-0.1178	-0.1178	-0.0944	-0.0555	-0.0121	0.0305	0.0772
5. 74.	-0.0233	-0.0006	0.0892	-0.1137	-0.1045	-0.0644	-0.0688	-0.0711	-0.0733	-0.0741	-0.0723	-0.0775	-0.0779	-0.0656	-0.0415	-0.0065	0.0342
5. 56.	-0.0047	0.0101	0.1095	-0.0574	-0.0304	-0.0320	-0.0354	-0.0360	-0.0370	-0.0415	-0.0402	-0.0432	-0.0394	-0.0279	-0.0116	0.0093	0.0316
5. 65.	-0.0020	0.0123	0.1205	-0.0259	0.0134	-0.0189	-0.0205	-0.0209	-0.0233	-0.0254	-0.0227	-0.0253	-0.0256	-0.0185	-0.0094	0.0051	0.0327

Table 7. Continued

(a) Concluded

Run Point	CP63	CP64	CP65	CP66	CP67	CP68	CP77	CP78	CP79	CP80	CP81	CP82	CP83	CP84	CP85	CP86	CP87
5. 103.	0.1634	0.2432	0.2598	0.3222	0.3875	0.4730	-0.0774	-0.1121	0.1151	0.2863	0.3986	-0.0913	-0.0989	-0.0776	-0.0958	-0.0860	-0.1130
5. 92.	0.1557	0.2152	0.2616	0.3167	0.3958	0.4428	-0.1008	-0.1227	0.0965	0.2725	0.4146	-0.1044	-0.1082	-0.1055	-0.1111	-0.1156	*****
5. 83.	0.1586	0.2151	0.2674	0.3322	0.4079	0.4357	-0.1012	-0.1237	0.0861	0.2765	0.4018	-0.1044	-0.1078	-0.1070	-0.1118	-0.1160	-0.1247
5. 74.	0.1074	0.1731	0.2338	0.2985	0.3609	0.3777	-0.0704	-0.0829	0.0310	0.2414	0.3619	-0.0730	-0.0782	-0.0771	-0.0784	-0.0824	-0.0876
5. 56.	0.0897	0.1478	0.1979	0.2491	0.2938	0.3080	-0.0290	-0.0352	0.0242	0.1989	0.3017	-0.0300	-0.0349	-0.0344	-0.0353	-0.0376	-0.0402
5. 65.	0.0772	0.1353	0.1787	0.2280	0.2587	0.2726	-0.0166	-0.0241	0.0275	0.1772	0.2627	-0.0187	-0.0226	-0.0218	-0.0221	-0.0253	-0.0279
Run Point	CP88	CP89	CP90	CP91	CP92	CP93	CP94	CP95	CP96	CP97	CP98	CP99	CP100	CP101	CP102	CP103	CP104
5. 103.	-0.1107	-0.1069	-0.0468	0.0247	0.1003	0.1624	0.2139	0.2451	0.2554	0.2642	0.2711	0.2737	0.3036	0.3398	0.3745	0.4160	0.4489
5. 92.	-0.1286	-0.1174	-0.0689	-0.0006	0.0764	0.1436	0.1968	0.2304	0.2498	0.2620	0.2734	0.2813	0.3068	0.3369	0.3716	0.4164	0.4568
5. 83.	-0.1276	-0.1168	-0.0756	-0.0156	0.0508	0.1177	0.1728	0.2148	0.2450	0.2648	0.2809	0.2955	0.3209	0.3502	0.3829	0.4219	0.4542
5. 74.	-0.0916	-0.0913	-0.0764	-0.0505	-0.0134	0.0316	0.0764	0.1218	0.1624	0.1964	0.2315	0.2590	0.2880	0.3147	0.3415	0.3705	0.3964
5. 56.	-0.0434	-0.0438	-0.0370	-0.0239	-0.0055	0.0193	0.0460	0.0756	0.1054	0.1350	0.1660	0.1935	0.2209	0.2464	0.2670	0.2879	0.3071
5. 65.	-0.0296	-0.0305	-0.0253	-0.0147	0.0004	0.0221	0.0447	0.0685	0.0928	0.1176	0.1441	0.1679	0.1953	0.2183	0.2378	0.2565	0.2707
Run Point	CP105	CP106															
5. 103.	0.4910	0.4773															
5. 92.	0.4939	0.4716															
5. 83.	0.4820	0.4581															
5. 74.	0.4246	0.3840															
5. 56.	0.3177	0.2967															
5. 65.	0.2747	0.2681															

Table 7. Continued

(b) $Z_s = 0.00$ in.

Run Point	M_∞	$R_\infty \times 10^{-6}$	p_∞ , psi	$p_{t,\infty}$, psi	q_∞ , psi	$T_{t,\infty}$, of	CP01	CP02	CP03	CP04	CP05	CP06	CP07	CP08	CP09	CP10	CP11
5. 105.	0.20	2.04	22.97	23.62	0.64	98.9	0.8873	-0.2177	-0.1873	-0.1744	-0.1532	-0.1130	-0.0940	-0.0852	-0.0621	-0.0286	-0.0358
5. 94.	0.40	3.68	19.87	22.25	2.28	99.8	0.9198	-0.2644	-0.2132	-0.2002	-0.1749	-0.1453	-0.1101	-0.0966	-0.0791	-0.0645	-0.0583
5. 85.	0.60	4.69	16.36	20.87	4.12	100.7	0.9915	-0.2951	-0.2281	-0.2116	-0.1847	-0.1528	-0.1104	-0.0947	-0.0761	-0.0625	-0.0552
5. 76.	0.80	3.80	9.30	14.17	4.16	99.8	1.1273	-0.3557	-0.2779	-0.2553	-0.2230	-0.1816	-0.1257	-0.1001	-0.0768	-0.0612	-0.0500
5. 58.	0.90	3.52	7.35	12.46	4.18	101.2	1.2029	-0.4175	-0.3783	-0.3780	-0.3698	-0.1651	-0.0957	-0.0701	-0.0477	-0.0337	-0.0229
5. 67.	0.95	3.41	6.61	11.83	4.19	100.7	1.2407	-0.3112	-0.2903	-0.3051	-0.3425	-0.3599	-0.3654	-0.3504	-0.0207	0.0487	0.0552
Run Point	CP12	CP13	CP14	CP15	CP16	CP17	CP18	CP19	CP20	CP21	CP22	CP23	CP24	CP25	CP26	CP27	CP28
5. 105.	-0.0463	-0.0325	-0.0252	-0.0209	-0.0234	-0.0331	-0.0191	-0.0081	-0.0164	-0.0072	0.0015	-0.0227	-0.0598	-0.0097	-0.0217	0.0281	0.0676
5. 94.	-0.0560	-0.0492	-0.0396	-0.0339	-0.0339	-0.0332	-0.0293	-0.0276	-0.0305	-0.0320	-0.0336	-0.0468	-0.0725	-0.0361	-0.0385	0.0076	0.0639
5. 85.	-0.0506	-0.0443	-0.0350	-0.0283	-0.0277	-0.0258	-0.0225	-0.0226	-0.0252	-0.0279	-0.0313	-0.0427	-0.0661	-0.0333	-0.0385	0.0108	0.0760
5. 76.	-0.0437	-0.0375	-0.0275	-0.0218	-0.0192	-0.0174	-0.0162	-0.0159	-0.0170	-0.0204	-0.0236	-0.0332	-0.0535	-0.0303	-0.0406	-0.0024	0.0794
5. 58.	-0.0166	-0.0112	-0.0022	0.0028	0.0052	0.0061	0.0073	0.0062	0.0041	0.0012	-0.0017	-0.0103	-0.0266	-0.0101	-0.0194	0.0139	0.0958
5. 67.	0.0479	0.0409	0.0351	0.0323	0.0291	0.0266	0.0241	0.0214	0.0165	0.0121	0.0069	-0.0038	-0.0216	-0.0070	-0.0169	0.0158	0.0990
Run Point	CP29	CP30	CP31	CP32	CP33	CP34	CP35	CP36	CP37	CP38	CP39	CP40	CP41	CP42	CP43	CP44	CP45
5. 105.	0.0690	-0.0895	-0.0737	-0.0468	-0.0541	-0.0234	-0.0173	-0.0356	-0.0283	-0.0159	-0.0194	-0.0468	-0.0248	-0.0203	-0.0096	-0.0146	-0.0210
5. 94.	0.0604	-0.1191	-0.1148	-0.0887	-0.0741	-0.0575	-0.0485	-0.0481	-0.0448	-0.0412	-0.0417	-0.0565	-0.0455	-0.0435	-0.0438	-0.0405	-0.0429
5. 85.	0.0793	-0.1441	-0.1371	-0.1064	-0.0846	-0.0685	-0.0601	-0.0564	-0.0541	-0.0499	-0.0532	-0.0701	-0.0609	-0.0577	-0.0572	-0.0597	-0.0633
5. 76.	0.0992	-0.2003	-0.1853	-0.1444	-0.1165	-0.1013	-0.0934	-0.0922	-0.0953	-0.1006	-0.1108	-0.1207	-0.1238	-0.1330	-0.1445	-0.1587	-0.1793
5. 58.	0.1320	-0.1708	-0.1396	-0.0930	-0.0618	-0.0429	-0.0312	-0.0251	-0.0248	-0.0275	-0.0348	-0.0445	-0.0454	-0.0527	-0.0641	-0.0795	-0.0993
5. 67.	0.1436	-0.1558	-0.1311	-0.0615	-0.0277	-0.0064	0.0069	0.0143	0.0171	0.0159	0.0117	0.0019	0.0034	-0.0016	-0.0110	-0.0239	-0.0411
Run Point	CP46	CP47	CP48	CP49	CP50	CP51	CP52	CP53	CP54	CP55	CP56	CP57	CP58	CP59	CP60	CP61	CP62
5. 105.	-0.0059	0.0348	0.0652	-0.0510	-0.0100	-0.1117	-0.0882	-0.1177	-0.1124	-0.1307	-0.1164	-0.0862	-0.0582	0.0178	0.0812	0.0817	0.1038
5. 94.	-0.0324	0.0196	0.0608	-0.0805	-0.0403	-0.1143	-0.1142	-0.1308	-0.1172	-0.1327	-0.1411	-0.1233	-0.0907	-0.0333	0.0018	0.0889	0.1131
5. 85.	-0.0508	0.0238	0.0793	-0.0945	-0.0501	-0.1130	-0.1099	-0.1164	-0.1313	-0.1398	-0.1180	-0.0953	-0.0641	-0.0193	0.0219	0.0772	0.1079
5. 76.	-0.0280	0.0119	0.0979	-0.1290	-0.1096	-0.0922	-0.0934	-0.0968	-0.0977	-0.0991	-0.0952	-0.0915	-0.0814	-0.0567	-0.0146	0.0354	0.0747
5. 58.	-0.0089	0.0272	0.1316	-0.0761	-0.0338	-0.0552	-0.0547	-0.0592	-0.0623	-0.0595	-0.0557	-0.0528	-0.0336	-0.0230	0.0035	0.0413	0.0784
5. 67.	-0.0058	0.0300	0.1429	-0.0430	0.0124	-0.0404	-0.0427	-0.0465	-0.0504	-0.0502	-0.0440	-0.0434	-0.0329	-0.0166	0.0109	0.0436	0.0707

Table 7. Continued

(b) Concluded

Run Point	CP63	CP64	CP65	CP66	CP67	CP68	CP77	CP78	CP79	CP80	CP81	CP82	CP83	CP84	CP85	CP86	CP87
5. 105.	0.2098	0.2431	0.2726	0.3193	0.4026	0.4750	-0.0893	-0.1190	0.1422	0.3068	0.3908	-0.1026	-0.1116	-0.0888	-0.1072	-0.1001	-0.1241
5. 94.	0.1736	0.2221	0.2676	0.3248	0.4134	0.4908	-0.1230	-0.1407	0.1193	0.2707	0.4264	-0.1239	-0.1287	-0.1253	-0.1306	-0.1362	-0.1460
5. 85.	0.1814	0.2337	0.2806	0.3431	0.4298	0.4474	-0.1178	-0.1317	0.1130	0.2904	0.4026	-0.1187	-0.1237	-0.1220	-0.1271	-0.1329	-0.1380
5. 76.	0.1467	0.2070	0.2769	0.3412	0.4087	0.4268	-0.0966	-0.1037	0.0785	0.2771	0.4033	-0.0984	-0.1041	-0.1023	-0.1032	-0.1069	-0.1101
5. 58.	0.1456	0.2011	0.2556	0.3091	0.3604	0.3848	-0.0860	-0.0898	0.0789	0.2567	0.3594	-0.0580	-0.0639	-0.0630	-0.0636	-0.0657	-0.0670
5. 67.	0.1348	0.1898	0.2417	0.2891	0.3281	0.3479	-0.0435	-0.0477	0.0766	0.2405	0.3440	-0.0450	-0.0514	-0.0502	-0.0488	-0.0504	-0.0527
Run Point	CP88	CP89	CP90	CP91	CP92	CP93	CP94	CP95	CP96	CP97	CP98	CP99	CP100	CP101	CP102	CP103	CP104
5. 105.	-0.1111	-0.0813	0.0027	0.0744	0.1424	0.1925	0.2319	0.2527	0.2587	0.2675	0.2712	0.2771	0.3071	0.3457	0.3804	0.4232	0.4630
5. 94.	-0.1343	-0.1016	-0.0318	0.0429	0.1106	0.1671	0.2088	0.2372	0.2539	0.2645	0.2760	0.2855	0.3115	0.3441	0.3836	0.4318	0.4804
5. 85.	-0.1277	-0.0958	-0.0376	0.0302	0.1014	0.1564	0.2017	0.2359	0.2575	0.2743	0.2888	0.3020	0.3286	0.3599	0.3961	0.4410	0.4851
5. 76.	-0.1064	-0.0924	-0.0601	-0.0162	0.0321	0.0791	0.1225	0.1648	0.2043	0.2373	0.2681	0.2937	0.3207	0.3488	0.3774	0.4083	0.4382
5. 58.	-0.0647	-0.0542	-0.0319	-0.0016	0.0350	0.0722	0.1056	0.1389	0.1711	0.2029	0.2351	0.2627	0.2902	0.3159	0.3370	0.3614	0.3831
5. 67.	-0.0508	-0.0427	-0.0231	0.0031	0.0358	0.0678	0.0967	0.1244	0.1550	0.1829	0.2116	0.2353	0.2611	0.2849	0.3052	0.3264	0.3443
Run Point	CP105	CP106															
5. 105.	0.5290	0.4681															
5. 94.	0.5268	0.4964															
5. 85.	0.5302	0.4983															
5. 76.	0.4709	0.4417															
5. 58.	0.4066	0.3763															
5. 67.	0.3617	0.3315															

Table 7. Continued

(c) $Z_s = 2.36$ in.

Run Point	M_∞	$R_\infty \times 10^{-6}$	p_∞ , psi	$p_{t,\infty}$, psi	q_∞ , psi	$T_{t,\infty}$, °F	CP01	CP02	CP03	CP04	CP05	CP06	CP07	CP08	CP09	CP10	CP11
5. 110.	0.20	2.03	22.96	23.60	0.64	99.1	0.8911	-0.2153	-0.1869	-0.1717	-0.1528	-0.1113	-0.0944	-0.0845	-0.0624	-0.0253	-0.0326
5. 101.	0.40	3.64	19.88	22.21	2.24	99.7	0.9108	-0.2536	-0.2037	-0.1913	-0.1663	-0.1375	-0.1031	-0.0911	-0.0732	-0.0580	-0.0537
5. 90.	0.60	4.70	16.33	20.85	4.13	100.6	0.9952	-0.2980	-0.2291	-0.2136	-0.1857	-0.1543	-0.1114	-0.0964	-0.0772	-0.0640	-0.0563
5. 81.	0.80	3.80	9.30	14.17	4.16	100.1	1.1277	-0.3575	-0.2780	-0.2547	-0.2231	-0.1815	-0.1256	-0.0998	-0.0764	-0.0605	-0.0495
5. 63.	0.90	3.52	7.37	12.47	4.19	100.6	1.2043	-0.4174	-0.3766	-0.3766	-0.3655	-0.1623	-0.0957	-0.0702	-0.0473	-0.0326	-0.0216
5. 72.	0.95	3.41	6.61	11.82	4.18	100.0	1.2408	-0.3120	-0.2914	-0.3057	-0.3428	-0.3603	-0.3658	-0.3467	-0.0147	0.0479	0.0540
Run Point	CP12	CP13	CP14	CP15	CP16	CP17	CP18	CP19	CP20	CP21	CP22	CP23	CP24	CP25	CP26	CP27	CP28
5. 110.	-0.0454	-0.0282	-0.0242	-0.0187	-0.0203	-0.0287	-0.0181	-0.0047	-0.0119	-0.0027	0.0095	-0.0160	-0.0511	-0.0064	-0.0207	0.0293	0.0556
5. 101.	-0.0511	-0.0446	-0.0363	-0.0299	-0.0276	-0.0276	-0.0238	-0.0208	-0.0236	-0.0232	-0.0231	-0.0353	-0.0578	-0.0275	-0.0324	0.0094	0.0661
5. 90.	-0.0516	-0.0462	-0.0366	-0.0315	-0.0279	-0.0264	-0.0233	-0.0213	-0.0232	-0.0245	-0.0260	-0.0352	-0.0582	-0.0310	-0.0379	0.0044	0.0735
5. 81.	-0.0435	-0.0373	-0.0273	-0.0208	-0.0176	-0.0157	-0.0138	-0.0135	-0.0146	-0.0161	-0.0187	-0.0271	-0.0439	-0.0257	-0.0373	-0.0092	0.0692
5. 63.	-0.0156	-0.0108	-0.0010	0.0040	0.0070	0.0087	0.0096	0.0094	0.0073	0.0051	0.0028	-0.0035	-0.0183	-0.0048	-0.0150	0.0084	0.0866
5. 72.	0.0461	0.0394	0.0347	0.0324	0.0295	0.0279	0.0255	0.0223	0.0178	0.0129	0.0091	0.0015	-0.0130	-0.0019	-0.0119	0.0113	0.0902
Run Point	CP29	CP30	CP31	CP32	CP33	CP34	CP35	CP36	CP37	CP38	CP39	CP40	CP41	CP42	CP43	CP44	CP45
5. 110.	0.0671	-0.0876	-0.0708	-0.0470	-0.0521	-0.0235	-0.0129	-0.0336	-0.0273	-0.0136	-0.0216	-0.0536	-0.0303	-0.0182	-0.0075	-0.0124	-0.0232
5. 101.	0.0632	-0.1027	-0.0978	-0.0757	-0.0643	-0.0487	-0.0419	-0.0429	-0.0395	-0.0346	-0.0342	-0.0533	-0.0428	-0.0383	-0.0355	-0.0331	-0.0335
5. 90.	0.0767	-0.1394	-0.1317	-0.1020	-0.0823	-0.0679	-0.0596	-0.0570	-0.0549	-0.0521	-0.0537	-0.0693	-0.0634	-0.0608	-0.0588	-0.0604	-0.0624
5. 81.	0.0905	-0.1860	-0.1716	-0.1365	-0.1121	-0.0974	-0.0901	-0.0892	-0.0924	-0.0977	-0.1091	-0.1162	-0.1196	-0.1315	-0.1446	-0.1618	-0.1825
5. 63.	0.1249	-0.1564	-0.1297	-0.0881	-0.0590	-0.0397	-0.0284	-0.0224	-0.0222	-0.0252	-0.0329	-0.0408	-0.0426	-0.0502	-0.0624	-0.0779	-0.0975
5. 72.	0.1362	-0.1488	-0.1115	-0.0603	-0.0292	-0.0079	0.0063	0.0138	0.0168	0.0157	0.0110	0.0021	0.0026	-0.0025	-0.0123	-0.0258	-0.0424
Run Point	CP46	CP47	CP48	CP49	CP50	CP51	CP52	CP53	CP54	CP55	CP56	CP57	CP58	CP59	CP60	CP61	CP62
5. 110.	-0.0026	0.0303	0.0621	-0.0479	-0.0100	-0.1133	-0.0875	-0.1280	-0.1263	-0.1280	-0.0999	-0.0976	-0.0683	-0.0227	0.0550	0.0853	0.1160
5. 101.	-0.0242	0.0197	0.0627	-0.0702	-0.0332	-0.1056	-0.1015	-0.1125	-0.1175	-0.1246	-0.1110	-0.1106	-0.0667	-0.0433	0.0101	0.0711	0.0760
5. 90.	-0.0279	0.0178	0.0748	-0.0936	-0.0516	-0.1097	-0.1105	-0.1133	-0.1234	-0.1260	-0.1231	-0.1109	-0.0821	-0.0729	-0.0060	0.0428	0.1109
5. 81.	-0.0235	0.0031	0.0885	-0.1248	-0.1072	-0.0837	-0.0859	-0.0862	-0.0885	-0.0901	-0.0869	-0.0936	-0.0787	-0.0604	-0.0235	0.0197	0.0610
5. 63.	-0.0029	0.0189	0.1241	-0.0742	-0.0315	-0.0398	-0.0412	-0.0438	-0.0446	-0.0476	-0.0474	-0.0547	-0.0434	-0.0290	-0.0081	0.0277	0.0666
5. 72.	-0.0004	0.0220	0.1366	-0.0436	0.0114	-0.0254	-0.0267	-0.0294	-0.0330	-0.0366	-0.0338	-0.0345	-0.0376	-0.0208	0.0041	0.0288	0.0599

Table 7. Concluded

(c) Concluded

Run	Point	CP63	CP64	CP65	CP66	CP67	CP68	CP77	CP78	CP79	CP80	CP81	CP82	CP83	CP84	CP85	CP86	CP87	
5.	110.	0.1838	0.2540	0.2834	0.3228	0.3896	0.4793	-0.0850	-0.1281	0.1239	0.3167	0.4158	-0.0986	-0.1065	-0.0837	-0.1021	-0.0959	-0.1278	
5.	101.	0.1532	0.2224	0.2751	0.3309	0.4019	0.4605	-0.1065	-0.1329	0.1050	0.2866	0.4289	-0.1091	-0.1136	-0.1099	-0.1186	-0.1227	-0.1370	
5.	90.	0.1796	0.2397	0.2874	0.3434	0.4201	0.4739	-0.1099	-0.1334	0.1094	0.2916	0.4447	-0.1099	-0.1142	-0.1141	-0.1192	-0.1265	-0.1365	
5.	81.	0.1356	0.1991	0.2558	0.3174	0.3721	0.3971	-0.0824	-0.0968	0.0629	0.2548	0.3869	-0.0839	-0.0883	-0.0874	-0.0902	-0.0955	-0.1020	
5.	63.	0.1303	0.1907	0.2449	0.2978	0.3383	0.3603	-0.0417	-0.0519	0.0630	0.2476	0.3600	-0.0428	-0.0470	-0.0465	-0.0485	-0.0523	-0.0567	
5.	72.	0.1195	0.1752	0.2312	0.2789	0.3166	0.3294	-0.0297	-0.0394	0.0613	0.2351	0.3335	-0.0293	-0.0339	-0.0337	-0.0345	-0.0387	-0.0424	
Run	Point	CP88	CP89	CP90	CP91	CP92	CP93	CP94	CP95	CP96	CP97	CP98	CP99	CP100	CP101	CP102	CP103	CP104	
5.	110.	-0.1204	-0.0947	-0.0092	0.0634	0.1334	0.1846	0.2243	0.2505	0.2587	0.2665	0.2690	0.2738	0.3062	0.3449	0.3777	0.4152	0.4395	
5.	101.	-0.1353	-0.1104	-0.0489	0.0270	0.1041	0.1606	0.2037	0.2343	0.2511	0.2637	0.2771	0.2891	0.3136	0.3423	0.3750	0.4130	0.4486	
5.	90.	-0.1353	-0.1160	-0.0605	0.0072	0.0767	0.1387	0.1868	0.2264	0.2543	0.2750	0.2911	0.3057	0.3292	0.3578	0.3888	0.4251	0.4556	
5.	81.	-0.1041	-0.0975	-0.0724	-0.0337	0.0135	0.0587	0.1017	0.1400	0.1770	0.2120	0.2440	0.2687	0.2971	0.3237	0.3488	0.3727	0.3939	
5.	63.	-0.0591	-0.0557	-0.0398	-0.0147	0.0199	0.0560	0.0896	0.1218	0.1515	0.1826	0.2142	0.2412	0.2692	0.2946	0.3175	0.3387	0.3559	
5.	72.	-0.0440	-0.0430	-0.0306	-0.0074	0.0229	0.0558	0.0828	0.1093	0.1381	0.1641	0.1931	0.2182	0.2441	0.2672	0.2884	0.3080	0.3247	
Run	Point	CP105	CP106																
5.	110.	0.4803	0.4555																
5.	101.	0.4791	0.4484																
5.	90.	0.4854	0.4615																
5.	81.	0.4131	0.3833																
5.	63.	0.3661	0.3368																
5.	72.	0.3269	0.3084																

Table 8. Pressure Coefficients for Configuration 8 With $h = 2.40$ in., $l = 26.00$ in., and $Y_s = 2.40$ in.(a) $Z_s = -0.90$ in.

Run Point	M_∞	$R_\infty \times 10^{-6}$	p_∞ , psi	$p_{t,\infty}$, psi	q_∞ , psi	$T_{t,\infty}$, °F	CP01	CP02	CP03	CP04	CP05	CP06	CP07	CP08	CP09	CP10	CP11
9. 347.	0.20	2.05	22.97	23.63	0.65	99.7	0.8694	-0.2418	-0.2100	-0.1946	-0.1808	-0.1388	-0.1196	-0.1105	-0.0885	-0.0489	-0.0596
9. 338.	0.40	3.63	19.92	22.24	2.22	100.2	0.9075	-0.2526	-0.2010	-0.1879	-0.1642	-0.1343	-0.1011	-0.0892	-0.0711	-0.0535	-0.0498
9. 329.	0.60	4.67	16.33	20.84	4.12	102.6	0.9917	-0.2941	-0.2291	-0.2134	-0.1874	-0.1551	-0.1127	-0.0971	-0.0777	-0.0616	-0.0567
9. 320.	0.80	3.81	9.31	14.18	4.16	99.1	1.1260	-0.3243	-0.2795	-0.2548	-0.2246	-0.1830	-0.1274	-0.1018	-0.0782	-0.0619	-0.0516
9. 311.	0.90	3.53	7.35	12.46	4.19	99.9	1.2030	-0.3606	-0.3454	-0.3695	-0.3460	-0.2010	-0.0983	-0.0677	-0.0461	-0.0309	-0.0213
9. 302.	0.95	3.39	6.61	11.83	4.18	101.8	1.2384	-0.2566	-0.2830	-0.3141	-0.3258	-0.3588	-0.3652	-0.3564	-0.0223	0.0476	0.0528
Run Point	CP12	CP13	CP14	CP15	CP16	CP17	CP18	CP19	CP20	CP21	CP22	CP23	CP24	CP25	CP26	CP27	CP28
9. 347.	-0.0693	-0.0527	-0.0466	-0.0479	-0.0463	-0.0581	-0.0403	-0.0318	-0.0417	-0.0222	-0.0120	-0.0391	-0.0730	-0.0225	-0.0464	0.0071	0.0377
9. 338.	-0.0480	-0.0410	-0.0332	-0.0290	-0.0265	-0.0271	-0.0230	-0.0204	-0.0245	-0.0226	-0.0233	-0.0355	-0.0605	-0.0244	-0.0300	0.0118	0.0663
9. 329.	-0.0522	-0.0461	-0.0379	-0.0334	-0.0312	-0.0299	-0.0267	-0.0244	-0.0274	-0.0264	-0.0282	-0.0391	-0.0615	-0.0314	-0.0388	0.0022	0.0696
9. 320.	-0.0448	-0.0393	-0.0283	-0.0228	-0.0197	-0.0176	-0.0155	-0.0156	-0.0172	-0.0185	-0.0210	-0.0292	-0.0460	-0.0274	-0.0361	-0.0137	0.0593
9. 311.	-0.0153	-0.0112	-0.0019	0.0024	0.0047	0.0056	0.0069	0.0069	0.0047	0.0031	0.0007	-0.0056	-0.0191	-0.0063	-0.0117	0.0022	0.0683
9. 302.	0.0460	0.0390	0.0333	0.0292	0.0283	0.0262	0.0237	0.0197	0.0155	0.0120	0.0075	0.0001	-0.0145	-0.0036	-0.0090	0.0044	0.0669
Run Point	CP29	CP30	CP31	CP32	CP33	CP34	CP35	CP36	CP37	CP38	CP39	CP40	CP41	CP42	CP43	CP44	CP45
9. 347.	0.0436	-0.1031	-0.0956	-0.0679	-0.0717	-0.0492	-0.0380	-0.0508	-0.0440	-0.0368	-0.0437	-0.0616	-0.0491	-0.0438	-0.0369	-0.0263	-0.0383
9. 338.	0.0673	-0.1003	-0.0961	-0.0722	-0.0605	-0.0461	-0.0371	-0.0368	-0.0335	-0.0302	-0.0331	-0.0399	-0.0320	-0.0292	-0.0284	-0.0279	-0.0339
9. 329.	0.0787	-0.1379	-0.1316	-0.1012	-0.0810	-0.0649	-0.0564	-0.0529	-0.0513	-0.0483	-0.0526	-0.0637	-0.0565	-0.0564	-0.0531	-0.0555	-0.0599
9. 320.	0.0874	-0.1757	-0.1617	-0.1278	-0.1059	-0.0932	-0.0865	-0.0854	-0.0882	-0.0963	-0.1083	-0.1139	-0.1177	-0.1286	-0.1465	-0.1628	-0.1813
9. 311.	0.1158	-0.1378	-0.1119	-0.0719	-0.0477	-0.0324	-0.0229	-0.0187	-0.0184	-0.0229	-0.0308	-0.0403	-0.0403	-0.0484	-0.0601	-0.0754	-0.0949
9. 302.	0.1258	-0.1253	-0.0962	-0.0444	-0.0162	0.0007	0.0116	0.0183	0.0207	0.0181	0.0124	0.0017	0.0038	-0.0018	-0.0094	-0.0225	-0.0394
Run Point	CP46	CP47	CP48	CP49	CP50	CP51	CP52	CP53	CP54	CP55	CP56	CP57	CP58	CP59	CP60	CP61	CP62
9. 347.	-0.0234	0.0054	0.0377	-0.0771	-0.0315	-0.1317	-0.1054	-0.1451	-0.1402	-0.1375	-0.1179	-0.1274	-0.1189	-0.0654	0.0178	0.0404	0.0542
9. 338.	-0.0220	0.0214	0.0638	-0.0748	-0.0294	-0.1048	-0.0984	-0.1089	-0.1140	-0.1037	-0.1068	-0.1190	-0.1053	-0.0353	0.0379	0.0551	0.1034
9. 329.	-0.0286	0.0143	0.0740	-0.0987	-0.0477	-0.1039	-0.1029	-0.1093	-0.1117	-0.1163	-0.1079	-0.1056	-0.1136	-0.0734	-0.0307	0.0484	0.0901
9. 320.	-0.0247	-0.0042	0.0833	-0.1226	-0.1063	-0.0692	-0.0755	-0.0782	-0.0756	-0.0766	-0.0745	-0.0761	-0.0736	-0.0690	-0.0421	-0.0167	0.0193
9. 311.	-0.0040	0.0091	0.1112	-0.0624	-0.0312	-0.0282	-0.0310	-0.0345	-0.0351	-0.0354	-0.0335	-0.0355	-0.0326	-0.0335	-0.0169	-0.0001	0.0252
9. 302.	-0.0023	0.0105	0.1211	-0.0306	0.0126	-0.0147	-0.0195	-0.0193	-0.0161	-0.0191	-0.0216	-0.0272	-0.0267	-0.0230	-0.0146	0.0006	0.0216

Table 8. Continued

(a) Concluded

Run Point	CP63	CP64	CP65	CP66	CP67	CP68	CP77	CP78	CP79	CP80	CP81	CP82	CP83	CP84	CP85	CP86	CP87
9. 347.	0.1664	0.2267	0.2532	0.3158	0.3639	0.4467	-0.0993	-0.1368	0.1120	0.2760	0.4243	-0.1149	-0.1180	-0.1049	-0.1242	-0.1119	-0.1428
9. 338.	0.1566	0.2188	0.2744	0.3339	0.4060	0.4633	-0.0982	-0.1150	0.1153	0.2714	0.4449	-0.1009	-0.1065	-0.1049	-0.1103	-0.1130	-0.1285
9. 329.	0.1557	0.2137	0.2694	0.3448	0.4218	0.4848	-0.1006	-0.1202	0.0933	0.2799	0.4372	-0.1047	-0.1086	-0.1086	-0.1139	-0.1154	-0.1259
9. 320.	0.0928	0.1756	0.2365	0.3077	0.3605	0.3890	-0.0713	-0.0842	0.0341	0.2375	0.3884	-0.0747	-0.0796	-0.0809	-0.0791	-0.0820	-0.0868
9. 311.	0.0854	0.1493	0.2093	0.2606	0.3021	0.3232	-0.0276	-0.0373	0.0301	0.2076	0.3288	-0.0321	-0.0362	-0.0371	-0.0359	-0.0376	-0.0412
9. 302.	0.0695	0.1270	0.1812	0.2377	0.2671	0.2812	-0.0166	-0.0255	0.0246	0.1786	0.2994	-0.0204	-0.0243	-0.0256	-0.0252	-0.0254	-0.0288
Run Point	CP88	CP89	CP90	CP91	CP92	CP93	CP94	CP95	CP96	CP97	CP98	CP99	CP100	CP101	CP102	CP103	CP104
9. 347.	-0.1375	-0.1274	-0.0631	0.0027	0.0865	0.1488	0.2086	0.2306	0.2404	0.2547	0.2475	0.2583	0.2886	0.3284	0.3617	0.4092	0.4379
9. 338.	-0.1286	-0.1151	-0.0657	-0.0031	0.0725	0.1425	0.1975	0.2334	0.2564	0.2676	0.2784	0.2886	0.3121	0.3446	0.3812	0.4251	0.4645
9. 329.	-0.1262	-0.1131	-0.0788	-0.0287	0.0377	0.1047	0.1646	0.2125	0.2439	0.2657	0.2833	0.2997	0.3254	0.3574	0.3929	0.4372	0.4737
9. 320.	-0.0884	-0.0875	-0.0771	-0.0566	-0.0242	0.0139	0.0561	0.0994	0.1431	0.1817	0.2208	0.2503	0.2788	0.3088	0.3346	0.3592	0.3819
9. 311.	-0.0426	-0.0443	-0.0392	-0.0283	-0.0092	0.0162	0.0438	0.0732	0.1077	0.1385	0.1719	0.2005	0.2303	0.2569	0.2781	0.3021	0.3215
9. 302.	-0.0311	-0.0330	-0.0293	-0.0200	-0.0030	0.0152	0.0369	0.0623	0.0900	0.1166	0.1448	0.1731	0.2003	0.2268	0.2498	0.2722	0.2908
Run Point	CP105	CP106															
9. 347.	0.4828	0.4638															
9. 338.	0.4944	0.4643															
9. 329.	0.5001	0.4686															
9. 320.	0.3962	0.3632															
9. 311.	0.3280	0.3183															
9. 302.	0.2877	0.2922															

Table 8. Continued
 (b) $Z_s = 0.00$ in.

Run Point	M_∞	$R_\infty \times 10^{-6}$	P_∞ , psi	$P_{t,\infty}$, psi	q_∞ , psi	$T_{t,\infty}$, °F	CP01	CP02	CP03	CP04	CP05	CP06	CP07	CP08	CP09	CP10	CP11
9. 349.	0.20	2.05	22.98	23.64	0.65	100.1	0.8755	-0.2356	-0.2050	-0.1882	-0.1748	-0.1313	-0.1142	-0.1041	-0.0820	-0.0411	-0.0519
9. 340.	0.40	3.62	19.92	22.22	2.22	100.7	0.9079	-0.2602	-0.2080	-0.1944	-0.1716	-0.1412	-0.1080	-0.0955	-0.0772	-0.0600	-0.0562
9. 331.	0.60	4.67	16.32	20.81	4.11	102.2	0.9906	-0.2947	-0.2304	-0.2143	-0.1883	-0.1564	-0.1135	-0.0988	-0.0791	-0.0634	-0.0579
9. 322.	0.80	3.80	9.31	14.18	4.16	100.8	1.1251	-0.3235	-0.2786	-0.2544	-0.2234	-0.1820	-0.1265	-0.1013	-0.0776	-0.0614	-0.0509
9. 313.	0.90	3.53	7.36	12.47	4.18	100.0	1.2016	-0.3622	-0.3452	-0.3691	-0.3459	-0.1904	-0.0959	-0.0703	-0.0479	-0.0321	-0.0230
9. 304.	0.95	3.39	6.61	11.82	4.18	101.9	1.2381	-0.2577	-0.2834	-0.3145	-0.3261	-0.3589	-0.3658	-0.3553	-0.0191	0.0473	0.0520
Run Point	CP12	CP13	CP14	CP15	CP16	CP17	CP18	CP19	CP20	CP21	CP22	CP23	CP24	CP25	CP26	CP27	CP28
9. 349.	-0.0628	-0.0464	-0.0411	-0.0402	-0.0400	-0.0537	-0.0360	-0.0251	-0.0363	-0.0178	-0.0065	-0.0347	-0.0710	-0.0171	-0.0399	0.0169	0.0444
9. 340.	-0.0543	-0.0474	-0.0394	-0.0346	-0.0319	-0.0327	-0.0271	-0.0240	-0.0281	-0.0255	-0.0273	-0.0408	-0.0664	-0.0296	-0.0361	0.0100	0.0640
9. 331.	-0.0532	-0.0471	-0.0387	-0.0341	-0.0311	-0.0301	-0.0259	-0.0246	-0.0284	-0.0280	-0.0309	-0.0427	-0.0689	-0.0328	-0.0407	0.0064	0.0719
9. 322.	-0.0446	-0.0391	-0.0283	-0.0233	-0.0191	-0.0178	-0.0159	-0.0147	-0.0171	-0.0193	-0.0238	-0.0327	-0.0552	-0.0296	-0.0410	-0.0051	0.0805
9. 313.	-0.0171	-0.0126	-0.0033	0.0013	0.0039	0.0052	0.0059	0.0055	0.0028	0.0007	-0.0026	-0.0108	-0.0297	-0.0111	-0.0208	0.0114	0.0971
9. 304.	0.0457	0.0385	0.0330	0.0293	0.0272	0.0250	0.0225	0.0192	0.0138	0.0097	0.0047	-0.0028	-0.0195	-0.0068	-0.0155	0.0127	0.0940
Run Point	CP29	CP30	CP31	CP32	CP33	CP34	CP35	CP36	CP37	CP38	CP39	CP40	CP41	CP42	CP43	CP44	CP45
9. 349.	0.0503	-0.1033	-0.0969	-0.0703	-0.0751	-0.0482	-0.0380	-0.0487	-0.0408	-0.0324	-0.0405	-0.0628	-0.0418	-0.0365	-0.0433	-0.0438	-0.0499
9. 340.	0.0637	-0.1101	-0.1081	-0.0844	-0.0714	-0.0560	-0.0453	-0.0429	-0.0396	-0.0366	-0.0399	-0.0499	-0.0442	-0.0454	-0.0344	-0.0331	-0.0420
9. 331.	0.0775	-0.1458	-0.1430	-0.1134	-0.0911	-0.0729	-0.0626	-0.0578	-0.0547	-0.0517	-0.0563	-0.0659	-0.0589	-0.0594	-0.0617	-0.0638	-0.0660
9. 322.	0.1020	-0.2002	-0.1887	-0.1495	-0.1216	-0.1035	-0.0932	-0.0899	-0.0918	-0.0977	-0.1079	-0.1129	-0.1156	-0.1262	-0.1390	-0.1561	-0.1753
9. 313.	0.1366	-0.1753	-0.1469	-0.0971	-0.0654	-0.0450	-0.0314	-0.0247	-0.0226	-0.0255	-0.0326	-0.0423	-0.0422	-0.0506	-0.0608	-0.0769	-0.0965
9. 304.	0.1443	-0.1562	-0.1333	-0.0631	-0.0291	-0.0088	0.0048	0.0130	0.0162	0.0146	0.0094	0.0002	0.0023	-0.0029	-0.0113	-0.0246	-0.0411
Run Point	CP46	CP47	CP48	CP49	CP50	CP51	CP52	CP53	CP54	CP55	CP56	CP57	CP58	CP59	CP60	CP61	CP62
9. 349.	-0.0179	0.0155	0.0411	-0.0804	-0.0282	-0.1286	-0.0983	-0.1389	-0.1503	-0.1388	-0.0993	-0.0758	-0.1202	-0.0303	0.0483	0.0565	0.1090
9. 340.	-0.0269	0.0211	0.0589	-0.0827	-0.0350	-0.1172	-0.1106	-0.1196	-0.1250	-0.1164	-0.0881	-0.1190	-0.1176	-0.0485	0.0454	0.0625	0.1106
9. 331.	-0.0325	0.0182	0.0721	-0.1073	-0.0510	-0.1138	-0.1116	-0.1225	-0.1286	-0.1375	-0.1245	-0.1337	-0.1072	-0.0473	0.0110	0.0735	0.1042
9. 322.	-0.0283	0.0121	0.0969	-0.1404	-0.1062	-0.0956	-0.0946	-0.0965	-0.0992	-0.1046	-0.1025	-0.0954	-0.0872	-0.0623	-0.0250	0.0230	0.0639
9. 313.	-0.0095	0.0279	0.1302	-0.0844	-0.0320	-0.0526	-0.0547	-0.0520	-0.0517	-0.0535	-0.0496	-0.0546	-0.0442	-0.0250	-0.0061	0.0274	0.0719
9. 304.	-0.0054	0.0296	0.1356	-0.0480	0.0102	-0.0361	-0.0367	-0.0377	-0.0372	-0.0413	-0.0394	-0.0444	-0.0384	-0.0180	0.0002	0.0269	0.0540

Table 8. Continued

(b) Concluded

Run	Point	CP63	CP64	CP65	CP66	CP67	CP68	CP77	CP78	CP79	CP80	CP81	CP82	CP83	CP84	CP85	CP86	CP87	
9.	349.	0.1855	0.2390	0.2537	0.3281	0.3857	0.4774	-0.1041	-0.1360	0.1341	0.2840	0.4345	-0.1205	-0.1259	-0.1137	-0.1364	-0.1234	-0.1504	
9.	340.	0.1653	0.2136	0.2766	0.3409	0.4104	0.4759	-0.1155	-0.1352	0.1299	0.2692	0.4358	-0.1155	-0.1204	-0.1201	-0.1273	-0.1310	-0.1409	
9.	331.	0.1650	0.2207	0.2809	0.3531	0.4335	0.4742	-0.1183	-0.1337	0.1130	0.2770	0.4563	-0.1171	-0.1229	-0.1236	-0.1298	-0.1327	-0.1399	
9.	322.	0.1412	0.2106	0.2792	0.3531	0.4124	0.4446	-0.0991	-0.1106	0.0808	0.2734	0.4375	-0.0956	-0.1010	-0.1038	-0.1048	-0.1095	-0.1116	
9.	313.	0.1401	0.2014	0.2692	0.3352	0.3765	0.4034	-0.0589	-0.0693	0.0866	0.2619	0.3904	-0.0546	-0.0586	-0.0606	-0.0614	-0.0638	-0.0662	
9.	304.	0.1126	0.1789	0.2338	0.2943	0.3398	0.3526	-0.0432	-0.0535	0.0805	0.2311	0.3557	-0.0404	-0.0427	-0.0459	-0.0479	-0.0494	-0.0510	
Run	Point	CP88	CP89	CP90	CP91	CP92	CP93	CP94	CP95	CP96	CP97	CP98	CP99	CP100	CP101	CP102	CP103	CP104	
9.	349.	-0.1335	-0.1063	-0.0377	0.0404	0.1246	0.1727	0.2216	0.2343	0.2420	0.2521	0.2425	0.2556	0.2892	0.3324	0.3657	0.4176	0.4421	
9.	340.	-0.1315	-0.1054	-0.0500	0.0230	0.0997	0.1626	0.2127	0.2377	0.2542	0.2648	0.2726	0.2855	0.3119	0.3461	0.3854	0.4335	0.4754	
9.	331.	-0.1326	-0.1098	-0.0589	0.0049	0.0756	0.1415	0.1931	0.2310	0.2544	0.2723	0.2849	0.3009	0.3284	0.3622	0.3997	0.4459	0.4874	
9.	322.	-0.1057	-0.0935	-0.0696	-0.0333	0.0117	0.0634	0.1160	0.1635	0.2059	0.2404	0.2728	0.2972	0.3245	0.3526	0.3820	0.4150	0.4436	
9.	313.	-0.0615	-0.0535	-0.0364	-0.0127	0.0185	0.0546	0.0927	0.1308	0.1700	0.2040	0.2387	0.2687	0.2966	0.3232	0.3473	0.3731	0.3949	
9.	304.	-0.0478	-0.0414	-0.0274	-0.0091	0.0159	0.0435	0.0747	0.1062	0.1388	0.1702	0.2003	0.2285	0.2553	0.2814	0.3019	0.3237	0.3424	
Run	Point	CP105	CP106																
9.	349.	0.4807	0.4349																
9.	340.	0.4998	0.4672																
9.	331.	0.5204	0.4772																
9.	322.	0.4708	0.4242																
9.	313.	0.4086	0.3730																
9.	304.	0.3448	0.3268																

Table 8. Continued

(c) $Z_s = 2.37$ in.

Run Point	M_∞	$R_\infty \times 10^{-6}$	p_∞ , psi	$p_{t,\infty}$, psi	q_∞ , psi	$T_{t,\infty}$, °F	CP01	CP02	CP03	CP04	CP05	CP06	CP07	CP08	CP09	CP10	CP11
9. 354.	0.20	2.05	22.97	23.62	0.65	100.4	0.8732	-0.2414	-0.2107	-0.1918	-0.1803	-0.1337	-0.1177	-0.1042	-0.0843	-0.0423	-0.0553
9. 345.	0.40	3.63	19.90	22.22	2.23	100.1	0.9048	-0.2589	-0.2076	-0.1937	-0.1710	-0.1415	-0.1081	-0.0970	-0.0791	-0.0607	-0.0575
9. 336.	0.60	4.66	16.31	20.80	4.10	102.2	0.9917	-0.2926	-0.2286	-0.2130	-0.1865	-0.1546	-0.1121	-0.0985	-0.0787	-0.0631	-0.0574
9. 327.	0.80	3.80	9.31	14.19	4.17	100.9	1.1262	-0.3228	-0.2779	-0.2541	-0.2232	-0.1820	-0.1264	-0.1014	-0.0774	-0.0607	-0.0505
9. 318.	0.90	3.52	7.36	12.46	4.18	100.2	1.2027	-0.3613	-0.3439	-0.3681	-0.3445	-0.1825	-0.0947	-0.0691	-0.0465	-0.0309	-0.0213
9. 309.	0.95	3.39	6.61	11.82	4.18	101.5	1.2386	-0.2572	-0.2829	-0.3142	-0.3258	-0.3583	-0.3654	-0.3537	-0.0164	0.0482	0.0526
Run Point	CP12	CP13	CP14	CP15	CP16	CP17	CP18	CP19	CP20	CP21	CP22	CP23	CP24	CP25	CP26	CP27	CP28
9. 354.	-0.0651	-0.0475	-0.0434	-0.0425	-0.0390	-0.0527	-0.0350	-0.0229	-0.0342	-0.0145	-0.0020	-0.0315	-0.0634	-0.0160	-0.0410	0.0148	0.0444
9. 345.	-0.0557	-0.0479	-0.0393	-0.0345	-0.0305	-0.0316	-0.0261	-0.0236	-0.0276	-0.0242	-0.0256	-0.0380	-0.0616	-0.0288	-0.0366	0.0080	0.0611
9. 336.	-0.0531	-0.0466	-0.0375	-0.0319	-0.0286	-0.0278	-0.0241	-0.0238	-0.0267	-0.0262	-0.0270	-0.0354	-0.0581	-0.0306	-0.0391	0.0040	0.0715
9. 327.	-0.0441	-0.0387	-0.0283	-0.0231	-0.0202	-0.0186	-0.0164	-0.0151	-0.0164	-0.0159	-0.0180	-0.0261	-0.0465	-0.0263	-0.0388	-0.0088	0.0707
9. 318.	-0.0158	-0.0116	-0.0021	0.0024	0.0046	0.0061	0.0076	0.0074	0.0057	0.0043	0.0028	-0.0034	-0.0169	-0.0052	-0.0145	0.0082	0.0854
9. 309.	0.0456	0.0387	0.0333	0.0301	0.0277	0.0257	0.0241	0.0209	0.0165	0.0121	0.0073	0.0010	-0.0108	-0.0026	-0.0107	0.0103	0.0881
Run Point	CP29	CP30	CP31	CP32	CP33	CP34	CP35	CP36	CP37	CP38	CP39	CP40	CP41	CP42	CP43	CP44	CP45
9. 354.	0.0493	-0.1012	-0.0927	-0.0626	-0.0708	-0.0429	-0.0326	-0.0477	-0.0409	-0.0290	-0.0395	-0.0628	-0.0397	-0.0397	-0.0359	-0.0308	-0.0427
9. 345.	0.0611	-0.1079	-0.1044	-0.0801	-0.0679	-0.0523	-0.0444	-0.0440	-0.0419	-0.0397	-0.0438	-0.0503	-0.0418	-0.0390	-0.0383	-0.0387	-0.0394
9. 336.	0.0769	-0.1412	-0.1364	-0.1052	-0.0845	-0.0686	-0.0594	-0.0553	-0.0536	-0.0519	-0.0560	-0.0666	-0.0591	-0.0574	-0.0601	-0.0643	-0.0661
9. 327.	0.0917	-0.1894	-0.1780	-0.1405	-0.1163	-0.1012	-0.0935	-0.0915	-0.0933	-0.0992	-0.1105	-0.1194	-0.1226	-0.1325	-0.1462	-0.1633	-0.1831
9. 318.	0.1245	-0.1569	-0.1306	-0.0878	-0.0597	-0.0417	-0.0304	-0.0245	-0.0228	-0.0268	-0.0345	-0.0433	-0.0443	-0.0524	-0.0639	-0.0792	-0.0982
9. 309.	0.1355	-0.1488	-0.1181	-0.0606	-0.0298	-0.0098	0.0036	0.0115	0.0147	0.0132	0.0080	-0.0010	-0.0001	-0.0059	-0.0142	-0.0270	-0.0442
Run Point	CP46	CP47	CP48	CP49	CP50	CP51	CP52	CP53	CP54	CP55	CP56	CP57	CP58	CP59	CP60	CP61	CP62
9. 354.	-0.0135	0.0122	0.0378	-0.0697	-0.0249	-0.1310	-0.0953	-0.1391	-0.1417	-0.1578	-0.1256	-0.1072	-0.1053	-0.0110	0.0114	0.0341	0.0807
9. 345.	-0.0255	0.0157	0.0547	-0.0760	-0.0361	-0.1075	-0.1015	-0.1102	-0.1115	-0.1305	-0.1335	-0.1235	-0.1280	-0.0373	-0.0164	0.0506	0.1240
9. 336.	-0.0261	0.0156	0.0711	-0.0966	-0.0516	-0.1197	-0.1167	-0.1187	-0.1198	-0.1353	-0.1265	-0.1126	-0.0709	-0.0472	0.0110	0.0614	0.1126
9. 327.	-0.0226	0.0018	0.0872	-0.1257	-0.1083	-0.0891	-0.0924	-0.0929	-0.0924	-0.0969	-0.0990	-0.1022	-0.0838	-0.0581	-0.0285	0.0151	0.0457
9. 318.	-0.0020	0.0176	0.1209	-0.0710	-0.0338	-0.0385	-0.0385	-0.0396	-0.0411	-0.0454	-0.0459	-0.0440	-0.0426	-0.0305	-0.0087	0.0219	0.0517
9. 309.	0.0001	0.0195	0.1328	-0.0429	0.0086	-0.0307	-0.0325	-0.0320	-0.0324	-0.0342	-0.0352	-0.0392	-0.0353	-0.0124	0.0010	0.0216	0.0468

Table 8. Concluded

(c) Concluded

Run	Point	CP63	CP64	CP65	CP66	CP67	CP68	CP77	CP78	CP79	CP80	CP81	CP82	CP83	CP84	CP85	CP86	CP87	
9.	354.	0.1581	0.2488	0.2729	0.3295	0.3938	0.4977	-0.1008	-0.1330	0.1113	0.2990	0.4485	-0.1195	-0.1228	-0.1106	-0.1322	-0.1202	-0.1516	
9.	345.	0.1669	0.2264	0.2730	0.3243	0.4056	0.4460	-0.1077	-0.1354	0.1010	0.2908	0.4512	-0.1133	-0.1178	-0.1160	-0.1235	-0.1277	-0.1414	
9.	336.	0.1428	0.2115	0.2806	0.3563	0.4243	0.4692	-0.1092	-0.1307	0.1000	0.2917	0.4473	-0.1118	-0.1154	-0.1166	-0.1226	-0.1278	-0.1388	
9.	327.	0.1285	0.1936	0.2584	0.3237	0.3861	0.4157	-0.0842	-0.1021	0.0713	0.2682	0.4052	-0.0847	-0.0900	-0.0914	-0.0924	-0.0962	-0.1020	
9.	318.	0.1190	0.1785	0.2420	0.2962	0.3380	0.3639	-0.0416	-0.0559	0.0740	0.2432	0.3538	-0.0422	-0.0473	-0.0482	-0.0489	-0.0522	-0.0563	
9.	309.	0.1057	0.1640	0.2217	0.2738	0.3128	0.3329	-0.0276	-0.0423	0.0737	0.2232	0.3159	-0.0297	-0.0342	-0.0353	-0.0363	-0.0390	-0.0429	
Run	Point	CP88	CP89	CP90	CP91	CP92	CP93	CP94	CP95	CP96	CP97	CP98	CP99	CP100	CP101	CP102	CP103	CP104	
9.	354.	-0.1379	-0.1074	-0.0399	0.0316	0.1068	0.1632	0.2250	0.2399	0.2507	0.2630	0.2494	0.2602	0.2939	0.3349	0.3629	0.4095	0.4350	
9.	345.	-0.1355	-0.1133	-0.0603	0.0151	0.0929	0.1604	0.2106	0.2373	0.2543	0.2667	0.2743	0.2871	0.3127	0.3451	0.3776	0.4217	0.4576	
9.	336.	-0.1348	-0.1142	-0.0687	-0.0076	0.0639	0.1316	0.1862	0.2254	0.2540	0.2728	0.2867	0.3023	0.3277	0.3579	0.3917	0.4317	0.4674	
9.	327.	-0.1017	-0.0946	-0.0734	-0.0419	0.0020	0.0492	0.0967	0.1418	0.1838	0.2194	0.2500	0.2768	0.3035	0.3303	0.3535	0.3796	0.4006	
9.	318.	-0.0560	-0.0530	-0.0397	-0.0195	0.0096	0.0419	0.0759	0.1105	0.1468	0.1786	0.2113	0.2391	0.2674	0.2927	0.3154	0.3361	0.3543	
9.	309.	-0.0432	-0.0401	-0.0291	-0.0125	0.0121	0.0392	0.0695	0.0996	0.1312	0.1620	0.1927	0.2184	0.2448	0.2690	0.2880	0.3097	0.3239	
Run	Point	CP105	CP106																
9.	354.	0.4832	0.4564																
9.	345.	0.4941	0.4585																
9.	336.	0.5006	0.4734																
9.	327.	0.4211	0.4006																
9.	318.	0.3651	0.3431																
9.	309.	0.3280	0.3135																

Table 9. Pressure Coefficients for Configuration 9 With $h = 2.40$ in., $l = 30.00$ in., and $Y_s = 0.00$ in.(a) $Z_s = -0.90$ in.

Run Point	M_∞	$R_\infty \times 10^{-6}$	P_∞ , psi	$P_{1,\infty}$, psi	q_∞ , psi	$T_{t,\infty}$, °F	CP01	CP02	CP03	CP04	CP05	CP06	CP07	CP08	CP09	CP10	CP11
6. 162.	0.20	2.02	22.98	23.62	0.63	99.7	0.8753	-0.2406	-0.2009	-0.1855	-0.1630	-0.1352	-0.1037	-0.0912	-0.0787	-0.0600	-0.0587
6. 152.	0.40	3.64	19.91	22.25	2.24	101.5	0.9068	-0.2616	-0.2069	-0.1924	-0.1680	-0.1419	-0.1045	-0.0900	-0.0758	-0.0636	-0.0574
6. 143.	0.60	4.69	16.33	20.86	4.14	101.6	0.9881	-0.3041	-0.2322	-0.2150	-0.1868	-0.1583	-0.1138	-0.0984	-0.0812	-0.0693	-0.0615
6. 134.	0.80	3.80	9.31	14.19	4.17	100.2	1.1270	-0.3556	-0.2796	-0.2555	-0.2225	-0.1831	-0.1251	-0.0995	-0.0775	-0.0632	-0.0514
6. 125.	0.90	3.52	7.37	12.46	4.18	99.8	1.2011	-0.4184	-0.3786	-0.3777	-0.3602	-0.1654	-0.0998	-0.0730	-0.0506	-0.0354	-0.0257
6. 116.	0.95	3.39	6.61	11.82	4.18	101.9	1.2372	-0.3092	-0.2926	-0.3039	-0.3455	-0.3614	-0.3675	-0.3535	-0.0262	0.0455	0.0490
Run Point	CP12	CP13	CP14	CP15	CP16	CP17	CP18	CP19	CP20	CP21	CP22	CP23	CP24	CP25	CP26	CP27	CP28
6. 162.	-0.0513	-0.0448	-0.0376	-0.0323	-0.0291	-0.0327	-0.0260	-0.0270	-0.0256	-0.0275	-0.0315	-0.0428	-0.0699	-0.0308	-0.0390	0.0082	0.0515
6. 152.	-0.0510	-0.0459	-0.0384	-0.0337	-0.0297	-0.0283	-0.0259	-0.0281	-0.0287	-0.0311	-0.0370	-0.0479	-0.0747	-0.0350	-0.0406	0.0028	0.0552
6. 143.	-0.0540	-0.0485	-0.0394	-0.0341	-0.0317	-0.0294	-0.0278	-0.0294	-0.0304	-0.0340	-0.0387	-0.0482	-0.0729	-0.0403	-0.0476	-0.0047	0.0590
6. 134.	-0.0433	-0.0388	-0.0280	-0.0220	-0.0192	-0.0168	-0.0168	-0.0178	-0.0188	-0.0238	-0.0304	-0.0393	-0.0640	-0.0372	-0.0512	-0.0184	0.0669
6. 125.	-0.0186	-0.0128	-0.0046	0.0003	0.0034	0.0044	0.0050	0.0036	0.0007	-0.0022	-0.0074	-0.0168	-0.0393	-0.0173	-0.0332	-0.0074	0.0799
6. 116.	0.0432	0.0389	0.0309	0.0272	0.0258	0.0225	0.0199	0.0155	0.0088	0.0061	0.0000	-0.0106	-0.0303	-0.0131	-0.0311	-0.0077	0.0715
Run Point	CP29	CP30	CP31	CP32	CP33	CP34	CP35	CP36	CP37	CP38	CP39	CP40	CP41	CP42	CP43	CP44	CP45
6. 162.	0.0690	0.0254	-0.0434	-0.0953	-0.0983	-0.0707	-0.0570	-0.0485	-0.0454	-0.0387	-0.0391	-0.0654	-0.0481	-0.0436	-0.0368	-0.0361	-0.0383
6. 152.	0.0722	0.0216	-0.0538	-0.1190	-0.1165	-0.0906	-0.0720	-0.0583	-0.0527	-0.0462	-0.0457	-0.0752	-0.0609	-0.0556	-0.0465	-0.0388	-0.0389
6. 143.	0.0833	0.0286	-0.0712	-0.1640	-0.1604	-0.1249	-0.0977	-0.0793	-0.0722	-0.0664	-0.0646	-0.0973	-0.0850	-0.0788	-0.0715	-0.0688	-0.0682
6. 134.	0.1126	0.0523	-0.0930	-0.2479	-0.2370	-0.1853	-0.1471	-0.1256	-0.1185	-0.1182	-0.1238	-0.1515	-0.1460	-0.1518	-0.1584	-0.1683	-0.1839
6. 125.	0.1521	0.0982	-0.0464	-0.2191	-0.1922	-0.1289	-0.0895	-0.0649	-0.0528	-0.0464	-0.0488	-0.0737	-0.0674	-0.0679	-0.0726	-0.0851	-0.1029
6. 116.	0.1562	0.1127	-0.0170	-0.1825	-0.1750	-0.0835	-0.0425	-0.0199	-0.0073	0.0014	-0.0012	-0.0191	-0.0113	-0.0125	-0.0189	-0.0306	-0.0470
Run Point	CP46	CP47	CP48	CP49	CP50	CP51	CP52	CP53	CP54	CP55	CP56	CP57	CP58	CP59	CP60	CP61	CP62
6. 162.	-0.0280	0.0173	0.0682	-0.1039	-0.0332	-0.1225	-0.1200	-0.1250	-0.1287	-0.1463	-0.1331	-0.1311	-0.0865	-0.0971	0.0046	0.0898	0.1154
6. 152.	-0.0343	0.0130	0.0709	-0.1260	-0.0448	-0.1213	-0.1216	-0.1284	-0.1325	-0.1284	-0.1355	-0.1522	-0.1297	-0.0864	-0.0228	0.0675	0.0911
6. 143.	-0.0382	0.0071	0.0832	-0.1720	-0.0639	-0.1243	-0.1289	-0.1262	-0.1265	-0.1416	-0.1495	-0.1494	-0.1231	-0.1043	-0.0303	0.0453	0.0792
6. 134.	-0.0349	-0.0035	0.1139	-0.2542	-0.1238	-0.1147	-0.1195	-0.1171	-0.1195	-0.1240	-0.1229	-0.1281	-0.1209	-0.0971	-0.0558	-0.0074	0.0327
6. 125.	-0.0156	0.0035	0.1525	-0.2260	-0.0467	-0.0745	-0.0760	-0.0785	-0.0781	-0.0815	-0.0773	-0.0840	-0.0719	-0.0633	-0.0416	-0.0128	0.0260
6. 116.	-0.0126	-0.0001	0.1561	-0.2032	0.0034	-0.0563	-0.0542	-0.0589	-0.0597	-0.0612	-0.0557	-0.0627	-0.0574	-0.0439	-0.0330	-0.0147	0.0153

Table 9. Continued

(a) Concluded

Run Point	CP63	CP64	CP65	CP66	CP67	CP68	CP69	CP70	CP77	CP78	CP79	CP80	CP81	CP82	CP83	CP84	CP85
6. 162.	0.1522	0.1586	0.1715	0.2060	0.2373	0.3049	0.3973	0.4875	-0.1179	-0.1451	0.1018	0.1971	0.3128	-0.1257	-0.1386	-0.1302	-0.1336
6. 152.	0.1244	0.1741	0.1857	0.2083	0.2440	0.3083	0.4044	0.4819	-0.1272	-0.1468	0.0750	0.1908	0.3188	-0.1266	-0.1322	-0.1323	-0.1371
6. 143.	0.1347	0.1571	0.1895	0.2206	0.2635	0.3342	0.4359	0.5173	-0.1319	-0.1485	0.0687	0.1995	0.3436	-0.1340	-0.1392	-0.1404	-0.1427
6. 134.	0.1079	0.1572	0.2054	0.2462	0.2987	0.3709	0.4622	0.4889	-0.1186	-0.1281	0.0337	0.2045	0.3834	-0.1177	-0.1228	-0.1239	-0.1245
6. 125.	0.0900	0.1554	0.2112	0.2648	0.3217	0.3876	0.4437	0.4523	-0.0762	-0.0823	0.0161	0.2127	0.3905	-0.0766	-0.0813	-0.0814	-0.0831
6. 116.	0.0733	0.1347	0.1861	0.2376	0.2949	0.3486	0.3857	0.3909	-0.0547	-0.0618	0.0094	0.1865	0.3479	-0.0568	-0.0616	-0.0607	-0.0652
Run Point	CP86	CP87	CP88	CP89	CP90	CP91	CP92	CP93	CP94	CP95	CP96	CP97	CP98	CP99	CP100	CP101	CP102
6. 162.	-0.1364	-0.1497	-0.1526	-0.1267	-0.0456	0.0496	0.1300	0.1862	0.2114	0.2231	0.2226	0.2145	0.2039	0.1953	0.2031	0.2144	0.2295
6. 152.	-0.1437	-0.1533	-0.1567	-0.1352	-0.0730	0.0162	0.1002	0.1629	0.1997	0.2148	0.2207	0.2172	0.2106	0.2049	0.2106	0.2205	0.2335
6. 143.	-0.1479	-0.1561	-0.1580	-0.1411	-0.0899	-0.0118	0.0674	0.1369	0.1843	0.2119	0.2241	0.2265	0.2245	0.2199	0.2273	0.2367	0.2515
6. 134.	-0.1297	-0.1332	-0.1373	-0.1320	-0.1095	-0.0667	-0.0125	0.0472	0.1037	0.1548	0.1931	0.2193	0.2397	0.2496	0.2630	0.2759	0.2933
6. 125.	-0.0840	-0.0884	-0.0913	-0.0891	-0.0769	-0.0544	-0.0238	0.0141	0.0563	0.0976	0.1380	0.1756	0.2097	0.2385	0.2654	0.2897	0.3108
6. 116.	-0.0625	-0.0669	-0.0712	-0.0701	-0.0605	-0.0445	-0.0226	0.0027	0.0352	0.0679	0.0989	0.1317	0.1612	0.1932	0.2234	0.2525	0.2758
Run Point	CP103	CP104	CP105	CP106	CP107	CP108	CP109	CP110									
6. 162.	0.2535	0.2771	0.3198	0.3519	0.4275	0.4857	0.5225	0.4688									
6. 152.	0.2555	0.2828	0.3240	0.3699	0.4348	0.4880	0.5201	0.4663									
6. 143.	0.2755	0.3061	0.3479	0.3961	0.4592	0.5137	0.5513	0.4894									
6. 134.	0.3176	0.3464	0.3826	0.4240	0.4704	0.5072	0.5362	0.4835									
6. 125.	0.3344	0.3587	0.3864	0.4123	0.4435	0.4717	0.4948	0.4442									
6. 116.	0.2998	0.3214	0.3456	0.3618	0.3884	0.4128	0.4236	0.3859									

Table 9. Continued

(b) $Z_s = 0.00$ in.

Run Point	M_∞	$R_\infty \times 10^{-6}$	p_∞ , psi	$p_{t,\infty}$, psi	q_∞ , psi	$T_{t,\infty}$, of	CP01	CP02	CP03	CP04	CP05	CP06	CP07	CP08	CP09	CP10	CP11
6. 163.	0.20	2.03	22.98	23.62	0.64	99.7	0.8747	-0.2359	-0.1977	-0.1836	-0.1613	-0.1327	-0.1004	-0.0859	-0.0734	-0.0560	-0.0559
6. 154.	0.40	3.62	19.91	22.23	2.23	101.2	0.9074	-0.2681	-0.2120	-0.1980	-0.1724	-0.1472	-0.1085	-0.0957	-0.0806	-0.0684	-0.0633
6. 145.	0.60	4.69	16.36	20.87	4.13	101.6	0.9897	-0.3042	-0.2319	-0.2151	-0.1866	-0.1571	-0.1130	-0.0969	-0.0799	-0.0684	-0.0598
6. 136.	0.80	3.80	9.31	14.18	4.16	100.3	1.1258	-0.3557	-0.2799	-0.2561	-0.2227	-0.1834	-0.1255	-0.0995	-0.0776	-0.0636	-0.0513
6. 127.	0.90	3.53	7.38	12.47	4.18	99.4	1.2021	-0.4193	-0.3786	-0.3774	-0.3587	-0.1654	-0.0999	-0.0728	-0.0502	-0.0350	-0.0257
6. 118.	0.95	3.39	6.61	11.81	4.17	101.3	1.2369	-0.3105	-0.2940	-0.3059	-0.3471	-0.3630	-0.3689	-0.3538	-0.0235	0.0444	0.0470
Run Point	CP12	CP13	CP14	CP15	CP16	CP17	CP18	CP19	CP20	CP21	CP22	CP23	CP24	CP25	CP26	CP27	CP28
6. 163.	-0.0485	-0.0422	-0.0361	-0.0298	-0.0267	-0.0301	-0.0225	-0.0222	-0.0243	-0.0250	-0.0289	-0.0413	-0.0737	-0.0261	-0.0353	0.0147	0.0554
6. 154.	-0.0562	-0.0518	-0.0441	-0.0394	-0.0352	-0.0343	-0.0311	-0.0319	-0.0333	-0.0352	-0.0401	-0.0508	-0.0784	-0.0390	-0.0444	0.0022	0.0518
6. 145.	-0.0529	-0.0483	-0.0397	-0.0340	-0.0308	-0.0285	-0.0280	-0.0290	-0.0305	-0.0348	-0.0402	-0.0495	-0.0770	-0.0415	-0.0488	0.0003	0.0610
6. 136.	-0.0432	-0.0393	-0.0287	-0.0227	-0.0198	-0.0179	-0.0175	-0.0178	-0.0197	-0.0266	-0.0343	-0.0451	-0.0716	-0.0412	-0.0552	-0.0105	0.0738
6. 127.	-0.0186	-0.0135	-0.0049	0.0002	0.0027	0.0041	0.0048	0.0027	-0.0002	-0.0034	-0.0090	-0.0197	-0.0457	-0.0207	-0.0406	0.0029	0.0991
6. 118.	0.0406	0.0369	0.0291	0.0257	0.0244	0.0209	0.0183	0.0135	0.0070	0.0044	-0.0019	-0.0142	-0.0397	-0.0175	-0.0449	0.0001	0.0966
Run Point	CP29	CP30	CP31	CP32	CP33	CP34	CP35	CP36	CP37	CP38	CP39	CP40	CP41	CP42	CP43	CP44	CP45
6. 163.	0.0716	0.0262	-0.0419	-0.0966	-0.1028	-0.0732	-0.0576	-0.0469	-0.0428	-0.0372	-0.0333	-0.0724	-0.0455	-0.0389	-0.0289	-0.0324	-0.0326
6. 154.	0.0676	0.0202	-0.0564	-0.1247	-0.1245	-0.0969	-0.0769	-0.0634	-0.0574	-0.0508	-0.0516	-0.0833	-0.0623	-0.0572	-0.0514	-0.0514	-0.0517
6. 145.	0.0831	0.0308	-0.0691	-0.1666	-0.1650	-0.1276	-0.0963	-0.0771	-0.0691	-0.0636	-0.0640	-0.0944	-0.0810	-0.0741	-0.0679	-0.0634	-0.0643
6. 136.	0.1125	0.0567	-0.0895	-0.2590	-0.2566	-0.2012	-0.1557	-0.1301	-0.1213	-0.1204	-0.1249	-0.1583	-0.1518	-0.1564	-0.1579	-0.1705	-0.1857
6. 127.	0.1613	0.1126	-0.0357	-0.2413	-0.2328	-0.1529	-0.1050	-0.0746	-0.0595	-0.0513	-0.0527	-0.0854	-0.0773	-0.0751	-0.0787	-0.0896	-0.1057
6. 118.	0.1749	0.1326	-0.0080	-0.2081	-0.2324	-0.1172	-0.0626	-0.0357	-0.0201	-0.0079	-0.0093	-0.0367	-0.0262	-0.0236	-0.0280	-0.0379	-0.0525
Run Point	CP46	CP47	CP48	CP49	CP50	CP51	CP52	CP53	CP54	CP55	CP56	CP57	CP58	CP59	CP60	CP61	CP62
6. 163.	-0.0255	0.0239	0.0708	-0.1061	-0.0306	-0.1358	-0.1315	-0.1411	-0.1352	-0.1586	-0.1444	-0.1429	-0.0769	-0.0014	0.0232	0.0931	0.0897
6. 154.	-0.0367	0.0138	0.0683	-0.1323	-0.0470	-0.1351	-0.1365	-0.1405	-0.1427	-0.1672	-0.1727	-0.1502	-0.0975	-0.0415	0.0249	0.0684	0.0866
6. 145.	-0.0379	0.0140	0.0837	-0.1759	-0.0646	-0.1386	-0.1414	-0.1417	-0.1533	-0.1654	-0.1599	-0.1523	-0.1229	-0.0523	0.0067	0.0719	0.1026
6. 136.	-0.0388	0.0076	0.1145	-0.2693	-0.1267	-0.1301	-0.1344	-0.1341	-0.1400	-0.1419	-0.1388	-0.1454	-0.1181	-0.0714	-0.0289	0.0291	0.0731
6. 127.	-0.0191	0.0196	0.1629	-0.2595	-0.0518	-0.1007	-0.1023	-0.1056	-0.1067	-0.1108	-0.1019	-0.1021	-0.0844	-0.0518	-0.0152	0.0251	0.0672
6. 118.	-0.0168	0.0144	0.1744	-0.2435	-0.0054	-0.0850	-0.0825	-0.0905	-0.0924	-0.0964	-0.0831	-0.0838	-0.0707	-0.0514	-0.0253	0.0064	0.0476

Table 9. Continued

(b) Concluded

Run Point	CP63	CP64	CP65	CP66	CP67	CP68	CP69	CP70	CP77	CP78	CP79	CP80	CP81	CP82	CP83	CP84	CP85
6. 163.	0.1450	0.1699	0.1696	0.2038	0.2337	0.3039	0.4062	0.4704	-0.1271	-0.1404	0.1095	0.1929	0.3179	-0.1298	-0.1461	-0.1365	-0.1432
6. 154.	0.1290	0.1537	0.1859	0.2097	0.2389	0.3034	0.4051	0.4851	-0.1425	-0.1608	0.0987	0.1795	0.3198	-0.1436	-0.1508	-0.1502	-0.1558
6. 145.	0.1486	0.1645	0.1880	0.2169	0.2585	0.3305	0.4352	0.5215	-0.1448	-0.1605	0.0928	0.1933	0.3459	-0.1457	-0.1506	-0.1521	-0.1552
6. 136.	0.1293	0.1695	0.2156	0.2503	0.2987	0.3710	0.4749	0.4987	-0.1397	-0.1482	0.0691	0.2123	0.3887	-0.1386	-0.1446	-0.1458	-0.1451
6. 127.	0.1373	0.1915	0.2364	0.2856	0.3399	0.4047	0.4722	0.4893	-0.1030	-0.1083	0.0663	0.2358	0.4135	-0.1043	-0.1103	-0.1098	-0.1112
6. 118.	0.1215	0.1782	0.2287	0.2819	0.3360	0.3966	0.4564	0.4572	-0.0869	-0.0931	0.0509	0.2332	0.3926	-0.0899	-0.0958	-0.0941	-0.0983
Run Point	CP86	CP87	CP88	CP89	CP90	CP91	CP92	CP93	CP94	CP95	CP96	CP97	CP98	CP99	CP100	CP101	CP102
6. 163.	-0.1511	-0.1577	-0.1477	-0.0951	-0.0095	0.0874	0.1457	0.1929	0.2070	0.2207	0.2191	0.2132	0.2028	0.1955	0.2020	0.2132	0.2281
6. 154.	-0.1632	-0.1703	-0.1594	-0.1153	-0.0340	0.0505	0.1285	0.1752	0.2016	0.2128	0.2125	0.2099	0.2046	0.1972	0.2050	0.2158	0.2286
6. 145.	-0.1637	-0.1687	-0.1586	-0.1186	-0.0502	0.0325	0.1044	0.1604	0.1944	0.2166	0.2253	0.2246	0.2214	0.2150	0.2228	0.2326	0.2479
6. 136.	-0.1527	-0.1560	-0.1512	-0.1272	-0.0846	-0.0261	0.0355	0.0956	0.1445	0.1859	0.2155	0.2332	0.2457	0.2491	0.2591	0.2696	0.2867
6. 127.	-0.1132	-0.1164	-0.1132	-0.0982	-0.0685	-0.0271	0.0188	0.0660	0.1121	0.1554	0.1935	0.2256	0.2513	0.2705	0.2903	0.3101	0.3288
6. 118.	-0.0941	-0.0977	-0.0976	-0.0868	-0.0618	-0.0285	0.0091	0.0463	0.0835	0.1219	0.1550	0.1895	0.2191	0.2460	0.2730	0.2980	0.3189
Run Point	CP103	CP104	CP105	CP106	CP107	CP108	CP109	CP110									
6. 163.	0.2519	0.2752	0.3175	0.3549	0.4328	0.4996	0.5493	0.4904									
6. 154.	0.2509	0.2796	0.3213	0.3708	0.4395	0.5057	0.5528	0.4712									
6. 145.	0.2725	0.3037	0.3470	0.3996	0.4658	0.5235	0.5682	0.5008									
6. 136.	0.3120	0.3439	0.3839	0.4311	0.4838	0.5304	0.5737	0.5106									
6. 127.	0.3530	0.3796	0.4125	0.4444	0.4845	0.5187	0.5494	0.5127									
6. 118.	0.3433	0.3666	0.3952	0.4191	0.4496	0.4800	0.5084	0.4676									

Table 9. Continued

(c) $Z_g = 2.37$ in.

Run Point	M_∞	$R_\infty \times 10^{-6}$	p_∞ psi	$p_{t,\infty}$ psi	q_∞ psi	$T_{t,\infty}$ °F	CP01	CP02	CP03	CP04	CP05	CP06	CP07	CP08	CP09	CP10	CP11
6. 168.	0.20	2.03	22.97	23.62	0.64	99.7	0.8857	-0.2278	-0.1899	-0.1732	-0.1504	-0.1236	-0.0923	-0.0780	-0.0654	-0.0457	-0.0468
6. 159.	0.40	3.63	19.92	22.25	2.24	101.9	0.9108	-0.2628	-0.2067	-0.1931	-0.1677	-0.1419	-0.1040	-0.0905	-0.0753	-0.0628	-0.0575
6. 150.	0.60	4.68	16.34	20.84	4.12	101.5	0.9949	-0.3023	-0.2310	-0.2143	-0.1857	-0.1566	-0.1118	-0.0961	-0.0787	-0.0673	-0.0594
6. 141.	0.80	3.80	9.31	14.18	4.17	100.4	1.1269	-0.3546	-0.2782	-0.2549	-0.2213	-0.1832	-0.1249	-0.0990	-0.0774	-0.0639	-0.0505
6. 132.	0.90	3.53	7.38	12.47	4.18	99.7	1.2015	-0.4142	-0.3789	-0.3777	-0.3588	-0.1644	-0.0997	-0.0729	-0.0504	-0.0350	-0.0253
6. 123.	0.95	3.39	6.60	11.79	4.17	100.5	1.2370	-0.3099	-0.2946	-0.3060	-0.3476	-0.3628	-0.3690	-0.3521	-0.0207	0.0457	0.0476
Run Point	CP12	CP13	CP14	CP15	CP16	CP17	CP18	CP19	CP20	CP21	CP22	CP23	CP24	CP25	CP26	CP27	CP28
6. 168.	-0.0395	-0.0346	-0.0259	-0.0219	-0.0181	-0.0200	-0.0138	-0.0165	-0.0154	-0.0172	-0.0188	-0.0289	-0.0614	-0.0206	-0.0286	0.0191	0.0619
6. 159.	-0.0507	-0.0456	-0.0388	-0.0337	-0.0307	-0.0293	-0.0266	-0.0259	-0.0271	-0.0290	-0.0335	-0.0425	-0.0675	-0.0328	-0.0407	0.0037	0.0550
6. 150.	-0.0518	-0.0474	-0.0382	-0.0336	-0.0292	-0.0264	-0.0247	-0.0257	-0.0270	-0.0296	-0.0350	-0.0443	-0.0716	-0.0372	-0.0468	-0.0026	0.0609
6. 141.	-0.0423	-0.0386	-0.0273	-0.0211	-0.0188	-0.0160	-0.0156	-0.0164	-0.0178	-0.0245	-0.0317	-0.0399	-0.0635	-0.0378	-0.0536	-0.0157	0.0715
6. 132.	-0.0186	-0.0133	-0.0044	0.0005	0.0037	0.0048	0.0052	0.0034	0.0007	-0.0024	-0.0073	-0.0168	-0.0404	-0.0178	-0.0389	-0.0028	0.0933
6. 123.	0.0411	0.0374	0.0297	0.0261	0.0247	0.0212	0.0193	0.0154	0.0087	0.0073	0.0009	-0.0120	-0.0367	-0.0141	-0.0429	-0.0045	0.0903
Run Point	CP29	CP30	CP31	CP32	CP33	CP34	CP35	CP36	CP37	CP38	CP39	CP40	CP41	CP42	CP43	CP44	CP45
6. 168.	0.0804	0.0329	-0.0299	-0.0841	-0.0874	-0.0601	-0.0454	-0.0337	-0.0296	-0.0223	-0.0234	-0.0581	-0.0326	-0.0324	-0.0278	-0.0247	-0.0283
6. 159.	0.0723	0.0232	-0.0499	-0.1147	-0.1148	-0.0886	-0.0693	-0.0559	-0.0496	-0.0440	-0.0435	-0.0722	-0.0579	-0.0526	-0.0468	-0.0461	-0.0441
6. 150.	0.0833	0.0292	-0.0670	-0.1596	-0.1565	-0.1221	-0.0944	-0.0757	-0.0669	-0.0604	-0.0597	-0.0892	-0.0782	-0.0724	-0.0639	-0.0619	-0.0618
6. 141.	0.1099	0.0530	-0.0862	-0.2478	-0.2400	-0.1906	-0.1509	-0.1272	-0.1188	-0.1185	-0.1215	-0.1467	-0.1441	-0.1509	-0.1570	-0.1713	-0.1876
6. 132.	0.1564	0.1101	-0.0327	-0.2336	-0.2171	-0.1463	-0.1017	-0.0724	-0.0571	-0.0487	-0.0490	-0.0778	-0.0712	-0.0713	-0.0776	-0.0897	-0.1063
6. 123.	0.1681	0.1299	-0.0047	-0.2016	-0.2148	-0.1077	-0.0584	-0.0319	-0.0162	-0.0038	-0.0063	-0.0277	-0.0181	-0.0187	-0.0261	-0.0368	-0.0532
Run Point	CP46	CP47	CP48	CP49	CP50	CP51	CP52	CP53	CP54	CP55	CP56	CP57	CP58	CP59	CP60	CP61	CP62
6. 168.	-0.0177	0.0284	0.0786	-0.0929	-0.0183	-0.1166	-0.1176	-0.1215	-0.1284	-0.1372	-0.1263	-0.1286	-0.1083	0.0044	0.0617	0.0941	0.1130
6. 159.	-0.0321	0.0147	0.0714	-0.1237	-0.0394	-0.1357	-0.1336	-0.1434	-0.1432	-0.1426	-0.1354	-0.1650	-0.1035	-0.0390	0.0093	0.0698	0.1086
6. 150.	-0.0359	0.0095	0.0823	-0.1686	-0.0598	-0.1366	-0.1410	-0.1438	-0.1493	-0.1560	-0.1556	-0.1373	-0.1150	-0.0696	-0.0001	0.0386	0.0885
6. 141.	-0.0357	0.0009	0.1116	-0.2587	-0.1225	-0.1275	-0.1318	-0.1266	-0.1297	-0.1361	-0.1380	-0.1390	-0.1346	-0.0967	-0.0455	0.0247	0.0651
6. 132.	-0.0161	0.0109	0.1569	-0.2508	-0.0487	-0.0960	-0.0956	-0.0978	-0.0994	-0.1029	-0.0972	-0.1020	-0.0895	-0.0687	-0.0228	0.0139	0.0542
6. 123.	-0.0137	0.0069	0.1665	-0.2353	-0.0016	-0.0863	-0.0818	-0.0880	-0.0891	-0.0928	-0.0847	-0.0925	-0.0733	-0.0534	-0.0258	0.0064	0.0461

Table 9. Concluded

(c) Concluded

Run Point	CP63	CP64	CP65	CP66	CP67	CP68	CP69	CP70	CP77	CP78	CP79	CP80	CP81	CP82	CP83	CP84	CP85
6. 168.	0.1393	0.1827	0.2003	0.2280	0.2569	0.3215	0.4057	0.4893	-0.1189	-0.1381	0.0972	0.2033	0.3260	-0.1221	-0.1348	-0.1298	-0.1343
6. 159.	0.1206	0.1702	0.1931	0.2146	0.2506	0.3099	0.3956	0.4847	-0.1347	-0.1587	0.0869	0.1931	0.3149	-0.1368	-0.1426	-0.1416	-0.1480
6. 150.	0.1399	0.1713	0.1979	0.2284	0.2648	0.3274	0.4195	0.4963	-0.1415	-0.1604	0.0840	0.1947	0.3413	-0.1414	-0.1462	-0.1477	-0.1521
6. 141.	0.1293	0.1736	0.2191	0.2546	0.3054	0.3689	0.4518	0.5200	-0.1347	-0.1462	0.0614	0.2133	0.3739	-0.1312	-0.1364	-0.1387	-0.1390
6. 132.	0.1247	0.1841	0.2361	0.2855	0.3378	0.3982	0.4662	0.4868	-0.0966	-0.1062	0.0521	0.2370	0.3969	-0.0967	-0.1011	-0.1020	-0.1049
6. 123.	0.1205	0.1810	0.2271	0.2796	0.3296	0.3891	0.4375	0.4682	-0.0801	-0.0916	0.0440	0.2306	0.3846	-0.0813	-0.0847	-0.0846	-0.0913
Run Point	CP86	CP87	CP88	CP89	CP90	CP91	CP92	CP93	CP94	CP95	CP96	CP97	CP98	CP99	CP100	CP101	CP102
6. 168.	-0.1406	-0.1543	-0.1498	-0.1091	-0.0160	0.0704	0.1466	0.1938	0.2142	0.2259	0.2253	0.2216	0.2148	0.2075	0.2140	0.2285	0.2430
6. 159.	-0.1558	-0.1660	-0.1629	-0.1236	-0.0462	0.0427	0.1179	0.1729	0.1986	0.2122	0.2153	0.2127	0.2091	0.2041	0.2117	0.2222	0.2368
6. 150.	-0.1609	-0.1690	-0.1666	-0.1349	-0.0678	0.0124	0.0912	0.1516	0.1897	0.2139	0.2246	0.2254	*****	*****	*****	*****	*****
6. 141.	-0.1481	-0.1545	-0.1555	-0.1393	-0.1008	-0.0400	0.0257	0.0864	0.1339	0.1738	0.2059	0.2256	0.2433	0.2496	0.2610	0.2723	0.2901
6. 132.	-0.1079	-0.1141	-0.1168	-0.1086	-0.0822	-0.0388	0.0105	0.0587	0.1030	0.1430	0.1796	0.2137	0.2436	0.2666	0.2864	0.3056	0.3243
6. 123.	-0.0890	-0.0949	-0.0991	-0.0941	-0.0732	-0.0393	0.0012	0.0404	0.0783	0.1144	0.1475	0.1813	0.2102	0.2397	0.2662	0.2910	0.3116
Run Point	CP103	CP104	CP105	CP106	CP107	CP108	CP109	CP110									
6. 168.	0.2669	0.2892	0.3330	0.3635	0.4301	0.4744	0.5142	0.4788									
6. 159.	0.2601	0.2894	0.3298	0.3735	0.4288	0.4752	0.5109	0.4736									
6. 150.	*****	*****	0.3458	0.3975	0.4518	0.4948	0.5284	0.4934									
6. 141.	0.3143	0.3448	0.3799	0.4198	0.4591	0.4907	0.5152	0.4968									
6. 132.	0.3479	0.3729	0.4024	0.4306	0.4634	0.4903	0.5108	0.4869									
6. 123.	0.3330	0.3539	0.3801	0.4005	0.4276	0.4527	0.4714	0.4391									

Table 10. Pressure Coefficients for Configuration 10 With $h = 2.40$ in., $l = 30.00$ in., and $Y_s = 2.40$ in.(a) $Z_s = -0.90$ in.

Run Point	M_∞	$R_{\infty} \times 10^{-6}$	p_{∞} , psi	$P_{t,\infty}$, psi	q_{∞} , psi	$T_{t,\infty}$, °F	CP01	CP02	CP03	CP04	CP05	CP06	CP07	CP08	CP09	CP10	CP11
7. 221.	0.20	2.04	22.97	23.63	0.65	101.8	0.8767	-0.2285	-0.1920	-0.1728	-0.1506	-0.1212	-0.0923	-0.0761	-0.0665	-0.0479	-0.0447
7. 212.	0.40	3.63	19.89	22.22	2.24	101.8	0.9053	-0.2582	-0.2073	-0.1934	-0.1683	-0.1424	-0.1053	-0.0911	-0.0764	-0.0650	-0.0570
7. 230.	0.60	4.69	16.34	20.87	4.14	102.1	0.9941	-0.2901	-0.2279	-0.2141	-0.1856	-0.1562	-0.1127	-0.0990	-0.0808	-0.0687	-0.0604
7. 257.	0.80	3.82	9.30	14.17	4.16	98.1	1.1268	-0.3265	-0.2758	-0.2541	-0.2227	-0.1830	-0.1261	-0.1005	-0.0783	-0.0652	-0.0529
7. 248.	0.90	3.53	7.37	12.49	4.20	100.6	1.2038	-0.3744	-0.3515	-0.3687	-0.3442	-0.1842	-0.0934	-0.0673	-0.0465	-0.0343	-0.0227
7. 239.	0.95	3.40	6.59	11.82	4.19	101.7	1.2403	-0.2659	-0.2782	-0.3119	-0.3284	-0.3560	-0.3604	-0.3543	-0.0492	0.0456	0.0573
Run Point	CP12	CP13	CP14	CP15	CP16	CP17	CP18	CP19	CP20	CP21	CP22	CP23	CP24	CP25	CP26	CP27	CP28
7. 221.	-0.0396	-0.0303	-0.0242	-0.0207	-0.0162	-0.0216	-0.0179	-0.0155	-0.0180	-0.0166	-0.0200	-0.0340	-0.0613	-0.0208	-0.0270	0.0206	0.0616
7. 212.	-0.0503	-0.0451	-0.0380	-0.0341	-0.0308	-0.0298	-0.0291	-0.0282	-0.0299	-0.0313	-0.0377	-0.0479	-0.0727	-0.0370	-0.0419	0.0014	0.0545
7. 230.	-0.0544	-0.0485	-0.0392	-0.0329	-0.0278	-0.0264	-0.0256	-0.0281	-0.0295	-0.0323	-0.0387	-0.0493	-0.0762	-0.0403	-0.0487	-0.0063	0.0581
7. 257.	-0.0448	-0.0395	-0.0304	-0.0247	-0.0208	-0.0185	-0.0173	-0.0198	-0.0218	-0.0256	-0.0319	-0.0421	-0.0674	-0.0386	-0.0554	-0.0199	0.0647
7. 248.	-0.0155	-0.0121	-0.0033	0.0013	0.0039	0.0055	0.0055	0.0029	0.0015	-0.0025	-0.0084	-0.0163	-0.0375	-0.0177	-0.0343	-0.0077	0.0850
7. 239.	0.0511	0.0431	0.0352	0.0310	0.0284	0.0265	0.0233	0.0173	0.0132	0.0079	0.0010	-0.0086	-0.0272	-0.0130	-0.0303	-0.0087	0.0750
Run Point	CP29	CP30	CP31	CP32	CP33	CP34	CP35	CP36	CP37	CP38	CP39	CP40	CP41	CP42	CP43	CP44	CP45
7. 221.	0.0805	0.0344	-0.0315	-0.0826	-0.0888	-0.0640	-0.0489	-0.0345	-0.0318	-0.0238	-0.0226	-0.0463	-0.0289	-0.0239	-0.0075	-0.0033	-0.0140
7. 212.	0.0727	0.0212	-0.0551	-0.1213	-0.1210	-0.0958	-0.0765	-0.0603	-0.0522	-0.0452	-0.0431	-0.0671	-0.0511	-0.0481	-0.0358	-0.0378	-0.0406
7. 230.	0.0842	0.0291	-0.0688	-0.1601	-0.1588	-0.1257	-0.0977	-0.0785	-0.0692	-0.0612	-0.0611	-0.0853	-0.0752	-0.0699	-0.0622	-0.0625	-0.0660
7. 257.	0.1128	0.0521	-0.0919	-0.2487	-0.2415	-0.1941	-0.1560	-0.1297	-0.1189	-0.1141	-0.1196	-0.1423	-0.1384	-0.1426	-0.1525	-0.1655	-0.1843
7. 248.	0.1588	0.1058	-0.0422	-0.2297	-0.2023	-0.1333	-0.0923	-0.0638	-0.0486	-0.0411	-0.0418	-0.0627	-0.0558	-0.0594	-0.0655	-0.0772	-0.0965
7. 239.	0.1624	0.1192	-0.0158	-0.1873	-0.1793	-0.0840	-0.0376	-0.0120	0.0005	0.0061	0.0053	-0.0073	-0.0017	-0.0044	-0.0124	-0.0236	-0.0393
Run Point	CP46	CP47	CP48	CP49	CP50	CP51	CP52	CP53	CP54	CP55	CP56	CP57	CP58	CP59	CP60	CP61	CP62
7. 221.	-0.0159	0.0313	0.0789	-0.0954	-0.0162	-0.1128	-0.1118	-0.1256	-0.1215	-0.1291	-0.1376	-0.1635	-0.0919	-0.0306	0.0522	0.0600	0.1030
7. 212.	-0.0338	0.0153	0.0721	-0.1320	-0.0424	-0.1272	-0.1262	-0.1271	-0.1346	-0.1407	-0.1406	-0.1377	-0.1132	-0.0622	-0.0101	0.0596	0.0912
7. 230.	-0.0375	0.0094	0.0824	-0.1738	-0.0598	-0.1319	-0.1311	-0.1300	-0.1310	-0.1454	-0.1505	-0.1474	-0.1191	-0.0751	-0.0246	0.0370	0.0721
7. 257.	-0.0369	-0.0030	0.1096	-0.2660	-0.1214	-0.1191	-0.1261	-0.1262	-0.1259	-0.1294	-0.1232	-0.1295	-0.1132	-0.0845	-0.0529	-0.0161	0.0293
7. 248.	-0.0155	0.0072	0.1547	-0.2456	-0.0444	-0.0743	-0.0836	-0.0833	-0.0826	-0.0839	-0.0798	-0.0881	-0.0847	-0.0680	-0.0460	-0.0111	0.0220
7. 239.	-0.0110	0.0029	0.1564	-0.2203	0.0061	-0.0554	-0.0624	-0.0622	-0.0622	-0.0615	-0.0593	-0.0674	-0.0682	-0.0548	-0.0391	-0.0131	0.0119

Table 10. Continued

(a) Concluded

Run Point	CP63	CP64	CP65	CP66	CP67	CP68	CP69	CP70	CP77	CP78	CP79	CP80	CP81	CP82	CP83	CP84	CP85
7. 221.	0.1884	0.1744	0.1934	0.2185	0.2531	0.3151	0.4031	0.4784	-0.1107	-0.1329	0.1133	0.1985	0.2978	-0.1137	-0.1271	-0.1163	-0.1276
7. 212.	0.1246	0.1745	0.1851	0.2129	0.2506	0.3217	0.4141	0.4799	-0.1302	-0.1487	0.1054	0.1844	0.2908	-0.1304	-0.1378	-0.1370	-0.1406
7. 230.	0.1246	0.1638	0.1933	0.2165	0.2685	0.3405	0.4369	0.5130	-0.1327	-0.1496	0.0859	0.1958	0.3207	-0.1345	-0.1408	-0.1413	-0.1438
7. 257.	0.1104	0.1579	0.2041	0.2510	0.3068	0.3816	0.4676	0.4867	-0.1222	-0.1332	0.0483	0.2057	0.3574	-0.1257	-0.1319	-0.1320	-0.1309
7. 248.	0.0946	0.1625	0.2159	0.2751	0.3329	0.4026	0.4670	0.4872	-0.0796	-0.0881	0.0286	0.2181	0.3856	-0.0816	-0.0883	-0.0890	-0.0862
7. 239.	0.0756	0.1331	0.1872	0.2414	0.2928	0.3486	0.3968	0.4173	-0.0558	-0.0629	0.0140	0.1875	0.3463	-0.0605	-0.0663	-0.0666	-0.0649
Run Point	CP86	CP87	CP88	CP89	CP90	CP91	CP92	CP93	CP94	CP95	CP96	CP97	CP98	CP99	CP100	CP101	CP102
7. 221.	-0.1283	-0.1399	-0.1406	-0.1156	-0.0497	0.0379	0.1235	0.1825	0.2150	0.2301	0.2261	0.2247	0.2220	0.2119	0.2186	0.2299	0.2439
7. 212.	-0.1482	-0.1569	-0.1569	-0.1331	-0.0715	0.0081	0.0951	0.1640	0.2042	0.2227	0.2219	0.2169	0.2121	0.2052	0.2110	0.2196	0.2342
7. 230.	-0.1495	-0.1576	-0.1570	-0.1372	-0.0890	-0.0225	0.0520	0.1274	0.1796	0.2115	0.2253	0.2275	0.2275	0.2218	0.2288	0.2378	0.2526
7. 257.	-0.1329	-0.1377	-0.1411	-0.1317	-0.1091	-0.0685	-0.0159	0.0420	0.0994	0.1535	0.1958	0.2229	0.2416	0.2514	0.2626	0.2754	0.2916
7. 248.	-0.0881	-0.0902	-0.0934	-0.0915	-0.0810	-0.0584	-0.0257	0.0136	0.0566	0.1019	0.1447	0.1837	0.2217	0.2496	0.2751	0.2984	0.3200
7. 239.	-0.0644	-0.0662	-0.0695	-0.0691	-0.0631	-0.0493	-0.0271	-0.0012	0.0301	0.0636	0.0994	0.1332	0.1684	0.1993	0.2278	0.2562	0.2813
Run Point	CP103	CP104	CP105	CP106	CP107	CP108	CP109	CP110									
7. 221.	0.2674	0.2905	0.3367	0.3753	0.4522	0.5072	0.5338	0.4931									
7. 212.	0.2578	0.2882	0.3329	0.3824	0.4520	0.5048	0.5196	0.4878									
7. 230.	0.2775	0.3097	0.3551	0.4082	0.4716	0.5191	0.5410	0.4969									
7. 257.	0.3163	0.3475	0.3873	0.4315	0.4815	0.5201	0.5392	0.4955									
7. 248.	0.3444	0.3714	0.4018	0.4299	0.4635	0.4933	0.5118	0.4623									
7. 239.	0.3082	0.3314	0.3553	0.3722	0.3990	0.4233	0.4279	0.3903									

Table 10. Continued

(b) $Z_s = 0.00$ in.

Run Point	M_∞	$R_\infty \times 10^{-6}$	p_∞ , psi	$p_{t,\infty}$, psi	q_∞ , psi	$T_{t,\infty}$, °F	CP01	CP02	CP03	CP04	CP05	CP06	CP07	CP08	CP09	CP10	CP11
7. 223.	0.20	2.05	22.97	23.63	0.66	101.8	0.8762	-0.2260	-0.1899	-0.1732	-0.1511	-0.1188	-0.0913	-0.0775	-0.0647	-0.0441	-0.0443
7. 214.	0.40	3.62	19.84	22.16	2.23	101.9	0.9057	-0.2585	-0.2081	-0.1942	-0.1689	-0.1426	-0.1056	-0.0924	-0.0770	-0.0655	-0.0582
7. 232.	0.60	4.70	16.33	20.86	4.15	101.8	0.9948	-0.2899	-0.2276	-0.2138	-0.1853	-0.1553	-0.1121	-0.0967	-0.0788	-0.0664	-0.0581
7. 259.	0.80	3.82	9.30	14.18	4.16	98.2	1.1281	-0.3266	-0.2765	-0.2543	-0.2233	-0.1829	-0.1260	-0.0992	-0.0772	-0.0639	-0.0521
7. 250.	0.90	3.53	7.37	12.49	4.19	100.7	1.2039	-0.3761	-0.3521	-0.3690	-0.3442	-0.1796	-0.0942	-0.0686	-0.0474	-0.0350	-0.0234
7. 241.	0.95	3.39	6.60	11.82	4.19	102.0	1.2407	-0.2671	-0.2794	-0.3129	-0.3293	-0.3571	-0.3612	-0.3548	-0.0456	0.0455	0.0566
Run Point	CP12	CP13	CP14	CP15	CP16	CP17	CP18	CP19	CP20	CP21	CP22	CP23	CP24	CP25	CP26	CP27	CP28
7. 223.	-0.0392	-0.0290	-0.0239	-0.0205	-0.0130	-0.0204	-0.0167	-0.0132	-0.0157	-0.0133	-0.0176	-0.0326	-0.0618	-0.0185	-0.0278	0.0235	0.0598
7. 214.	-0.0520	-0.0462	-0.0391	-0.0339	-0.0303	-0.0299	-0.0282	-0.0293	-0.0309	-0.0334	-0.0378	-0.0500	-0.0768	-0.0371	-0.0421	0.0043	0.0545
7. 232.	-0.0516	-0.0468	-0.0381	-0.0334	-0.0298	-0.0279	-0.0271	-0.0282	-0.0301	-0.0345	-0.0416	-0.0532	-0.0794	-0.0430	-0.0502	-0.0025	0.0599
7. 259.	-0.0442	-0.0391	-0.0300	-0.0250	-0.0215	-0.0194	-0.0179	-0.0206	-0.0221	-0.0259	-0.0330	-0.0443	-0.0714	-0.0398	-0.0570	-0.0129	0.0717
7. 250.	-0.0164	-0.0124	-0.0038	0.0011	0.0044	0.0060	0.0060	0.0033	0.0010	-0.0033	-0.0105	-0.0210	-0.0463	-0.0214	-0.0409	0.0013	0.1022
7. 241.	0.0506	0.0425	0.0346	0.0306	0.0276	0.0258	0.0228	0.0169	0.0121	0.0050	-0.0036	-0.0148	-0.0377	-0.0185	-0.0421	-0.0020	0.1016
Run Point	CP29	CP30	CP31	CP32	CP33	CP34	CP35	CP36	CP37	CP38	CP39	CP40	CP41	CP42	CP43	CP44	CP45
7. 223.	0.0806	0.0317	-0.0333	-0.0861	-0.0900	-0.0644	-0.0462	-0.0374	-0.0336	-0.0236	-0.0256	-0.0522	-0.0443	-0.0362	-0.0285	-0.0098	-0.0181
7. 214.	0.0723	0.0220	-0.0543	-0.1207	-0.1215	-0.0961	-0.0745	-0.0586	-0.0515	-0.0447	-0.0448	-0.0576	-0.0479	-0.0458	-0.0328	-0.0309	-0.0340
7. 232.	0.0834	0.0285	-0.0704	-0.1642	-0.1639	-0.1302	-0.1015	-0.0812	-0.0709	-0.0628	-0.0614	-0.0847	-0.0739	-0.0695	-0.0625	-0.0626	-0.0650
7. 259.	0.1137	0.0537	-0.0920	-0.2527	-0.2492	-0.2028	-0.1623	-0.1348	-0.1223	-0.1173	-0.1216	-0.1433	-0.1379	-0.1421	-0.1518	-0.1653	-0.1833
7. 250.	0.1661	0.1130	-0.0391	-0.2406	-0.2282	-0.1555	-0.1095	-0.0759	-0.0570	-0.0467	-0.0460	-0.0675	-0.0591	-0.0606	-0.0680	-0.0805	-0.0990
7. 241.	0.1822	0.1340	-0.0121	-0.2118	-0.2248	-0.1235	-0.0600	-0.0285	-0.0110	-0.0013	0.0010	-0.0163	-0.0075	-0.0080	-0.0149	-0.0258	-0.0415
Run Point	CP46	CP47	CP48	CP49	CP50	CP51	CP52	CP53	CP54	CP55	CP56	CP57	CP58	CP59	CP60	CP61	CP62
7. 223.	-0.0147	0.0320	0.0790	-0.1007	-0.0183	-0.1192	-0.1167	-0.1295	-0.1354	-0.1504	-0.1289	-0.1022	-0.0836	-0.0483	0.0184	0.0908	0.1163
7. 214.	-0.0349	0.0177	0.0708	-0.1350	-0.0409	-0.1299	-0.1340	-0.1419	-0.1511	-0.1646	-0.1380	-0.1319	-0.1136	-0.0733	0.0028	0.0499	0.0735
7. 232.	-0.0392	0.0138	0.0830	-0.1799	-0.0606	-0.1309	-0.1299	-0.1375	-0.1469	-0.1511	-0.1504	-0.1527	-0.0021	-0.0702	-0.0137	0.0500	0.0891
7. 259.	-0.0375	0.0069	0.1109	-0.2758	-0.1217	-0.1300	-0.1318	-0.1336	-0.1343	-0.1405	-0.1353	-0.1393	-0.1167	-0.0874	-0.0491	0.0165	0.0573
7. 250.	-0.0197	0.0234	0.1621	-0.2722	-0.0479	-0.1026	-0.1032	-0.0994	-0.1023	-0.1067	-0.0999	-0.1039	-0.0879	-0.0573	-0.0233	0.0184	0.0591
7. 241.	-0.0174	0.0201	0.1761	-0.2554	-0.0006	-0.0846	-0.0860	-0.0849	-0.0879	-0.0883	-0.0801	-0.0841	-0.0780	-0.0559	-0.0279	0.0109	0.0436

Table 10. Continued

(b) Concluded

Run Point	CP63	CP64	CP65	CP66	CP67	CP68	CP69	CP70	CP77	CP78	CP79	CP80	CP81	CP82	CP83	CP84	CP85
7. 223.	0.1472	0.1851	0.1901	0.2159	0.2458	0.3159	0.4122	0.4782	-0.1219	-0.1419	0.1130	0.1972	0.2964	-0.1231	-0.1366	-0.1278	-0.1369
7. 214.	0.1318	0.1708	0.1922	0.2095	0.2468	0.3178	0.4132	0.4895	-0.1422	-0.1649	0.1020	0.1753	0.2928	-0.1394	-0.1472	-0.1482	-0.1534
7. 232.	0.1324	0.1681	0.2755	0.2993	0.3391	0.3419	0.4352	0.5223	-0.1469	-0.1653	0.0966	0.1911	0.3178	-0.1427	-0.1498	-0.1508	-0.1542
7. 259.	0.1241	0.1718	0.2131	0.2530	0.3066	0.3803	0.4738	0.5093	-0.1401	-0.1513	0.0729	0.2103	0.3590	-0.1355	-0.1422	-0.1447	-0.1465
7. 250.	0.1293	0.1879	0.2438	0.2918	0.3481	0.4152	0.4866	0.5077	-0.1069	-0.1177	0.0719	0.2422	0.3946	-0.1065	-0.1085	-0.1104	-0.1109
7. 241.	0.1149	0.1787	0.2360	0.2881	0.3434	0.3994	0.4461	0.4618	-0.0898	-0.0997	0.0605	0.2286	0.3899	-0.0869	-0.0915	-0.0935	-0.0945
Run Point	CP86	CP87	CP88	CP89	CP90	CP91	CP92	CP93	CP94	CP95	CP96	CP97	CP98	CP99	CP100	CP101	CP102
7. 223.	-0.1414	-0.1487	-0.1433	-0.1027	-0.0229	0.0670	0.1469	0.2027	0.2229	0.2306	0.2234	0.2179	0.2151	0.2061	0.2140	0.2250	0.2390
7. 214.	-0.1616	-0.1678	-0.1588	-0.1161	-0.0460	0.0386	0.1231	0.1797	0.2102	0.2204	0.2185	0.2122	0.2066	0.1986	0.2061	0.2160	0.2308
7. 232.	-0.1625	-0.1678	-0.1604	-0.1274	-0.0674	0.0093	0.0919	0.1569	0.1986	0.2206	0.2266	0.2233	0.2217	0.2149	0.2221	0.2319	0.2474
7. 259.	-0.1510	-0.1532	-0.1495	-0.1304	-0.0965	-0.0449	0.0186	0.0813	0.1381	0.1843	0.2142	0.2334	0.2448	0.2479	0.2572	0.2682	0.2847
7. 250.	-0.1146	-0.1147	-0.1113	-0.0983	-0.0756	-0.0405	0.0059	0.0567	0.1088	0.1583	0.2005	0.2321	0.2582	0.2755	0.2925	0.3099	0.3287
7. 241.	-0.0970	-0.0962	-0.0934	-0.0839	-0.0670	-0.0395	-0.0064	0.0325	0.0749	0.1162	0.1564	0.1929	0.2272	0.2533	0.2781	0.3018	0.3236
Run Point	CP103	CP104	CP105	CP106	CP107	CP108	CP109	CP110									
7. 223.	0.2622	0.2871	0.3380	0.3775	0.4544	0.5080	0.5267	0.4994									
7. 214.	0.2547	0.2865	0.3318	0.3846	0.4531	0.5086	0.5275	0.4989									
7. 232.	0.2741	0.3072	0.3545	0.4111	0.5115	0.5511	0.5581	0.5507									
7. 259.	0.3107	0.3446	0.3877	0.4362	0.4922	0.5362	0.5600	0.5018									
7. 250.	0.3536	0.3827	0.4169	0.4519	0.4924	0.5255	0.5450	0.4848									
7. 241.	0.3474	0.3724	0.3997	0.4232	0.4554	0.4832	0.4937	0.4467									

Table 10. Continued

(c) $Z_g = 2.37$ in.

Run Point	M_∞	$R_\infty \times 10^{-6}$	p_∞ , psi	$P_{t,\infty}$, psi	q_∞ , psi	$T_{t,\infty}$, °F	CP01	CP02	CP03	CP04	CP05	CP06	CP07	CP08	CP09	CP10	CP11
7. 228.	0.20	2.04	22.97	23.63	0.65	101.7	0.8700	-0.2400	-0.2032	-0.1855	-0.1648	-0.1314	-0.1047	-0.0894	-0.0788	-0.0559	-0.0582
7. 219.	0.40	3.62	19.91	22.23	2.23	101.8	0.9111	-0.2572	-0.2065	-0.1928	-0.1673	-0.1413	-0.1037	-0.0905	-0.0751	-0.0629	-0.0559
7. 237.	0.60	4.69	16.33	20.85	4.14	101.6	0.9946	-0.2904	-0.2285	-0.2143	-0.1856	-0.1554	-0.1123	-0.0974	-0.0790	-0.0681	-0.0595
7. 264.	0.80	3.81	9.31	14.18	4.17	99.6	1.1274	-0.3266	-0.2756	-0.2538	-0.2222	-0.1822	-0.1255	-0.0991	-0.0768	-0.0635	-0.0509
7. 255.	0.90	3.52	7.37	12.48	4.19	100.9	1.2035	-0.3766	-0.3521	-0.3689	-0.3438	-0.1782	-0.0943	-0.0678	-0.0470	-0.0345	-0.0231
7. 246.	0.95	3.40	6.59	11.81	4.18	101.2	1.2400	-0.2673	-0.2794	-0.3129	-0.3287	-0.3573	-0.3610	-0.3538	-0.0385	0.0452	0.0552
Run Point	CP12	CP13	CP14	CP15	CP16	CP17	CP18	CP19	CP20	CP21	CP22	CP23	CP24	CP25	CP26	CP27	CP28
7. 228.	-0.0519	-0.0411	-0.0364	-0.0318	-0.0269	-0.0350	-0.0287	-0.0245	-0.0279	-0.0221	-0.0256	-0.0407	-0.0691	-0.0295	-0.0391	0.0087	0.0497
7. 219.	-0.0494	-0.0443	-0.0365	-0.0316	-0.0272	-0.0267	-0.0248	-0.0250	-0.0271	-0.0282	-0.0330	-0.0439	-0.0707	-0.0343	-0.0408	0.0027	0.0554
7. 237.	-0.0533	-0.0479	-0.0386	-0.0328	-0.0305	-0.0290	-0.0280	-0.0281	-0.0288	-0.0320	-0.0374	-0.0478	-0.0762	-0.0421	-0.0512	-0.0063	0.0580
7. 264.	-0.0430	-0.0384	-0.0288	-0.0231	-0.0197	-0.0170	-0.0166	-0.0189	-0.0200	-0.0235	-0.0294	-0.0393	-0.0647	-0.0371	-0.0558	-0.0165	0.0693
7. 255.	-0.0161	-0.0123	-0.0040	0.0004	0.0035	0.0055	0.0057	0.0035	-0.0023	-0.0023	-0.0083	-0.0171	-0.0394	-0.0182	-0.0396	-0.0029	0.0970
7. 246.	0.0497	0.0412	0.0343	0.0303	0.0276	0.0258	0.0227	0.0170	0.0128	0.0069	-0.0010	-0.0105	-0.0325	-0.0150	-0.0398	-0.0057	0.0980
Run Point	CP29	CP30	CP31	CP32	CP33	CP34	CP35	CP36	CP37	CP38	CP39	CP40	CP41	CP42	CP43	CP44	CP45
7. 228.	0.0696	0.0200	-0.0444	-0.0949	-0.0986	-0.0716	-0.0577	-0.0486	-0.0469	-0.0363	-0.0355	-0.0636	-0.0396	-0.0409	-0.0267	-0.0306	-0.0277
7. 219.	0.0733	0.0232	-0.0518	-0.1162	-0.1143	-0.0895	-0.0694	-0.0557	-0.0496	-0.0433	-0.0422	-0.0620	-0.0513	-0.0482	-0.0482	-0.0407	-0.0368
7. 237.	0.0831	0.0275	-0.0705	-0.1630	-0.1584	-0.1242	-0.0978	-0.0795	-0.0705	-0.0640	-0.0621	-0.0871	-0.0766	-0.0710	-0.0688	-0.0672	-0.0636
7. 264.	0.1118	0.0513	-0.0893	-0.2504	-0.2430	-0.1920	-0.1526	-0.1269	-0.1172	-0.1143	-0.1203	-0.1445	-0.1417	-0.1452	-0.1549	-0.1670	-0.1844
7. 255.	0.1613	0.1115	-0.0338	-0.2355	-0.2194	-0.1476	-0.1035	-0.0719	-0.0554	-0.0471	-0.0468	-0.0739	-0.0664	-0.0676	-0.0755	-0.0867	-0.1035
7. 246.	0.1762	0.1345	-0.0030	-0.2064	-0.2178	-0.1118	-0.0573	-0.0277	-0.0112	-0.0023	0.0000	-0.0220	-0.0139	-0.0142	-0.0200	-0.0306	-0.0456
Run Point	CP46	CP47	CP48	CP49	CP50	CP51	CP52	CP53	CP54	CP55	CP56	CP57	CP58	CP59	CP60	CP61	CP62
7. 228.	-0.0225	0.0168	0.0647	-0.1074	-0.0284	-0.1307	-0.1266	-0.1430	-0.1371	-0.1492	-0.1358	-0.1423	-0.1285	-0.0840	0.0339	0.0292	0.1001
7. 219.	-0.0304	0.0147	0.0714	-0.1246	-0.0389	-0.1354	-0.1334	-0.1328	-0.1382	-0.1341	-0.1420	-0.1636	-0.1030	-0.0849	-0.0070	0.0539	0.0909
7. 237.	-0.0355	0.0083	0.0802	-0.1709	-0.0613	-0.1478	-0.1502	-0.1462	-0.1462	-0.1510	-0.1570	-0.1561	-0.1045	-0.0634	-0.0161	0.0396	0.0824
7. 264.	-0.0334	-0.0006	0.1079	-0.2642	-0.1197	-0.1333	-0.1384	-0.1359	-0.1381	-0.1402	-0.1330	-0.1415	-0.1187	-0.0848	-0.0408	0.0098	0.0539
7. 255.	-0.0148	0.0133	0.1586	-0.2478	-0.0473	-0.0949	-0.0999	-0.0975	-0.0993	-0.1031	-0.0986	-0.1053	-0.0925	-0.0668	-0.0359	0.0086	0.0508
7. 246.	-0.0126	0.0109	0.1741	-0.2356	-0.0006	-0.0761	-0.0803	-0.0774	-0.0782	-0.0827	-0.0794	-0.0847	-0.0793	-0.0627	-0.0296	0.0010	0.0364

Table 10. Concluded

(c) Concluded

Run Point	CP63	CP64	CP65	CP66	CP67	CP68	CP69	CP70	CP77	CP78	CP79	CP80	CP81	CP82	CP83	CP84	CP85
7. 228.	0.1602	0.1748	0.1864	0.2053	0.2459	0.3092	0.3921	0.4559	-0.1269	-0.1521	0.0828	0.2053	0.3088	-0.1333	-0.1493	-0.1380	-0.1485
7. 219.	0.1353	0.1636	0.1916	0.2201	0.2522	0.3155	0.3990	0.5081	-0.1346	-0.1591	0.0825	0.1989	0.3227	-0.1356	-0.1421	-0.1413	-0.1464
7. 237.	0.1338	0.1728	0.1867	0.2177	0.2634	0.3315	0.4283	0.5085	-0.1431	-0.1647	0.0723	0.1981	0.3374	-0.1429	-0.1495	-0.1500	-0.1531
7. 264.	0.1181	0.1672	0.2154	0.2548	0.3043	0.3701	0.4484	0.5116	-0.1319	-0.1475	0.0607	0.2158	0.3715	-0.1323	-0.1386	-0.1394	-0.1409
7. 255.	0.1263	0.1850	0.2378	0.2907	0.3446	0.4078	0.4718	0.4976	-0.0979	-0.1101	0.0580	0.2412	0.4050	-0.0978	-0.1036	-0.1051	-0.1051
7. 246.	0.1039	0.1742	0.2300	0.2842	0.3410	0.3925	0.4499	0.4756	-0.0805	-0.0923	0.0536	0.2303	0.3861	-0.0808	-0.0872	-0.0880	-0.0873
Run Point	CP86	CP87	CP88	CP89	CP90	CP91	CP92	CP93	CP94	CP95	CP96	CP97	CP98	CP99	CP100	CP101	CP102
7. 228.	-0.1489	-0.1610	-0.1527	-0.1137	-0.0423	0.0569	0.1321	0.1829	0.2102	0.2231	0.2160	0.2103	0.2093	0.2002	0.2060	0.2227	0.2370
7. 219.	-0.1553	-0.1638	-0.1606	-0.1286	-0.0653	0.0179	0.1041	0.1668	0.2037	0.2207	0.2237	0.2196	0.2165	0.2089	0.2166	0.2259	0.2398
7. 237.	-0.1619	-0.1690	-0.1634	-0.1344	-0.0789	-0.0029	0.0767	0.1443	0.1892	0.2159	0.2248	0.2262	0.2265	0.2203	0.2287	0.2378	0.2534
7. 264.	-0.1467	-0.1522	-0.1523	-0.1370	-0.1028	-0.0518	0.0104	0.0722	0.1276	0.1744	0.2078	0.2282	0.2437	0.2504	0.2614	0.2733	0.2901
7. 255.	-0.1089	-0.1125	-0.1133	-0.1030	-0.0800	-0.0440	0.0018	0.0514	0.0992	0.1466	0.1893	0.2223	0.2522	0.2723	0.2914	0.3098	0.3286
7. 246.	-0.0905	-0.0931	-0.0941	-0.0879	-0.0716	-0.0449	-0.0105	0.0292	0.0707	0.1123	0.1523	0.1897	0.2237	0.2512	0.2767	0.2999	0.3213
Run Point	CP103	CP104	CP105	CP106	CP107	CP108	CP109	CP110									
7. 228.	0.2604	0.2835	0.3312	0.3606	0.4380	0.4907	0.5136	0.4854									
7. 219.	0.2628	0.2919	0.3342	0.3797	0.4423	0.4960	0.5240	0.4940									
7. 237.	0.2781	0.3092	0.3518	0.4000	0.4600	0.5121	0.5352	0.5065									
7. 264.	0.3144	0.3446	0.3815	0.4188	0.4652	0.5018	0.5214	0.4969									
7. 255.	0.3520	0.3784	0.4085	0.4380	0.4728	0.5015	0.5224	0.4904									
7. 246.	0.3445	0.3683	0.3932	0.4156	0.4440	0.4667	0.4819	0.4575									

Table 11. Pressure Coefficients for Configuration 11 With $h = 4.80$ in., $l = 26.00$ in., $Y_s = 0.00$ in., and $Z_s = -3.00$ in.

Run Point	M_∞	$R_\infty \times 10^{-6}$	p_∞ , psi	$p_{t,\infty}$, psi	q_∞ , psi	$T_{t,\infty}$, °F	CP01	CP02	CP03	CP04	CP05	CP06	CP07	CP08	CP09	CP10	CP11
16. 658.	0.20	2.05	22.94	23.60	0.65	98.6	0.8729	-0.2413	-0.1962	-0.1808	-0.1558	-0.1321	-0.1026	-0.0822	-0.0737	-0.0644	-0.0525
16. 650.	0.40	3.61	19.92	22.23	2.22	101.6	0.9132	-0.2505	-0.2076	-0.1927	-0.1661	-0.1429	-0.1055	-0.0915	-0.0767	-0.0664	-0.0575
16. 641.	0.60	2.81	9.80	12.50	2.47	100.5	0.9989	-0.2783	-0.2365	-0.2165	-0.1917	-0.1606	-0.1230	-0.1042	-0.0856	-0.0680	-0.0631
16. 633.	0.80	2.53	6.19	9.44	2.78	100.1	1.1312	-0.3206	-0.2780	-0.2516	-0.2226	-0.1813	-0.1296	-0.1011	-0.0785	-0.0600	-0.0512
16. 617.	0.95	2.41	4.67	8.35	2.95	99.6	1.2377	-0.2613	-0.2737	-0.2988	-0.3212	-0.3524	-0.3630	-0.3470	-0.0144	0.0418	0.0474
Run Point	CP12	CP13	CP14	CP15	CP16	CP17	CP18	CP19	CP20	CP21	CP22	CP23	CP24	CP25	CP26	CP27	CP28
16. 658.	-0.0445	-0.0447	-0.0314	-0.0261	-0.0216	-0.0225	-0.0168	-0.0143	-0.0065	-0.0141	-0.0126	-0.0074	-0.0008	-0.0119	0.0029	-0.0020	-0.0092
16. 650.	-0.0502	-0.0475	-0.0379	-0.0311	-0.0255	-0.0235	-0.0183	-0.0159	-0.0145	-0.0128	-0.0098	-0.0073	-0.0089	-0.0115	-0.0053	-0.0083	-0.0172
16. 641.	-0.0577	-0.0511	-0.0425	-0.0386	-0.0343	-0.0329	-0.0276	-0.0225	-0.0240	-0.0187	-0.0152	-0.0182	-0.0247	-0.0172	-0.0155	-0.0163	-0.0145
16. 633.	-0.0451	-0.0383	-0.0274	-0.0214	-0.0164	-0.0138	-0.0100	-0.0065	-0.0086	-0.0062	-0.0058	-0.0095	-0.0164	-0.0088	-0.0044	-0.0079	0.0003
16. 617.	0.0427	0.0358	0.0308	0.0288	0.0286	0.0276	0.0259	0.0232	0.0208	0.0176	0.0151	0.0152	0.0143	0.0123	0.0277	0.0231	0.0329
Run Point	CP29	CP30	CP31	CP32	CP33	CP34	CP35	CP36	CP37	CP38	CP39	CP40	CP41	CP42	CP43	CP44	CP45
16. 658.	-0.0302	-0.0331	-0.0305	-0.0302	-0.0207	-0.0253	-0.0210	-0.0193	-0.0192	-0.0294	-0.0250	-0.0296	-0.0205	-0.0247	-0.0262	-0.0217	-0.0266
16. 650.	-0.0143	-0.0438	-0.0433	-0.0387	-0.0320	-0.0328	-0.0309	-0.0285	-0.0288	-0.0293	-0.0318	-0.0347	-0.0273	-0.0291	-0.0322	-0.0326	-0.0336
16. 641.	-0.0047	-0.0904	-0.0858	-0.0717	-0.0643	-0.0560	-0.0529	-0.0520	-0.0518	-0.0535	-0.0587	-0.0616	-0.0539	-0.0562	-0.0593	-0.0636	-0.0680
16. 633.	0.0038	-0.1220	-0.1135	-0.0945	-0.0842	-0.0769	-0.0759	-0.0781	-0.0826	-0.0912	-0.1049	-0.1054	-0.1069	-0.1184	-0.1334	-0.1502	-0.1712
16. 617.	0.0369	-0.0739	-0.0578	-0.0308	-0.0103	0.0031	0.0108	0.0167	0.0172	0.0158	0.0094	0.0039	0.0056	-0.0007	-0.0106	-0.0241	-0.0414
Run Point	CP46	CP47	CP48	CP49	CP50	CP51	CP52	CP53	CP54	CP55	CP56	CP57	CP58	CP59	CP60	CP61	CP62
16. 658.	-0.0071	-0.0037	-0.0152	-0.0264	-0.0281	0.0174	0.0106	0.0153	0.0145	0.0087	-0.0115	0.0064	-0.0259	-0.0333	-0.0260	0.0205	0.0386
16. 650.	-0.0102	-0.0095	-0.0145	-0.0376	-0.0316	0.0012	-0.0036	0.0059	0.0075	-0.0063	-0.0122	-0.0065	-0.0128	-0.0236	-0.0230	-0.0089	-0.0253
16. 641.	-0.0158	-0.0191	-0.0087	-0.0695	-0.0566	-0.0076	-0.0057	-0.0178	-0.0257	-0.0399	-0.0335	-0.0343	-0.0361	-0.0476	-0.0668	-0.0820	-0.0769
16. 633.	-0.0074	-0.0094	0.0013	-0.0911	-0.1011	0.0124	0.0115	0.0067	0.0047	0.0000	-0.0009	-0.0013	-0.0088	-0.0334	-0.0409	-0.0515	-0.0485
16. 617.	0.0130	0.0254	0.0382	-0.0230	0.0103	0.0386	0.0346	0.0312	0.0273	0.0206	0.0126	0.0018	-0.0031	-0.0012	-0.0077	0.0021	0.0023

Table 11. Concluded

Run Point	CP63	CP64	CP65	CP66	CP67	CP68	CP71	CP72	CP73	CP74	CP75	CP76	CP77	CP78	CP79	CP80	CP81
16. 658.	-0.0112	-0.0554	-0.1000	-0.0996	-0.0346	-0.0280	0.0065	-0.0074	-0.0811	0.0187	0.0006	-0.0710	0.0050	0.0051	-0.0183	-0.0615	-0.0224
16. 650.	-0.0362	-0.0518	-0.0064	0.0116	0.0116	0.0420	-0.0061	-0.0152	-0.0216	0.0000	-0.0075	-0.0322	-0.0010	-0.0015	-0.0353	-0.0608	0.0178
16. 641.	-0.0317	0.0066	0.0495	0.0779	0.0576	0.0359	-0.0074	-0.0236	0.0464	-0.0067	-0.0215	0.0456	-0.0109	-0.0313	-0.0607	0.0447	0.0260
16. 633.	-0.0213	0.0216	0.0580	0.0741	0.0431	0.0313	0.0118	-0.0042	0.0460	0.0118	-0.0028	0.0353	-0.0061	-0.0227	-0.0456	0.0542	0.0243
16. 617.	0.0165	0.0528	0.0709	0.0733	0.0686	0.0625	0.0334	0.0174	0.0673	0.0352	0.0190	0.0646	0.0309	0.0151	0.0096	0.0578	0.0487
Run Point	CP82	CP83	CP84	CP85	CP86	CP87	CP88	CP89	CP90	CP91	CP92	CP93	CP94	CP95	CP96	CP97	CP98
16. 658.	0.0133	-0.0021	0.0016	0.0055	-0.0059	-0.0020	-0.0013	-0.0084	-0.0182	-0.0267	-0.0253	-0.0241	-0.0310	-0.0425	-0.0474	-0.0590	-0.0620
16. 650.	0.0041	-0.0019	-0.0034	-0.0048	-0.0106	-0.0128	-0.0156	-0.0192	-0.0249	-0.0313	-0.0367	-0.0434	-0.0487	-0.0528	-0.0544	-0.0521	-0.0468
16. 641.	-0.0135	-0.0171	-0.0192	-0.0239	-0.0254	-0.0322	-0.0355	-0.0412	-0.0450	-0.0526	-0.0570	-0.0561	-0.0497	-0.0423	-0.0310	-0.0200	-0.0087
16. 633.	-0.0027	-0.0061	-0.0066	-0.0112	-0.0135	-0.0184	-0.0228	-0.0285	-0.0344	-0.0406	-0.0431	-0.0432	-0.0371	-0.0286	-0.0160	-0.0017	0.0112
16. 617.	0.0296	0.0256	0.0230	0.0188	0.0182	0.0141	0.0096	0.0056	0.0013	-0.0028	-0.0019	-0.0035	0.0003	0.0094	0.0164	0.0257	0.0333
Run Point	CP99	CP100	CP101	CP102	CP103	CP104	CP105	CP106									
16. 658.	-0.0733	-0.0834	-0.0929	-0.0863	-0.0669	-0.0284	0.0403	0.1858									
16. 650.	-0.0421	-0.0321	-0.0211	-0.0058	0.0112	0.0388	0.0946	0.2073									
16. 641.	0.0016	0.0205	0.0375	0.0471	0.0622	0.0773	0.1160	0.2286									
16. 633.	0.0243	0.0358	0.0480	0.0623	0.0721	0.0790	0.1273	0.2488									
16. 617.	0.0431	0.0515	0.0616	0.0667	0.0739	0.0881	0.1359	0.2606									

Table 12. Pressure Coefficients for Configuration 12 With $h = 4.80$ in., $l = 26.00$ in., and $Y_s = 0.00$ in.(a) $Z_s = 0.00$ in.

Run Point	M_∞	$R_\infty \times 10^{-6}$	p_∞ , psi	$p_{t,\infty}$, psi	q_∞ , psi	$T_{t,\infty}$, °F	CP01	CP02	CP03	CP04	CP05	CP06	CP07	CP08	CP09	CP10	CP11
15. 606.	0.20	2.04	22.97	23.62	0.65	100.5	0.8791	-0.2392	-0.2041	-0.1819	-0.1802	-0.1315	-0.1117	-0.1008	-0.0837	-0.0336	-0.0631
15. 597.	0.40	3.63	19.91	22.23	2.24	101.7	0.9129	-0.2445	-0.2082	-0.1912	-0.1709	-0.1413	-0.1064	-0.0950	-0.0771	-0.0568	-0.0600
15. 588.	0.60	2.82	9.81	12.51	2.47	100.5	1.0000	-0.2707	-0.2300	-0.2088	-0.1860	-0.1567	-0.1183	-0.0988	-0.0806	-0.0620	-0.0590
15. 579.	0.80	2.54	6.20	9.46	2.78	99.7	1.1316	-0.3204	-0.2770	-0.2499	-0.2222	-0.1825	-0.1303	-0.1015	-0.0784	-0.0599	-0.0527
15. 570.	0.90	2.36	4.93	8.34	2.79	99.6	1.2040	-0.3738	-0.3221	-0.3351	-0.3362	-0.1994	-0.1060	-0.0727	-0.0506	-0.0331	-0.0257
15. 561.	0.95	2.40	4.65	8.34	2.96	101.1	1.2370	-0.2633	-0.2671	-0.2945	-0.3183	-0.3501	-0.3598	-0.3488	-0.0222	0.0417	0.0464
Run Point	CP12	CP13	CP14	CP15	CP16	CP17	CP18	CP19	CP20	CP21	CP22	CP23	CP24	CP25	CP26	CP27	CP28
15. 606.	-0.0628	-0.0373	-0.0416	-0.0420	-0.0348	-0.0546	-0.0308	-0.0201	-0.0357	0.0057	0.0256	0.0040	-0.0155	0.0162	-0.0238	0.0029	-0.0461
15. 597.	-0.0553	-0.0447	-0.0405	-0.0367	-0.0335	-0.0355	-0.0272	-0.0227	-0.0264	-0.0131	-0.0068	-0.0111	-0.0163	-0.0077	-0.0153	-0.0081	-0.0176
15. 588.	-0.0529	-0.0446	-0.0386	-0.0346	-0.0294	-0.0300	-0.0229	-0.0193	-0.0221	-0.0130	-0.0114	-0.0173	-0.0205	-0.0135	-0.0155	-0.0119	0.0011
15. 579.	-0.0453	-0.0375	-0.0295	-0.0233	-0.0190	-0.0190	-0.0151	-0.0144	-0.0161	-0.0114	-0.0086	-0.0098	-0.0139	-0.0098	-0.0090	-0.0124	0.0016
15. 570.	-0.0184	-0.0120	-0.0047	0.0009	0.0053	0.0055	0.0080	0.0082	0.0071	0.0100	0.0116	0.0097	0.0053	0.0092	0.0153	0.0145	0.0299
15. 561.	0.0415	0.0355	0.0297	0.0274	0.0274	0.0249	0.0242	0.0217	0.0180	0.0159	0.0139	0.0131	0.0112	0.0111	0.0228	0.0194	0.0428
Run Point	CP29	CP30	CP31	CP32	CP33	CP34	CP35	CP36	CP37	CP38	CP39	CP40	CP41	CP42	CP43	CP44	CP45
15. 606.	-0.0294	-0.0444	-0.0239	-0.0123	-0.0410	-0.0095	-0.0176	-0.0354	-0.0382	-0.0124	-0.0448	-0.0596	-0.0240	-0.0224	-0.0179	-0.0246	-0.0374
15. 597.	-0.0066	-0.0599	-0.0504	-0.0397	-0.0411	-0.0292	-0.0309	-0.0358	-0.0378	-0.0288	-0.0407	-0.0456	-0.0300	-0.0296	-0.0293	-0.0317	-0.0377
15. 588.	0.0181	-0.0991	-0.0900	-0.0734	-0.0656	-0.0526	-0.0491	-0.0494	-0.0503	-0.0458	-0.0559	-0.0593	-0.0495	-0.0502	-0.0517	-0.0556	-0.0615
15. 579.	0.0134	-0.1347	-0.1218	-0.1011	-0.0903	-0.0800	-0.0787	-0.0822	-0.0880	-0.0924	-0.1090	-0.1104	-0.1131	-0.1222	-0.1353	-0.1537	-0.1752
15. 570.	0.0448	-0.1024	-0.0839	-0.0578	-0.0406	-0.0263	-0.0214	-0.0204	-0.0212	-0.0232	-0.0359	-0.0397	-0.0378	-0.0468	-0.0599	-0.0769	-0.0978
15. 561.	0.0571	-0.0948	-0.0727	-0.0395	-0.0167	0.0001	0.0087	0.0150	0.0170	0.0172	0.0083	0.0036	0.0066	0.0002	-0.0095	-0.0230	-0.0408
Run Point	CP46	CP47	CP48	CP49	CP50	CP51	CP52	CP53	CP54	CP55	CP56	CP57	CP58	CP59	CP60	CP61	CP62
15. 606.	0.0134	-0.0198	-0.0456	-0.0374	-0.0055	-0.0255	0.0243	-0.0435	-0.0288	-0.0343	-0.0062	-0.0043	0.0081	0.0462	0.0277	-0.0743	-0.0391
15. 597.	-0.0064	-0.0155	-0.0090	-0.0451	-0.0251	-0.0064	0.0021	-0.0218	-0.0190	-0.0248	-0.0267	-0.0246	-0.0141	-0.0239	-0.0268	-0.0375	-0.0251
15. 588.	-0.0133	-0.0163	0.0132	-0.0722	-0.0469	-0.0131	-0.0079	-0.0344	-0.0380	-0.0516	-0.0594	-0.0882	-0.1176	-0.1067	-0.1196	-0.0780	-0.0595
15. 579.	-0.0086	-0.0138	0.0093	-0.0959	-0.1024	-0.0083	-0.0049	-0.0153	-0.0212	-0.0266	-0.0296	-0.0319	-0.0384	-0.0437	-0.0528	-0.0624	-0.0480
15. 570.	0.0108	0.0119	0.0408	-0.0519	-0.0301	0.0168	0.0192	0.0110	0.0048	-0.0036	-0.0053	-0.0006	-0.0018	-0.0008	-0.0108	-0.0191	-0.0169
15. 561.	0.0118	0.0191	0.0561	-0.0292	0.0127	0.0268	0.0270	0.0214	0.0147	0.0129	0.0096	0.0086	0.0056	-0.0013	-0.0046	-0.0097	-0.0017

Table 12. Continued

(a) Concluded

Run Point	CP63	CP64	CP65	CP66	CP67	CP68	CP71	CP72	CP73	CP74	CP75	CP76	CP77	CP78	CP79	CP80	CP81
15. 606.	-0.0226	0.0071	-0.0920	-0.0637	-0.0292	0.0304	0.0316	-0.0261	-0.0999	-0.0176	-0.0313	-0.0557	0.0217	-0.0035	-0.0295	-0.0462	0.0156
15. 597.	-0.0297	-0.0206	-0.0254	0.0188	0.0246	0.0081	0.0086	-0.0162	-0.0463	-0.0020	-0.0219	-0.0235	0.0004	-0.0200	-0.0395	0.0010	0.0132
15. 588.	-0.0213	0.0515	0.0861	0.1079	0.0940	0.0809	-0.0056	-0.0690	0.0904	-0.0212	-0.0632	0.0888	-0.0205	-0.0478	-0.0679	0.0803	0.1089
15. 579.	-0.0200	0.0310	0.0603	0.0819	0.0723	0.0475	-0.0043	-0.0243	0.0472	-0.0091	-0.0246	0.0378	-0.0069	-0.0230	-0.0417	0.0514	0.0532
15. 570.	0.0040	0.0424	0.0814	0.1036	0.0847	0.0564	0.0195	0.0028	0.0690	0.0149	0.0061	0.0650	0.0179	0.0022	-0.0160	0.0862	0.0557
15. 561.	0.0263	0.0658	0.0886	0.1047	0.0814	0.0657	0.0254	0.0148	0.0679	0.0245	0.0164	0.0630	0.0255	0.0085	-0.0039	0.0888	0.0700
Run Point	CP82	CP83	CP84	CP85	CP86	CP87	CP88	CP89	CP90	CP91	CP92	CP93	CP94	CP95	CP96	CP97	CP98
15. 606.	-0.0031	0.0012	0.0258	-0.0169	0.0325	-0.0010	-0.0096	-0.0183	0.0045	-0.0025	-0.0168	-0.0373	-0.0223	-0.0264	-0.0522	-0.0430	-0.1020
15. 597.	-0.0064	-0.0074	-0.0030	-0.0180	-0.0067	-0.0204	-0.0264	-0.0316	-0.0290	-0.0350	-0.0376	-0.0448	-0.0406	-0.0393	-0.0427	-0.0352	-0.0452
15. 588.	-0.0214	-0.0246	-0.0228	-0.0331	-0.0277	-0.0360	-0.0428	-0.0514	-0.0534	-0.0567	-0.0557	-0.0532	-0.0376	-0.0150	0.0064	0.0321	0.0453
15. 579.	-0.0077	-0.0104	-0.0100	-0.0176	-0.0147	-0.0223	-0.0288	-0.0360	-0.0383	-0.0440	-0.0466	-0.0474	-0.0408	-0.0274	-0.0146	0.0024	0.0116
15. 570.	0.0147	0.0125	0.0131	0.0069	0.0097	0.0041	-0.0003	-0.0064	-0.0085	-0.0122	-0.0139	-0.0140	-0.0078	0.0037	0.0133	0.0277	0.0339
15. 561.	0.0245	0.0212	0.0204	0.0151	0.0174	0.0130	0.0074	0.0029	0.0005	-0.0020	-0.0023	-0.0024	0.0031	0.0133	0.0223	0.0341	0.0407
Run Point	CP99	CP100	CP101	CP102	CP103	CP104	CP105	CP106									
15. 606.	-0.0970	-0.0874	-0.0600	-0.0651	-0.0514	-0.0486	0.0345	0.1243									
15. 597.	-0.0348	-0.0200	-0.0040	0.0029	0.0196	0.0326	0.0917	0.1915									
15. 588.	0.0674	0.0869	0.1037	0.1119	0.1235	0.1301	0.1623	0.2381									
15. 579.	0.0273	0.0434	0.0615	0.0763	0.0951	0.1133	0.1451	0.2332									
15. 570.	0.0478	0.0578	0.0713	0.0842	0.1003	0.1124	0.1575	0.2530									
15. 561.	0.0514	0.0640	0.0787	0.0930	0.1110	0.1269	0.1647	0.2611									

Table 12. Continued

(b) $Z_s = 2.31$ in.

Run Point	M_∞	$R_\infty \times 10^{-6}$	p_∞ , psi	$p_{t,\infty}$, psi	q_∞ , psi	$T_{t,\infty}$, °F	CP01	CP02	CP03	CP04	CP05	CP06	CP07	CP08	CP09	CP10	CP11
15. 611.	0.20	2.03	22.97	23.62	0.64	101.2	0.8772	-0.2373	-0.2032	-0.1807	-0.1803	-0.1300	-0.1079	-0.0981	-0.0797	-0.0292	-0.0612
15. 602.	0.40	3.63	19.91	22.23	2.24	101.4	0.9167	-0.2434	-0.2066	-0.1892	-0.1700	-0.1397	-0.1047	-0.0924	-0.0749	-0.0539	-0.0565
15. 593.	0.60	2.81	9.81	12.52	2.48	101.5	1.0008	-0.2697	-0.2294	-0.2074	-0.1861	-0.1548	-0.1168	-0.0972	-0.0789	-0.0604	-0.0579
15. 584.	0.80	2.54	6.20	9.45	2.78	99.6	1.1308	-0.3193	-0.2763	-0.2487	-0.2222	-0.1814	-0.1293	-0.1007	-0.0783	-0.0585	-0.0510
15. 575.	0.90	2.36	4.93	8.34	2.80	99.7	1.2035	-0.3737	-0.3228	-0.3358	-0.3364	-0.1944	-0.1059	-0.0739	-0.0511	-0.0334	-0.0260
15. 566.	0.95	2.40	4.66	8.34	2.95	100.4	1.2401	-0.2628	-0.2673	-0.2947	-0.3186	-0.3494	-0.3599	-0.3467	-0.0173	0.0453	0.0478
Run Point	CP12	CP13	CP14	CP15	CP16	CP17	CP18	CP19	CP20	CP21	CP22	CP23	CP24	CP25	CP26	CP27	CP28
15. 611.	-0.0621	-0.0343	-0.0385	-0.0400	-0.0318	-0.0537	-0.0277	-0.0168	-0.0325	0.0080	0.0303	0.0086	-0.0122	0.0197	-0.0239	0.0040	-0.0497
15. 602.	-0.0524	-0.0419	-0.0369	-0.0325	-0.0254	-0.0281	-0.0197	-0.0162	-0.0200	-0.0064	0.0016	0.0002	-0.0055	-0.0024	-0.0099	-0.0069	-0.0176
15. 593.	-0.0522	-0.0428	-0.0368	-0.0316	-0.0263	-0.0273	-0.0209	-0.0181	-0.0197	-0.0109	-0.0067	-0.0088	-0.0124	-0.0078	-0.0120	-0.0079	0.0076
15. 584.	-0.0436	-0.0350	-0.0267	-0.0210	-0.0171	-0.0167	-0.0131	-0.0134	-0.0143	-0.0106	-0.0071	-0.0072	-0.0058	-0.0078	-0.0070	-0.0114	0.0009
15. 575.	-0.0189	-0.0120	-0.0044	0.0009	0.0053	0.0052	0.0087	0.0089	0.0078	0.0118	0.0139	0.0141	0.0124	0.0128	0.0183	0.0150	0.0306
15. 566.	0.0423	0.0377	0.0315	0.0292	0.0291	0.0267	0.0264	0.0248	0.0212	0.0215	0.0210	0.0193	0.0165	0.0176	0.0262	0.0233	0.0422
Run Point	CP29	CP30	CP31	CP32	CP33	CP34	CP35	CP36	CP37	CP38	CP39	CP40	CP41	CP42	CP43	CP44	CP45
15. 611.	-0.0307	-0.0503	-0.0295	-0.0157	-0.0390	-0.0095	-0.0177	-0.0389	-0.0373	-0.0136	-0.0473	-0.0545	-0.0177	-0.0193	-0.0244	-0.0314	-0.0482
15. 602.	-0.0079	-0.0602	-0.0510	-0.0390	-0.0404	-0.0285	-0.0274	-0.0327	-0.0347	-0.0258	-0.0367	-0.0434	-0.0300	-0.0299	-0.0290	-0.0323	-0.0386
15. 593.	0.0143	-0.1049	-0.0918	-0.0721	-0.0635	-0.0491	-0.0456	-0.0478	-0.0482	-0.0445	-0.0535	-0.0555	-0.0449	-0.0462	-0.0491	-0.0538	-0.0597
15. 584.	0.0086	-0.1335	-0.1206	-0.0995	-0.0887	-0.0779	-0.0768	-0.0799	-0.0849	-0.0892	-0.1052	-0.1099	-0.1069	-0.1175	-0.1346	-0.1517	-0.1722
15. 575.	0.0381	-0.1046	-0.0861	-0.0595	-0.0423	-0.0278	-0.0224	-0.0211	-0.0227	-0.0238	-0.0361	-0.0399	-0.0393	-0.0480	-0.0599	-0.0769	-0.0979
15. 566.	0.0504	-0.0937	-0.0704	-0.0390	-0.0179	0.0002	0.0090	0.0137	0.0154	0.0165	0.0076	0.0039	0.0069	0.0002	-0.0090	-0.0240	-0.0427
Run Point	CP46	CP47	CP48	CP49	CP50	CP51	CP52	CP53	CP54	CP55	CP56	CP57	CP58	CP59	CP60	CP61	CP62
15. 611.	0.0169	-0.0199	-0.0537	-0.0409	-0.0010	-0.0200	0.0298	-0.0416	-0.0245	-0.0292	0.0086	0.0077	-0.0135	0.0132	-0.0039	-0.0445	-0.0191
15. 602.	-0.0010	-0.0139	-0.0106	-0.0435	-0.0258	-0.0039	0.0124	-0.0103	-0.0081	-0.0230	-0.0282	-0.0284	-0.0381	-0.0275	-0.0555	-0.0859	-0.1006
15. 593.	-0.0069	-0.0131	0.0152	-0.0706	-0.0433	-0.0160	-0.0090	-0.0228	-0.0229	-0.0312	-0.0307	-0.0259	-0.0242	-0.0418	-0.0504	-0.0602	-0.0530
15. 584.	-0.0063	-0.0117	0.0059	-0.0971	-0.0995	-0.0021	-0.0015	-0.0169	-0.0174	-0.0188	-0.0238	-0.0231	-0.0335	-0.0376	-0.0473	-0.0465	-0.0353
15. 575.	0.0144	0.0114	0.0385	-0.0531	-0.0312	0.0260	0.0281	0.0194	0.0171	0.0127	0.0137	0.0132	0.0052	-0.0122	-0.0199	-0.0191	-0.0049
15. 566.	0.0192	0.0231	0.0504	-0.0304	0.0120	0.0359	0.0379	0.0309	0.0254	0.0185	0.0161	0.0122	0.0122	0.0055	-0.0002	-0.0031	0.0100

Table 12. Concluded

(b) Concluded

Run Point	CP63	CP64	CP65	CP66	CP67	CP68	CP71	CP72	CP73	CP74	CP75	CP76	CP77	CP78	CP79	CP80	CP81
15. 611.	-0.0205	-0.0242	-0.0714	-0.0280	-0.0014	0.0138	0.0393	-0.0230	-0.0929	-0.0145	-0.0303	-0.0355	0.0277	-0.0035	-0.0130	-0.0050	0.0346
15. 602.	-0.0835	-0.0283	0.0011	0.0249	0.0018	-0.0150	0.0157	-0.0221	0.0026	-0.0014	-0.0237	-0.0222	0.0064	-0.0050	-0.0321	-0.0103	-0.0079
15. 593.	-0.0187	0.0281	0.0911	0.1137	0.0452	0.0372	-0.0048	-0.0354	0.0667	-0.0198	-0.0267	0.0400	-0.0115	-0.0302	-0.0743	0.0971	0.0475
15. 584.	-0.0123	0.0285	0.0575	0.0774	0.0473	0.0225	0.0012	-0.0256	0.0340	-0.0076	-0.0226	0.0299	-0.0048	-0.0211	-0.0398	0.0648	0.0213
15. 575.	0.0122	0.0543	0.0727	0.0840	0.0676	0.0561	0.0291	0.0107	0.0518	0.0250	0.0117	0.0545	0.0200	0.0046	-0.0150	0.0808	0.0530
15. 566.	0.0266	0.0761	0.0952	0.1066	0.0850	0.0707	0.0355	0.0161	0.0767	0.0329	0.0234	0.0716	0.0296	0.0134	0.0010	0.0938	0.0638
Run Point	CP82	CP83	CP84	CP85	CP86	CP87	CP88	CP89	CP90	CP91	CP92	CP93	CP94	CP95	CP96	CP97	CP98
15. 611.	-0.0053	-0.0021	0.0217	-0.0247	0.0293	-0.0042	-0.0129	-0.0206	0.0057	-0.0025	-0.0126	-0.0408	-0.0255	-0.0330	-0.0642	-0.0583	-0.1215
15. 602.	-0.0033	-0.0058	-0.0018	-0.0155	-0.0040	-0.0155	-0.0214	-0.0263	-0.0240	-0.0308	-0.0370	-0.0463	-0.0449	-0.0471	-0.0538	-0.0470	-0.0558
15. 593.	-0.0165	-0.0191	-0.0174	-0.0285	-0.0217	-0.0296	-0.0356	-0.0426	-0.0440	-0.0470	-0.0492	-0.0480	-0.0345	-0.0192	-0.0055	0.0161	0.0224
15. 584.	-0.0065	-0.0091	-0.0083	-0.0168	-0.0131	-0.0208	-0.0266	-0.0331	-0.0359	-0.0405	-0.0427	-0.0424	-0.0343	-0.0229	-0.0119	0.0019	0.0117
15. 575.	0.0190	0.0166	0.0169	0.0102	0.0129	0.0063	0.0009	-0.0049	-0.0063	-0.0106	-0.0114	-0.0110	-0.0032	0.0084	0.0173	0.0289	0.0331
15. 566.	0.0289	0.0257	0.0250	0.0192	0.0227	0.0170	0.0115	0.0060	0.0032	0.0002	0.0000	-0.0005	0.0053	0.0155	0.0231	0.0334	0.0369
Run Point	CP99	CP100	CP101	CP102	CP103	CP104	CP105	CP106									
15. 611.	-0.1176	-0.0968	-0.0559	-0.0687	-0.0517	-0.0521	0.0389	0.1677									
15. 602.	-0.0470	-0.0365	-0.0165	-0.0076	0.0065	0.0284	0.0902	0.1840									
15. 593.	0.0345	0.0497	0.0679	0.0846	0.1014	0.1090	0.1468	0.2517									
15. 584.	0.0287	0.0441	0.0573	0.0688	0.0812	0.0878	0.1269	0.2434									
15. 575.	0.0457	0.0590	0.0725	0.0849	0.0972	0.1062	0.1505	0.2638									
15. 566.	0.0462	0.0581	0.0730	0.0820	0.0925	0.1054	0.1460	0.2594									

Table 13. Pressure Coefficients for Configuration 13 With $h = 4.80$ in., $l = 26.00$ in., $Y_s = 2.40$ in., and $Z_s = -3.00$ in.

Run Point	M_∞	$R_\infty \times 10^{-6}$	p_∞ , psi	$p_{t,\infty}$, psi	q_∞ , psi	$T_{t,\infty}$, °F	CP01	CP02	CP03	CP04	CP05	CP06	CP07	CP08	CP09	CP10	CP11
21. 828.	0.20	2.04	22.98	23.63	0.64	98.6	0.8865	-0.2415	-0.1953	-0.1805	-0.1549	-0.1325	-0.1030	-0.0859	-0.0760	-0.0613	-0.0471
21. 820.	0.40	3.62	19.92	22.23	2.22	101.2	0.9168	-0.2560	-0.2029	-0.1873	-0.1615	-0.1383	-0.1013	-0.0870	-0.0724	-0.0605	-0.0517
21. 812.	0.60	2.81	9.78	12.48	2.47	101.0	1.0006	-0.2687	-0.2310	-0.2098	-0.1846	-0.1562	-0.1179	-0.0995	-0.0803	-0.0649	-0.0585
20. 777.	0.80	2.53	6.20	9.45	2.78	100.9	1.1304	-0.3135	-0.2780	-0.2505	-0.2200	-0.1830	-0.1299	-0.1001	-0.0787	-0.0653	-0.0522
20. 785.	0.90	2.35	4.93	8.34	2.80	102.1	1.2050	-0.3653	-0.3250	-0.3371	-0.3404	-0.1976	-0.1037	-0.0711	-0.0491	-0.0287	-0.0241
21. 804.	0.95	2.40	4.65	8.32	2.94	100.3	1.2415	-0.2562	-0.2649	-0.2957	-0.3222	-0.3491	-0.3604	-0.3475	-0.0147	0.0489	0.0462
Run Point	CP12	CP13	CP14	CP15	CP16	CP17	CP18	CP19	CP20	CP21	CP22	CP23	CP24	CP25	CP26	CP27	CP28
21. 828.	-0.0436	-0.0442	-0.0343	-0.0225	-0.0223	-0.0196	-0.0184	-0.0153	-0.0096	-0.0129	-0.0088	-0.0056	-0.0014	-0.0160	0.0024	-0.0036	-0.0151
21. 820.	-0.0454	-0.0418	-0.0327	-0.0257	-0.0222	-0.0200	-0.0174	-0.0171	-0.0147	-0.0134	-0.0103	-0.0078	-0.0085	-0.0127	-0.0048	-0.0056	0.0023
21. 812.	-0.0532	-0.0477	-0.0387	-0.0331	-0.0278	-0.0267	-0.0227	-0.0202	-0.0195	-0.0152	-0.0116	-0.0106	-0.0165	-0.0126	-0.0107	-0.0090	-0.0001
20. 777.	-0.0431	-0.0394	-0.0287	-0.0218	-0.0182	-0.0145	-0.0118	-0.0127	-0.0109	-0.0134	-0.0143	-0.0121	-0.0138	-0.0149	-0.0062	-0.0110	0.0195
20. 785.	-0.0172	-0.0094	-0.0027	0.0011	0.0068	0.0060	0.0100	0.0109	0.0081	0.0153	0.0165	0.0139	0.0089	0.0137	0.0164	0.0168	0.0419
21. 804.	0.0400	0.0377	0.0310	0.0273	0.0286	0.0237	0.0245	0.0230	0.0175	0.0224	0.0235	0.0187	0.0135	0.0184	0.0213	0.0258	0.0486
Run Point	CP29	CP30	CP31	CP32	CP33	CP34	CP35	CP36	CP37	CP38	CP39	CP40	CP41	CP42	CP43	CP44	CP45
21. 828.	-0.0298	-0.0220	-0.0207	-0.0227	-0.0154	-0.0191	-0.0152	-0.0161	-0.0185	-0.0251	-0.0197	-0.0227	-0.0156	-0.0156	-0.0201	-0.0217	-0.0206
21. 820.	0.0066	-0.0670	-0.0617	-0.0497	-0.0370	-0.0318	-0.0278	-0.0278	-0.0304	-0.0316	-0.0336	-0.0363	-0.0280	-0.0267	-0.0256	-0.0274	-0.0287
21. 812.	0.0121	-0.0928	-0.0845	-0.0689	-0.0587	-0.0502	-0.0473	-0.0462	-0.0466	-0.0472	-0.0521	-0.0563	-0.0495	-0.0507	-0.0545	-0.0566	-0.0616
20. 777.	0.0232	-0.1478	-0.1336	-0.1114	-0.0910	-0.0825	-0.0801	-0.0786	-0.0826	-0.0906	-0.1020	-0.1045	-0.1074	-0.1182	-0.1331	-0.1498	-0.1691
20. 785.	0.0543	-0.1204	-0.1003	-0.0698	-0.0491	-0.0302	-0.0247	-0.0233	-0.0247	-0.0241	-0.0381	-0.0425	-0.0383	-0.0467	-0.0589	-0.0769	-0.0987
21. 804.	0.0637	-0.1073	-0.0822	-0.0458	-0.0231	-0.0010	0.0091	0.0128	0.0153	0.0168	0.0068	0.0017	0.0069	0.0012	-0.0089	-0.0231	-0.0425
Run Point	CP46	CP47	CP48	CP49	CP50	CP51	CP52	CP53	CP54	CP55	CP56	CP57	CP58	CP59	CP60	CP61	CP62
21. 828.	-0.0064	-0.0036	-0.0261	-0.0232	-0.0220	0.0278	0.0181	0.0227	0.0248	0.0162	0.0018	0.0172	0.0191	0.0217	0.0088	0.0001	0.0123
21. 820.	-0.0077	-0.0066	0.0097	-0.0463	-0.0281	0.0032	-0.0048	-0.0090	-0.0202	-0.0207	-0.0022	-0.0239	-0.0392	-0.0245	-0.0277	-0.0467	-0.0665
21. 812.	-0.0100	-0.0151	0.0055	-0.0657	-0.0496	-0.0110	-0.0090	-0.0132	-0.0117	-0.0075	-0.0147	-0.0289	-0.0341	-0.0504	-0.0594	-0.0526	-0.0497
20. 777.	-0.0114	-0.0117	0.0159	-0.0993	-0.1034	-0.0084	-0.0126	-0.0083	-0.0131	-0.0201	-0.0297	-0.0403	-0.0425	-0.0316	-0.0338	-0.0376	-0.0404
20. 785.	0.0151	0.0114	0.0424	-0.0607	-0.0314	0.0174	0.0215	0.0102	0.0104	0.0088	0.0105	0.0064	-0.0001	-0.0104	-0.0181	-0.0259	-0.0154
21. 804.	0.0189	0.0205	0.0533	-0.0339	0.0132	0.0225	0.0259	0.0133	0.0134	0.0106	0.0121	0.0125	0.0135	0.0085	0.0006	-0.0149	-0.0025

Table 13. Concluded

Run Point	CP63	CP64	CP65	CP66	CP67	CP68	CP71	CP72	CP73	CP74	CP75	CP76	CP77	CP78	CP79	CP80	CP81
21. 828.	-0.0058	-0.0899	-0.1319	-0.0833	-0.0686	0.0009	0.0176	0.0177	-0.1269	0.0287	0.0207	-0.1034	0.0146	0.0097	-0.0309	-0.0725	-0.0105
21. 820.	-0.0175	-0.0146	0.0157	0.0564	0.0722	0.0551	-0.0057	-0.0173	0.0119	-0.0006	-0.0131	-0.0049	-0.0063	-0.0166	-0.0573	0.0428	0.0148
21. 812.	-0.0250	0.0279	0.0617	0.0819	0.0670	0.0399	-0.0085	-0.0172	0.0467	-0.0109	-0.0201	0.0384	-0.0107	-0.0322	-0.0605	0.0760	0.0365
20. 777.	-0.0099	0.0366	0.0829	0.0914	0.0482	0.0214	-0.0170	-0.0234	0.0609	-0.0095	-0.0208	0.0358	-0.0082	-0.0259	-0.0431	0.0746	0.0074
20. 785.	0.0124	0.0673	0.1004	0.1213	0.0734	0.0701	0.0216	0.0084	0.0738	0.0153	0.0076	0.0681	0.0238	0.0018	-0.0145	0.1082	0.0448
21. 804.	0.0371	0.0718	0.1046	0.1220	0.0839	0.0728	0.0276	0.0151	0.0793	0.0204	0.0147	0.0811	0.0350	0.0128	-0.0021	0.1117	0.0552
Run Point	CP82	CP83	CP84	CP85	CP86	CP87	CP88	CP89	CP90	CP91	CP92	CP93	CP94	CP95	CP96	CP97	CP98
21. 828.	0.0105	-0.0014	0.0026	0.0094	-0.0022	-0.0055	-0.0036	-0.0078	-0.0130	-0.0194	-0.0200	-0.0182	-0.0295	-0.0439	-0.0525	-0.0650	-0.0719
21. 820.	-0.0050	-0.0111	-0.0111	-0.0104	-0.0151	-0.0190	-0.0239	-0.0272	-0.0298	-0.0359	-0.0403	-0.0432	-0.0472	-0.0449	-0.0368	-0.0320	-0.0230
21. 812.	-0.0117	-0.0164	-0.0183	-0.0246	-0.0256	-0.0306	-0.0347	-0.0387	-0.0427	-0.0484	-0.0515	-0.0527	-0.0487	-0.0402	-0.0265	-0.0092	0.0066
20. 777.	-0.0094	-0.0154	-0.0178	-0.0173	-0.0215	-0.0236	-0.0273	-0.0318	-0.0396	-0.0456	-0.0475	-0.0438	-0.0389	-0.0238	-0.0059	0.0086	0.0250
20. 785.	0.0145	0.0121	0.0131	0.0036	0.0101	0.0018	-0.0041	-0.0089	-0.0093	-0.0140	-0.0160	-0.0160	-0.0081	0.0053	0.0127	0.0286	0.0325
21. 804.	0.0264	0.0238	0.0249	0.0152	0.0222	0.0138	0.0090	0.0040	0.0036	-0.0020	-0.0044	-0.0053	0.0017	0.0148	0.0238	0.0365	0.0389
Run Point	CP99	CP100	CP101	CP102	CP103	CP104	CP105	CP106									
21. 828.	-0.0923	-0.1004	-0.1007	-0.0817	-0.0536	-0.0128	0.0638	0.2178									
21. 820.	-0.0167	0.0004	0.0173	0.0416	0.0628	0.0789	0.1349	0.2468									
21. 812.	0.0173	0.0330	0.0487	0.0595	0.0787	0.1008	0.1397	0.2531									
20. 777.	0.0371	0.0469	0.0637	0.0869	0.1139	0.1281	0.1720	0.2935									
20. 785.	0.0440	0.0604	0.0848	0.1054	0.1294	0.1402	0.1808	0.3007									
21. 804.	0.0490	0.0656	0.0858	0.1034	0.1276	0.1411	0.1841	0.3012									

Table 14. Pressure Coefficients for Configuration 14 With $h = 4.80$ in., $l = 26.00$ in., and $Y_s = 2.40$ in.(a) $Z_s = 0.00$ in.

Run Point	M_∞	$R_\infty \times 10^{-6}$	p_∞ , psi	$P_{t,\infty}$, psi	q_∞ , psi	$T_{t,\infty}$, °F	CP01	CP02	CP03	CP04	CP05	CP06	CP07	CP08	CP09	CP10	CP11
10. 409.	0.20	2.04	22.97	23.62	0.64	99.3	0.8780	-0.2376	-0.2034	-0.1837	-0.1625	-0.1368	-0.1069	-0.0850	-0.0786	-0.0637	-0.0551
10. 399.	0.40	3.63	19.92	22.24	2.22	100.1	0.9157	-0.2445	-0.2052	-0.1899	-0.1650	-0.1414	-0.1034	-0.0889	-0.0747	-0.0642	-0.0551
10. 390.	0.60	2.82	9.80	12.50	2.47	100.1	1.0031	-0.2609	-0.2309	-0.2094	-0.1865	-0.1532	-0.1177	-0.0987	-0.0794	-0.0577	-0.0558
10. 381.	0.80	2.54	6.18	9.42	2.77	99.3	1.1336	-0.3075	-0.2776	-0.2498	-0.2217	-0.1790	-0.1301	-0.1010	-0.0770	-0.0551	-0.0487
10. 372.	0.90	2.36	4.94	8.36	2.80	100.5	1.2043	-0.3782	-0.3198	-0.3403	-0.3429	-0.1943	-0.1051	-0.0733	-0.0496	-0.0297	-0.0225
10. 363.	0.95	2.41	4.67	8.36	2.96	100.8	1.2393	-0.2735	-0.2720	-0.2986	-0.3215	-0.3513	-0.3631	-0.3502	-0.0197	0.0448	0.0478
Run Point	CP12	CP13	CP14	CP15	CP16	CP17	CP18	CP19	CP20	CP21	CP22	CP23	CP24	CP25	CP26	CP27	CP28
10. 409.	-0.0489	-0.0462	-0.0369	-0.0317	-0.0259	-0.0277	-0.0208	-0.0170	-0.0158	-0.0129	-0.0118	-0.0126	-0.0116	-0.0170	-0.0085	-0.0126	-0.0172
10. 399.	-0.0479	-0.0439	-0.0347	-0.0287	-0.0267	-0.0239	-0.0213	-0.0177	-0.0156	-0.0128	-0.0106	-0.0108	-0.0111	-0.0117	-0.0061	-0.0079	-0.0130
10. 390.	-0.0529	-0.0447	-0.0373	-0.0330	-0.0289	-0.0291	-0.0284	-0.0186	-0.0212	-0.0140	-0.0098	-0.0144	-0.0211	-0.0130	-0.0148	-0.0103	-0.0097
10. 381.	-0.0438	-0.0354	-0.0265	-0.0214	-0.0171	-0.0156	-0.0121	-0.0093	-0.0118	-0.0074	-0.0041	-0.0090	-0.0132	-0.0091	-0.0076	-0.0075	-0.0041
10. 372.	-0.0178	-0.0106	-0.0017	0.0019	0.0050	0.0054	0.0086	0.0106	0.0085	0.0121	0.0148	0.0112	0.0067	0.0107	0.0158	0.0163	0.0188
10. 363.	0.0414	0.0363	0.0304	0.0270	0.0259	0.0249	0.0242	0.0226	0.0187	0.0189	0.0177	0.0150	0.0114	0.0125	0.0227	0.0228	0.0212
Run Point	CP29	CP30	CP31	CP32	CP33	CP34	CP35	CP36	CP37	CP38	CP39	CP40	CP41	CP42	CP43	CP44	CP45
10. 409.	-0.0234	-0.0361	-0.0379	-0.0361	-0.0339	-0.0307	-0.0284	-0.0311	-0.0327	-0.0367	-0.0314	-0.0374	-0.0304	-0.0321	-0.0309	-0.0321	-0.0327
10. 399.	-0.0133	-0.0439	-0.0431	-0.0384	-0.0342	-0.0323	-0.0297	-0.0284	-0.0288	-0.0330	-0.0329	-0.0378	-0.0307	-0.0309	-0.0362	-0.0390	-0.0411
10. 390.	0.0015	-0.0831	-0.0763	-0.0619	-0.0597	-0.0483	-0.0447	-0.0480	-0.0484	-0.0477	-0.0561	-0.0579	-0.0491	-0.0508	-0.0518	-0.0558	-0.0630
10. 381.	0.0020	-0.1160	-0.1062	-0.0890	-0.0822	-0.0736	-0.0703	-0.0771	-0.0833	-0.0910	-0.1052	-0.1070	-0.1079	-0.1195	-0.1336	-0.1518	-0.1743
10. 372.	0.0279	-0.0818	-0.0673	-0.0456	-0.0340	-0.0221	-0.0156	-0.0166	-0.0187	-0.0232	-0.0336	-0.0385	-0.0371	-0.0460	-0.0563	-0.0724	-0.0945
10. 363.	0.0316	-0.0621	-0.0456	-0.0198	-0.0034	0.0093	0.0179	0.0213	0.0218	0.0189	0.0114	0.0054	0.0077	0.0018	-0.0082	-0.0214	-0.0396
Run Point	CP46	CP47	CP48	CP49	CP50	CP51	CP52	CP53	CP54	CP55	CP56	CP57	CP58	CP59	CP60	CP61	CP62
10. 409.	-0.0100	-0.0071	-0.0409	-0.0371	-0.0354	0.0051	-0.0001	-0.0022	-0.0022	-0.0067	-0.0079	-0.0060	-0.0151	-0.0223	-0.0097	-0.0174	-0.0227
10. 399.	-0.0107	-0.0092	-0.0190	-0.0408	-0.0329	0.0057	-0.0003	0.0011	-0.0045	-0.0166	-0.0271	-0.0236	-0.0111	-0.0452	-0.0667	-0.0361	-0.0357
10. 390.	-0.0105	-0.0197	0.0022	-0.0662	-0.0479	-0.0158	-0.0142	-0.0313	-0.0304	-0.0312	-0.0364	-0.0422	-0.0502	-0.0620	-0.0687	-0.0615	-0.0535
10. 381.	-0.0061	-0.0116	0.0018	-0.0916	-0.1001	0.0051	0.0025	-0.0113	-0.0119	-0.0168	-0.0168	-0.0129	-0.0143	-0.0185	-0.0296	-0.0466	-0.0398
10. 372.	0.0132	0.0120	0.0304	-0.0456	-0.0286	0.0233	0.0233	0.0165	0.0167	0.0134	0.0107	0.0165	0.0110	-0.0011	-0.0119	-0.0136	-0.0118
10. 363.	0.0142	0.0188	0.0318	-0.0157	0.0148	0.0384	0.0358	0.0300	0.0273	0.0226	0.0205	0.0171	0.0102	0.0110	0.0025	-0.0011	-0.0020

Table 14. Continued

(a) Concluded

Run Point	CP63	CP64	CP65	CP66	CP67	CP68	CP71	CP72	CP73	CP74	CP75	CP76	CP77	CP78	CP79	CP80	CP81
10. 409.	-0.0253	-0.0686	-0.0561	-0.0102	-0.0082	0.0148	-0.0030	-0.0118	-0.0709	0.0016	-0.0026	-0.0697	-0.0040	-0.0161	-0.0135	-0.0375	-0.0278
10. 399.	-0.0398	-0.0367	-0.0048	-0.0244	-0.0140	0.0507	-0.0017	-0.0221	-0.0238	-0.0004	-0.0174	-0.0372	-0.0004	-0.0188	-0.0309	-0.0056	0.0080
10. 390.	-0.0125	0.0107	0.0305	0.0428	0.0584	0.0598	-0.0109	-0.0419	0.0350	-0.0176	-0.0376	0.0312	-0.0089	-0.0354	-0.0513	0.0690	0.0400
10. 381.	-0.0169	0.0127	0.0340	0.0432	0.0483	0.0452	0.0035	-0.0148	0.0192	-0.0008	-0.0107	0.0180	-0.0027	-0.0247	-0.0155	0.0565	0.0045
10. 372.	0.0066	0.0427	0.0601	0.0845	0.0797	0.0788	0.0247	0.0103	0.0552	0.0233	0.0152	0.0569	0.0188	-0.0011	0.0096	0.0798	0.0382
10. 363.	0.0082	0.0400	0.0537	0.0648	0.0711	0.0735	0.0374	0.0194	0.0492	0.0351	0.0225	0.0464	0.0302	0.0128	0.0149	0.0699	0.0354
Run Point	CP82	CP83	CP84	CP85	CP86	CP87	CP88	CP89	CP90	CP91	CP92	CP93	CP94	CP95	CP96	CP97	CP98
10. 409.	-0.0168	-0.0265	-0.0233	-0.0205	-0.0235	-0.0205	-0.0219	-0.0209	-0.0285	-0.0339	-0.0321	-0.0346	-0.0370	-0.0460	-0.0501	-0.0582	-0.0647
10. 399.	-0.0040	-0.0093	-0.0091	-0.0098	-0.0140	-0.0160	-0.0207	-0.0256	-0.0312	-0.0375	-0.0392	-0.0420	-0.0420	-0.0411	-0.0411	-0.0404	-0.0409
10. 390.	-0.0167	-0.0196	-0.0188	-0.0261	-0.0227	-0.0326	-0.0335	-0.0391	-0.0402	-0.0449	-0.0472	-0.0494	-0.0412	-0.0293	-0.0155	-0.0001	0.0093
10. 381.	-0.0104	-0.0137	-0.0130	-0.0174	-0.0166	-0.0237	-0.0249	-0.0299	-0.0323	-0.0380	-0.0411	-0.0436	-0.0377	-0.0289	-0.0174	-0.0049	0.0046
10. 372.	0.0163	0.0140	0.0146	0.0093	0.0088	0.0006	-0.0004	-0.0042	-0.0056	-0.0118	-0.0143	-0.0154	-0.0108	-0.0040	0.0062	0.0174	0.0247
10. 363.	0.0270	0.0231	0.0223	0.0181	0.0171	0.0122	0.0098	0.0075	0.0052	0.0023	-0.0004	-0.0024	-0.0001	0.0037	0.0098	0.0157	0.0200
Run Point	CP99	CP100	CP101	CP102	CP103	CP104	CP105	CP106									
10. 409.	-0.0692	-0.0632	-0.0620	-0.0554	-0.0429	-0.0118	0.0433	0.1746									
10. 399.	-0.0433	-0.0356	-0.0260	-0.0193	-0.0028	0.0207	0.0772	0.2123									
10. 390.	0.0206	0.0341	0.0481	0.0567	0.0726	0.0827	0.1257	0.2356									
10. 381.	0.0141	0.0290	0.0435	0.0510	0.0590	0.0692	0.1146	0.2356									
10. 372.	0.0329	0.0437	0.0556	0.0608	0.0714	0.0857	0.1349	0.2551									
10. 363.	0.0259	0.0323	0.0396	0.0476	0.0594	0.0757	0.1237	0.2447									

Table 14. Continued

(b) $Z_g = 2.31$ in.

Run Point	M_∞	$R_\infty \times 10^{-6}$	p_∞ , psi	$p_{t,\infty}$, psi	q_∞ , psi	$T_{t,\infty}$, °F	CP01	CP02	CP03	CP04	CP05	CP06	CP07	CP08	CP09	CP10	CP11
10. 414.	0.20	2.04	22.98	23.63	0.64	99.0	0.8787	-0.2359	-0.2005	-0.1841	-0.1639	-0.1371	-0.1071	-0.0874	-0.0787	-0.0650	-0.0564
10. 404.	0.40	3.62	19.92	22.23	2.22	100.5	0.9202	-0.2441	-0.2051	-0.1892	-0.1630	-0.1399	-0.1016	-0.0865	-0.0725	-0.0620	-0.0532
10. 395.	0.60	2.82	9.79	12.49	2.47	100.2	1.0020	-0.2586	-0.2278	-0.2068	-0.1834	-0.1514	-0.1163	-0.0978	-0.0780	-0.0559	-0.0534
10. 386.	0.80	2.53	6.19	9.43	2.77	100.2	1.1328	-0.3069	-0.2768	-0.2490	-0.2209	-0.1783	-0.1288	-0.0995	-0.0757	-0.0536	-0.0471
10. 377.	0.90	2.36	4.94	8.36	2.80	100.6	1.2040	-0.3799	-0.3208	-0.3370	-0.3350	-0.1943	-0.1065	-0.0738	-0.0497	-0.0292	-0.0213
10. 368.	0.95	2.40	4.67	8.36	2.95	100.7	1.2400	-0.2729	-0.2718	-0.2985	-0.3221	-0.3512	-0.3628	-0.3427	-0.0116	0.0456	0.0474
Run Point	CP12	CP13	CP14	CP15	CP16	CP17	CP18	CP19	CP20	CP21	CP22	CP23	CP24	CP25	CP26	CP27	CP28
10. 414.	-0.0524	-0.0473	-0.0347	-0.0295	-0.0260	-0.0278	-0.0198	-0.0148	-0.0136	-0.0107	-0.0062	-0.0058	-0.0038	-0.0104	-0.0030	-0.0049	-0.0128
10. 404.	-0.0464	-0.0437	-0.0341	-0.0284	-0.0236	-0.0207	-0.0169	-0.0141	-0.0127	-0.0112	-0.0089	-0.0062	-0.0060	-0.0120	-0.0061	-0.0079	-0.0057
10. 395.	-0.0509	-0.0405	-0.0332	-0.0301	-0.0278	-0.0279	-0.0214	-0.0162	-0.0186	-0.0082	-0.0013	-0.0059	-0.0211	-0.0084	-0.0114	-0.0080	0.0052
10. 386.	-0.0427	-0.0343	-0.0247	-0.0206	-0.0171	-0.0161	-0.0121	-0.0088	-0.0097	-0.0033	0.0006	-0.0030	-0.0084	-0.0053	-0.0056	-0.0085	0.0077
10. 377.	-0.0167	-0.0091	-0.0007	0.0027	0.0060	0.0073	0.0103	0.0124	0.0109	0.0157	0.0189	0.0166	0.0143	0.0147	0.0184	0.0168	0.0345
10. 368.	0.0407	0.0361	0.0314	0.0280	0.0283	0.0267	0.0254	0.0241	0.0202	0.0209	0.0209	0.0200	0.0191	0.0168	0.0249	0.0231	0.0400
Run Point	CP29	CP30	CP31	CP32	CP33	CP34	CP35	CP36	CP37	CP38	CP39	CP40	CP41	CP42	CP43	CP44	CP45
10. 414.	-0.0190	-0.0216	-0.0194	-0.0171	-0.0143	-0.0144	-0.0130	-0.0126	-0.0109	-0.0173	-0.0161	-0.0221	-0.0154	-0.0182	-0.0201	-0.0189	-0.0199
10. 404.	-0.0035	-0.0563	-0.0532	-0.0456	-0.0392	-0.0358	-0.0339	-0.0312	-0.0320	-0.0350	-0.0358	-0.0384	-0.0320	-0.0340	-0.0334	-0.0327	-0.0353
10. 395.	0.0137	-0.1024	-0.0896	-0.0698	-0.0640	-0.0489	-0.0430	-0.0471	-0.0475	-0.0456	-0.0529	-0.0545	-0.0460	-0.0469	-0.0507	-0.0541	-0.0613
10. 386.	0.0108	-0.1394	-0.1256	-0.1033	-0.0928	-0.0799	-0.0752	-0.0804	-0.0853	-0.0915	-0.1057	-0.1062	-0.1069	-0.1188	-0.1331	-0.1505	-0.1738
10. 377.	0.0449	-0.1084	-0.0895	-0.0613	-0.0450	-0.0279	-0.0194	-0.0193	-0.0209	-0.0251	-0.0356	-0.0381	-0.0364	-0.0453	-0.0596	-0.0766	-0.0985
10. 368.	0.0494	-0.0912	-0.0697	-0.0366	-0.0164	0.0015	0.0129	0.0166	0.0179	0.0165	0.0095	0.0050	0.0073	0.0012	-0.0079	-0.0219	-0.0415
Run Point	CP46	CP47	CP48	CP49	CP50	CP51	CP52	CP53	CP54	CP55	CP56	CP57	CP58	CP59	CP60	CP61	CP62
10. 414.	-0.0010	-0.0060	-0.0219	-0.0175	-0.0130	0.0164	0.0094	0.0065	0.0034	-0.0014	0.0059	0.0137	0.0088	-0.0131	-0.0185	-0.0034	0.0029
10. 404.	-0.0068	-0.0138	-0.0043	-0.0415	-0.0343	0.0041	0.0021	-0.0127	-0.0132	-0.0117	0.0020	-0.0284	-0.0459	-0.0513	-0.0620	-0.0121	-0.0302
10. 395.	-0.0056	-0.0158	0.0138	-0.0719	-0.0441	-0.0106	-0.0018	-0.0132	-0.0298	-0.0480	-0.0447	-0.0243	-0.0041	-0.0003	-0.0244	-0.0731	-0.0718
10. 386.	-0.0017	-0.0134	0.0117	-0.1014	-0.1014	-0.0032	-0.0019	-0.0146	-0.0188	-0.0271	-0.0352	-0.0333	-0.0392	-0.0393	-0.0398	-0.0546	-0.0507
10. 377.	0.0178	0.0094	0.0454	-0.0549	-0.0310	0.0244	0.0255	0.0152	0.0116	0.0085	0.0078	0.0165	0.0130	0.0066	-0.0034	-0.0222	-0.0147
10. 368.	0.0196	0.0178	0.0528	-0.0300	0.0116	0.0385	0.0351	0.0253	0.0229	0.0212	0.0164	0.0207	0.0154	0.0110	-0.0013	-0.0077	-0.0022

Table 14. Concluded

(b) Concluded

Run Point	CP63	CP64	CP65	CP66	CP67	CP68	CP71	CP72	CP73	CP74	CP75	CP76	CP77	CP78	CP79	CP80	CP81
10. 414.	-0.0443	-0.0355	-0.0733	-0.0421	-0.0440	0.0215	0.0067	0.0110	-0.0721	0.0091	0.0134	-0.0397	0.0099	0.0042	-0.0202	-0.0226	0.0111
10. 404.	-0.0492	-0.0552	0.0136	0.0478	0.0141	0.0272	-0.0023	-0.0095	-0.0051	0.0027	-0.0106	-0.0132	-0.0033	-0.0148	-0.0424	-0.0025	0.0092
10. 395.	-0.0197	0.0485	0.0856	0.1073	0.0884	0.0907	-0.0106	-0.0044	0.0684	-0.0090	-0.0048	0.0817	-0.0101	-0.0388	-0.0283	0.0784	0.0463
10. 386.	-0.0037	0.0547	0.0764	0.0888	0.0439	0.0374	-0.0027	-0.0260	0.0588	-0.0080	-0.0234	0.0504	-0.0019	-0.0219	-0.0240	0.0893	0.0091
10. 377.	0.0074	0.0597	0.0963	0.1068	0.0800	0.0481	0.0284	0.0145	0.0772	0.0243	0.0157	0.0621	0.0247	0.0050	0.0094	0.1009	0.0312
10. 368.	0.0341	0.0634	0.0792	0.0915	0.0710	0.0658	0.0358	0.0204	0.0612	0.0333	0.0209	0.0554	0.0327	0.0145	0.0176	0.0973	0.0440
Run Point	CP82	CP83	CP84	CP85	CP86	CP87	CP88	CP89	CP90	CP91	CP92	CP93	CP94	CP95	CP96	CP97	CP98
10. 414.	0.0127	0.0024	0.0040	0.0016	-0.0028	-0.0035	-0.0045	-0.0068	-0.0123	-0.0215	-0.0204	-0.0227	-0.0254	-0.0352	-0.0427	-0.0561	-0.0649
10. 404.	-0.0047	-0.0103	-0.0113	-0.0133	-0.0183	-0.0203	-0.0226	-0.0253	-0.0300	-0.0398	-0.0408	-0.0404	-0.0405	-0.0402	-0.0396	-0.0367	-0.0336
10. 395.	-0.0162	-0.0199	-0.0185	-0.0269	-0.0232	-0.0348	-0.0361	-0.0434	-0.0452	-0.0525	-0.0539	-0.0520	-0.0385	-0.0223	-0.0039	0.0164	0.0330
10. 386.	-0.0091	-0.0119	-0.0113	-0.0169	-0.0168	-0.0244	-0.0269	-0.0344	-0.0386	-0.0442	-0.0468	-0.0466	-0.0382	-0.0269	-0.0117	0.0048	0.0182
10. 377.	0.0181	0.0145	0.0149	0.0098	0.0099	0.0026	0.0011	-0.0040	-0.0056	-0.0113	-0.0141	-0.0145	-0.0086	0.0012	0.0138	0.0282	0.0380
10. 368.	0.0292	0.0256	0.0243	0.0201	0.0194	0.0134	0.0105	0.0071	0.0038	-0.0006	-0.0020	-0.0021	0.0030	0.0108	0.0219	0.0312	0.0392
Run Point	CP99	CP100	CP101	CP102	CP103	CP104	CP105	CP106									
10. 414.	-0.0727	-0.0711	-0.0622	-0.0523	-0.0386	-0.0140	0.0455	0.1918									
10. 404.	-0.0307	-0.0222	-0.0135	-0.0081	0.0114	0.0350	0.0947	0.2184									
10. 395.	0.0542	0.0744	0.0907	0.1019	0.1159	0.1205	0.1578	0.2712									
10. 386.	0.0309	0.0449	0.0600	0.0734	0.0870	0.0939	0.1429	0.2791									
10. 377.	0.0478	0.0593	0.0697	0.0807	0.0959	0.1037	0.1479	0.2713									
10. 368.	0.0492	0.0596	0.0700	0.0798	0.0931	0.1043	0.1475	0.2697									

Table 15. Pressure Coefficients for Configuration 15 With $h = 4.80$ in., $l = 30.00$ in., $Y_s = 0.00$ in., and $Z_s = -3.00$ in.

Run Point	M_∞	$R_\infty \times 10^{-6}$	P_∞ psi	$P_{t,\infty}$ psi	q_∞ psi	$T_{t,\infty}$ °F	CP01	CP02	CP03	CP04	CP05	CP06	CP07	CP08	CP09	CP10	CP11
18. 714.	0.20	2.05	22.95	23.60	0.65	97.8	0.8876	-0.2256	-0.1934	-0.1764	-0.1634	-0.1169	-0.1014	-0.0914	-0.0718	-0.0247	-0.0399
18. 706.	0.40	3.65	19.90	22.23	2.24	99.2	0.9142	-0.2376	-0.2024	-0.1880	-0.1653	-0.1360	-0.1030	-0.0911	-0.0737	-0.0543	-0.0527
18. 698.	0.60	2.81	9.79	12.49	2.47	100.5	1.0014	-0.2679	-0.2284	-0.2077	-0.1839	-0.1550	-0.1151	-0.0972	-0.0788	-0.0642	-0.0574
17. 686.	0.80	2.54	6.19	9.44	2.78	98.2	1.1307	-0.3159	-0.2780	-0.2504	-0.2226	-0.1822	-0.1290	-0.0995	-0.0772	-0.0583	-0.0514
17. 678.	0.90	2.37	4.94	8.36	2.81	99.9	1.2046	-0.3637	-0.3269	-0.3478	-0.3405	-0.2174	-0.1034	-0.0702	-0.0482	-0.0320	-0.0245
17. 670.	0.95	2.40	4.66	8.35	2.95	100.3	1.2391	-0.2576	-0.2739	-0.2995	-0.3223	-0.3541	-0.3628	-0.3472	-0.0167	0.0411	0.0468
Run Point	CP12	CP13	CP14	CP15	CP16	CP17	CP18	CP19	CP20	CP21	CP22	CP23	CP24	CP25	CP26	CP27	CP28
18. 714.	-0.0519	-0.0338	-0.0279	-0.0276	-0.0285	-0.0382	-0.0226	-0.0062	-0.0142	0.0063	0.0296	0.0050	-0.0052	0.0109	-0.0076	0.0037	-0.0237
18. 706.	-0.0512	-0.0436	-0.0355	-0.0329	-0.0291	-0.0292	-0.0224	-0.0148	-0.0166	-0.0097	-0.0034	-0.0096	-0.0147	-0.0083	-0.0115	-0.0088	-0.0073
18. 698.	-0.0522	-0.0454	-0.0362	-0.0318	-0.0275	-0.0264	-0.0216	-0.0169	-0.0173	-0.0125	-0.0106	-0.0144	-0.0207	-0.0141	-0.0133	-0.0142	-0.0057
17. 686.	-0.0446	-0.0361	-0.0281	-0.0226	-0.0160	-0.0158	-0.0114	-0.0104	-0.0141	-0.0111	-0.0108	-0.0126	-0.0145	-0.0116	-0.0115	-0.0155	0.0112
17. 678.	-0.0170	-0.0105	-0.0025	0.0027	0.0068	0.0071	0.0085	0.0094	0.0079	0.0107	0.0112	0.0087	0.0024	0.0084	0.0147	0.0135	0.0195
17. 670.	0.0414	0.0349	0.0300	0.0275	0.0272	0.0263	0.0242	0.0223	0.0196	0.0161	0.0129	0.0110	0.0074	0.0078	0.0217	0.0191	0.0301
Run Point	CP29	CP30	CP31	CP32	CP33	CP34	CP35	CP36	CP37	CP38	CP39	CP40	CP41	CP42	CP43	CP44	CP45
18. 714.	-0.0112	-0.0256	-0.0174	-0.0184	-0.0448	-0.0153	-0.0070	-0.0244	-0.0279	-0.0179	-0.0332	-0.0425	-0.0186	-0.0099	-0.0122	-0.0107	-0.0191
18. 706.	0.0304	-0.0165	-0.0564	-0.0784	-0.0794	-0.0590	-0.0441	-0.0398	-0.0364	-0.0300	-0.0368	-0.0435	-0.0315	-0.0293	-0.0310	-0.0311	-0.0342
18. 698.	0.0381	-0.0286	-0.0804	-0.1087	-0.1022	-0.0831	-0.0705	-0.0622	-0.0567	-0.0547	-0.0588	-0.0556	-0.0481	-0.0469	-0.0522	-0.0540	-0.0581
17. 686.	0.0597	-0.0419	-0.1290	-0.1812	-0.1723	-0.1438	-0.1253	-0.1137	-0.1095	-0.1076	-0.1189	-0.1175	-0.1154	-0.1260	-0.1384	-0.1554	-0.1758
17. 678.	0.0760	0.0059	-0.0738	-0.1229	-0.1114	-0.0812	-0.0604	-0.0455	-0.0380	-0.0340	-0.0421	-0.0444	-0.0395	-0.0477	-0.0584	-0.0753	-0.0971
17. 670.	0.0732	0.0230	-0.0456	-0.0948	-0.0791	-0.0481	-0.0239	-0.0064	0.0037	0.0072	0.0032	-0.0007	0.0034	-0.0015	-0.0110	-0.0237	-0.0416
Run Point	CP46	CP47	CP48	CP49	CP50	CP51	CP52	CP53	CP54	CP55	CP56	CP57	CP58	CP59	CP60	CP61	CP62
18. 714.	0.0153	-0.0070	-0.0272	-0.0357	-0.0095	-0.0179	0.0209	-0.0213	-0.0173	-0.0185	0.0063	0.0234	0.0049	0.0147	0.0190	-0.0173	-0.0197
18. 706.	-0.0059	-0.0102	0.0227	-0.0784	-0.0302	-0.0101	-0.0016	-0.0123	-0.0134	-0.0245	-0.0289	-0.0188	-0.0287	-0.0389	-0.0472	-0.0561	-0.0353
18. 698.	-0.0125	-0.0159	0.0312	-0.1059	-0.0515	-0.0239	-0.0222	-0.0261	-0.0266	-0.0338	-0.0383	-0.0439	-0.0407	-0.0367	-0.0442	-0.0634	-0.0696
17. 686.	-0.0099	-0.0182	0.0555	-0.1844	-0.1111	-0.0058	-0.0023	-0.0103	-0.0113	-0.0156	-0.0224	-0.0322	-0.0451	-0.0714	-0.0857	-0.0903	-0.0732
17. 678.	0.0104	0.0089	0.0742	-0.1240	-0.0373	0.0190	0.0217	0.0176	0.0152	0.0094	0.0067	-0.0016	-0.0046	-0.0054	-0.0180	-0.0299	-0.0306
17. 670.	0.0104	0.0152	0.0736	-0.0922	0.0052	0.0272	0.0248	0.0269	0.0247	0.0179	0.0140	0.0091	-0.0001	-0.0096	-0.0118	-0.0054	-0.0078

Table 15. Concluded

Run Point	CP63	CP64	CP65	CP66	CP67	CP68	CP69	CP70	CP71	CP72	CP73	CP74	CP75	CP76	CP77	CP78	CP79
18. 714.	-0.0589	-0.0676	-0.0631	-0.0114	-0.0058	-0.0054	-0.0230	-0.0085	0.0282	-0.0119	-0.0682	0.0007	-0.0088	-0.0483	0.0213	-0.0008	-0.0245
18. 706.	-0.0533	-0.0416	0.0110	0.0689	0.1269	0.1142	0.0714	0.0004	0.0011	-0.0220	0.0125	-0.0047	-0.0185	0.0257	-0.0063	-0.0247	-0.0610
18. 698.	-0.0566	-0.0300	0.0294	0.0819	0.1049	0.0804	0.0395	0.0815	-0.0222	-0.0320	0.0379	-0.0237	-0.0293	0.0393	-0.0131	-0.0268	-0.0598
17. 686.	-0.0380	0.0186	0.0532	0.1001	0.1250	0.1181	0.0840	0.1274	-0.0053	-0.0262	0.0550	-0.0091	-0.0237	0.0605	-0.0163	-0.0348	-0.0627
17. 678.	-0.0186	0.0171	0.0499	0.1007	0.1360	0.1245	0.0861	0.1008	0.0209	0.0081	0.0424	0.0188	0.0106	0.0490	0.0154	0.0036	-0.0272
17. 670.	-0.0016	0.0246	0.0602	0.0925	0.1086	0.1038	0.0759	0.0890	0.0225	0.0129	0.0477	0.0246	0.0171	0.0449	0.0230	0.0129	-0.0162
Run Point	CP80	CP81	CP82	CP83	CP84	CP85	CP86	CP87	CP88	CP89	CP90	CP91	CP92	CP93	CP94	CP95	CP96
18. 714.	-0.0120	-0.0077	0.0091	0.0089	0.0265	0.0072	0.0254	0.0021	0.0052	-0.0017	0.0061	-0.0029	-0.0104	-0.0218	-0.0178	-0.0299	-0.0430
18. 706.	0.0274	0.0998	-0.0085	-0.0106	-0.0078	-0.0161	-0.0149	-0.0240	-0.0265	-0.0312	-0.0332	-0.0393	-0.0477	-0.0568	-0.0592	-0.0593	-0.0562
18. 698.	0.0160	0.0979	-0.0170	-0.0194	-0.0192	-0.0228	-0.0224	-0.0269	-0.0308	-0.0367	-0.0418	-0.0487	-0.0540	-0.0588	-0.0576	-0.0495	-0.0372
17. 686.	0.0471	0.1251	-0.0213	-0.0233	-0.0233	-0.0320	-0.0276	-0.0371	-0.0454	-0.0531	-0.0582	-0.0669	-0.0705	-0.0704	-0.0618	-0.0401	-0.0192
17. 678.	0.0566	0.1223	0.0139	0.0121	0.0116	0.0046	0.0086	0.0020	-0.0028	-0.0074	-0.0094	-0.0172	-0.0234	-0.0293	-0.0286	-0.0212	-0.0119
17. 670.	0.0721	0.1071	0.0251	0.0224	0.0210	0.0168	0.0180	0.0138	0.0092	0.0052	0.0016	-0.0046	-0.0081	-0.0115	-0.0105	-0.0039	0.0032
Run Point	CP97	CP98	CP99	CP100	CP101	CP102	CP103	CP104	CP105	CP106	CP107	CP108	CP109	CP110			
18. 714.	-0.0457	-0.0697	-0.0747	-0.0604	-0.0404	-0.0490	-0.0407	-0.0564	-0.0292	-0.0335	-0.0124	0.0227	0.0853	0.1813			
18. 706.	-0.0441	-0.0318	-0.0111	0.0149	0.0404	0.0559	0.0723	0.0825	0.1002	0.1039	0.1040	0.1127	0.1485	0.2650			
18. 698.	-0.0206	-0.0053	0.0141	0.0387	0.0594	0.0785	0.1008	0.1141	0.1282	0.1359	0.1357	0.1321	0.1509	0.2766			
17. 686.	0.0071	0.0256	0.0550	0.0869	0.1176	0.1395	0.1666	0.1865	0.2180	0.2347	0.2517	0.2399	0.2145	0.3426			
17. 678.	0.0051	0.0162	0.0366	0.0598	0.0827	0.0988	0.1163	0.1288	0.1470	0.1579	0.1710	0.1672	0.1832	0.3193			
17. 670.	0.0137	0.0237	0.0390	0.0564	0.0728	0.0864	0.1006	0.1143	0.1296	0.1352	0.1426	0.1405	0.1697	0.3070			

Table 16. Pressure Coefficients for Configuration 16 With $h = 4.80$ in., $l = 30.00$ in., and $Y_s = 0.00$ in.(a) $Z_s = 0.00$ in.

Run Point	M_∞	$R_\infty \times 10^{-6}$	P_∞ , psi	P_t^∞ , psi	q_∞ , psi	$T_{t,\infty}$, °F	CP01	CP02	CP03	CP04	CP05	CP06	CP07	CP08	CP09	CP10	CP11
14. 540.	0.20	2.06	22.96	23.62	0.65	99.0	0.8791	-0.2414	-0.1979	-0.1817	-0.1554	-0.1338	-0.1037	-0.0865	-0.0742	-0.0623	-0.0532
14. 531.	0.40	3.64	19.90	22.24	2.24	100.5	0.9127	-0.2439	-0.2071	-0.1904	-0.1690	-0.1401	-0.1044	-0.0920	-0.0747	-0.0578	-0.0563
14. 522.	0.60	2.82	9.81	12.51	2.47	100.6	1.0000	-0.2658	-0.2295	-0.2085	-0.1845	-0.1550	-0.1162	-0.0970	-0.0787	-0.0638	-0.0580
14. 513.	0.80	2.53	6.20	9.45	2.78	100.7	1.1318	-0.3214	-0.2781	-0.2508	-0.2222	-0.1814	-0.1293	-0.0997	-0.0771	-0.0603	-0.0514
14. 504.	0.90	2.36	4.94	8.35	2.80	100.1	1.2035	-0.3707	-0.3221	-0.3385	-0.3346	-0.2105	-0.1051	-0.0721	-0.0497	-0.0348	-0.0254
14. 495.	0.95	2.40	4.67	8.36	2.96	101.3	1.2398	-0.2644	-0.2700	-0.2982	-0.3193	-0.3512	-0.3600	-0.3412	-0.0121	0.0412	0.0465
Run Point	CP12	CP13	CP14	CP15	CP16	CP17	CP18	CP19	CP20	CP21	CP22	CP23	CP24	CP25	CP26	CP27	CP28
14. 540.	-0.0458	-0.0436	-0.0332	-0.0287	-0.0234	-0.0287	-0.0207	-0.0172	-0.0152	-0.0163	-0.0118	-0.0121	-0.0125	-0.0158	-0.0077	-0.0097	-0.0111
14. 531.	-0.0523	-0.0424	-0.0371	-0.0321	-0.0277	-0.0283	-0.0227	-0.0212	-0.0230	-0.0141	-0.0097	-0.0146	-0.0231	-0.0112	-0.0156	-0.0087	-0.0078
14. 522.	-0.0532	-0.0445	-0.0376	-0.0322	-0.0284	-0.0276	-0.0242	-0.0229	-0.0231	-0.0185	-0.0151	-0.0164	-0.0220	-0.0158	-0.0167	-0.0144	-0.0061
14. 513.	-0.0448	-0.0374	-0.0291	-0.0233	-0.0171	-0.0148	-0.0118	-0.0127	-0.0140	-0.0119	-0.0099	-0.0077	-0.0135	-0.0113	-0.0108	-0.0202	0.0113
14. 504.	-0.0186	-0.0127	-0.0054	0.0001	0.0047	0.0062	0.0083	0.0091	0.0078	0.0078	0.0065	0.0043	-0.0004	0.0042	0.0104	0.0090	0.0178
14. 495.	0.0409	0.0348	0.0301	0.0285	0.0282	0.0271	0.0249	0.0224	0.0197	0.0154	0.0123	0.0107	0.0073	0.0083	0.0199	0.0164	0.0325
Run Point	CP29	CP30	CP31	CP32	CP33	CP34	CP35	CP36	CP37	CP38	CP39	CP40	CP41	CP42	CP43	CP44	CP45
14. 540.	-0.0155	-0.0182	-0.0290	-0.0396	-0.0403	-0.0360	-0.0358	-0.0309	-0.0350	-0.0359	-0.0349	-0.0433	-0.0355	-0.0280	-0.0330	-0.0310	-0.0302
14. 531.	0.0277	-0.0096	-0.0553	-0.0798	-0.0796	-0.0608	-0.0513	-0.0472	-0.0438	-0.0378	-0.0458	-0.0458	-0.0336	-0.0331	-0.0346	-0.0366	-0.0388
14. 522.	0.0304	-0.0180	-0.0720	-0.1036	-0.1003	-0.0818	-0.0705	-0.0637	-0.0594	-0.0546	-0.0593	-0.0610	-0.0510	-0.0509	-0.0548	-0.0581	-0.0614
14. 513.	0.0478	-0.0169	-0.1110	-0.1735	-0.1663	-0.1403	-0.1222	-0.1111	-0.1076	-0.1071	-0.1165	-0.1205	-0.1208	-0.1305	-0.1383	-0.1549	-0.1751
14. 504.	0.0714	0.0160	-0.0687	-0.1247	-0.1111	-0.0808	-0.0593	-0.0453	-0.0383	-0.0359	-0.0429	-0.0444	-0.0429	-0.0489	-0.0627	-0.0782	-0.0984
14. 495.	0.0827	0.0343	-0.0485	-0.1074	-0.0904	-0.0555	-0.0290	-0.0092	0.0013	0.0054	0.0021	-0.0013	0.0023	-0.0027	-0.0126	-0.0249	-0.0415
Run Point	CP46	CP47	CP48	CP49	CP50	CP51	CP52	CP53	CP54	CP55	CP56	CP57	CP58	CP59	CP60	CP61	CP62
14. 540.	-0.0120	-0.0077	-0.0141	-0.0482	-0.0284	-0.0085	-0.0115	-0.0123	-0.0052	-0.0212	-0.0255	-0.0269	-0.0212	-0.0151	-0.0360	-0.0231	-0.0195
14. 531.	-0.0099	-0.0123	0.0211	-0.0892	-0.0305	-0.0259	-0.0188	-0.0368	-0.0346	-0.0279	-0.0192	-0.0302	-0.0342	-0.0673	-0.0754	-0.0326	-0.0283
14. 522.	-0.0138	-0.0176	0.0303	-0.1084	-0.0518	-0.0249	-0.0200	-0.0294	-0.0357	-0.0503	-0.0509	-0.0457	-0.0436	-0.0555	-0.0677	-0.0619	-0.0532
14. 513.	-0.0093	-0.0194	0.0452	-0.1764	-0.1140	-0.0126	-0.0125	-0.0267	-0.0315	-0.0321	-0.0362	-0.0420	-0.0502	-0.0737	-0.0877	-0.0897	-0.0727
14. 504.	0.0057	0.0063	0.0744	-0.1263	-0.0388	0.0106	0.0094	0.0024	-0.0019	-0.0041	-0.0064	-0.0136	-0.0202	-0.0169	-0.0175	-0.0199	-0.0177
14. 495.	0.0105	0.0159	0.0815	-0.1047	0.0042	0.0213	0.0195	0.0182	0.0154	0.0092	0.0052	0.0025	0.0000	-0.0002	-0.0010	-0.0057	-0.0099

Table 16. Continued

(a) Concluded

Run	Point	CP63	CP64	CP65	CP66	CP67	CP68	CP69	CP70	CP71	CP72	CP73	CP74	CP75	CP76	CP77	CP78	CP79	
14.	540.	-0.0483	-0.0119	-0.0217	-0.0273	-0.0332	-0.0245	-0.0115	-0.0253	-0.0120	-0.0208	-0.0121	-0.0097	-0.0177	-0.0202	-0.0116	-0.0103	-0.0356	
14.	531.	-0.0567	-0.0295	0.0255	0.0440	0.0675	0.1378	0.1105	0.0604	-0.0144	-0.0389	0.0313	-0.0259	-0.0371	0.0135	-0.0130	-0.0281	-0.0546	
14.	522.	-0.0250	0.0066	0.0341	0.0545	0.0795	0.1063	0.1081	0.0691	-0.0197	-0.0383	0.0358	-0.0265	-0.0449	0.0274	-0.0234	-0.0382	-0.0644	
14.	513.	-0.0473	0.0083	0.0514	0.0833	0.1098	0.1345	0.1408	0.2200	-0.0091	-0.0361	0.0595	-0.0162	-0.0400	0.0624	-0.0244	-0.0422	-0.0625	
14.	504.	-0.0165	0.0084	0.0470	0.0955	0.1297	0.1363	0.1085	0.1228	0.0098	-0.0052	0.0419	0.0068	-0.0049	0.0413	0.0087	-0.0021	-0.0264	
14.	495.	-0.0052	0.0255	0.0586	0.0948	0.1375	0.1405	0.1068	0.0961	0.0184	0.0097	0.0547	0.0185	0.0105	0.0482	0.0179	0.0080	-0.0132	
Run	Point	CP80	CP81	CP82	CP83	CP84	CP85	CP86	CP87	CP88	CP89	CP90	CP91	CP92	CP93	CP94	CP95	CP96	
14.	540.	-0.0224	-0.0216	-0.0128	-0.0217	-0.0161	-0.0162	-0.0179	-0.0186	-0.0207	-0.0273	-0.0339	-0.0345	-0.0349	-0.0349	-0.0371	-0.0366	-0.0375	
14.	531.	0.0331	0.1300	-0.0199	-0.0222	-0.0201	-0.0289	-0.0212	-0.0280	-0.0343	-0.0391	-0.0381	-0.0436	-0.0470	-0.0541	-0.0511	-0.0452	-0.0418	
14.	522.	0.0391	0.1222	-0.0256	-0.0270	-0.0267	-0.0319	-0.0286	-0.0358	-0.0417	-0.0460	-0.0491	-0.0538	-0.0556	-0.0569	-0.0518	-0.0440	-0.0362	
14.	513.	0.0468	0.1356	-0.0254	-0.0279	-0.0291	-0.0353	-0.0343	-0.0421	-0.0515	-0.0612	-0.0694	-0.0752	-0.0739	-0.0688	-0.0572	-0.0332	-0.0117	
14.	504.	0.0466	0.1523	0.0077	0.0057	0.0037	-0.0001	0.0014	-0.0020	-0.0072	-0.0111	-0.0152	-0.0194	-0.0220	-0.0243	-0.0226	-0.0162	-0.0096	
14.	495.	0.0606	0.1306	0.0177	0.0151	0.0123	0.0099	0.0089	0.0061	0.0017	-0.0019	-0.0059	-0.0097	-0.0115	-0.0110	-0.0103	-0.0031	0.0037	
Run	Point	CP97	CP98	CP99	CP100	CP101	CP102	CP103	CP104	CP105	CP106	CP107	CP108	CP109	CP110				
14.	540.	-0.0361	-0.0390	-0.0360	-0.0310	-0.0280	-0.0345	-0.0412	-0.0442	-0.0355	-0.0385	-0.0155	0.0065	0.0451	0.1766				
14.	531.	-0.0302	-0.0268	-0.0082	0.0197	0.0459	0.0622	0.0781	0.0896	0.1076	0.1059	0.1249	0.1415	0.1475	0.2390				
14.	522.	-0.0181	-0.0057	0.0158	0.0406	0.0659	0.0843	0.0988	0.1075	0.1206	0.1228	0.1319	0.1422	0.1521	0.2456				
14.	513.	0.0114	0.0336	0.0596	0.0844	0.1129	0.1367	0.1649	0.1885	0.2134	0.2274	0.2472	0.2572	0.2551	0.3146				
14.	504.	0.0027	0.0146	0.0327	0.0529	0.0734	0.0921	0.1116	0.1265	0.1439	0.1546	0.1744	0.1803	0.2003	0.2992				
14.	495.	0.0127	0.0267	0.0426	0.0591	0.0751	0.0926	0.1083	0.1216	0.1370	0.1525	0.1692	0.1817	0.1996	0.2974				

Table 16. Continued

(b) $Z_s = 2.31$ in.

Run Point	M_∞	$R_\infty \times 10^{-6}$	p_∞ , psi	$p_{t,\infty}$, psi	q_∞ , psi	$T_{t,\infty}$, °F	CP01	CP02	CP03	CP04	CP05	CP06	CP07	CP08	CP09	CP10	CP11
14. 545.	0.20	2.05	22.94	23.60	0.65	99.6	0.8861	-0.2411	-0.1974	-0.1812	-0.1570	-0.1353	-0.1029	-0.0868	-0.0733	-0.0614	-0.0522
14. 536.	0.40	3.63	19.92	22.24	2.22	100.7	0.9160	-0.2425	-0.2065	-0.1891	-0.1681	-0.1389	-0.1035	-0.0904	-0.0739	-0.0562	-0.0544
14. 527.	0.60	2.82	9.81	12.52	2.48	100.3	1.0009	-0.2639	-0.2275	-0.2070	-0.1841	-0.1535	-0.1153	-0.0961	-0.0781	-0.0620	-0.0574
14. 518.	0.80	2.53	6.20	9.45	2.78	100.9	1.1313	-0.3198	-0.2768	-0.2499	-0.2212	-0.1811	-0.1285	-0.1004	-0.0773	-0.0600	-0.0509
14. 509.	0.90	2.36	4.94	8.35	2.80	100.4	1.2050	-0.3701	-0.3208	-0.3368	-0.3325	-0.2060	-0.1030	-0.0713	-0.0487	-0.0329	-0.0233
14. 500.	0.95	2.41	4.67	8.36	2.95	100.5	1.2403	-0.2634	-0.2693	-0.2975	-0.3189	-0.3499	-0.3595	-0.3412	-0.0119	0.0414	0.0456
Run Point	CP12	CP13	CP14	CP15	CP16	CP17	CP18	CP19	CP20	CP21	CP22	CP23	CP24	CP25	CP26	CP27	CP28
14. 545.	-0.0448	-0.0427	-0.0333	-0.0287	-0.0224	-0.0254	-0.0186	-0.0161	-0.0120	-0.0109	-0.0041	-0.0021	-0.0027	-0.0104	-0.0034	-0.0065	-0.0089
14. 536.	-0.0507	-0.0407	-0.0347	-0.0306	-0.0250	-0.0256	-0.0196	-0.0177	-0.0199	-0.0103	-0.0055	-0.0092	-0.0152	-0.0080	-0.0137	-0.0093	-0.0132
14. 527.	-0.0523	-0.0442	-0.0373	-0.0319	-0.0273	-0.0264	-0.0219	-0.0203	-0.0205	-0.0139	-0.0119	-0.0140	-0.0200	-0.0129	-0.0158	-0.0147	-0.0082
14. 518.	-0.0435	-0.0354	-0.0273	-0.0217	-0.0179	-0.0164	-0.0135	-0.0116	-0.0119	-0.0071	-0.0063	-0.0102	-0.0186	-0.0105	-0.0121	-0.0195	0.0067
14. 509.	-0.0168	-0.0105	-0.0028	0.0030	0.0071	0.0085	0.0098	0.0093	0.0088	0.0099	0.0106	0.0118	0.0094	0.0097	0.0137	0.0092	0.0118
14. 500.	0.0396	0.0346	0.0292	0.0282	0.0287	0.0286	0.0275	0.0251	0.0214	0.0181	0.0157	0.0141	0.0121	0.0118	0.0209	0.0164	0.0265
Run Point	CP29	CP30	CP31	CP32	CP33	CP34	CP35	CP36	CP37	CP38	CP39	CP40	CP41	CP42	CP43	CP44	CP45
14. 545.	-0.0067	-0.0093	-0.0216	-0.0353	-0.0350	-0.0285	-0.0261	-0.0255	-0.0233	-0.0236	-0.0263	-0.0284	-0.0228	-0.0217	-0.0246	-0.0224	-0.0250
14. 536.	0.0190	-0.0129	-0.0466	-0.0671	-0.0682	-0.0533	-0.0478	-0.0416	-0.0412	-0.0334	-0.0388	-0.0404	-0.0273	-0.0262	-0.0301	-0.0321	-0.0326
14. 527.	0.0341	-0.0253	-0.0802	-0.1088	-0.1042	-0.0846	-0.0722	-0.0637	-0.0591	-0.0539	-0.0595	-0.0607	-0.0521	-0.0520	-0.0545	-0.0575	-0.0622
14. 518.	0.0504	-0.0298	-0.1227	-0.1789	-0.1713	-0.1443	-0.1245	-0.1119	-0.1076	-0.1074	-0.1193	-0.1185	-0.1173	-0.1263	-0.1420	-0.1582	-0.1771
14. 509.	0.0635	0.0165	-0.0582	-0.1105	-0.0991	-0.0725	-0.0544	-0.0420	-0.0373	-0.0362	-0.0431	-0.0441	-0.0436	-0.0513	-0.0597	-0.0761	-0.0969
14. 500.	0.0740	0.0347	-0.0405	-0.0967	-0.0816	-0.0489	-0.0252	-0.0083	0.0006	0.0057	0.0014	-0.0027	0.0014	-0.0051	-0.0126	-0.0253	-0.0428
Run Point	CP46	CP47	CP48	CP49	CP50	CP51	CP52	CP53	CP54	CP55	CP56	CP57	CP58	CP59	CP60	CP61	CP62
14. 545.	-0.0065	-0.0032	-0.0164	-0.0397	-0.0196	0.0103	0.0134	0.0112	0.0091	-0.0035	0.0005	0.0063	0.0086	0.0007	-0.0026	-0.0306	-0.0447
14. 536.	-0.0077	-0.0143	0.0103	-0.0797	-0.0330	-0.0102	-0.0046	-0.0189	-0.0114	-0.0171	-0.0190	-0.0222	-0.0307	-0.0216	-0.0252	-0.0371	-0.0505
14. 527.	-0.0121	-0.0173	0.0297	-0.1137	-0.0547	-0.0278	-0.0222	-0.0294	-0.0310	-0.0382	-0.0396	-0.0361	-0.0236	-0.0316	-0.0452	-0.0714	-0.0518
14. 518.	-0.0096	-0.0194	0.0502	-0.1814	-0.1114	-0.0237	-0.0213	-0.0294	-0.0313	-0.0370	-0.0394	-0.0419	-0.0459	-0.0511	-0.0621	-0.0728	-0.0675
14. 509.	0.0110	0.0058	0.0612	-0.1133	-0.0404	0.0083	0.0087	0.0048	0.0042	0.0027	0.0019	-0.0006	-0.0045	-0.0140	-0.0167	-0.0194	-0.0202
14. 500.	0.0134	0.0149	0.0751	-0.0986	0.0038	0.0220	0.0215	0.0187	0.0163	0.0117	0.0100	0.0070	0.0021	-0.0012	-0.0061	-0.0127	-0.0136

Table 16. Concluded

(b) Concluded

Run Point	CP63	CP64	CP65	CP66	CP67	CP68	CP69	CP70	CP71	CP72	CP73	CP74	CP75	CP76	CP77	CP78	CP79
14. 545.	-0.0111	-0.0140	-0.0259	-0.0441	-0.0311	0.0283	0.0152	0.0290	0.0082	0.0037	-0.0305	0.0114	0.0055	-0.0372	0.0043	0.0023	-0.0171
14. 536.	-0.0304	0.0127	-0.0113	0.0267	0.0623	0.0996	0.0942	0.0354	-0.0023	-0.0213	-0.0166	-0.0137	-0.0215	0.0021	-0.0090	-0.0206	-0.0499
14. 527.	-0.0401	-0.0046	0.0283	0.0771	0.1099	0.1196	0.0693	0.1021	-0.0228	-0.0293	0.0202	-0.0268	-0.0288	0.0257	-0.0177	-0.0324	-0.0569
14. 518.	-0.0375	0.0034	0.0428	0.0840	0.1245	0.1347	0.0993	0.1417	-0.0225	-0.0333	0.0474	-0.0264	-0.0341	0.0502	-0.0180	-0.0331	-0.0569
14. 509.	-0.0196	0.0069	0.0484	0.0901	0.1109	0.1111	0.1025	0.1212	0.0088	0.0000	0.0391	0.0058	0.0008	0.0395	0.0137	0.0035	-0.0226
14. 500.	-0.0033	0.0227	0.0579	0.0890	0.1253	0.1296	0.1101	0.1175	0.0205	0.0108	0.0528	0.0185	0.0114	0.0473	0.0224	0.0126	-0.0055
Run Point	CP80	CP81	CP82	CP83	CP84	CP85	CP86	CP87	CP88	CP89	CP90	CP91	CP92	CP93	CP94	CP95	CP96
14. 545.	-0.0056	-0.0299	0.0012	-0.0064	-0.0032	-0.0011	-0.0066	-0.0082	-0.0068	-0.0135	-0.0169	-0.0235	-0.0255	-0.0296	-0.0309	-0.0313	-0.0344
14. 536.	-0.0112	0.1259	-0.0134	-0.0155	-0.0149	-0.0243	-0.0157	-0.0248	-0.0304	-0.0331	-0.0328	-0.0377	-0.0406	-0.0454	-0.0438	-0.0417	-0.0433
14. 527.	0.0214	0.1087	-0.0197	-0.0218	-0.0224	-0.0302	-0.0257	-0.0324	-0.0389	-0.0435	-0.0460	-0.0514	-0.0536	-0.0572	-0.0551	-0.0508	-0.0459
14. 518.	0.0453	0.1280	-0.0206	-0.0235	-0.0248	-0.0307	-0.0293	-0.0350	-0.0420	-0.0492	-0.0542	-0.0604	-0.0633	-0.0638	-0.0577	-0.0410	-0.0258
14. 509.	0.0458	0.1301	0.0107	0.0085	0.0079	0.0042	0.0059	0.0028	-0.0022	-0.0069	-0.0107	-0.0160	-0.0197	-0.0241	-0.0245	-0.0190	-0.0135
14. 500.	0.0487	0.1285	0.0229	0.0204	0.0187	0.0159	0.0156	0.0123	0.0069	0.0031	-0.0019	-0.0061	-0.0081	-0.0110	-0.0110	-0.0036	0.0023
Run Point	CP97	CP98	CP99	CP100	CP101	CP102	CP103	CP104	CP105	CP106	CP107	CP108	CP109	CP110			
14. 545.	-0.0362	-0.0424	-0.0460	-0.0463	-0.0489	-0.0452	-0.0402	-0.0410	-0.0315	-0.0364	-0.0079	0.0198	0.0601	0.1772			
14. 536.	-0.0344	-0.0337	-0.0198	0.0007	0.0247	0.0403	0.0549	0.0627	0.0765	0.0832	0.1000	0.1081	0.1399	0.2405			
14. 527.	-0.0290	-0.0175	0.0040	0.0282	0.0540	0.0700	0.0872	0.1000	0.1128	0.1175	0.1321	0.1439	0.1596	0.2673			
14. 518.	-0.0070	0.0113	0.0367	0.0621	0.0889	0.1120	0.1354	0.1559	0.1833	0.2023	0.2246	0.2288	0.2294	0.3309			
14. 509.	-0.0024	0.0092	0.0278	0.0483	0.0692	0.0864	0.1013	0.1126	0.1264	0.1337	0.1537	0.1633	0.1807	0.2835			
14. 500.	0.0127	0.0223	0.0339	0.0494	0.0654	0.0800	0.0934	0.1079	0.1232	0.1372	0.1542	0.1635	0.1825	0.2959			

Table 17. Pressure Coefficients for Configuration 17 With $h = 4.80$ in., $l = 30.00$ in., $Y_s = 2.40$ in., and $Z_s = -3.00$ in.

Run Point	M_∞	$R_\infty \times 10^{-6}$	p_∞ , psi	$p_{t,\infty}$, psi	q_∞ , psi	$T_{t,\infty}$, °F	CP01	CP02	CP03	CP04	CP05	CP06	CP07	CP08	CP09	CP10	CP11
19. 766.	0.20	2.04	22.95	23.61	0.65	100.4	0.8793	-0.2337	-0.1943	-0.1750	-0.1621	-0.1246	-0.0992	-0.0856	-0.0688	-0.0411	-0.0465
19. 758.	0.40	3.64	19.90	22.23	2.24	100.9	0.9167	-0.2454	-0.2064	-0.1910	-0.1678	-0.1407	-0.1049	-0.0919	-0.0758	-0.0608	-0.0570
19. 750.	0.60	2.82	9.82	12.52	2.47	100.9	1.0011	-0.2711	-0.2296	-0.2101	-0.1838	-0.1553	-0.1163	-0.0966	-0.0790	-0.0658	-0.0575
19. 742.	0.80	2.54	6.19	9.45	2.78	99.1	1.1322	-0.3112	-0.2764	-0.2484	-0.2205	-0.1804	-0.1272	-0.0983	-0.0757	-0.0578	-0.0496
19. 734.	0.90	2.36	4.93	8.34	2.80	100.1	1.2043	-0.3658	-0.3240	-0.3388	-0.3285	-0.2188	-0.1045	-0.0702	-0.0485	-0.0331	-0.0242
19. 726.	0.95	2.40	4.67	8.34	2.95	100.1	1.2384	-0.2597	-0.2704	-0.2991	-0.3196	-0.3533	-0.3620	-0.3414	-0.0131	0.0377	0.0453
Run Point	CP12	CP13	CP14	CP15	CP16	CP17	CP18	CP19	CP20	CP21	CP22	CP23	CP24	CP25	CP26	CP27	CP28
19. 766.	-0.0476	-0.0341	-0.0294	-0.0263	-0.0211	-0.0302	-0.0210	-0.0117	-0.0145	0.0021	0.0108	0.0004	-0.0099	0.0049	-0.0073	0.0022	-0.0143
19. 758.	-0.0521	-0.0458	-0.0382	-0.0324	-0.0260	-0.0248	-0.0197	-0.0176	-0.0180	-0.0129	-0.0105	-0.0128	-0.0201	-0.0116	-0.0127	-0.0099	-0.0074
19. 750.	-0.0513	-0.0460	-0.0369	-0.0317	-0.0275	-0.0257	-0.0221	-0.0195	-0.0188	-0.0162	-0.0162	-0.0154	-0.0187	-0.0162	-0.0146	-0.0164	-0.0058
19. 742.	-0.0427	-0.0345	-0.0266	-0.0210	-0.0158	-0.0155	-0.0121	-0.0108	-0.0119	-0.0077	-0.0063	-0.0103	-0.0153	-0.0097	-0.0101	-0.0144	0.0116
19. 734.	-0.0169	-0.0119	-0.0039	0.0013	0.0056	0.0074	0.0108	0.0112	0.0097	0.0118	0.0111	0.0095	0.0066	0.0081	0.0134	0.0105	0.0231
19. 726.	0.0411	0.0330	0.0294	0.0282	0.0282	0.0283	0.0261	0.0218	0.0205	0.0134	0.0103	0.0117	0.0111	0.0077	0.0207	0.0171	0.0358
Run Point	CP29	CP30	CP31	CP32	CP33	CP34	CP35	CP36	CP37	CP38	CP39	CP40	CP41	CP42	CP43	CP44	CP45
19. 766.	0.0053	-0.0113	-0.0296	-0.0422	-0.0463	-0.0323	-0.0266	-0.0338	-0.0309	-0.0245	-0.0280	-0.0372	-0.0245	-0.0243	-0.0206	-0.0212	-0.0235
19. 758.	0.0322	-0.0159	-0.0653	-0.0922	-0.0835	-0.0659	-0.0521	-0.0437	-0.0400	-0.0357	-0.0383	-0.0415	-0.0292	-0.0285	-0.0324	-0.0322	-0.0363
19. 750.	0.0432	-0.0219	-0.0818	-0.1139	-0.1054	-0.0889	-0.0740	-0.0634	-0.0571	-0.0543	-0.0554	-0.0577	-0.0513	-0.0522	-0.0558	-0.0578	-0.0617
19. 742.	0.0605	-0.0390	-0.1349	-0.1882	-0.1774	-0.1467	-0.1244	-0.1109	-0.1052	-0.1039	-0.1142	-0.1139	-0.1107	-0.1192	-0.1350	-0.1521	-0.1722
19. 734.	0.0855	0.0100	-0.0829	-0.1428	-0.1287	-0.0946	-0.0693	-0.0517	-0.0423	-0.0374	-0.0436	-0.0517	-0.0439	-0.0511	-0.0626	-0.0791	-0.1003
19. 726.	0.0913	0.0291	-0.0604	-0.1207	-0.1016	-0.0650	-0.0351	-0.0131	-0.0007	0.0031	0.0029	-0.0055	0.0014	-0.0017	-0.0138	-0.0264	-0.0432
Run Point	CP46	CP47	CP48	CP49	CP50	CP51	CP52	CP53	CP54	CP55	CP56	CP57	CP58	CP59	CP60	CP61	CP62
19. 766.	0.0025	-0.0085	0.0029	-0.0547	-0.0193	0.0011	0.0099	-0.0181	-0.0076	-0.0129	-0.0011	0.0057	-0.0063	0.0088	0.0031	-0.0290	-0.0344
19. 758.	-0.0099	-0.0148	0.0336	-0.0953	-0.0355	-0.0158	-0.0144	-0.0204	-0.0240	-0.0235	-0.0195	-0.0192	-0.0169	-0.0201	-0.0386	-0.0432	-0.0416
19. 750.	-0.0145	-0.0190	0.0443	-0.1174	-0.0549	-0.0178	-0.0219	-0.0227	-0.0199	-0.0215	-0.0265	-0.0372	-0.0455	-0.0508	-0.0618	-0.0662	-0.0455
19. 742.	-0.0084	-0.0196	0.0675	-0.1878	-0.1094	-0.0149	-0.0112	-0.0206	-0.0232	-0.0308	-0.0314	-0.0322	-0.0362	-0.0406	-0.0556	-0.0748	-0.0659
19. 734.	0.0102	0.0051	0.0949	-0.1424	-0.0403	0.0188	0.0165	0.0122	0.0100	0.0093	0.0072	0.0019	-0.0064	-0.0139	-0.0209	-0.0198	-0.0213
19. 726.	0.0102	0.0158	0.0981	-0.1155	0.0002	0.0284	0.0214	0.0255	0.0221	0.0174	0.0096	0.0016	-0.0044	-0.0088	-0.0098	-0.0028	-0.0123

Table 17. Concluded

Run Point	CP63	CP64	CP65	CP66	CP67	CP68	CP69	CP70	CP71	CP72	CP73	CP74	CP75	CP76	CP77	CP78	CP79
19. 766.	-0.0557	-0.0087	-0.0291	-0.0006	0.0350	0.0307	0.0522	0.0642	0.0173	-0.0100	-0.0202	-0.0022	-0.0092	-0.0127	0.0141	0.0006	-0.0234
19. 758.	-0.0062	-0.0176	-0.0072	0.0597	0.1123	0.1420	0.0737	0.0606	-0.0125	-0.0236	-0.0151	-0.0166	-0.0231	0.0019	-0.0087	-0.0270	-0.0661
19. 750.	-0.0389	-0.0353	-0.0093	0.0490	0.1060	0.1237	0.0760	0.0725	-0.0203	-0.0262	-0.0142	-0.0220	-0.0238	-0.0094	-0.0147	-0.0301	-0.0663
19. 742.	-0.0354	-0.0036	0.0423	0.0862	0.1299	0.1133	0.0701	0.1429	-0.0109	-0.0267	0.0326	-0.0171	-0.0257	0.0421	-0.0131	-0.0296	-0.0670
19. 734.	-0.0157	0.0169	0.0473	0.0927	0.1376	0.1453	0.1007	0.1072	0.0152	0.0050	0.0391	0.0139	0.0069	0.0373	0.0171	0.0018	-0.0315
19. 726.	-0.0122	0.0158	0.0608	0.1057	0.1388	0.1397	0.0971	0.1006	0.0212	0.0137	0.0485	0.0237	0.0173	0.0398	0.0210	0.0110	-0.0180
Run Point	CP80	CP81	CP82	CP83	CP84	CP85	CP86	CP87	CP88	CP89	CP90	CP91	CP92	CP93	CP94	CP95	CP96
19. 766.	0.0113	0.0411	-0.0025	-0.0146	-0.0003	-0.0144	0.0012	-0.0104	-0.0120	-0.0116	-0.0089	-0.0185	-0.0228	-0.0322	-0.0293	-0.0365	-0.0391
19. 758.	0.0596	0.1148	-0.0131	-0.0183	-0.0187	-0.0223	-0.0193	-0.0252	-0.0311	-0.0352	-0.0368	-0.0408	-0.0457	-0.0503	-0.0519	-0.0543	-0.0502
19. 750.	0.0320	0.1195	-0.0229	-0.0281	-0.0286	-0.0313	-0.0323	-0.0338	-0.0370	-0.0412	-0.0471	-0.0551	-0.0606	-0.0651	-0.0642	-0.0588	-0.0444
19. 742.	0.0591	0.1260	-0.0187	-0.0218	-0.0215	-0.0287	-0.0244	-0.0315	-0.0379	-0.0447	-0.0496	-0.0578	-0.0628	-0.0643	-0.0600	-0.0452	-0.0304
19. 734.	0.0597	0.1258	0.0110	0.0077	0.0062	0.0008	0.0033	-0.0017	-0.0070	-0.0112	-0.0142	-0.0217	-0.0272	-0.0312	-0.0301	-0.0223	-0.0129
19. 726.	0.0684	0.1421	0.0206	0.0156	0.0131	0.0118	0.0095	0.0085	0.0057	0.0028	-0.0031	-0.0088	-0.0127	-0.0144	-0.0156	-0.0086	0.0015
Run Point	CP97	CP98	CP99	CP100	CP101	CP102	CP103	CP104	CP105	CP106	CP107	CP108	CP109	CP110			
19. 766.	-0.0341	-0.0466	-0.0415	-0.0321	-0.0162	-0.0136	-0.0121	-0.0073	0.0088	0.0099	0.0353	0.0650	0.1128	0.2248			
19. 758.	-0.0388	-0.0260	-0.0076	0.0125	0.0386	0.0565	0.0808	0.0846	0.0925	0.1092	0.1230	0.1290	0.1617	0.2764			
19. 750.	-0.0282	-0.0090	0.0152	0.0414	0.0661	0.0886	0.1121	0.1258	0.1410	0.1423	0.1643	0.1650	0.1637	0.2951			
19. 742.	-0.0086	0.0121	0.0400	0.0675	0.0960	0.1185	0.1422	0.1635	0.1932	0.2124	0.2412	0.2466	0.2313	0.3611			
19. 734.	0.0022	0.0180	0.0412	0.0658	0.0904	0.1084	0.1282	0.1472	0.1717	0.1859	0.2124	0.2208	0.2238	0.3537			
19. 726.	0.0127	0.0304	0.0476	0.0662	0.0825	0.0979	0.1135	0.1281	0.1459	0.1655	0.1846	0.1903	0.2048	0.3353			

Table 18. Pressure Coefficients for Configuration 18 With $h = 4.80$ in., $l = 30.00$ in., and $Y_s = 2.40$ in.(a) $Z_s = 0.00$ in.

Run Point	M_∞	$R_\infty \times 10^{-6}$	P_∞ , psi	$P_{t,\infty}$, psi	q_∞ , psi	$T_{t,\infty}$, °F	CP01	CP02	CP03	CP04	CP05	CP06	CP07	CP08	CP09	CP10	CP11
13. 482.	0.20	2.06	22.94	23.61	0.66	100.1	0.8832	-0.2237	-0.1912	-0.1716	-0.1554	-0.1228	-0.1011	-0.0853	-0.0685	-0.0444	-0.0446
13. 473.	0.40	3.64	19.88	22.21	2.24	100.5	0.9131	-0.2505	-0.2064	-0.1905	-0.1673	-0.1413	-0.1058	-0.0924	-0.0750	-0.0609	-0.0552
13. 464.	0.60	2.82	9.80	12.50	2.48	100.3	1.0024	-0.2650	-0.2276	-0.2080	-0.1818	-0.1547	-0.1164	-0.0960	-0.0781	-0.0660	-0.0570
13. 455.	0.80	2.54	6.20	9.46	2.78	99.8	1.1316	-0.3175	-0.2772	-0.2491	-0.2235	-0.1822	-0.1287	-0.1014	-0.0786	-0.0579	-0.0529
13. 446.	0.90	2.35	4.92	8.33	2.79	101.2	1.2034	-0.3714	-0.3219	-0.3397	-0.3344	-0.2129	-0.1049	-0.0719	-0.0504	-0.0335	-0.0257
12. 428.	0.95	2.40	4.67	8.35	2.95	100.6	1.2403	-0.2679	-0.2697	-0.2979	-0.3200	-0.3503	-0.3611	-0.3437	-0.0126	0.0435	0.0468
Run Point	CP12	CP13	CP14	CP15	CP16	CP17	CP18	CP19	CP20	CP21	CP22	CP23	CP24	CP25	CP26	CP27	CP28
13. 482.	-0.0432	-0.0362	-0.0277	-0.0259	-0.0230	-0.0299	-0.0155	-0.0094	-0.0126	-0.0004	0.0107	0.0038	-0.0040	0.0027	-0.0066	0.0083	-0.0103
13. 473.	-0.0501	-0.0439	-0.0356	-0.0312	-0.0286	-0.0269	-0.0213	-0.0177	-0.0191	-0.0148	-0.0113	-0.0140	-0.0184	-0.0135	-0.0131	-0.0093	-0.0136
13. 464.	-0.0494	-0.0465	-0.0368	-0.0311	-0.0258	-0.0237	-0.0215	-0.0218	-0.0210	-0.0203	-0.0190	-0.0191	-0.0252	-0.0190	-0.0173	-0.0144	-0.0039
13. 455.	-0.0459	-0.0363	-0.0287	-0.0236	-0.0171	-0.0176	-0.0130	-0.0113	-0.0150	-0.0096	-0.0078	-0.0122	-0.0201	-0.0111	-0.0150	-0.0157	0.0052
13. 446.	-0.0185	-0.0125	-0.0052	-0.0007	0.0042	0.0044	0.0061	0.0075	0.0065	0.0104	0.0106	0.0078	0.0002	0.0069	0.0095	0.0102	0.0133
12. 428.	0.0403	0.0345	0.0296	0.0271	0.0266	0.0257	0.0242	0.0226	0.0195	0.0185	0.0167	0.0130	0.0085	0.0099	0.0180	0.0197	0.0245
Run Point	CP29	CP30	CP31	CP32	CP33	CP34	CP35	CP36	CP37	CP38	CP39	CP40	CP41	CP42	CP43	CP44	CP45
13. 482.	-0.0173	-0.0159	-0.0159	-0.0215	-0.0294	-0.0195	-0.0177	-0.0253	-0.0226	-0.0228	-0.0308	-0.0297	-0.0118	-0.0145	-0.0171	-0.0206	-0.0219
13. 473.	0.0038	-0.0079	-0.0335	-0.0540	-0.0553	-0.0443	-0.0374	-0.0355	-0.0321	-0.0306	-0.0359	-0.0383	-0.0302	-0.0322	-0.0312	-0.0321	-0.0336
13. 464.	0.0255	-0.0144	-0.0681	-0.1025	-0.0981	-0.0825	-0.0698	-0.0610	-0.0551	-0.0546	-0.0540	-0.0599	-0.0527	-0.0545	-0.0514	-0.0531	-0.0574
13. 455.	0.0453	-0.0330	-0.1213	-0.1723	-0.1645	-0.1359	-0.1181	-0.1089	-0.1066	-0.1045	-0.1165	-0.1174	-0.1140	-0.1242	-0.1371	-0.1537	-0.1737
13. 446.	0.0566	0.0156	-0.0574	-0.1102	-0.0995	-0.0719	-0.0535	-0.0409	-0.0364	-0.0339	-0.0414	-0.0460	-0.0418	-0.0461	-0.0610	-0.0771	-0.0978
12. 428.	0.0657	0.0284	-0.0386	-0.0855	-0.0714	-0.0401	-0.0169	-0.0026	0.0066	0.0081	0.0052	0.0038	0.0036	-0.0027	-0.0121	-0.0247	-0.0420
Run Point	CP46	CP47	CP48	CP49	CP50	CP51	CP52	CP53	CP54	CP55	CP56	CP57	CP58	CP59	CP60	CP61	CP62
13. 482.	0.0053	-0.0020	-0.0212	-0.0390	-0.0122	0.0024	0.0177	-0.0044	0.0017	-0.0014	-0.0006	-0.0015	0.0093	0.0185	-0.0004	-0.0170	-0.0051
13. 473.	-0.0106	-0.0135	0.0076	-0.0683	-0.0290	-0.0112	-0.0072	-0.0233	-0.0200	-0.0120	-0.0175	-0.0250	-0.0282	-0.0281	-0.0531	-0.0634	-0.0332
13. 464.	-0.0177	-0.0172	0.0398	-0.1164	-0.0548	-0.0232	-0.0235	-0.0258	-0.0299	-0.0444	-0.0521	-0.0470	-0.0436	-0.0507	-0.0666	-0.0754	-0.0616
13. 455.	-0.0096	-0.0209	0.0492	-0.1792	-0.1100	-0.0180	-0.0131	-0.0251	-0.0258	-0.0292	-0.0301	-0.0321	-0.0398	-0.0504	-0.0627	-0.0733	-0.0651
13. 446.	0.0077	0.0030	0.0657	-0.1182	-0.0375	0.0130	0.0141	0.0111	0.0102	0.0033	0.0000	-0.0029	-0.0055	-0.0038	-0.0087	-0.0167	-0.0184
12. 428.	0.0122	0.0143	0.0752	-0.0910	0.0052	0.0269	0.0240	0.0214	0.0202	0.0169	0.0122	0.0110	0.0056	0.0054	0.0036	-0.0034	-0.0026

Table 18. Continued

(a) Concluded

Run Point	CP63	CP64	CP65	CP66	CP67	CP68	CP69	CP70	CP71	CP72	CP73	CP74	CP75	CP76	CP77	CP78	CP79
13. 482.	-0.0116	0.0001	-0.0307	-0.0228	0.0052	-0.0052	0.0406	0.0706	0.0176	-0.0093	-0.0472	0.0049	-0.0009	-0.0274	0.0187	0.0039	-0.0075
13. 473.	-0.0383	-0.0234	-0.0222	-0.0055	0.0582	0.0661	0.0693	0.0801	-0.0052	-0.0169	-0.0241	-0.0086	-0.0161	-0.0222	-0.0049	-0.0153	-0.0223
13. 464.	-0.0320	0.0119	0.0220	0.0627	0.1175	0.1205	0.0978	0.1179	-0.0240	-0.0336	0.0214	-0.0262	-0.0293	0.0225	-0.0236	-0.0394	-0.0567
13. 455.	-0.0359	0.0129	0.0406	0.0954	0.1213	0.1145	0.0792	0.1285	-0.0134	-0.0283	0.0464	-0.0191	-0.0296	0.0571	-0.0148	-0.0383	-0.0452
13. 446.	-0.0073	0.0059	0.0405	0.0883	0.1261	0.1250	0.0998	0.0936	0.0093	0.0044	0.0363	0.0084	0.0076	0.0402	0.0118	-0.0037	-0.0177
12. 428.	-0.0029	0.0173	0.0514	0.0928	0.1056	0.1135	0.0902	0.0816	0.0227	0.0194	0.0427	0.0228	0.0204	0.0401	0.0236	0.0101	-0.0005
Run Point	CP80	CP81	CP82	CP83	CP84	CP85	CP86	CP87	CP88	CP89	CP90	CP91	CP92	CP93	CP94	CP95	CP96
13. 482.	-0.0016	0.0041	0.0040	-0.0008	0.0082	0.0013	0.0081	-0.0014	-0.0043	-0.0061	-0.0007	-0.0078	-0.0098	-0.0184	-0.0150	-0.0185	-0.0226
13. 473.	0.0017	0.0468	-0.0118	-0.0149	-0.0134	-0.0183	-0.0159	-0.0198	-0.0214	-0.0249	-0.0270	-0.0330	-0.0377	-0.0442	-0.0456	-0.0457	-0.0462
13. 464.	0.0367	0.1627	-0.0237	-0.0287	-0.0313	-0.0334	-0.0346	-0.0357	-0.0379	-0.0414	-0.0448	-0.0508	-0.0538	-0.0566	-0.0564	-0.0512	-0.0377
13. 455.	0.0393	0.1741	-0.0228	-0.0243	-0.0235	-0.0316	-0.0255	-0.0333	-0.0399	-0.0460	-0.0487	-0.0553	-0.0589	-0.0612	-0.0541	-0.0364	-0.0211
13. 446.	0.0439	0.1449	0.0087	0.0057	0.0042	-0.0009	0.0031	-0.0018	-0.0061	-0.0085	-0.0110	-0.0154	-0.0191	-0.0233	-0.0224	-0.0165	-0.0106
12. 428.	0.0517	0.1238	0.0190	0.0167	0.0148	0.0125	0.0129	0.0095	0.0076	0.0050	0.0012	-0.0041	-0.0036	-0.0106	-0.0090	-0.0058	0.0005
Run Point	CP97	CP98	CP99	CP100	CP101	CP102	CP103	CP104	CP105	CP106	CP107	CP108	CP109	CP110			
13. 482.	-0.0217	-0.0363	-0.0388	-0.0355	-0.0327	-0.0412	-0.0427	-0.0545	-0.0430	-0.0334	-0.0126	0.0170	0.0865	0.1839			
13. 473.	-0.0393	-0.0350	-0.0262	-0.0156	-0.0020	0.0074	0.0219	0.0314	0.0432	0.0476	0.0629	0.0831	0.1157	0.2274			
13. 464.	-0.0219	-0.0005	0.0203	0.0428	0.0613	0.0782	0.0950	0.1084	0.1226	0.1389	0.1382	0.1420	0.1689	0.2748			
13. 455.	0.0042	0.0189	0.0429	0.0696	0.0969	0.1171	0.1361	0.1490	0.1726	0.1866	0.2060	0.2105	0.2078	0.3218			
13. 446.	0.0018	0.0118	0.0295	0.0483	0.0667	0.0816	0.0952	0.1073	0.1195	0.1245	0.1364	0.1432	0.1626	0.2859			
12. 428.	0.0098	0.0204	0.0346	0.0495	0.0647	0.0761	0.0875	0.0952	0.1070	0.1091	0.1147	0.1240	0.1558	0.2854			

Table 18. Continued

(b) $Z_s = 2.31$ in.

Run Point	M_∞	$R_\infty \times 10^{-6}$	p_∞ , psi	$p_{h,\infty}$, psi	q_∞ , psi	$T_{t,\infty}$, °F	CP01	CP02	CP03	CP04	CP05	CP06	CP07	CP08	CP09	CP10	CP11
13. 487.	0.20	2.03	22.96	23.61	0.64	100.5	0.8857	-0.2380	-0.2010	-0.1832	-0.1674	-0.1330	-0.1107	-0.0943	-0.0782	-0.0513	-0.0548
13. 478.	0.40	3.64	19.90	22.23	2.24	100.8	0.9193	-0.2492	-0.2050	-0.1894	-0.1653	-0.1395	-0.1037	-0.0906	-0.0725	-0.0593	-0.0543
13. 469.	0.60	2.82	9.80	12.50	2.48	100.3	1.0030	-0.2670	-0.2290	-0.2089	-0.1832	-0.1555	-0.1169	-0.0971	-0.0787	-0.0660	-0.0576
13. 460.	0.80	2.54	6.21	9.45	2.78	99.9	1.1315	-0.3147	-0.2753	-0.2476	-0.2225	-0.1802	-0.1281	-0.1000	-0.0776	-0.0565	-0.0515
13. 451.	0.90	2.36	4.94	8.35	2.80	100.9	1.2021	-0.3730	-0.3235	-0.3382	-0.3308	-0.2124	-0.1063	-0.0743	-0.0516	-0.0332	-0.0277
12. 433.	0.95	2.40	4.68	8.35	2.95	100.5	1.2393	-0.2694	-0.2705	-0.2997	-0.3202	-0.3505	-0.3611	-0.3280	-0.0033	0.0431	0.0452
Run Point	CP12	CP13	CP14	CP15	CP16	CP17	CP18	CP19	CP20	CP21	CP22	CP23	CP24	CP25	CP26	CP27	CP28
13. 487.	-0.0522	-0.0415	-0.0351	-0.0355	-0.0310	-0.0363	-0.0234	-0.0140	-0.0195	-0.0013	0.0089	0.0029	-0.0029	-0.0004	-0.0132	-0.0001	-0.0204
13. 478.	-0.0489	-0.0452	-0.0369	-0.0322	-0.0317	-0.0298	-0.0244	-0.0200	-0.0194	-0.0148	-0.0110	-0.0115	-0.0130	-0.0144	-0.0147	-0.0122	-0.0107
13. 469.	-0.0500	-0.0470	-0.0371	-0.0317	-0.0281	-0.0252	-0.0212	-0.0203	-0.0198	-0.0194	-0.0178	-0.0167	-0.0206	-0.0187	-0.0173	-0.0155	-0.0014
13. 460.	-0.0455	-0.0364	-0.0290	-0.0241	-0.0179	-0.0192	-0.0145	-0.0108	-0.0138	-0.0065	-0.0052	-0.0117	-0.0186	-0.0106	-0.0168	-0.0155	0.0062
13. 451.	-0.0203	-0.0122	-0.0055	-0.0012	0.0066	0.0067	0.0099	0.0104	0.0075	0.0107	0.0111	0.0086	0.0068	0.0094	0.0108	0.0099	0.0154
12. 433.	0.0386	0.0334	0.0294	0.0271	0.0271	0.0260	0.0254	0.0234	0.0208	0.0197	0.0192	0.0175	0.0140	0.0140	0.0200	0.0183	0.0299
Run Point	CP29	CP30	CP31	CP32	CP33	CP34	CP35	CP36	CP37	CP38	CP39	CP40	CP41	CP42	CP43	CP44	CP45
13. 487.	-0.0109	-0.0218	-0.0248	-0.0321	-0.0421	-0.0264	-0.0236	-0.0314	-0.0275	-0.0233	-0.0272	-0.0424	-0.0281	-0.0288	-0.0174	-0.0166	-0.0245
13. 478.	0.0246	-0.0170	-0.0572	-0.0792	-0.0735	-0.0568	-0.0457	-0.0409	-0.0378	-0.0362	-0.0384	-0.0399	-0.0314	-0.0322	-0.0346	-0.0359	-0.0360
13. 469.	0.0432	-0.0258	-0.0912	-0.1232	-0.1139	-0.0943	-0.0781	-0.0672	-0.0616	-0.0590	-0.0582	-0.0602	-0.0526	-0.0551	-0.0570	-0.0591	-0.0602
13. 460.	0.0571	-0.0442	-0.1345	-0.1868	-0.1781	-0.1459	-0.1256	-0.1138	-0.1100	-0.1070	-0.1194	-0.1191	-0.1151	-0.1251	-0.1358	-0.1514	-0.1710
13. 451.	0.0701	0.0097	-0.0700	-0.1231	-0.1121	-0.0801	-0.0582	-0.0441	-0.0386	-0.0336	-0.0436	-0.0472	-0.0418	-0.0512	-0.0630	-0.0787	-0.1001
12. 433.	0.0828	0.0307	-0.0502	-0.1070	-0.0911	-0.0553	-0.0275	-0.0097	0.0012	0.0047	0.0022	-0.0024	0.0018	-0.0044	-0.0135	-0.0262	-0.0432
Run Point	CP46	CP47	CP48	CP49	CP50	CP51	CP52	CP53	CP54	CP55	CP56	CP57	CP58	CP59	CP60	CP61	CP62
13. 487.	0.0034	-0.0143	-0.0239	-0.0356	-0.0158	0.0004	0.0152	-0.0141	-0.0070	-0.0119	-0.0079	0.0008	-0.0033	-0.0061	-0.0134	-0.0162	-0.0158
13. 478.	-0.0094	-0.0162	0.0214	-0.0843	-0.0323	-0.0067	-0.0048	-0.0142	-0.0133	-0.0156	-0.0257	-0.0366	-0.0276	-0.0014	-0.0141	-0.0638	-0.0635
13. 469.	-0.0148	-0.0207	0.0453	-0.1232	-0.0571	-0.0171	-0.0227	-0.0261	-0.0276	-0.0303	-0.0378	-0.0325	-0.0323	-0.0316	-0.0335	-0.0560	-0.0735
13. 460.	-0.0078	-0.0210	0.0574	-0.1886	-0.1121	-0.0129	-0.0063	-0.0162	-0.0150	-0.0242	-0.0260	-0.0378	-0.0545	-0.0532	-0.0606	-0.0598	-0.0577
13. 451.	0.0121	0.0009	0.0759	-0.1253	-0.0377	0.0061	0.0085	-0.0048	-0.0072	-0.0079	-0.0132	-0.0129	-0.0135	-0.0115	-0.0165	-0.0216	-0.0213
12. 433.	0.0171	0.0104	0.0893	-0.1060	0.0011	0.0345	0.0344	0.0326	0.0323	0.0250	0.0249	0.0213	0.0179	0.0127	0.0065	-0.0064	-0.0079

Table 18. Concluded

(b) Concluded

Run Point	CP63	CP64	CP65	CP66	CP67	CP68	CP69	CP70	CP71	CP72	CP73	CP74	CP75	CP76	CP77	CP78	CP79
13. 487.	-0.0051	-0.0171	-0.0762	-0.0616	-0.0135	-0.0265	0.0082	-0.0157	0.0205	-0.0126	-0.0616	0.0020	-0.0082	-0.0378	0.0113	0.0021	-0.0065
13. 478.	-0.0569	-0.0117	0.0227	0.0738	0.0551	0.0767	0.0534	-0.0147	-0.0040	-0.0210	0.0073	-0.0096	-0.0174	0.0096	-0.0089	-0.0193	-0.0319
13. 469.	-0.0612	-0.0335	0.0324	0.1029	0.1395	0.1278	0.0831	0.0753	-0.0234	-0.0319	0.0302	-0.0220	-0.0296	0.0323	-0.0239	-0.0363	-0.0584
13. 460.	-0.0318	0.0157	0.0515	0.0876	0.1266	0.1198	0.0691	0.1074	-0.0106	-0.0286	0.0380	-0.0149	-0.0262	0.0471	-0.0151	-0.0345	-0.0407
13. 451.	-0.0119	0.0199	0.0527	0.0918	0.1113	0.1123	0.0829	0.1071	0.0115	-0.0115	0.0486	0.0032	-0.0103	0.0456	0.0176	0.0051	-0.0147
12. 433.	-0.0014	0.0220	0.0594	0.1015	0.1262	0.1207	0.1017	0.0933	0.0330	0.0273	0.0516	0.0336	0.0279	0.0446	0.0262	0.0148	-0.0010
Run Point	CP80	CP81	CP82	CP83	CP84	CP85	CP86	CP87	CP88	CP89	CP90	CP91	CP92	CP93	CP94	CP95	CP96
13. 487.	-0.0133	-0.0680	-0.0056	-0.0106	-0.0012	-0.0127	0.0016	-0.0087	-0.0097	-0.0104	-0.0049	-0.0135	-0.0163	-0.0264	-0.0259	-0.0319	-0.0359
13. 478.	0.0204	0.0972	-0.0156	-0.0181	-0.0171	-0.0215	-0.0209	-0.0246	-0.0286	-0.0327	-0.0350	-0.0401	-0.0442	-0.0480	-0.0502	-0.0501	-0.0466
13. 469.	0.0444	0.1241	-0.0279	-0.0328	-0.0344	-0.0368	-0.0375	-0.0395	-0.0430	-0.0470	-0.0520	-0.0581	-0.0601	-0.0609	-0.0584	-0.0509	-0.0385
13. 460.	0.0301	0.1364	-0.0214	-0.0231	-0.0218	-0.0320	-0.0255	-0.0344	-0.0397	-0.0457	-0.0484	-0.0563	-0.0596	-0.0628	-0.0572	-0.0408	-0.0271
13. 451.	0.0455	0.1281	0.0124	0.0098	0.0107	0.0027	0.0089	0.0023	-0.0026	-0.0070	-0.0093	-0.0141	-0.0189	-0.0248	-0.0238	-0.0180	-0.0131
12. 433.	0.0629	0.1313	0.0210	0.0194	0.0179	0.0154	0.0146	0.0109	0.0090	0.0050	0.0000	-0.0053	-0.0052	-0.0110	-0.0097	-0.0051	0.0015
Run Point	CP97	CP98	CP99	CP100	CP101	CP102	CP103	CP104	CP105	CP106	CP107	CP108	CP109	CP110			
13. 487.	-0.0351	-0.0538	-0.0576	-0.0563	-0.0513	-0.0541	-0.0438	-0.0515	-0.0325	-0.0499	-0.0128	0.0221	0.0557	0.1828			
13. 478.	-0.0390	-0.0309	-0.0173	0.0066	0.0341	0.0457	0.0560	0.0592	0.0705	0.0792	0.0934	0.1076	0.1403	0.2595			
13. 469.	-0.0219	0.0013	0.0238	0.0506	0.0754	0.0958	0.1157	0.1252	0.1392	0.1468	0.1617	0.1611	0.1725	0.3012			
13. 460.	-0.0047	0.0115	0.0384	0.0662	0.0962	0.1150	0.1353	0.1490	0.1737	0.1935	0.2161	0.2193	0.2085	0.3493			
13. 451.	0.0023	0.0102	0.0294	0.0508	0.0730	0.0894	0.1069	0.1188	0.1334	0.1396	0.1624	0.1733	0.1941	0.3202			
12. 433.	0.0112	0.0239	0.0415	0.0593	0.0779	0.0915	0.1060	0.1177	0.1371	0.1489	0.1714	0.1746	0.1908	0.3244			

Table 19. Force and Moment Data for Configuration 7 With $h = 2.40$ in., $l = 26.00$ in., and $Y_g = 0.00$ in.

Run	Point	M_∞	$R_\infty \times 10^{-6}$	P_∞ , psi	$P_{t,\infty}$, psi	q_∞ , psi	$T_{t,\infty}$, of	Z_s , in.	C_N	C_m	C_A	C_{A_B}	C_Y	C_n
5	103	0.20	2.04	22.93	23.58	0.64	98.7	-0.90	-0.76	6.42	-0.231	-0.374	0.068	0.171
5	104	0.20	2.04	22.95	23.60	0.64	98.9	-0.50	-0.77	7.93	-0.071	-0.302	0.056	0.334
5	105	0.20	2.04	22.97	23.62	0.64	98.9	0.00	-0.68	9.06	0.243	-0.042	0.086	0.353
5	106	0.20	2.04	22.97	23.62	0.64	99.0	0.50	-0.81	8.67	0.498	0.211	0.110	0.109
5	107	0.20	2.04	22.97	23.62	0.64	99.0	1.00	-1.03	9.19	0.729	0.446	0.107	-0.051
5	108	0.20	2.04	22.96	23.61	0.64	99.1	1.50	-1.08	8.88	0.836	0.538	0.079	0.049
5	109	0.20	2.03	22.98	23.62	0.64	99.1	2.00	-1.03	7.99	0.836	0.524	0.066	0.079
5	110	0.20	2.03	22.96	23.60	0.64	99.1	2.36	-0.96	7.17	0.804	0.485	0.080	0.048
5	92	0.40	3.64	19.93	22.24	2.22	98.6	-0.90	-0.67	5.99	-0.344	-0.382	0.013	-0.139
5	93	0.40	3.62	19.91	22.22	2.21	99.7	-0.50	-0.67	7.65	-0.181	-0.325	0.004	0.156
5	94	0.40	3.68	19.87	22.25	2.28	99.8	0.00	-0.62	8.80	0.149	-0.041	0.024	0.029
5	95	0.40	3.65	19.90	22.24	2.25	99.9	0.50	-0.78	8.23	0.403	0.222	0.025	-0.099
5	96	0.40	3.65	19.89	22.23	2.25	100.0	1.00	-0.98	9.02	0.634	0.462	0.043	-0.240
5	97	0.40	3.65	19.88	22.22	2.25	99.9	1.50	-1.01	8.68	0.722	0.525	0.019	-0.148
5	98	0.40	3.64	19.89	22.22	2.24	99.8	1.50	-1.01	8.74	0.728	0.534	0.027	-0.181
5	99	0.40	3.64	19.89	22.22	2.24	99.8	1.50	-1.01	8.71	0.725	0.531	0.015	-0.130
5	100	0.40	3.66	19.90	22.24	2.25	99.7	2.00	-0.95	7.76	0.718	0.523	0.019	-0.130
5	101	0.40	3.64	19.88	22.21	2.24	99.7	2.37	-0.88	6.99	0.685	0.491	0.011	-0.085
5	83	0.60	4.70	16.35	20.87	4.14	100.9	-0.90	-0.63	5.47	-0.370	-0.388	-0.006	-0.166
5	84	0.60	4.69	16.36	20.86	4.11	100.7	-0.50	-0.62	7.27	-0.222	-0.346	-0.015	0.073
5	85	0.60	4.69	16.36	20.87	4.12	100.7	0.00	-0.57	8.45	0.110	-0.058	-0.015	0.144
5	86	0.60	4.70	16.32	20.84	4.13	100.7	0.50	-0.75	8.08	0.379	0.229	0.017	-0.097
5	87	0.60	4.71	16.32	20.85	4.15	100.7	1.00	-0.95	8.80	0.587	0.439	0.017	-0.192
5	88	0.60	4.70	16.30	20.82	4.13	100.7	1.50	-0.99	8.68	0.681	0.522	0.018	-0.230
5	89	0.60	4.70	16.34	20.86	4.13	100.6	2.00	-0.94	7.82	0.685	0.526	0.008	-0.161
5	90	0.60	4.70	16.33	20.85	4.13	100.6	2.36	-0.89	7.15	0.669	0.501	0.002	-0.109
5	74	0.80	3.80	9.32	14.20	4.17	100.9	-0.90	-0.40	3.48	-0.302	-0.329	-0.012	0.027
5	75	0.80	3.79	9.30	14.15	4.15	100.5	-0.50	-0.44	4.83	-0.178	-0.304	-0.011	0.144
5	76	0.80	3.80	9.30	14.17	4.16	99.8	0.00	-0.53	6.69	0.098	-0.084	0.002	0.070
5	77	0.80	3.81	9.31	14.17	4.16	99.3	0.50	-0.67	6.40	0.374	0.213	0.000	0.016
5	78	0.80	3.79	9.33	14.18	4.15	101.4	1.00	-0.84	7.10	0.555	0.390	0.011	-0.148
5	79	0.80	3.79	9.30	14.17	4.16	101.2	1.50	-0.87	6.96	0.655	0.484	0.010	-0.202
5	80	0.80	3.80	9.30	14.18	4.17	100.6	2.00	-0.84	6.54	0.683	0.506	0.014	-0.262
5	81	0.80	3.80	9.30	14.17	4.16	100.1	2.36	-0.81	6.13	0.676	0.493	0.016	-0.295

Table 19. Concluded

Run	Point	M_{∞}	$R_{\infty} \times 10^{-6}$	p_{∞} , psi	$p_{t,\infty}$, psi	q_{∞} , psi	$T_{t,\infty}$, °F	Z_s in.	C_N	C_m	C_A	C_{AB}	C_Y	C_n
5	56	0.90	3.52	7.35	12.46	4.18	101.0	-0.90	-0.20	1.72	-0.228	-0.273	0.001	0.001
5	57	0.90	3.52	7.36	12.47	4.19	101.2	-0.50	-0.30	2.97	-0.127	-0.241	-0.002	0.123
5	58	0.90	3.52	7.35	12.46	4.18	101.2	0.00	-0.40	4.69	0.091	-0.109	0.013	0.073
5	59	0.90	3.52	7.36	12.47	4.19	101.2	0.50	-0.49	4.58	0.352	0.157	0.007	0.051
5	60	0.90	3.52	7.36	12.46	4.18	100.9	1.00	-0.62	4.93	0.502	0.304	0.001	-0.042
5	61	0.90	3.52	7.36	12.46	4.18	100.9	1.50	-0.67	4.89	0.604	0.398	0.006	-0.143
5	62	0.90	3.52	7.36	12.46	4.18	100.8	2.00	-0.67	4.70	0.637	0.428	0.016	-0.270
5	63	0.90	3.52	7.37	12.47	4.19	100.6	2.36	-0.66	4.44	0.639	0.429	0.014	-0.279
5	65	0.95	3.40	6.61	11.83	4.19	101.0	-0.90	-0.15	1.21	-0.201	-0.253	0.003	-0.072
5	66	0.95	3.40	6.61	11.82	4.18	100.9	-0.50	-0.21	2.12	-0.097	-0.206	0.016	-0.017
5	67	0.95	3.41	6.61	11.83	4.19	100.7	0.00	-0.34	3.59	0.092	-0.105	0.012	0.049
5	68	0.95	3.40	6.61	11.82	4.18	100.6	0.50	-0.39	3.52	0.346	0.137	0.001	0.047
5	69	0.95	3.41	6.61	11.84	4.19	100.5	1.00	-0.51	3.71	0.479	0.272	0.004	0.001
5	70	0.95	3.41	6.61	11.82	4.18	100.1	1.50	-0.56	3.70	0.573	0.357	0.004	-0.150
5	71	0.95	3.41	6.61	11.82	4.18	99.9	2.00	-0.57	3.53	0.604	0.388	0.012	-0.187
5	72	0.95	3.41	6.61	11.82	4.18	100.0	2.36	-0.56	3.33	0.611	0.393	0.013	-0.165

Table 20. Force and Moment Data for Configuration 8 With $h = 2.40$ in., $l = 26.00$ in., and $Y_s = 2.40$ in.

Run	Point	M_∞	$R_\infty \times 10^{-6}$	p_∞ , psi	$P_{t,\infty}$, psi	q_∞ , psi	$T_{t,\infty}$, °F	Z_s in.	C_N	C_m	C_A	C_{A_B}	C_Y	C_n
9	347	0.20	2.05	22.97	23.63	0.65	99.7	-0.90	-0.60	6.04	-0.355	-0.398	-0.081	2.310
9	348	0.20	2.05	22.97	23.63	0.65	100.0	-0.50	-0.57	7.94	-0.122	-0.342	-0.132	2.671
9	349	0.20	2.05	22.98	23.64	0.65	100.1	0.00	-0.57	9.06	0.237	-0.056	-0.182	3.291
9	350	0.20	2.05	22.96	23.62	0.65	100.2	0.50	-0.85	9.06	0.475	0.316	-0.185	3.252
9	351	0.20	2.05	22.96	23.62	0.65	100.2	1.00	-1.00	9.16	0.716	0.541	-0.161	3.283
9	352	0.20	2.05	22.96	23.62	0.65	100.3	1.50	-1.01	8.49	0.836	0.624	-0.136	2.962
9	353	0.20	2.04	22.97	23.63	0.65	100.3	2.00	-0.96	7.35	0.827	0.584	-0.111	2.717
9	354	0.20	2.05	22.97	23.62	0.65	100.4	2.37	-0.89	6.40	0.782	0.534	-0.071	2.337
9	338	0.40	3.63	19.92	22.24	2.22	100.2	-0.90	-0.56	5.88	-0.357	-0.412	-0.153	2.165
9	339	0.40	3.63	19.91	22.23	2.23	101.0	-0.50	-0.54	7.75	-0.158	-0.345	-0.220	2.491
9	340	0.40	3.62	19.92	22.22	2.22	100.7	0.00	-0.57	8.89	0.187	-0.070	-0.242	2.967
9	341	0.40	3.64	19.91	22.24	2.23	100.5	0.50	-0.81	8.84	0.422	0.295	-0.251	2.979
9	342	0.40	3.62	19.90	22.21	2.22	100.1	1.00	-0.98	9.25	0.658	0.517	-0.250	3.166
9	343	0.40	3.64	19.91	22.24	2.24	99.9	1.50	-0.98	8.41	0.750	0.585	-0.215	2.821
9	344	0.40	3.64	19.92	22.24	2.23	99.8	2.00	-0.92	7.43	0.753	0.567	-0.193	2.572
9	345	0.40	3.63	19.90	22.22	2.23	100.1	2.37	-0.84	6.48	0.690	0.516	-0.155	2.243
9	329	0.60	4.67	16.33	20.84	4.12	102.6	-0.90	-0.53	5.56	-0.367	-0.409	-0.138	1.934
9	330	0.60	4.68	16.34	20.86	4.13	102.4	-0.50	-0.50	7.49	-0.185	-0.357	-0.183	2.311
9	331	0.60	4.67	16.32	20.81	4.11	102.2	0.00	-0.52	8.64	0.158	-0.074	-0.227	2.885
9	332	0.60	4.68	16.29	20.80	4.12	101.8	0.50	-0.81	8.77	0.408	0.288	-0.243	2.835
9	333	0.60	4.68	16.30	20.82	4.13	101.8	1.00	-0.95	9.03	0.624	0.488	-0.253	3.108
9	334	0.60	4.68	16.30	20.82	4.13	102.0	1.50	-0.97	8.47	0.717	0.572	-0.227	2.852
9	335	0.60	4.67	16.32	20.82	4.11	102.2	2.00	-0.91	7.49	0.712	0.561	-0.199	2.593
9	336	0.60	4.66	16.31	20.80	4.10	102.2	2.37	-0.85	6.71	0.681	0.524	-0.173	2.325
9	320	0.80	3.81	9.31	14.18	4.16	99.1	-0.90	-0.33	3.51	-0.302	-0.324	-0.078	1.103
9	321	0.80	3.81	9.31	14.18	4.16	99.8	-0.50	-0.42	5.68	-0.192	-0.319	-0.112	1.300
9	322	0.80	3.80	9.31	14.18	4.16	100.8	0.00	-0.48	7.04	0.116	-0.087	-0.148	2.005
9	323	0.80	3.80	9.31	14.19	4.17	100.7	0.50	-0.71	6.92	0.379	0.248	-0.179	1.994
9	324	0.80	3.80	9.31	14.18	4.17	100.6	1.00	-0.87	7.50	0.592	0.442	-0.210	2.350
9	325	0.80	3.80	9.31	14.18	4.17	100.8	1.50	-0.87	7.02	0.684	0.527	-0.196	2.282
9	326	0.80	3.80	9.31	14.19	4.17	100.7	2.00	-0.83	6.33	0.695	0.532	-0.180	2.048
9	327	0.80	3.80	9.31	14.19	4.17	100.9	2.37	-0.78	5.79	0.682	0.516	-0.170	1.956

Table 20. Concluded

Run	Point	M_∞	$R_\infty \times 10^{-6}$	p_∞ , psi	$P_{t,\infty}$, psi	q_∞ , psi	$T_{t,\infty}$, °F	Z_s in.	C_N	C_m	C_A	C_{AB}	C_Y	C_n
9	311	0.90	3.53	7.35	12.46	4.19	99.9	-0.90	-0.20	2.14	-0.247	-0.285	-0.035	0.545
9	312	0.90	3.53	7.36	12.46	4.19	99.8	-0.50	-0.26	3.44	-0.134	-0.258	-0.071	0.583
9	313	0.90	3.53	7.36	12.47	4.18	100.9	0.00	-0.37	5.07	0.113	-0.108	-0.055	1.051
9	314	0.90	3.53	7.36	12.47	4.19	99.9	0.50	-0.54	4.99	0.351	0.186	-0.110	1.464
9	315	0.90	3.53	7.36	12.47	4.19	100.1	1.00	-0.67	5.27	0.521	0.339	-0.155	1.746
9	316	0.90	3.53	7.36	12.47	4.19	100.1	1.50	-0.69	5.00	0.619	0.429	-0.149	1.630
9	317	0.90	3.53	7.37	12.47	4.19	100.1	2.00	-0.68	4.52	0.641	0.450	-0.134	1.433
9	318	0.90	3.52	7.36	12.46	4.18	100.2	2.37	-0.64	4.09	0.640	0.445	-0.132	1.352
9	302	0.95	3.39	6.61	11.83	4.18	101.8	-0.90	-0.15	1.65	-0.221	-0.266	-0.044	0.466
9	303	0.95	3.39	6.61	11.83	4.18	102.0	-0.50	-0.18	2.35	-0.102	-0.219	-0.094	0.539
9	304	0.95	3.39	6.61	11.82	4.18	101.9	0.00	-0.31	3.84	0.118	-0.095	-0.030	0.651
9	305	0.95	3.40	6.61	11.83	4.18	101.8	0.50	-0.42	3.79	0.347	0.165	-0.082	1.185
9	306	0.95	3.39	6.61	11.82	4.18	101.5	1.00	-0.54	3.99	0.492	0.300	-0.128	1.517
9	307	0.95	3.39	6.61	11.82	4.18	101.6	1.50	-0.57	3.71	0.585	0.384	-0.121	1.298
9	308	0.95	3.40	6.61	11.82	4.18	101.5	2.00	-0.56	3.33	0.612	0.411	-0.109	1.201
9	309	0.95	3.39	6.61	11.82	4.18	101.5	2.37	-0.54	3.09	0.618	0.415	-0.110	1.152

Table 21. Force and Moment Data for Configuration 9 With $h = 2.40$ in., $l = 30.00$ in., and $Y_s = 0.00$ in.

Run	Point	M_{∞}	$R_{\infty} \times 10^{-6}$	p_{∞} , psi	$p_{t,\infty}$, psi	q_{∞} , psi	$T_{t,\infty}$, °F	Z_s in.	C_N	C_m	C_A	C_{AB}	C_Y	C_n
6	162	0.20	2.02	22.98	23.62	0.63	99.7	-0.90	-0.16	3.06	-0.317	-0.308	-0.027	-0.034
6	161	0.20	2.08	22.95	23.63	0.67	99.6	-0.50	-0.02	4.12	-0.237	-0.280	0.005	0.091
6	163	0.20	2.03	22.98	23.62	0.64	99.7	0.00	0.09	5.17	-0.139	-0.245	-0.007	0.046
6	164	0.20	2.03	22.98	23.63	0.64	99.7	0.50	-0.12	5.15	-0.057	-0.207	0.004	-0.052
6	165	0.20	2.03	22.98	23.63	0.64	99.7	1.00	-0.22	5.19	0.018	-0.140	0.002	-0.130
6	166	0.20	2.04	22.98	23.63	0.64	99.7	1.50	-0.29	4.98	0.072	-0.086	-0.013	-0.128
6	167	0.20	2.03	22.97	23.62	0.64	99.7	2.00	-0.34	4.68	0.126	-0.053	-0.013	-0.128
6	168	0.20	2.03	22.97	23.62	0.64	99.7	2.37	-0.33	4.40	0.164	-0.031	-0.014	-0.128
6	152	0.40	3.64	19.91	22.25	2.24	101.5	-0.90	-0.16	2.99	-0.355	-0.315	-0.035	-0.072
6	153	0.40	3.64	19.90	22.24	2.25	100.7	-0.50	-0.01	4.02	-0.278	-0.281	-0.007	0.089
6	154	0.40	3.62	19.91	22.23	2.23	101.2	0.00	0.09	5.08	-0.188	-0.251	0.002	0.019
6	155	0.40	3.63	19.90	22.23	2.24	101.5	0.50	-0.13	5.09	-0.105	-0.214	-0.009	-0.071
6	156	0.40	3.62	19.90	22.23	2.23	101.8	1.00	-0.23	5.25	-0.031	-0.140	0.001	-0.188
6	157	0.40	3.63	19.92	22.25	2.24	102.1	1.50	-0.28	5.08	0.020	-0.090	-0.015	-0.130
6	158	0.40	3.62	19.90	22.23	2.24	102.0	2.00	-0.32	4.81	0.064	-0.057	-0.012	-0.108
6	159	0.40	3.63	19.92	22.25	2.24	101.9	2.37	-0.33	4.58	0.096	-0.032	-0.016	-0.111
6	143	0.60	4.69	16.33	20.86	4.14	101.6	-0.90	-0.16	2.85	-0.394	-0.334	-0.017	-0.047
6	144	0.60	4.69	16.34	20.86	4.14	101.5	-0.50	0.00	3.79	-0.314	-0.306	-0.005	0.019
6	145	0.60	4.69	16.36	20.87	4.13	101.6	0.00	0.09	4.82	-0.223	-0.276	-0.013	-0.009
6	146	0.60	4.69	16.35	20.86	4.13	101.4	0.50	-0.14	4.89	-0.145	-0.239	-0.006	-0.107
6	147	0.60	4.69	16.34	20.86	4.13	101.5	1.00	-0.23	5.13	-0.070	-0.169	-0.014	-0.164
6	148	0.60	4.68	16.36	20.86	4.12	101.5	1.50	-0.29	5.08	-0.018	-0.118	-0.017	-0.126
6	149	0.60	4.69	16.34	20.86	4.13	101.5	2.00	-0.31	4.84	0.025	-0.083	-0.019	-0.100
6	150	0.60	4.68	16.34	20.84	4.12	101.5	2.37	-0.32	4.64	0.056	-0.057	-0.017	-0.106
6	134	0.80	3.80	9.31	14.19	4.17	100.2	-0.90	-0.12	2.35	-0.400	-0.343	-0.031	-0.067
6	135	0.80	3.80	9.31	14.18	4.17	100.3	-0.50	0.00	3.18	-0.337	-0.323	-0.003	0.022
6	136	0.80	3.80	9.31	14.18	4.16	100.3	0.00	0.06	4.02	-0.258	-0.305	0.009	0.017
6	137	0.80	3.80	9.31	14.18	4.17	100.2	0.50	-0.17	4.22	-0.172	-0.271	-0.009	-0.111
6	138	0.80	3.80	9.31	14.19	4.17	100.5	1.00	-0.26	4.58	-0.100	-0.204	-0.015	-0.177
6	139	0.80	3.80	9.31	14.19	4.17	100.4	1.50	-0.30	4.61	-0.053	-0.160	-0.024	-0.196
6	140	0.80	3.80	9.32	14.18	4.16	100.4	2.00	-0.32	4.47	-0.011	-0.124	-0.022	-0.241
6	141	0.80	3.80	9.31	14.18	4.17	100.4	2.37	-0.33	4.30	0.017	-0.100	-0.020	-0.256

Table 21. Concluded

Run	Point	M_∞	$R_\infty \times 10^{-6}$	p_∞ , psi	$p_{t,\infty}$, psi	q_∞ , psi	$T_{t,\infty}$, °F	Z_s in.	C_N	C_m	C_A	C_{AB}	C_Y	C_n
6	125	0.90	3.52	7.37	12.46	4.18	99.8	-0.90	-0.08	1.54	-0.368	-0.341	-0.016	-0.020
6	126	0.90	3.53	7.37	12.47	4.18	99.4	-0.50	0.01	2.21	-0.312	-0.322	-0.010	0.032
6	127	0.90	3.53	7.38	12.47	4.18	99.4	0.00	0.07	3.08	-0.255	-0.319	-0.002	0.012
6	128	0.90	3.53	7.38	12.47	4.18	99.3	0.50	-0.13	3.15	-0.167	-0.287	-0.005	-0.073
6	129	0.90	3.53	7.38	12.47	4.18	99.5	1.00	-0.23	3.57	-0.112	-0.241	-0.013	-0.173
6	130	0.90	3.53	7.37	12.47	4.18	99.6	1.50	-0.28	3.71	-0.068	-0.201	-0.031	-0.270
6	131	0.90	3.53	7.38	12.48	4.18	99.8	2.00	-0.30	3.69	-0.037	-0.237	-0.029	-0.301
6	132	0.90	3.53	7.38	12.47	4.18	99.7	2.37	-0.31	3.60	-0.013	-0.151	-0.028	-0.336
6	116	0.95	3.39	6.61	11.82	4.18	101.9	-0.90	-0.05	1.01	-0.330	-0.314	-0.021	-0.039
6	117	0.95	3.39	6.61	11.82	4.18	101.4	-0.50	0.00	1.47	-0.261	-0.288	-0.001	-0.020
6	118	0.95	3.39	6.61	11.81	4.17	101.3	0.00	0.07	2.22	-0.224	-0.297	-0.001	0.009
6	119	0.95	3.40	6.60	11.81	4.17	101.0	0.50	-0.08	2.32	-0.140	-0.266	-0.008	-0.071
6	120	0.95	3.39	6.60	11.80	4.17	100.6	1.00	-0.20	2.65	-0.094	-0.234	-0.013	-0.137
6	121	0.95	3.40	6.60	11.80	4.17	100.7	1.50	-0.25	2.82	-0.059	-0.202	-0.027	-0.213
6	122	0.95	3.40	6.60	11.80	4.17	100.6	2.00	-0.28	2.84	-0.032	-0.176	-0.025	-0.241
6	123	0.95	3.39	6.60	11.79	4.17	100.5	2.37	-0.28	2.81	-0.008	-0.156	-0.019	-0.273

Table 22. Force and Moment Data for Configuration 10 With $h = 2.40$ in., $l = 30.00$ in., and $Y_s = 2.40$ in.

Run	Point	M_∞	$R_\infty \times 10^{-6}$	p_∞ , psi	$p_{t,\infty}$, psi	q_∞ , psi	$T_{t,\infty}$, °F	Z_s , in.	C_N	C_m	C_A	C_{AB}	C_Y	C_n
7	221	0.20	2.04	22.97	23.63	0.65	101.8	-0.90	-0.09	3.17	-0.255	-0.293	0.164	1.239
7	222	0.20	2.05	22.96	23.62	0.66	101.8	-0.50	0.07	4.33	-0.176	-0.257	0.152	1.300
7	223	0.20	2.05	22.97	23.63	0.66	101.8	0.00	0.13	5.31	-0.095	-0.224	0.157	1.776
7	224	0.20	2.05	22.97	23.64	0.65	101.8	0.50	-0.11	5.34	-0.001	-0.165	0.102	2.140
7	225	0.20	2.04	22.97	23.63	0.65	101.7	1.00	-0.21	5.16	0.072	-0.111	0.116	2.346
7	226	0.20	2.03	22.99	23.64	0.64	101.8	1.50	-0.28	4.86	0.129	-0.062	0.143	2.201
7	227	0.20	2.03	22.98	23.64	0.64	101.8	2.00	-0.32	4.41	0.174	-0.038	0.127	1.966
7	228	0.20	2.04	22.97	23.63	0.65	101.7	2.37	-0.36	4.06	0.198	-0.008	0.110	1.820
7	212	0.40	3.63	19.89	22.22	2.24	101.8	-0.90	-0.06	3.23	-0.302	-0.294	0.053	1.089
7	213	0.40	3.62	19.86	22.19	2.23	101.9	-0.50	0.10	4.35	-0.229	-0.263	0.021	1.139
7	214	0.40	3.62	19.84	22.16	2.23	101.9	0.00	0.14	5.23	-0.141	-0.226	0.049	1.617
7	215	0.40	3.63	19.92	22.25	2.24	102.1	0.50	-0.12	5.31	-0.052	-0.169	0.000	2.037
7	216	0.40	3.63	19.90	22.24	2.24	101.9	1.00	-0.21	5.19	0.015	-0.111	0.016	2.171
7	217	0.40	3.63	19.92	22.24	2.24	101.8	1.50	-0.28	4.92	0.059	-0.073	0.017	1.982
7	218	0.40	3.63	19.91	22.24	2.24	101.8	2.00	-0.32	4.54	0.099	-0.040	0.015	1.788
7	219	0.40	3.62	19.91	22.23	2.23	101.8	2.37	-0.33	4.25	0.131	-0.016	0.026	1.686
7	230	0.60	4.69	16.34	20.87	4.14	102.1	-0.90	-0.04	3.09	-0.340	-0.314	0.056	0.952
7	231	0.60	4.70	16.32	20.85	4.15	101.7	-0.50	0.14	4.17	-0.273	-0.291	0.019	1.036
7	232	0.60	4.70	16.33	20.86	4.15	101.8	0.00	0.15	5.03	-0.187	-0.255	0.037	1.507
7	233	0.60	4.69	16.33	20.85	4.14	101.6	0.50	-0.13	5.18	-0.095	-0.196	-0.009	1.996
7	234	0.60	4.69	16.34	20.85	4.13	101.6	1.00	-0.20	5.14	-0.030	-0.137	0.008	2.157
7	235	0.60	4.69	16.33	20.86	4.14	101.9	1.50	-0.27	4.91	0.016	-0.098	0.002	1.985
7	236	0.60	4.69	16.33	20.86	4.14	101.7	2.00	-0.32	4.61	0.057	-0.064	0.000	1.828
7	237	0.60	4.69	16.33	20.85	4.14	101.6	2.37	-0.33	4.33	0.088	-0.039	0.010	1.716
7	257	0.80	3.82	9.30	14.17	4.16	98.1	-0.90	-0.04	2.64	-0.373	-0.332	0.035	0.759
7	258	0.80	3.82	9.31	14.18	4.16	98.1	-0.50	0.11	3.61	-0.316	-0.320	0.023	0.721
7	259	0.80	3.82	9.30	14.18	4.16	98.2	0.00	0.11	4.40	-0.230	-0.293	0.037	1.281
7	260	0.80	3.82	9.30	14.18	4.17	98.4	0.50	-0.16	4.64	-0.136	-0.236	-0.019	1.816
7	261	0.80	3.81	9.30	14.18	4.16	98.8	1.00	-0.23	4.69	-0.072	-0.175	-0.004	1.998
7	262	0.80	3.81	9.31	14.18	4.17	99.3	1.50	-0.29	4.55	-0.026	-0.136	-0.010	1.881
7	263	0.80	3.81	9.30	14.18	4.17	99.5	2.00	-0.32	4.31	0.014	-0.103	-0.011	1.762
7	264	0.80	3.81	9.31	14.18	4.17	99.6	2.37	-0.34	4.11	0.043	-0.079	-0.003	1.664

Table 22. Concluded

Run	Point	M_∞	$R_\infty \times 10^{-6}$	P_∞ , psi	$P_{t,\infty}$, psi	q_∞ , psi	$T_{t,\infty}$, °F	Z_s in.	C_N	C_m	C_A	C_{AB}	C_Y	C_n
7	248	0.90	3.53	7.37	12.49	4.20	100.6	-0.90	0.00	1.76	-0.357	-0.340	0.045	0.463
7	249	0.90	3.53	7.37	12.49	4.19	100.8	-0.50	0.10	2.84	-0.322	-0.342	0.035	0.384
7	250	0.90	3.53	7.37	12.49	4.19	100.7	0.00	0.11	3.61	-0.247	-0.326	0.055	0.869
7	251	0.90	3.53	7.37	12.49	4.19	100.8	0.50	-0.14	3.74	-0.148	-0.275	-0.020	1.370
7	252	0.90	3.52	7.37	12.48	4.19	100.8	1.00	-0.23	3.81	-0.086	-0.219	-0.018	1.552
7	253	0.90	3.52	7.37	12.48	4.19	101.1	1.50	-0.28	3.75	-0.050	-0.186	-0.021	1.436
7	254	0.90	3.52	7.37	12.48	4.19	101.1	2.00	-0.31	3.60	-0.015	-0.154	-0.032	1.387
7	255	0.90	3.52	7.37	12.48	4.19	100.9	2.37	-0.32	3.46	0.013	-0.132	-0.035	1.326
7	239	0.95	3.40	6.59	11.82	4.19	101.7	-0.90	0.02	1.07	-0.310	-0.304	0.025	0.357
7	240	0.95	3.39	6.59	11.82	4.19	102.0	-0.50	0.12	1.78	-0.273	-0.310	0.030	0.141
7	241	0.95	3.39	6.60	11.82	4.19	102.0	0.00	0.12	2.76	-0.225	-0.312	0.067	0.425
7	242	0.95	3.40	6.60	11.82	4.19	101.9	0.50	-0.10	2.79	-0.124	-0.264	0.003	0.959
7	243	0.95	3.39	6.60	11.82	4.19	101.9	1.00	-0.21	2.94	-0.072	-0.218	-0.008	1.117
7	244	0.95	3.39	6.59	11.82	4.19	101.8	1.50	-0.26	2.90	-0.041	-0.191	-0.019	1.033
7	245	0.95	3.40	6.59	11.82	4.19	101.6	2.00	-0.28	2.82	-0.006	-0.162	-0.022	0.999
7	246	0.95	3.40	6.59	11.81	4.18	101.2	2.37	-0.29	2.75	0.013	-0.144	-0.024	1.027

Table 23. Force and Moment Data for Configuration 11 With $h = 4.80$ in., $l = 26.00$ in., and $Y_s = 0.00$ in.

Run	Point	M_{∞}	$R_{\infty} \times 10^{-6}$	p_{∞} , psi	$p_{t,\infty}$, psi	q_{∞} , psi	$T_{t,\infty}$, °F	Z_s in.	C_N	C_m	C_A	C_{A_B}	C_Y	C_n
16	658	0.20	2.05	22.94	23.60	0.65	98.6	-3.00	-0.09	-0.81	-0.024	-0.035	0.175	-0.680
16	659	0.20	2.06	22.95	23.61	0.65	98.6	-2.50	0.04	-1.55	0.025	-0.022	0.083	-0.022
16	660	0.20	2.05	22.96	23.62	0.65	98.7	-2.00	0.15	-1.93	0.010	-0.043	0.097	-0.216
16	661	0.20	2.06	22.96	23.63	0.65	98.7	-1.50	0.29	-2.36	-0.020	-0.104	0.151	-0.342
16	662	0.20	2.05	22.97	23.62	0.65	98.8	-1.00	0.31	-2.03	-0.032	-0.159	0.087	0.070
16	663	0.20	2.05	22.96	23.62	0.65	98.8	-0.50	0.21	-1.31	0.053	-0.060	0.072	-0.071
16	664	0.20	2.05	22.97	23.62	0.65	98.8	0.00	0.13	-0.42	0.265	0.091	0.059	0.171
16	650	0.40	3.61	19.92	22.23	2.22	101.6	-3.00	-0.09	-1.09	-0.073	-0.096	0.086	-0.218
16	651	0.40	3.61	19.94	22.24	2.21	101.8	-2.50	0.09	-1.89	-0.069	-0.111	0.055	-0.289
16	652	0.40	3.61	19.93	22.23	2.21	101.9	-2.00	0.14	-1.96	-0.075	-0.138	0.013	0.123
16	653	0.40	3.61	19.92	22.23	2.22	101.6	-1.50	0.19	-1.92	-0.092	-0.179	-0.003	-0.055
16	654	0.40	3.61	19.93	22.23	2.21	101.0	-1.00	0.07	-1.18	-0.107	-0.211	0.017	0.138
16	655	0.40	3.62	19.93	22.24	2.22	100.9	-0.50	0.10	-0.50	0.020	-0.106	0.037	-0.012
16	656	0.40	3.63	19.92	22.24	2.23	100.9	0.00	0.08	0.53	0.262	0.055	0.029	-0.113
16	641	0.60	2.81	9.80	12.50	2.47	100.5	-3.00	-0.07	-1.60	-0.124	-0.136	0.013	0.013
16	642	0.60	2.82	9.81	12.51	2.47	100.0	-2.50	0.03	-1.90	-0.116	-0.156	0.002	-0.218
16	643	0.60	2.82	9.80	12.51	2.47	99.6	-2.00	0.14	-2.12	-0.132	-0.202	0.014	-0.181
16	644	0.60	2.83	9.80	12.51	2.48	99.4	-1.50	0.16	-2.08	-0.177	-0.285	0.025	-0.094
16	645	0.60	2.83	9.80	12.51	2.48	99.5	-1.00	0.02	-0.98	-0.199	-0.300	-0.007	0.084
16	646	0.60	2.82	9.81	12.52	2.48	99.9	-0.50	0.11	0.16	-0.032	-0.181	-0.041	-0.115
16	647	0.60	2.82	9.80	12.51	2.48	100.3	0.00	0.32	1.29	0.257	-0.007	-0.040	0.042
16	633	0.80	2.53	6.19	9.44	2.78	100.1	-3.00	-0.05	-1.76	-0.111	-0.147	0.011	-0.053
16	634	0.80	2.53	6.19	9.44	2.78	100.1	-2.50	0.03	-2.24	-0.105	-0.169	0.008	-0.103
16	635	0.80	2.53	6.19	9.44	2.77	100.0	-2.00	0.09	-2.21	-0.144	-0.236	0.002	-0.089
16	636	0.80	2.53	6.19	9.44	2.77	99.9	-1.50	0.17	-2.17	-0.185	-0.312	-0.006	0.034
16	637	0.80	2.53	6.20	9.44	2.77	100.2	-1.00	0.15	-1.26	-0.195	-0.325	-0.009	-0.022
16	638	0.80	2.53	6.19	9.45	2.78	100.5	-0.50	0.19	-0.29	-0.041	-0.210	-0.048	0.046
16	639	0.80	2.53	6.19	9.45	2.78	100.5	0.00	0.32	0.49	0.197	-0.050	-0.004	0.041

Table 23. Concluded

Run	Point	M_∞	$R_\infty \times 10^{-6}$	p_∞ , psi	$p_{t,\infty}$, psi	q_∞ , psi	$T_{t,\infty}$, °F	Z_s in.	C_N	C_m	C_A	C_{AB}	C_Y	C_n
16	625	0.90	2.36	4.94	8.35	2.80	100.6	-2.50	0.09	-2.01	-0.077	-0.163	-0.004	-0.076
16	626	0.90	2.36	4.94	8.35	2.80	100.7	-2.00	0.14	-2.08	-0.118	-0.221	-0.001	-0.176
16	627	0.90	2.36	4.94	8.35	2.80	100.6	-1.50	0.17	-2.07	-0.172	-0.321	-0.012	0.049
16	628	0.90	2.36	4.94	8.35	2.80	100.5	-1.00	0.17	-1.44	-0.200	-0.364	-0.012	-0.080
16	629	0.90	2.36	4.93	8.35	2.80	100.6	-0.50	0.22	-0.52	-0.072	-0.242	-0.013	-0.032
16	630	0.90	2.36	4.93	8.35	2.80	100.5	0.00	0.25	0.29	0.178	-0.076	-0.021	0.064
16	617	0.95	2.41	4.67	8.35	2.95	99.6	-3.00	-0.01	-1.63	-0.086	-0.148	-0.001	0.054
16	618	0.95	2.40	4.67	8.35	2.95	100.0	-2.50	0.09	-2.03	-0.081	-0.169	-0.002	-0.218
16	619	0.95	2.40	4.67	8.35	2.95	100.2	-2.00	0.13	-2.26	-0.120	-0.237	-0.007	-0.113
16	620	0.95	2.40	4.67	8.35	2.95	100.5	-1.50	0.17	-1.96	-0.161	-0.319	0.004	0.020
16	621	0.95	2.40	4.67	8.35	2.95	100.5	-1.00	0.19	-1.54	-0.203	-0.378	-0.011	-0.075
16	622	0.95	2.40	4.67	8.35	2.95	100.5	-0.50	0.18	-0.51	-0.069	-0.247	-0.018	0.080
16	623	0.95	2.40	4.67	8.35	2.95	100.9	0.00	0.27	0.05	0.162	-0.100	-0.020	0.065

Table 24. Force and Moment Data for Configuration 12 With $h = 4.80$ in., $l = 26.00$ in., and $Y_s = 0.00$ in.

Run	Point	M_∞	$R_\infty \times 10^{-6}$	p_∞ , psi	$p_{h,\infty}$, psi	q_∞ , psi	$T_{h,\infty}$, °F	Z_s in.	C_N	C_m	C_A	C_{AB}	C_Y	C_n
15	604	0.20	2.03	22.97	23.62	0.64	100.1	-0.90	0.30	-2.12	-0.072	-0.136	0.005	0.148
15	605	0.20	2.04	22.97	23.62	0.65	100.5	-0.50	0.25	-1.48	0.016	-0.041	0.018	0.083
15	606	0.20	2.04	22.97	23.62	0.65	100.5	0.00	0.12	-0.74	0.211	0.097	0.032	0.231
15	607	0.20	2.04	22.97	23.62	0.65	100.7	0.50	0.18	-0.89	0.408	0.171	0.071	-0.351
15	608	0.20	2.03	22.97	23.62	0.64	100.8	1.00	0.04	-0.73	0.461	0.242	0.096	-0.477
15	609	0.20	2.03	22.97	23.62	0.64	100.9	1.50	0.01	-1.15	0.441	0.246	0.042	-0.125
15	610	0.20	2.03	22.97	23.62	0.65	101.0	2.00	-0.04	-1.20	0.418	0.221	0.055	-0.025
15	611	0.20	2.03	22.97	23.62	0.64	101.2	2.31	-0.04	-1.45	0.395	0.208	0.029	0.185
15	595	0.40	3.65	19.88	22.24	2.26	101.7	-0.90	0.07	-1.42	-0.118	-0.212	0.004	0.042
15	596	0.40	3.63	19.91	22.23	2.24	101.9	-0.50	0.06	-0.53	0.022	-0.102	0.021	0.066
15	597	0.40	3.63	19.91	22.23	2.24	101.7	0.00	0.11	0.13	0.263	0.074	0.006	-0.054
15	598	0.40	3.63	19.90	22.23	2.24	101.6	0.50	0.25	0.12	0.473	0.191	-0.016	0.098
15	599	0.40	3.63	19.91	22.24	2.24	101.5	1.00	0.12	0.02	0.493	0.269	-0.010	0.035
15	600	0.40	3.63	19.89	22.23	2.24	101.6	1.50	0.06	-0.04	0.500	0.273	0.014	0.081
15	601	0.40	3.63	19.90	22.23	2.24	101.5	2.00	-0.02	-0.20	0.476	0.253	0.000	-0.016
15	602	0.40	3.63	19.91	22.23	2.24	101.4	2.31	-0.06	-0.18	0.465	0.247	0.004	0.040
15	586	0.60	2.82	9.80	12.52	2.48	100.9	-0.90	-0.06	-0.81	-0.188	-0.269	-0.004	0.046
15	587	0.60	2.82	9.80	12.51	2.48	100.2	-0.50	0.09	0.53	-0.044	-0.187	0.003	0.179
15	588	0.60	2.82	9.81	12.51	2.47	100.5	0.00	0.30	1.60	0.268	0.017	0.007	0.279
15	589	0.60	2.82	9.80	12.51	2.48	100.6	0.50	0.32	1.50	0.498	0.220	-0.002	-0.090
15	590	0.60	2.82	9.80	12.51	2.48	100.5	1.00	0.16	1.57	0.551	0.317	-0.020	0.104
15	591	0.60	2.82	9.80	12.51	2.48	100.6	1.50	0.04	1.13	0.560	0.326	-0.005	-0.012
15	592	0.60	2.81	9.81	12.51	2.47	101.1	2.00	-0.04	0.80	0.547	0.320	-0.003	0.009
15	593	0.60	2.81	9.81	12.52	2.48	101.5	2.31	-0.10	0.90	0.541	0.318	-0.007	-0.066
15	577	0.80	2.54	6.20	9.46	2.78	99.9	-0.90	0.06	-1.03	-0.186	-0.304	-0.019	0.045
15	578	0.80	2.54	6.20	9.46	2.78	99.7	-0.50	0.16	-0.32	-0.045	-0.200	-0.001	0.026
15	579	0.80	2.54	6.20	9.46	2.78	99.7	0.00	0.23	0.42	0.216	-0.014	-0.009	0.070
15	580	0.80	2.54	6.20	9.45	2.78	99.7	0.50	0.21	0.83	0.467	0.180	-0.018	0.063
15	581	0.80	2.54	6.20	9.45	2.78	99.6	1.00	0.05	1.36	0.558	0.312	-0.013	0.165
15	582	0.80	2.54	6.20	9.45	2.78	99.6	1.50	-0.03	1.08	0.590	0.349	-0.002	0.062
15	583	0.80	2.54	6.20	9.45	2.78	99.6	2.00	-0.09	0.79	0.600	0.363	-0.016	0.028
15	584	0.80	2.54	6.20	9.45	2.78	99.6	2.31	-0.13	0.69	0.594	0.360	-0.013	0.032

Table 24. Concluded

Run	Point	M_∞	$R_\infty \times 10^{-6}$	p_∞ , psi	$p_{t,\infty}$, psi	q_∞ , psi	$T_{t,\infty}$, °F	Z_s in.	C_N	C_m	C_A	C_{AB}	C_Y	C_n
15	568	0.90	2.36	4.93	8.33	2.79	99.3	-0.90	0.09	-1.30	-0.188	-0.333	-0.006	0.033
15	569	0.90	2.36	4.93	8.33	2.79	99.6	-0.50	0.09	-0.31	-0.064	-0.218	-0.008	0.012
15	570	0.90	2.36	4.93	8.34	2.79	99.6	0.00	0.20	0.12	0.180	-0.049	-0.016	0.067
15	571	0.90	2.36	4.93	8.35	2.80	99.7	0.50	0.18	0.38	0.425	0.129	-0.013	-0.063
15	572	0.90	2.36	4.94	8.35	2.80	99.8	1.00	0.07	0.56	0.530	0.267	-0.027	-0.099
15	573	0.90	2.36	4.94	8.35	2.80	99.6	1.50	0.00	0.32	0.568	0.313	-0.018	0.109
15	574	0.90	2.36	4.94	8.35	2.80	99.7	2.00	-0.05	0.18	0.582	0.329	-0.016	0.058
15	575	0.90	2.36	4.93	8.34	2.80	99.7	2.31	-0.11	0.24	0.593	0.336	-0.017	-0.019
15	559	0.95	2.40	4.65	8.34	2.95	101.4	-0.90	0.08	-1.18	-0.184	-0.351	0.003	0.022
15	560	0.95	2.40	4.66	8.35	2.96	101.3	-0.50	0.12	-0.48	-0.069	-0.239	-0.023	0.012
15	561	0.95	2.40	4.65	8.34	2.96	101.1	0.00	0.21	-0.04	0.157	-0.072	-0.021	-0.017
15	562	0.95	2.40	4.66	8.34	2.95	101.0	0.50	0.17	0.18	0.401	0.105	-0.045	0.100
15	563	0.95	2.40	4.66	8.34	2.95	100.8	1.00	0.08	0.28	0.510	0.245	-0.016	0.054
15	564	0.95	2.40	4.66	8.34	2.95	100.7	1.50	0.02	-0.01	0.562	0.299	-0.011	0.082
15	565	0.95	2.40	4.66	8.34	2.95	100.5	2.00	-0.04	-0.15	0.580	0.323	-0.010	-0.015
15	566	0.95	2.40	4.66	8.34	2.95	100.4	2.31	-0.07	-0.17	0.599	0.330	-0.010	0.019

Table 25. Force and Moment Data for Configuration 13 With $h = 4.80$ in., $l = 26.00$ in., and $Y_s = 2.40$ in.

Run	Point	M_{∞}	$R_{\infty} \times 10^{-6}$	p_{∞} , psi	$P_{h,\infty}$, psi	q_{∞} , psi	$T_{h,\infty}$, °F	Z_s in.	C_N	C_m	C_A	C_{AB}	C_Y	C_n
21	828	0.20	2.04	22.98	23.63	0.64	98.6	-3.00	-0.15	-0.67	0.010	-0.041	0.124	-0.249
21	827	0.20	2.04	22.98	23.63	0.64	98.6	-2.50	-0.04	-1.04	0.040	-0.029	0.085	0.175
21	826	0.20	2.04	22.98	23.62	0.64	98.4	-2.00	0.09	-1.70	0.045	-0.050	0.004	0.351
21	825	0.20	2.04	22.98	23.63	0.64	98.4	-1.50	0.15	-1.75	0.067	-0.066	-0.023	0.371
21	824	0.20	2.04	22.98	23.63	0.64	98.3	-1.00	0.21	-1.55	0.080	-0.078	-0.046	0.984
21	823	0.20	2.04	22.97	23.62	0.64	98.2	-0.50	0.19	-0.90	0.172	-0.015	-0.088	0.904
21	822	0.20	2.03	22.99	23.63	0.64	98.2	0.00	0.20	-0.75	0.347	0.125	0.092	0.758
21	820	0.40	3.62	19.92	22.23	2.22	101.2	-3.00	-0.21	-0.59	-0.051	-0.084	-0.152	1.069
21	819	0.40	3.62	19.91	22.22	2.22	101.2	-2.50	-0.15	-1.06	-0.018	-0.072	-0.176	1.017
21	818	0.40	3.62	19.92	22.24	2.22	101.3	-2.00	0.00	-1.95	-0.018	-0.091	-0.179	0.269
21	817	0.40	3.62	19.92	22.23	2.22	101.3	-1.50	-0.02	-2.00	-0.001	-0.113	-0.102	-0.045
21	816	0.40	3.61	19.90	22.21	2.22	101.3	-1.00	0.03	-1.72	0.014	-0.113	0.072	0.029
21	815	0.40	3.61	19.91	22.21	2.21	101.3	-0.50	0.02	-0.28	0.122	-0.036	0.169	-0.090
21	814	0.40	3.62	19.92	22.23	2.22	101.4	0.00	0.16	-0.06	0.343	0.116	0.245	-0.214
21	812	0.60	2.81	9.78	12.48	2.47	101.0	-3.00	-0.32	-0.57	-0.078	-0.112	-0.271	1.850
21	811	0.60	2.80	9.77	12.46	2.46	101.0	-2.50	-0.17	-1.07	-0.035	-0.094	-0.226	1.326
21	810	0.60	2.80	9.77	12.47	2.47	101.1	-2.00	-0.09	-1.59	-0.020	-0.108	-0.199	0.894
21	809	0.60	2.80	9.77	12.47	2.47	101.2	-1.50	-0.06	-2.02	-0.016	-0.134	0.069	0.983
21	808	0.60	2.81	9.81	12.52	2.47	101.3	-1.00	-0.01	-1.07	0.007	-0.132	0.299	1.037
21	807	0.60	2.81	9.83	12.52	2.46	101.1	-0.50	0.19	0.52	0.233	-0.016	0.335	-0.097
21	806	0.60	2.81	9.83	12.51	2.46	100.8	0.00	0.38	0.60	0.413	0.132	0.211	-0.736
21	777	0.80	2.53	6.20	9.45	2.78	100.9	-3.00	-0.39	-0.35	-0.087	-0.118	-0.316	2.606
21	778	0.80	2.53	6.20	9.46	2.78	101.5	-2.50	-0.24	-0.77	-0.043	-0.104	-0.233	2.294
21	779	0.80	2.53	6.20	9.45	2.78	101.4	-2.00	-0.09	-1.38	-0.014	-0.104	-0.131	1.946
21	780	0.80	2.53	6.20	9.45	2.78	100.9	-1.50	0.05	-1.70	-0.003	-0.122	0.150	1.523
21	781	0.80	2.53	6.20	9.46	2.78	100.9	-1.00	0.17	-1.00	0.056	-0.115	0.248	1.122
21	782	0.80	2.53	6.20	9.45	2.78	101.1	-0.50	0.21	0.34	0.197	-0.003	0.216	0.308
21	783	0.80	2.53	6.20	9.45	2.78	101.5	0.00	0.31	0.67	0.408	0.154	0.255	0.041

Table 25. Concluded

Run	Point	M_{∞}	$R_{\infty} \times 10^{-6}$	p_{∞} , psi	$p_{t,\infty}$, psi	q_{∞} , psi	$T_{t,\infty}$, °F	Z_s in.	C_N	C_m	C_A	C_{AB}	C_Y	C_n
20	785	0.90	2.35	4.93	8.34	2.80	102.1	-3.00	-0.36	-0.35	-0.080	-0.128	-0.280	2.309
20	786	0.90	2.35	4.94	8.35	2.80	101.5	-2.50	-0.25	-0.71	-0.027	-0.107	-0.227	1.993
20	787	0.90	2.35	4.94	8.36	2.80	101.6	-2.00	-0.09	-1.43	-0.011	-0.109	-0.139	1.092
20	788	0.90	2.35	4.93	8.35	2.80	101.0	-1.50	0.03	-1.56	0.014	-0.122	-0.015	0.829
20	789	0.90	2.36	4.93	8.35	2.80	101.0	-1.00	0.05	-1.03	0.028	-0.133	0.174	0.528
20	790	0.90	2.36	4.94	8.35	2.80	101.0	-0.50	0.10	0.29	0.170	-0.031	0.233	-0.035
20	791	0.90	2.36	4.93	8.35	2.80	101.0	0.00	0.26	0.50	0.366	0.112	0.194	-0.066
21	804	0.95	2.40	4.65	8.32	2.94	100.3	-3.00	-0.32	-0.31	-0.057	-0.130	-0.264	2.012
21	803	0.95	2.40	4.65	8.32	2.94	100.3	-2.50	-0.25	-0.81	-0.013	-0.113	-0.208	1.722
21	802	0.95	2.40	4.65	8.32	2.94	100.3	-2.00	-0.08	-1.25	0.021	-0.117	-0.124	1.393
21	801	0.95	2.40	4.65	8.32	2.94	100.5	-1.50	0.01	-1.67	0.027	-0.130	0.030	0.765
21	800	0.95	2.39	4.66	8.32	2.94	100.3	-1.00	0.10	-0.98	0.062	-0.136	0.224	0.427
21	799	0.95	2.40	4.66	8.32	2.94	99.9	-0.50	0.11	0.16	0.169	-0.045	0.212	-0.119
21	798	0.95	2.40	4.65	8.32	2.94	100.0	0.00	0.23	0.50	0.344	0.084	0.172	-0.154

Table 26. Force and Moment Data for Configuration 14 With $h = 4.80$ in., $l = 26.00$ in., and $Y_s = 2.40$ in.

Run	Point	M_{∞}	$R_{\infty} \times 10^{-6}$	p_{∞} , psi	$p_{t,\infty}$, psi	q_{∞} , psi	$T_{t,\infty}$, of	Z_s in.	C_N	C_m	C_A	C_{AB}	C_Y	C_n
10	406	0.20	2.03	22.98	23.63	0.64	99.2	-0.90	0.18	-1.14	0.043	-0.083	0.030	-0.228
10	407	0.20	2.03	22.99	23.63	0.64	99.3	-0.50	0.16	-0.82	0.121	-0.029	-0.036	0.477
10	409	0.20	2.04	22.97	23.62	0.64	99.3	0.00	0.13	-0.49	0.315	0.131	0.117	0.630
10	410	0.20	2.04	22.98	23.63	0.64	99.3	0.50	0.13	-0.51	0.480	0.204	0.184	0.338
10	411	0.20	2.04	22.97	23.62	0.64	99.3	1.00	0.02	-0.56	0.510	0.241	0.125	-0.094
10	412	0.20	2.04	22.97	23.63	0.64	99.3	1.50	-0.02	-0.65	0.534	0.245	0.096	-0.142
10	413	0.20	2.04	22.98	23.63	0.64	99.1	2.00	-0.05	-1.00	0.567	0.226	0.125	0.115
10	414	0.20	2.04	22.98	23.63	0.64	99.0	2.31	-0.13	-1.39	0.653	0.213	0.222	0.323
10	397	0.40	3.66	19.89	22.25	2.26	100.8	-0.90	0.03	-1.13	-0.015	-0.120	0.102	0.021
10	398	0.40	3.64	19.91	22.24	2.24	100.6	-0.50	-0.02	-0.48	0.100	-0.038	0.185	-0.239
10	399	0.40	3.63	19.92	22.24	2.22	100.1	0.00	0.18	-0.04	0.345	0.121	0.204	-0.407
10	400	0.40	3.63	19.92	22.24	2.23	100.1	0.50	0.25	-0.01	0.528	0.243	0.158	-0.209
10	401	0.40	3.62	19.92	22.22	2.22	100.5	1.00	0.14	-0.01	0.543	0.296	0.081	-0.245
10	402	0.40	3.63	19.92	22.24	2.23	100.7	1.50	0.05	-0.07	0.550	0.288	0.037	-0.037
10	403	0.40	3.63	19.91	22.24	2.24	100.6	2.00	0.01	-0.45	0.552	0.282	0.064	-0.028
10	404	0.40	3.62	19.92	22.23	2.22	100.5	2.31	-0.07	-0.44	0.560	0.276	0.071	0.014
10	388	0.60	2.82	9.82	12.52	2.47	100.0	-0.90	-0.06	-0.17	0.016	-0.134	0.299	0.697
10	389	0.60	2.82	9.80	12.51	2.48	99.8	-0.50	0.15	0.96	0.187	-0.044	0.347	-0.178
10	390	0.60	2.82	9.80	12.50	2.47	100.1	0.00	0.33	0.99	0.415	0.144	0.241	-0.920
10	391	0.60	2.82	9.79	12.50	2.47	100.2	0.50	0.40	0.72	0.594	0.307	0.159	-0.290
10	392	0.60	2.82	9.79	12.50	2.48	100.3	1.00	0.24	0.69	0.632	0.368	0.134	0.022
10	393	0.60	2.82	9.78	12.49	2.47	100.3	1.50	0.12	0.24	0.637	0.372	0.110	0.037
10	394	0.60	2.81	9.80	12.50	2.47	100.3	2.00	0.01	0.16	0.657	0.383	0.144	-0.034
10	395	0.60	2.82	9.79	12.49	2.47	100.2	2.31	-0.08	0.19	0.673	0.389	0.151	0.059
10	379	0.80	2.51	6.13	9.35	2.75	99.8	-0.90	0.10	-0.69	0.065	-0.109	0.223	0.457
10	380	0.80	2.53	6.17	9.42	2.77	99.4	-0.50	0.17	0.28	0.185	-0.014	0.207	-0.130
10	381	0.80	2.54	6.18	9.42	2.77	99.3	0.00	0.28	0.80	0.412	0.148	0.188	-0.377
10	382	0.80	2.53	6.19	9.43	2.77	99.5	0.50	0.33	0.35	0.610	0.331	0.135	0.386
10	383	0.80	2.53	6.19	9.43	2.77	99.7	1.00	0.18	0.21	0.661	0.401	0.099	0.542
10	384	0.80	2.53	6.19	9.44	2.77	100.0	1.50	0.08	0.01	0.680	0.412	0.096	0.303
10	385	0.80	2.53	6.19	9.43	2.78	100.1	2.00	-0.01	-0.09	0.701	0.425	0.116	0.188
10	386	0.80	2.53	6.19	9.43	2.77	100.2	2.31	-0.08	-0.29	0.710	0.418	0.118	0.192

Table 26. Concluded

Run	Point	M_∞	$R_\infty \times 10^{-6}$	p_∞ , psi	$P_{t,\infty}$, psi	q_∞ , psi	$T_{t,\infty}$, °F	Z_s , in.	C_N	C_m	C_A	C_{AB}	C_Y	C_n
10	370	0.90	2.35	4.92	8.32	2.79	100.1	-0.90	0.01	-0.77	0.041	-0.142	0.252	0.165
10	371	0.90	2.36	4.94	8.35	2.80	100.4	-0.50	0.04	0.30	0.163	-0.041	0.251	-0.627
10	372	0.90	2.36	4.94	8.36	2.80	100.5	0.00	0.25	0.58	0.388	0.109	0.195	-0.405
10	373	0.90	2.36	4.94	8.36	2.80	100.7	0.50	0.28	0.14	0.558	0.250	0.146	-0.146
10	374	0.90	2.36	4.94	8.36	2.80	100.5	1.00	0.17	-0.18	0.616	0.345	0.093	0.255
10	375	0.90	2.36	4.94	8.36	2.80	100.5	1.50	0.07	-0.37	0.640	0.365	0.078	0.223
10	376	0.90	2.36	4.94	8.36	2.80	100.8	2.00	-0.01	-0.50	0.658	0.373	0.086	0.116
10	377	0.90	2.36	4.94	8.36	2.80	100.6	2.31	-0.07	-0.57	0.685	0.380	0.104	0.116
10	362	0.95	2.41	4.67	8.36	2.96	101.0	-0.50	0.08	0.15	0.159	-0.051	0.215	-0.393
10	363	0.95	2.41	4.67	8.36	2.96	100.8	0.00	0.20	0.44	0.332	0.083	0.120	-0.582
10	364	0.95	2.41	4.67	8.36	2.96	100.7	0.50	0.28	-0.20	0.537	0.231	0.159	-0.079
10	365	0.95	2.41	4.67	8.36	2.96	100.6	1.00	0.18	-0.38	0.597	0.316	0.105	0.161
10	366	0.95	2.41	4.67	8.36	2.96	100.8	1.50	0.09	-0.72	0.632	0.345	0.074	0.201
10	367	0.95	2.41	4.67	8.36	2.96	100.7	2.00	0.01	-0.75	0.655	0.362	0.082	0.167
10	368	0.95	2.40	4.67	8.36	2.95	100.7	2.31	-0.05	-0.90	0.664	0.362	0.083	0.125

Table 27. Force and Moment Data for Configuration 15 With $h = 4.80$ in., $l = 30.00$ in., and $Y_s = 0.00$ in.

Run	Point	M_∞	$R_\infty \times 10^{-6}$	p_∞ , psi	$p_{t,\infty}$, psi	q_∞ , psi	$T_{t,\infty}$, °F	Z_s in.	C_N	C_m	C_A	C_{AB}	C_Y	C_n
18	714	0.20	2.05	22.95	23.60	0.65	97.8	-3.00	-0.14	0.16	0.080	0.065	0.154	0.166
18	715	0.20	2.05	22.96	23.61	0.65	97.7	-2.50	-0.08	0.13	0.126	0.095	0.208	-0.186
18	716	0.20	2.06	22.97	23.62	0.65	97.5	-2.00	-0.01	-0.21	0.166	0.117	0.113	0.038
18	717	0.20	2.06	22.96	23.62	0.65	97.4	-1.50	0.10	-0.56	0.187	0.129	0.171	0.323
18	718	0.20	2.06	22.96	23.62	0.65	97.3	-1.00	0.15	-0.52	0.231	0.143	0.129	0.084
18	719	0.20	2.06	22.97	23.62	0.65	97.1	-0.50	0.13	-0.25	0.295	0.154	0.170	0.099
18	720	0.20	2.06	22.96	23.62	0.65	96.9	0.00	0.18	-0.40	0.381	0.162	0.144	0.195
18	706	0.40	3.65	19.90	22.23	2.24	99.2	-3.00	-0.25	0.08	-0.032	-0.018	0.053	-0.074
18	707	0.40	3.63	19.93	22.25	2.22	99.8	-2.50	-0.09	-0.55	-0.006	-0.010	0.039	-0.006
18	708	0.40	3.61	19.92	22.22	2.21	100.9	-2.00	-0.02	-0.73	0.034	0.018	0.077	0.100
18	709	0.40	3.64	19.91	22.25	2.25	101.7	-1.50	0.06	-0.83	0.095	0.053	0.038	0.173
18	710	0.40	3.61	19.93	22.24	2.22	101.9	-1.00	0.07	-0.99	0.098	0.049	0.041	0.044
18	711	0.40	3.62	19.92	22.24	2.22	101.3	-0.50	0.20	-0.47	0.155	0.054	0.036	0.178
18	712	0.40	3.63	19.90	22.22	2.22	100.6	0.00	0.35	-0.43	0.255	0.079	0.048	-0.094
18	698	0.60	2.81	9.79	12.49	2.47	100.5	-3.00	-0.28	0.05	-0.078	-0.060	-0.002	0.085
18	699	0.60	2.82	9.79	12.50	2.48	100.5	-2.50	-0.11	-0.58	-0.027	-0.028	0.024	0.069
18	700	0.60	2.82	9.79	12.49	2.47	100.5	-2.00	0.02	-0.97	-0.001	-0.013	0.018	0.014
18	701	0.60	2.82	9.78	12.49	2.48	100.6	-1.50	0.05	-0.93	0.043	0.011	0.027	0.231
18	702	0.60	2.81	9.78	12.49	2.48	100.7	-1.00	0.13	-1.32	0.087	0.031	0.090	-0.122
18	703	0.60	2.81	9.79	12.49	2.47	100.8	-0.50	0.32	-1.05	0.150	0.051	0.000	0.016
18	704	0.60	2.81	9.78	12.49	2.47	100.8	0.00	0.47	-0.40	0.243	0.071	0.010	0.031
18	686	0.80	2.54	6.19	9.44	2.78	98.2	-3.00	-0.29	-0.28	-0.162	-0.121	0.012	-0.082
18	687	0.80	2.54	6.21	9.46	2.78	99.0	-2.50	-0.17	-0.84	-0.121	-0.103	0.009	-0.233
18	688	0.80	2.54	6.22	9.48	2.78	100.0	-2.00	-0.03	-1.27	-0.093	-0.093	0.001	-0.151
18	689	0.80	2.53	6.20	9.44	2.77	100.6	-1.50	0.14	-1.29	-0.077	-0.098	-0.025	-0.026
18	690	0.80	2.53	6.21	9.45	2.77	100.7	-1.00	0.39	-1.28	-0.034	-0.086	0.014	-0.029
18	691	0.80	2.53	6.21	9.45	2.77	100.7	-0.50	0.53	-0.91	0.067	-0.041	-0.007	-0.116
18	692	0.80	2.53	6.21	9.46	2.78	100.6	0.00	0.64	-0.60	0.153	-0.007	0.024	-0.009

Table 27. Concluded

Run	Point	M_∞	$R_\infty \times 10^{-6}$	p_∞ , psi	$p_{t,\infty}$, psi	q_∞ , psi	$T_{t,\infty}$, °F	Z_s in.	C_N	C_m	C_A	C_{AB}	C_Y	C_n
17	678	0.90	2.37	4.94	8.36	2.81	99.9	-3.00	-0.23	-0.25	-0.079	-0.072	-0.012	-0.007
17	679	0.90	2.36	4.93	8.35	2.80	100.5	-2.50	-0.14	-0.63	-0.032	-0.041	0.020	-0.116
17	680	0.90	2.36	4.93	8.35	2.80	100.6	-2.00	0.01	-1.12	-0.004	-0.017	-0.003	0.027
17	681	0.90	2.36	4.94	8.35	2.80	100.5	-1.50	0.08	-1.38	0.030	-0.003	-0.034	0.216
17	682	0.90	2.36	4.93	8.35	2.80	100.5	-1.00	0.20	-1.46	0.060	0.011	-0.021	-0.041
17	683	0.90	2.36	4.94	8.35	2.80	100.6	-0.50	0.35	-1.47	0.129	0.027	-0.006	0.035
17	684	0.90	2.36	4.94	8.35	2.80	100.5	0.00	0.40	-1.13	0.224	0.059	-0.002	0.001
17	670	0.95	2.40	4.66	8.35	2.95	100.3	-3.00	-0.22	-0.16	-0.052	-0.058	-0.018	-0.079
17	671	0.95	2.41	4.68	8.36	2.96	100.5	-2.50	-0.11	-0.68	-0.013	-0.031	0.001	-0.014
17	672	0.95	2.41	4.67	8.36	2.95	100.5	-2.00	0.00	-1.08	0.017	-0.007	-0.012	0.118
17	673	0.95	2.40	4.67	8.34	2.95	100.5	-1.50	0.12	-1.45	0.041	-0.005	-0.020	0.012
17	674	0.95	2.40	4.67	8.35	2.95	100.7	-1.00	0.21	-1.63	0.073	0.007	-0.005	-0.049
17	675	0.95	2.40	4.67	8.35	2.95	100.5	-0.50	0.33	-1.57	0.131	0.024	-0.018	-0.033
17	676	0.95	2.40	4.67	8.34	2.95	100.4	0.00	0.38	-1.24	0.224	0.052	-0.017	0.069

Table 28. Force and Moment Data for Configuration 16 With $h = 4.80$ in., $l = 30.00$ in., and $Y_s = 0.00$ in.

Run	Point	M_∞	$R_\infty \times 10^{-6}$	p_∞ , psi	$p_{t,\infty}$, psi	q_∞ , psi	$T_{t,\infty}$, of F	Z_s , in.	C_N	C_m	C_A	C_{AB}	C_Y	C_n
14	538	0.20	2.07	22.96	23.63	0.66	98.6	-0.90	0.12	-0.53	0.238	0.166	0.017	-0.007
14	539	0.20	2.06	22.96	23.63	0.65	98.9	-0.50	0.14	-0.42	0.326	0.175	0.031	0.168
14	540	0.20	2.06	22.96	23.62	0.65	99.0	0.00	0.16	-0.42	0.378	0.163	0.058	0.120
14	541	0.20	2.02	22.98	23.62	0.63	99.2	0.50	0.22	-1.06	0.459	0.179	0.018	0.173
14	542	0.20	2.03	22.98	23.63	0.64	99.3	1.00	0.15	-1.37	0.499	0.173	0.031	0.058
14	543	0.20	2.03	22.98	23.63	0.64	99.4	1.50	0.10	-1.71	0.496	0.178	0.029	-0.088
14	544	0.20	2.06	22.94	23.60	0.66	99.5	2.00	0.03	-1.48	0.478	0.172	0.042	0.026
14	545	0.20	2.05	22.94	23.60	0.65	99.6	2.31	0.00	-1.36	0.467	0.167	0.028	0.074
14	529	0.40	3.64	19.90	22.24	2.24	100.4	-0.90	0.09	-1.23	0.124	0.061	-0.007	0.118
14	530	0.40	3.64	19.90	22.24	2.24	100.5	-0.50	0.28	-1.11	0.159	0.060	-0.036	0.108
14	531	0.40	3.64	19.90	22.24	2.24	100.5	0.00	0.37	-0.56	0.262	0.086	0.009	0.129
14	532	0.40	3.64	19.90	22.23	2.24	100.6	0.50	0.33	-0.63	0.344	0.116	-0.004	-0.065
14	533	0.40	3.64	19.90	22.24	2.24	100.6	1.00	0.29	-1.07	0.374	0.126	0.010	-0.148
14	534	0.40	3.64	19.90	22.24	2.24	100.6	1.50	0.20	-0.98	0.374	0.130	0.006	-0.027
14	535	0.40	3.64	19.90	22.24	2.24	100.6	2.00	0.09	-0.65	0.365	0.127	-0.007	-0.044
14	536	0.40	3.63	19.92	22.24	2.22	100.7	2.31	0.04	-0.43	0.362	0.123	-0.011	0.021
14	520	0.60	2.82	9.79	12.49	2.47	100.0	-0.90	0.11	-1.11	0.082	0.031	-0.028	-0.038
14	521	0.60	2.82	9.81	12.52	2.47	100.5	-0.50	0.28	-1.01	0.145	0.048	-0.011	-0.036
14	522	0.60	2.82	9.81	12.51	2.47	100.6	0.00	0.39	-0.37	0.247	0.070	-0.010	-0.045
14	523	0.60	2.82	9.81	12.52	2.48	100.5	0.50	0.43	-0.27	0.307	0.077	-0.026	0.063
14	524	0.60	2.82	9.80	12.51	2.47	100.3	1.00	0.38	-0.63	0.337	0.088	-0.013	0.110
14	525	0.60	2.82	9.81	12.52	2.48	100.3	1.50	0.24	-0.50	0.355	0.106	-0.004	0.019
14	526	0.60	2.82	9.80	12.51	2.48	100.3	2.00	0.11	-0.21	0.359	0.111	-0.016	0.012
14	527	0.60	2.82	9.81	12.52	2.48	100.3	2.31	0.04	-0.04	0.362	0.112	-0.003	0.013
14	511	0.80	2.54	6.20	9.47	2.79	100.1	-0.90	0.39	-1.24	0.017	-0.059	-0.011	0.123
14	512	0.80	2.53	6.20	9.45	2.78	100.5	-0.50	0.54	-1.15	0.089	-0.026	-0.039	-0.123
14	513	0.80	2.53	6.20	9.45	2.78	100.7	0.00	0.57	-0.65	0.185	0.003	-0.015	0.145
14	514	0.80	2.53	6.20	9.45	2.78	100.8	0.50	0.53	-0.68	0.274	0.025	-0.031	0.109
14	515	0.80	2.53	6.20	9.45	2.78	100.9	1.00	0.43	-0.79	0.326	0.063	-0.037	0.032
14	516	0.80	2.53	6.20	9.45	2.78	100.7	1.50	0.28	-0.54	0.336	0.087	-0.003	-0.013
14	517	0.80	2.53	6.20	9.45	2.78	100.7	2.00	0.15	-0.32	0.348	0.101	-0.014	-0.026
14	518	0.80	2.53	6.20	9.45	2.78	100.9	2.31	0.09	-0.13	0.356	0.106	-0.015	0.034

Table 28. Concluded

Run	Point	M_{∞}	$R_{\infty} \times 10^{-6}$	p_{∞} , psi	$p_{t,\infty}$, psi	q_{∞} , psi	$T_{t,\infty}$, °F	Z_s in.	C_N	C_m	C_A	C_{A_B}	C_Y	C_n
14	502	0.90	2.36	4.94	8.35	2.80	100.7	-0.90	0.18	-1.36	0.101	0.007	-0.036	0.127
14	503	0.90	2.36	4.94	8.36	2.80	100.5	-0.50	0.25	-1.11	0.154	0.022	-0.003	0.084
14	504	0.90	2.36	4.94	8.35	2.80	100.1	0.00	0.40	-1.24	0.258	0.054	-0.012	-0.051
14	505	0.90	2.36	4.93	8.35	2.80	99.9	0.50	0.45	-1.35	0.326	0.066	0.005	0.049
14	506	0.90	2.36	4.94	8.35	2.80	100.1	1.00	0.36	-1.50	0.356	0.079	-0.003	-0.065
14	507	0.90	2.36	4.94	8.35	2.80	100.3	1.50	0.23	-1.29	0.369	0.089	-0.007	0.084
14	508	0.90	2.36	4.94	8.35	2.80	100.5	2.00	0.11	-0.95	0.376	0.093	-0.015	0.023
14	509	0.90	2.36	4.94	8.35	2.80	100.4	2.31	0.04	-0.74	0.375	0.094	-0.015	0.083
14	493	0.95	2.40	4.66	8.34	2.95	101.0	-0.90	0.20	-1.56	0.104	0.011	-0.023	-0.049
14	494	0.95	2.40	4.67	8.35	2.95	101.2	-0.50	0.29	-1.46	0.161	0.024	-0.018	0.038
14	495	0.95	2.40	4.67	8.36	2.96	101.3	0.00	0.38	-1.32	0.257	0.057	-0.041	0.017
14	496	0.95	2.40	4.68	8.37	2.96	101.4	0.50	0.39	-1.45	0.318	0.062	-0.023	0.033
14	497	0.95	2.41	4.67	8.35	2.95	100.1	1.00	0.33	-1.78	0.365	0.084	-0.024	0.059
14	498	0.95	2.41	4.67	8.35	2.95	99.9	1.50	0.22	-1.59	0.371	0.088	-0.017	0.014
14	499	0.95	2.41	4.68	8.36	2.96	100.3	2.00	0.10	-1.18	0.370	0.090	-0.015	-0.017
14	500	0.95	2.41	4.67	8.36	2.95	100.5	2.31	0.05	-1.03	0.371	0.087	0.000	-0.048

Table 29. Force and Moment Data for Configuration 17 With $h = 4.80$ in., $l = 30.00$ in., and $Y_s = 2.40$ in.

Run	Point	M_∞	$R_\infty \times 10^{-6}$	P_∞ , psi	$P_{t,\infty}$, psi	q_∞ , psi	$T_{t,\infty}$, °F	Z_s in.	C_N	C_m	C_A	C_{AB}	C_Y	C_n
19	766	0.20	2.04	22.95	23.61	0.65	100.4	-3.00	-0.23	0.28	0.048	0.040	0.123	-0.127
19	767	0.20	2.04	22.95	23.60	0.65	100.5	-2.50	-0.15	0.01	0.091	0.057	0.163	-0.465
19	768	0.20	2.03	22.95	23.60	0.64	100.4	-2.00	0.03	-0.92	0.128	0.080	0.134	-1.064
19	769	0.20	2.03	22.96	23.60	0.64	100.4	-1.50	0.01	-0.43	0.189	0.113	0.015	-0.241
19	770	0.20	2.03	22.95	23.60	0.64	100.4	-1.00	0.06	-0.28	0.231	0.136	0.071	-0.306
19	771	0.20	2.03	22.95	23.60	0.64	100.4	-0.50	0.10	-0.31	0.287	0.157	0.072	0.002
19	772	0.20	2.03	22.96	23.61	0.64	100.4	0.00	0.21	-0.28	0.396	0.163	0.278	-0.521
19	758	0.40	3.64	19.90	22.23	2.24	100.9	-3.00	-0.19	-0.36	0.000	0.012	0.052	-0.184
19	759	0.40	3.64	19.90	22.24	2.25	100.8	-2.50	-0.06	-0.97	0.035	0.025	0.042	-0.758
19	760	0.40	3.64	19.91	22.24	2.24	100.8	-2.00	0.03	-1.40	0.061	0.039	0.033	-1.171
19	761	0.40	3.64	19.90	22.24	2.24	100.9	-1.50	0.08	-1.52	0.101	0.065	0.115	-1.474
19	762	0.40	3.63	19.92	22.24	2.23	100.9	-1.00	0.11	-1.37	0.124	0.068	0.268	-1.332
19	763	0.40	3.62	19.92	22.23	2.22	100.9	-0.50	0.34	-1.15	0.195	0.081	0.442	-1.675
19	764	0.40	3.63	19.90	22.23	2.24	100.9	0.00	0.43	-0.60	0.304	0.111	0.397	-1.818
19	750	0.60	2.82	9.82	12.52	2.47	100.9	-3.00	-0.21	-0.46	-0.052	-0.031	0.014	-0.243
19	751	0.60	2.82	9.81	12.51	2.47	100.9	-2.50	-0.08	-1.19	0.003	-0.003	0.058	-0.828
19	752	0.60	2.81	9.80	12.51	2.47	101.0	-2.00	0.02	-1.73	0.055	0.028	0.102	-1.452
19	753	0.60	2.81	9.80	12.50	2.47	100.9	-1.50	0.07	-1.91	0.092	0.049	0.215	-1.932
19	754	0.60	2.81	9.79	12.49	2.47	101.0	-1.00	0.17	-1.72	0.106	0.047	0.388	-1.591
19	755	0.60	2.81	9.79	12.50	2.48	100.9	-0.50	0.33	-0.89	0.170	0.057	0.432	-1.674
19	756	0.60	2.81	9.80	12.50	2.47	100.9	0.00	0.52	-0.32	0.282	0.088	0.472	-2.200
19	742	0.80	2.54	6.19	9.45	2.78	99.1	-3.00	-0.33	-0.19	-0.052	-0.047	0.056	-0.091
19	743	0.80	2.54	6.20	9.46	2.78	99.8	-2.50	-0.14	-0.93	0.020	-0.001	0.197	-0.957
19	744	0.80	2.53	6.19	9.43	2.77	99.8	-2.00	0.03	-1.57	0.062	0.025	0.331	-1.835
19	745	0.80	2.53	6.19	9.44	2.78	100.3	-1.50	0.26	-1.97	0.097	0.031	0.443	-2.322
19	746	0.80	2.53	6.20	9.45	2.78	101.3	-1.00	0.50	-1.95	0.141	0.045	0.421	-2.634
19	747	0.80	2.53	6.20	9.46	2.78	100.7	-0.50	0.61	-1.04	0.194	0.053	0.399	-2.414
19	748	0.80	2.53	6.20	9.45	2.78	100.5	0.00	0.65	-0.51	0.273	0.073	0.418	-2.087

Table 29. Concluded

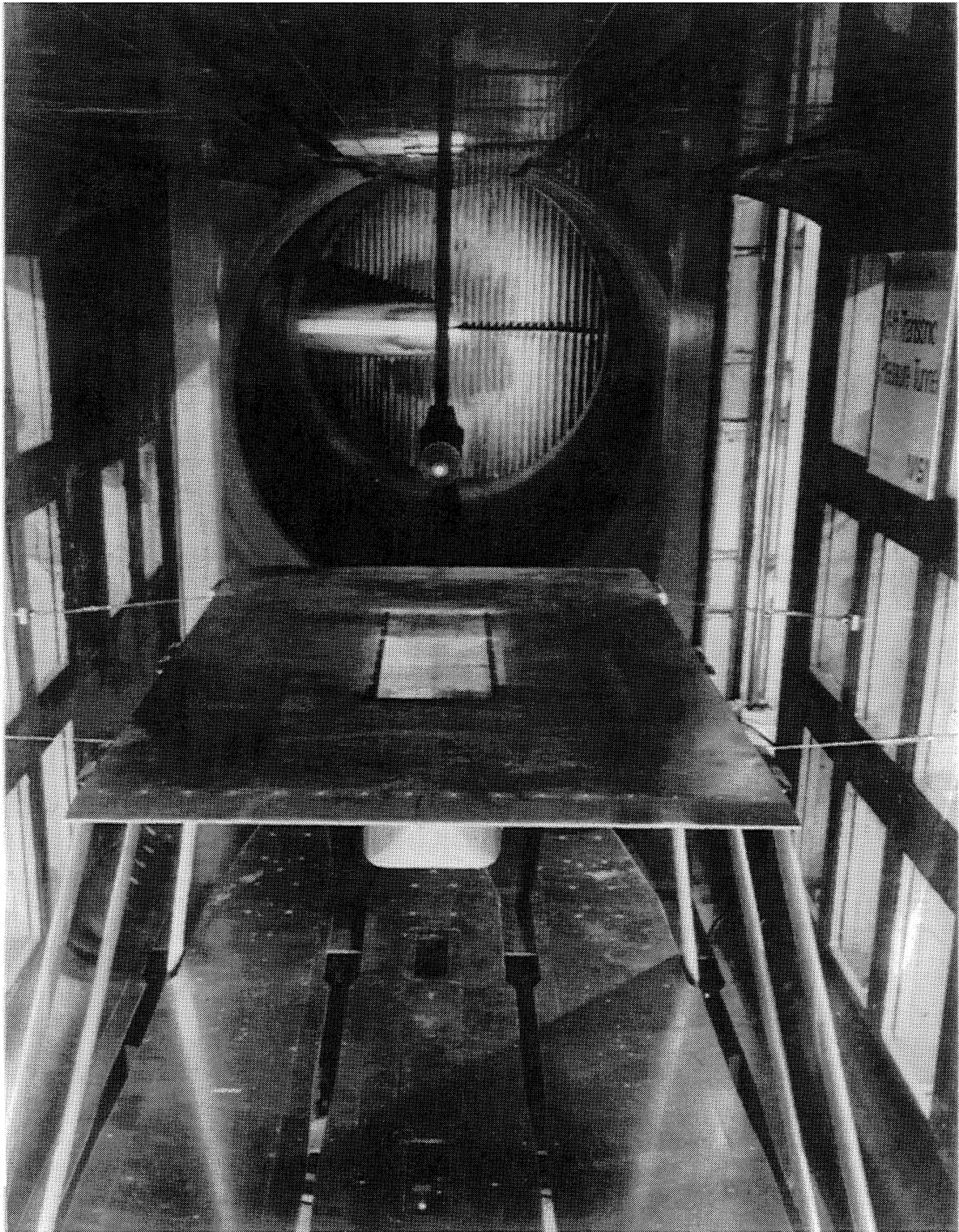
Run	Point	M_∞	$R_\infty \times 10^{-6}$	P_∞ , psi	$P_{t,\infty}$, psi	q_∞ , psi	$T_{t,\infty}$, °F	Z_s in.	C_N	C_m	C_A	C_{A_B}	C_Y	C_n
19	734	0.90	2.36	4.93	8.34	2.80	100.1	-3.00	-0.29	-0.08	-0.018	-0.053	0.063	-0.072
19	735	0.90	2.36	4.94	8.36	2.80	100.6	-2.50	-0.13	-0.73	0.026	-0.012	0.120	-0.903
19	736	0.90	2.36	4.95	8.37	2.80	100.8	-2.00	0.01	-1.49	0.064	0.014	0.248	-1.853
19	737	0.90	2.35	4.94	8.35	2.80	101.2	-1.50	0.16	-1.89	0.098	0.021	0.346	-2.288
19	738	0.90	2.35	4.94	8.35	2.80	101.0	-1.00	0.25	-1.64	0.128	0.032	0.473	-2.573
19	739	0.90	2.35	4.93	8.35	2.80	101.1	-0.50	0.34	-0.92	0.179	0.038	0.438	-2.296
19	740	0.90	2.35	4.93	8.35	2.80	101.1	0.00	0.45	-0.60	0.288	0.069	0.412	-2.177
19	726	0.95	2.40	4.67	8.34	2.95	100.1	-3.00	-0.28	-0.06	-0.015	-0.042	0.058	-0.334
19	727	0.95	2.41	4.68	8.36	2.95	100.5	-2.50	-0.11	-0.84	0.039	-0.008	0.142	-1.070
19	728	0.95	2.41	4.68	8.36	2.95	100.5	-2.00	-0.01	-1.39	0.074	0.013	0.219	-1.879
19	729	0.95	2.41	4.68	8.36	2.95	100.6	-1.50	0.13	-1.73	0.093	0.020	0.342	-2.340
19	730	0.95	2.40	4.67	8.34	2.95	100.6	-1.00	0.24	-1.74	0.129	0.023	0.483	-2.627
19	731	0.95	2.40	4.67	8.34	2.95	100.5	-0.50	0.30	-0.91	0.179	0.032	0.453	-2.450
19	732	0.95	2.40	4.67	8.35	2.95	100.6	0.00	0.37	-0.61	0.274	0.061	0.371	-2.200

Table 30. Force and Moment Data for Configuration 18 With $h = 4.80$ in., $l = 30.00$ in., and $Y_s = 2.40$ in.

Run	Point	M_{∞}	$R_{\infty} \times 10^{-6}$	P_{∞} , psi	$P_{t,\infty}$, psi	q_{∞} , psi	$T_{t,\infty}$, °F	Z_s in.	C_N	C_m	C_A	C_{AB}	C_Y	C_n
13	480	0.20	2.03	22.97	23.61	0.64	99.7	-0.90	0.02	-0.58	0.184	0.131	-0.001	-0.500
13	481	0.20	2.05	22.94	23.61	0.65	99.9	-0.50	0.03	-0.39	0.247	0.135	0.029	-0.026
13	482	0.20	2.06	22.94	23.61	0.66	100.1	0.00	0.08	-0.69	0.354	0.176	0.135	-0.280
13	483	0.20	2.03	22.96	23.61	0.64	100.2	0.50	0.13	-0.84	0.389	0.159	0.302	-1.139
13	484	0.20	2.03	22.97	23.62	0.64	100.2	1.00	0.07	-1.11	0.424	0.184	0.205	-0.790
13	485	0.20	2.03	22.98	23.62	0.64	100.4	1.50	0.02	-1.24	0.442	0.168	0.151	-0.532
13	486	0.20	2.03	22.97	23.61	0.64	100.4	2.00	-0.01	-1.24	0.424	0.160	0.124	-0.353
13	487	0.20	2.03	22.96	23.61	0.64	100.5	2.31	-0.14	-1.87	0.584	0.179	0.221	0.276
13	471	0.40	3.63	19.90	22.22	2.23	100.1	-0.90	0.15	-1.14	0.096	0.049	0.250	-1.152
13	472	0.40	3.64	19.88	22.22	2.25	100.4	-0.50	0.29	-1.05	0.165	0.062	0.358	-1.580
13	473	0.40	3.64	19.88	22.21	2.24	100.5	0.00	0.32	-0.78	0.293	0.118	0.314	-1.328
13	474	0.40	3.64	19.88	22.21	2.24	100.6	0.50	0.44	-0.78	0.354	0.129	0.351	-2.090
13	475	0.40	3.63	19.88	22.21	2.23	100.6	1.00	0.24	-0.69	0.384	0.143	0.230	-1.413
13	476	0.40	3.64	19.88	22.21	2.24	100.7	1.50	0.13	-0.44	0.380	0.142	0.163	-0.925
13	477	0.40	3.64	19.90	22.24	2.25	100.8	2.00	0.02	0.02	0.360	0.136	0.140	-0.676
13	478	0.40	3.64	19.90	22.23	2.24	100.8	2.31	-0.08	-0.03	0.402	0.136	0.140	-0.409
13	462	0.60	2.82	9.81	12.51	2.47	100.2	-0.90	0.16	-1.40	0.089	0.038	0.366	-1.552
13	463	0.60	2.82	9.80	12.51	2.48	100.2	-0.50	0.27	-1.03	0.163	0.062	0.356	-1.544
13	464	0.60	2.82	9.80	12.50	2.48	100.3	0.00	0.48	-0.37	0.261	0.081	0.428	-2.190
13	465	0.60	2.82	9.79	12.51	2.48	100.2	0.50	0.54	0.09	0.326	0.095	0.308	-1.910
13	466	0.60	2.82	9.80	12.51	2.47	100.3	1.00	0.32	0.17	0.356	0.109	0.259	-1.418
13	467	0.60	2.82	9.80	12.51	2.47	100.4	1.50	0.17	0.11	0.362	0.122	0.194	-1.063
13	468	0.60	2.82	9.80	12.50	2.48	100.2	2.00	0.02	0.51	0.383	0.136	0.201	-0.813
13	469	0.60	2.82	9.80	12.50	2.48	100.3	2.31	-0.09	0.55	0.393	0.130	0.187	-0.516
13	453	0.80	2.54	6.19	9.45	2.78	99.4	-0.90	0.44	-1.46	0.080	0.011	0.408	-2.415
13	454	0.80	2.54	6.20	9.46	2.78	99.8	-0.50	0.56	-1.07	0.149	0.040	0.391	-2.397
13	455	0.80	2.54	6.20	9.46	2.78	99.8	0.00	0.60	-0.62	0.247	0.065	0.354	-2.335
13	456	0.80	2.54	6.21	9.46	2.78	100.0	0.50	0.54	-0.37	0.328	0.088	0.296	-1.842
13	457	0.80	2.54	6.21	9.47	2.78	99.9	1.00	0.35	-0.42	0.360	0.110	0.305	-1.542
13	458	0.80	2.54	6.21	9.47	2.78	99.9	1.50	0.19	-0.16	0.358	0.120	0.242	-1.129
13	459	0.80	2.54	6.21	9.46	2.78	100.1	2.00	0.05	0.16	0.373	0.136	0.201	-0.818
13	460	0.80	2.54	6.21	9.45	2.78	99.9	2.31	-0.06	0.27	0.398	0.135	0.188	-0.552

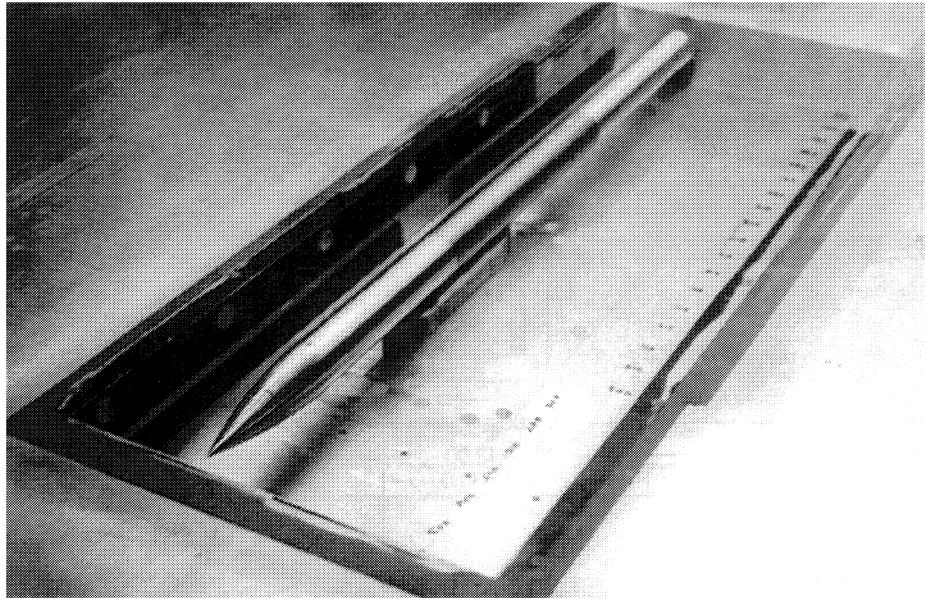
Table 30. Concluded

Run	Point	M_∞	$R_\infty \times 10^{-6}$	p_∞ , psi	$p_{t,\infty}$, psi	q_∞ , psi	$T_{t,\infty}$, °F	Z_s in.	C_N	C_m	C_A	C_{AB}	C_Y	C_n
13	444	0.90	2.34	4.92	8.33	2.79	102.0	-0.90	0.22	-1.47	0.099	0.019	0.454	-2.525
13	445	0.90	2.35	4.92	8.33	2.79	101.5	-0.50	0.28	-0.89	0.156	0.031	0.393	-2.403
13	446	0.90	2.35	4.92	8.33	2.79	101.2	0.00	0.38	-0.73	0.261	0.059	0.340	-2.331
13	447	0.90	2.35	4.92	8.33	2.79	100.9	0.50	0.39	-0.88	0.332	0.074	0.291	-2.043
13	448	0.90	2.35	4.93	8.33	2.79	100.9	1.00	0.24	-0.90	0.347	0.080	0.258	-1.435
13	449	0.90	2.35	4.93	8.33	2.79	100.9	1.50	0.12	-0.64	0.367	0.094	0.212	-0.951
13	450	0.90	2.35	4.93	8.34	2.79	100.6	2.00	0.00	-0.32	0.377	0.103	0.170	-0.770
13	451	0.90	2.36	4.94	8.35	2.80	100.9	2.31	-0.07	-0.33	0.388	0.109	0.180	-0.591
12	426	0.95	2.40	4.67	8.35	2.95	100.8	-0.90	0.15	-1.33	0.110	0.015	0.441	-2.417
12	427	0.95	2.40	4.67	8.35	2.95	100.5	-0.50	0.22	-0.88	0.168	0.029	0.376	-2.370
12	428	0.95	2.40	4.67	8.35	2.95	100.6	0.00	0.35	-0.79	0.272	0.057	0.312	-2.338
12	429	0.95	2.40	4.67	8.35	2.95	100.8	0.50	0.36	-1.10	0.334	0.068	0.266	-1.895
12	430	0.95	2.40	4.67	8.35	2.95	100.7	1.00	0.24	-1.17	0.352	0.072	0.222	-1.468
12	431	0.95	2.40	4.67	8.35	2.95	100.6	1.50	0.10	-0.92	0.362	0.080	0.196	-1.084
12	432	0.95	2.40	4.67	8.35	2.95	100.5	2.00	0.02	-0.71	0.366	0.086	0.158	-0.815
12	433	0.95	2.40	4.68	8.35	2.95	100.5	2.31	-0.06	-0.61	0.380	0.091	0.158	-0.625



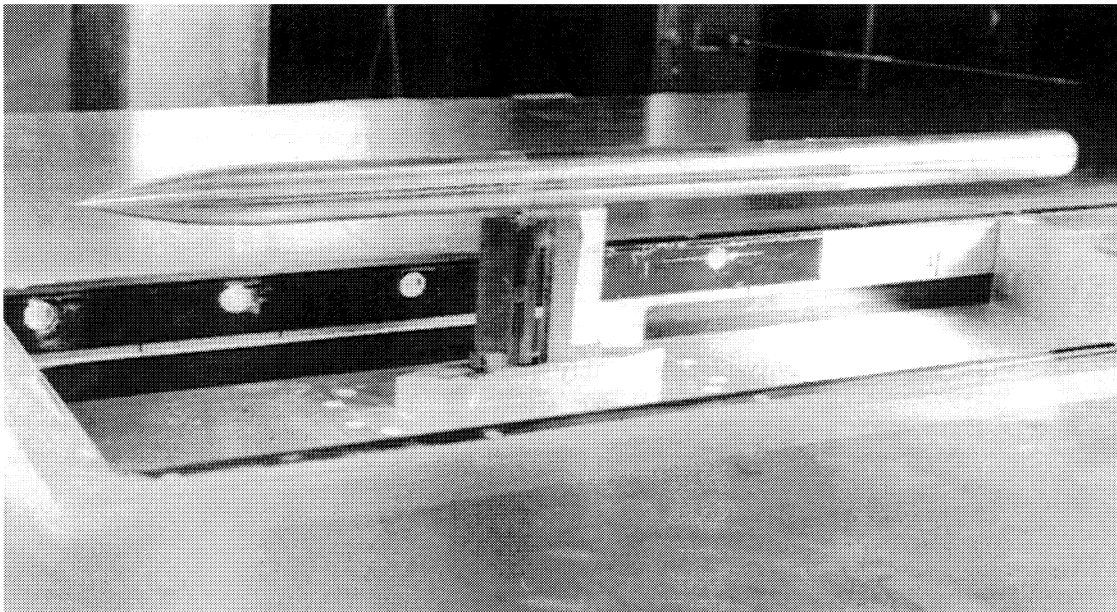
L-92-1502

Figure 1. Cavity-plate assembly installed in test section of Langley 8-Foot Transonic Pressure Tunnel. (View looking downstream.)



L-92-01063

(a) $Z_s = -0.90$ in.



L-92-01062

(b) $Z_s = 2.37$ in.

Figure 2. Store model assembly installed in cavity. $h = 2.40$ in.; $l = 26.00$ in.; $Y_s = 2.40$ in.

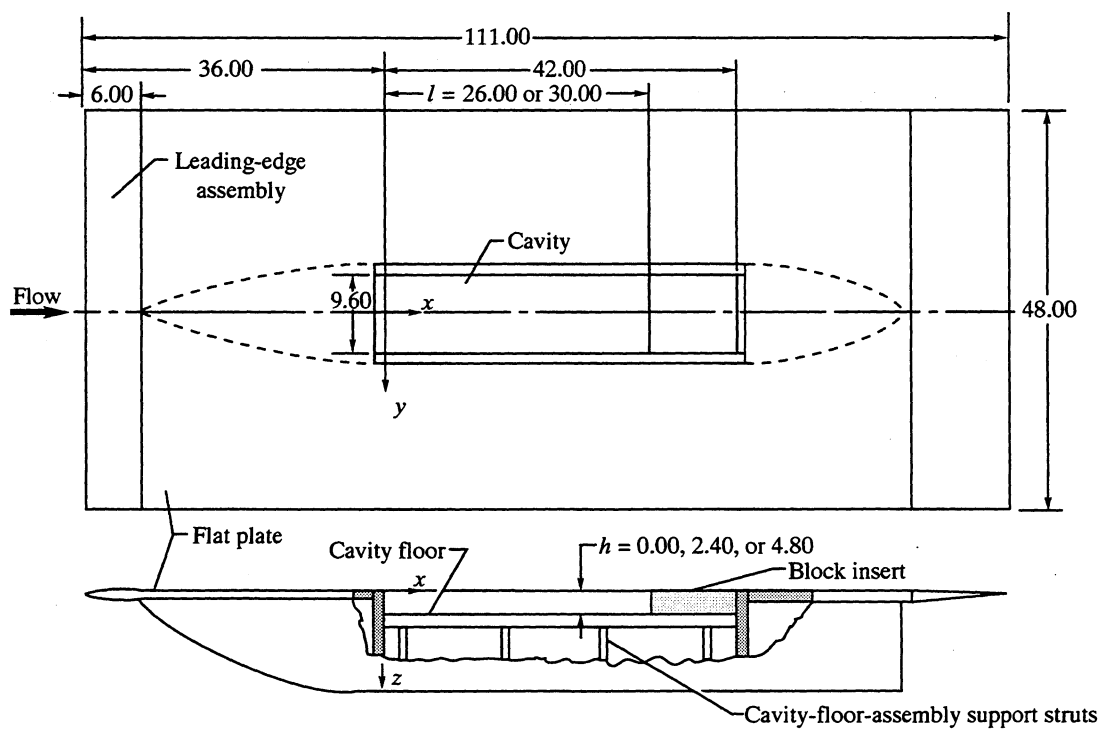
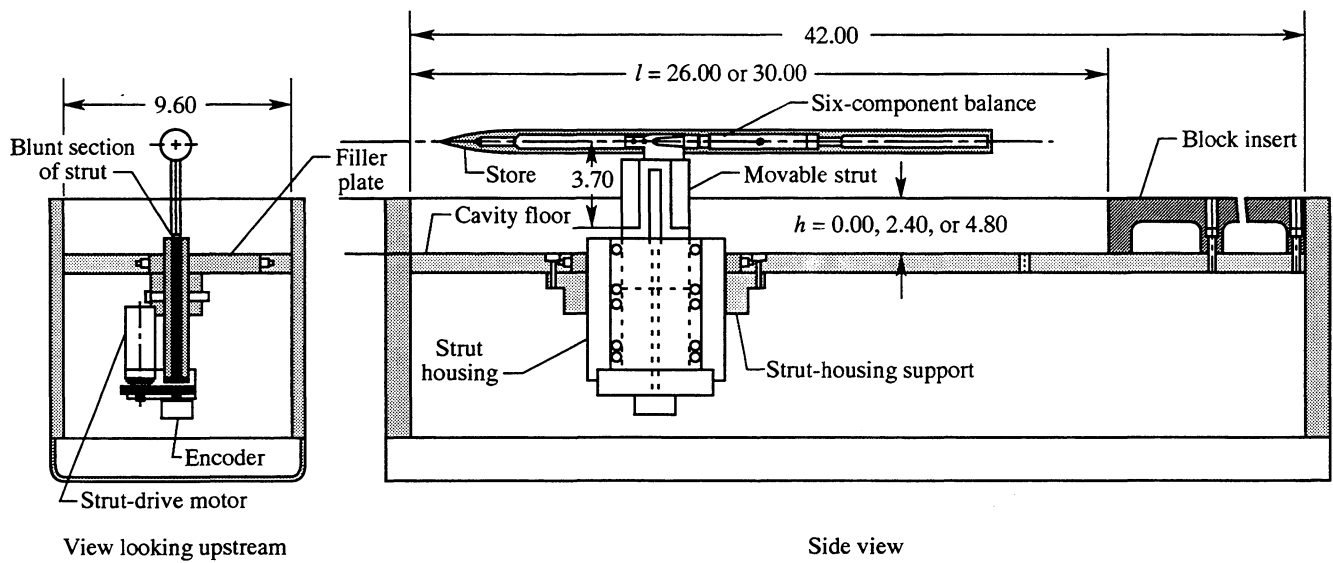
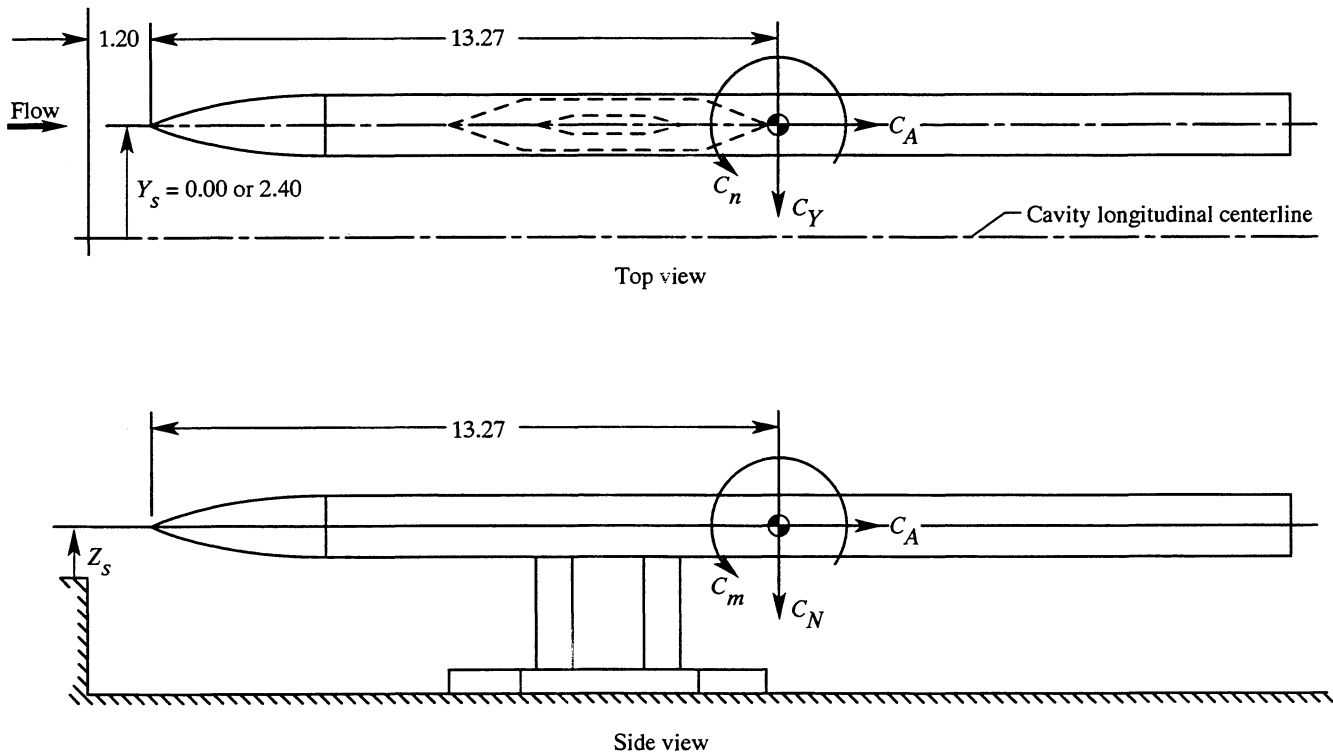


Figure 3. Cavity-plate assembly. (All dimensions in inches.)

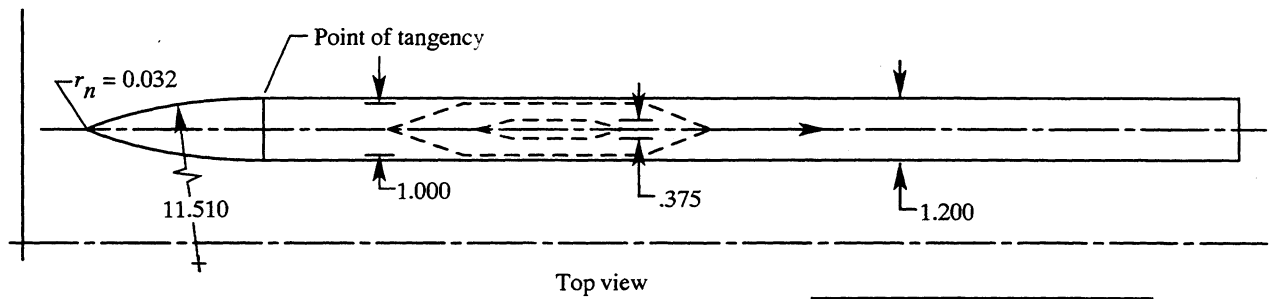


(a) General assembly.



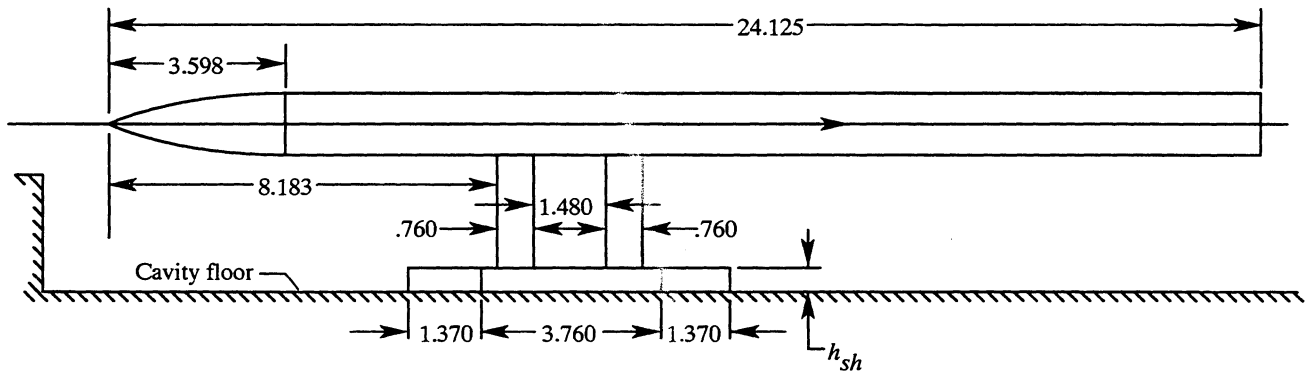
(b) General arrangement of store model in cavity.

Figure 4. Sketches of store model and cavity assembly. (All dimensions in inches.)



Top view

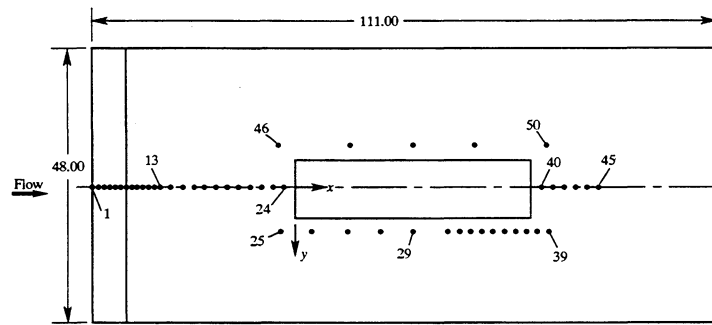
h_{sh}	Configuration
0.450	6-11, 13, 15, 17
2.850	12, 14, 16, 18



Side view

(c) Dimensions of store model and strut assembly.

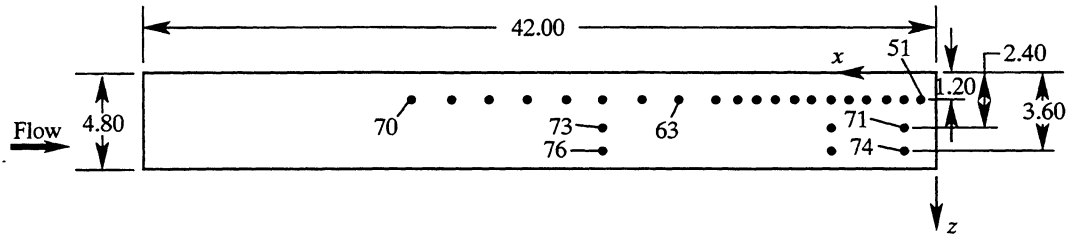
Figure 4. Concluded.



Orifice number	x, in.	y, in.	z, in.	Orifice location on plate
1	-36.0	0.00	0.500	Leading-edge assembly
2	-35.0		.224	
3	-34.0		.127	
4	-33.0		.067	
5	-32.0		.029	
6	-31.0		.007	
7	-30.0		.000	
8	-29.0			Forward of cavity
9	-28.0			
10	-27.0			
11	-26.0			
12	-25.0			
13	-24.0			
14	-22.0			
15	-20.0			
16	-18.0			
17	-16.0			
18	-14.0			
19	-12.0			
20	-10.0			
21	-8.0			
22	-6.0			
23	-4.0			
24	-2.0			Left of cavity
25	-3.0	7.80		
26	3.0			
27	9.0			
28	15.0			
29	21.0			
30	27.0			
31	29.0			
32	31.0			
33	33.0			
34	35.0			
35	37.0			
36	39.0			
37	41.0			
38	43.0			
39	45.0			
40	44.0	0.00		Aft of cavity
41	46.0			
42	48.0			
43	50.0			
44	52.0			
45	54.0			
46	-3.0	-7.80		
47	10.0			
48	21.0			
49	32.0			
50	45.0			

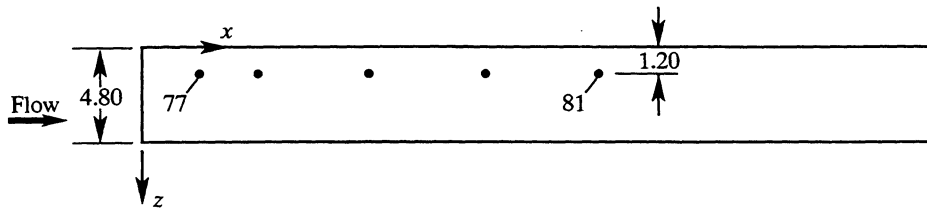
(a) Flat plate.

Figure 5. Pressure orifice locations on flat plate and cavity surfaces. (All dimensions in inches.)



Orifice number	x , in.	y , in.	z , in.
51	1.0	4.80	1.200
52	2.0		
53	3.0		
54	4.0		
55	5.0		
56	6.0		
57	7.0		
58	8.0		
59	9.0		
60	10.0		
61	11.0		
62	12.0		
63	14.0		
64	16.0		
65	18.0		
66	20.0		
67	22.0		
68	24.0		
69	26.0		
70	28.0		2.400
71	2.0		3.600
72	6.0		
73	18.0		
74	2.0		
75	6.0		
76	18.0		

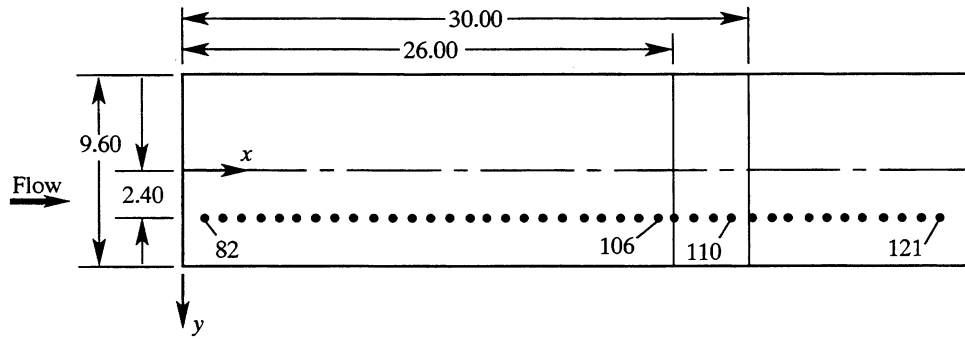
(b) Cavity left sidewall.



Orifice number	x , in.	y , in.	z , in.
77	3.0	-4.80	1.200
78	6.0		
79	12.0		
80	18.0		
81	24.0		

(c) Cavity right sidewall.

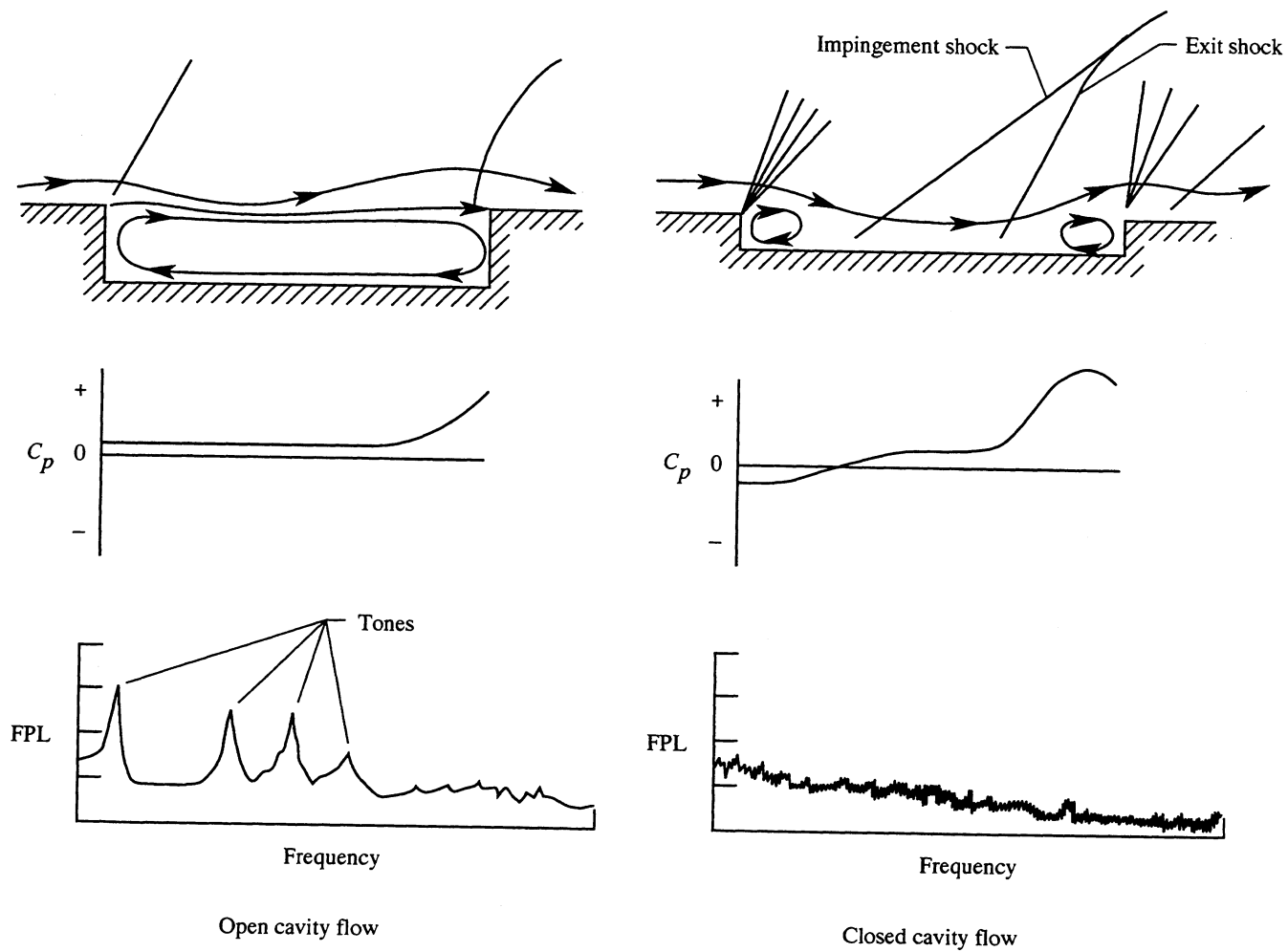
Figure 5. Continued.



Orifice number	x , in.	y , in.	z , in.
82	1.0	2.40	Variable
83	2.0		
84	3.0		
85	4.0		
86	5.0		
87	6.0		
88	7.0		
89	8.0		
90	9.0		
91	10.0		
92	11.0		
93	12.0		
94	13.0		
95	14.0		
96	15.0		
97	16.0		
98	17.0		
99	18.0		
100	19.0		
101	20.0		
102	21.0		
103	22.0		
104	23.0		
105	24.0		
106	25.0		
107	26.0		
108	27.0		
109	28.0		
110	29.0		
111	30.0		
112	31.0		
113	32.0		
114	33.0		
115	34.0		
116	35.0		
117	36.0		
118	37.0		
119	38.0		
120	39.0		
121	40.0		

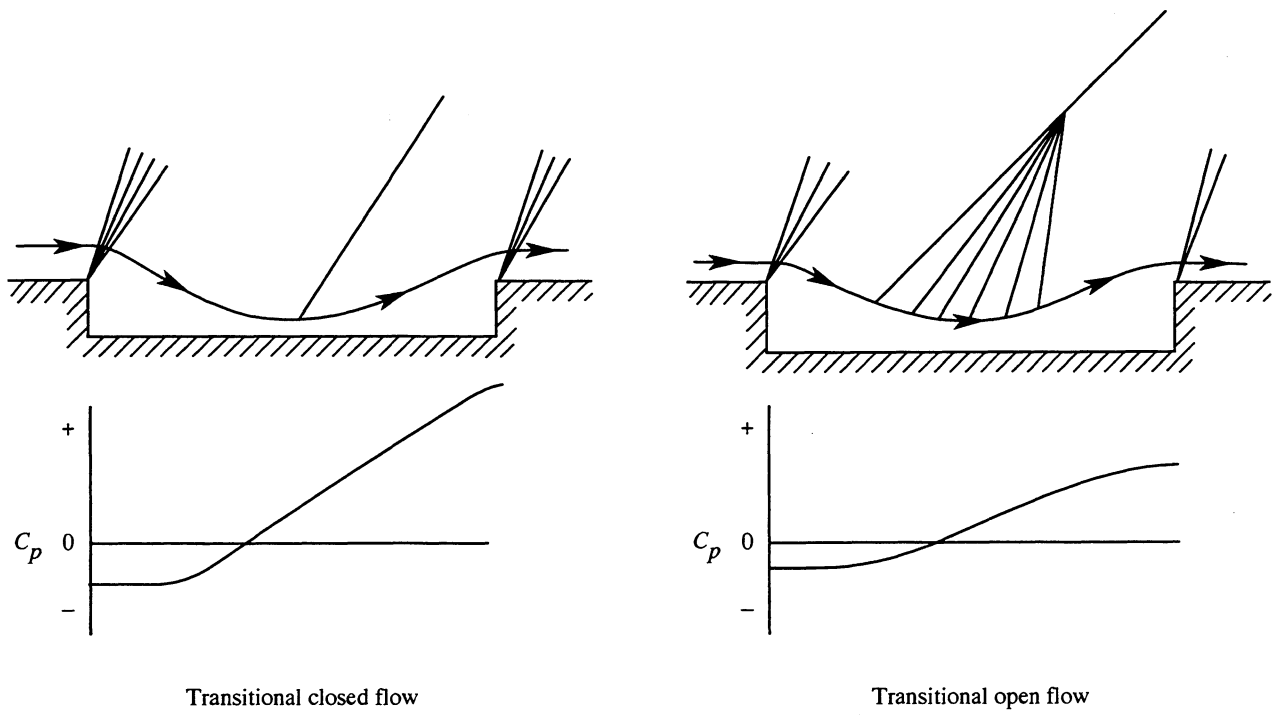
(d) Cavity floor.

Figure 5. Concluded.



(a) Basic cavity flow-field models.

Figure 6. Sketches of cavity flow-field models for supersonic speeds.



(b) Transitional cavity flow-field models.

Figure 6. Concluded.

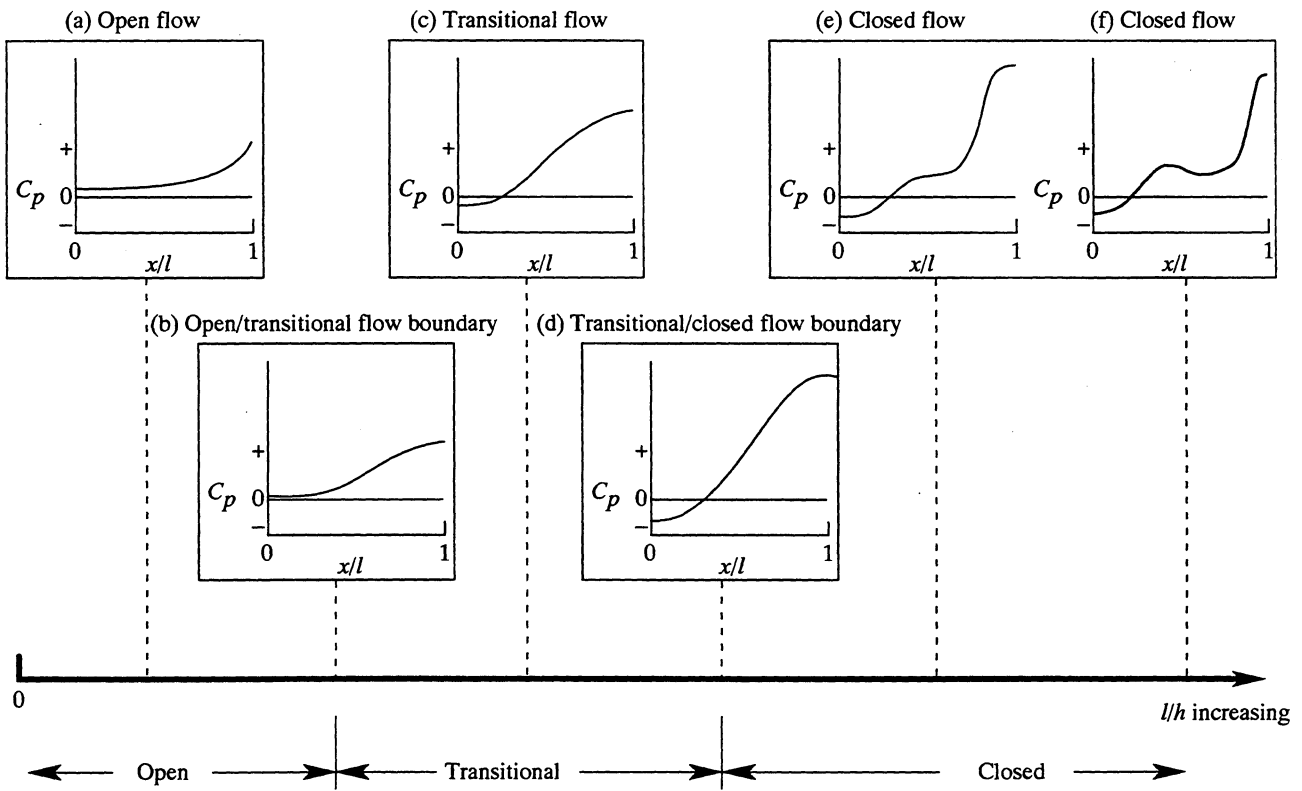


Figure 7. Representative cavity floor pressure distributions for different types of cavity flow at subsonic and transonic speeds (ref. 5).

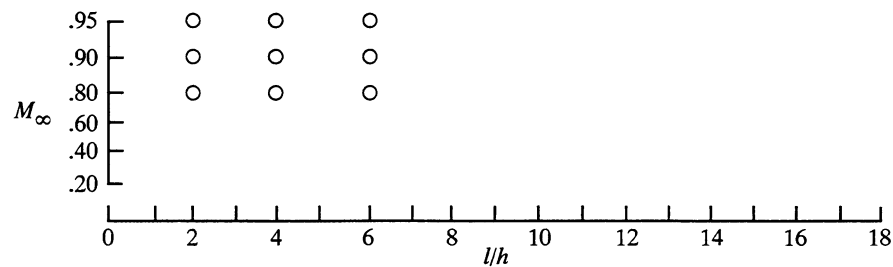
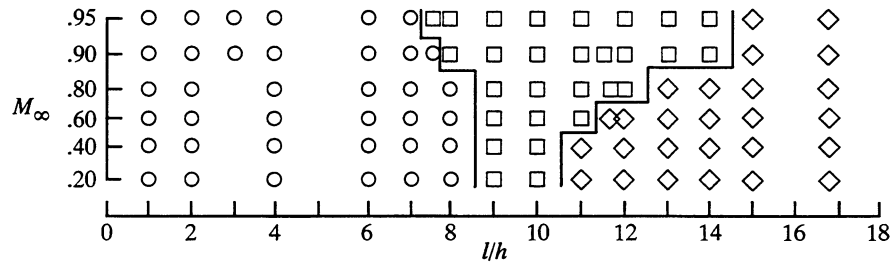
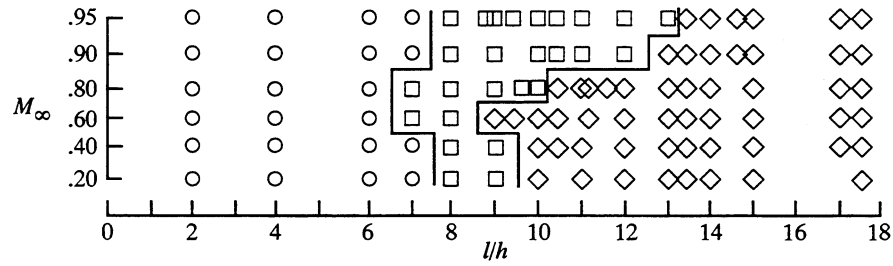
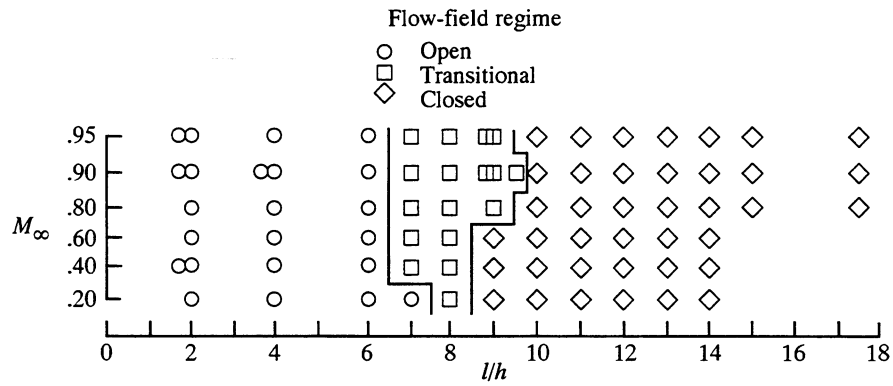
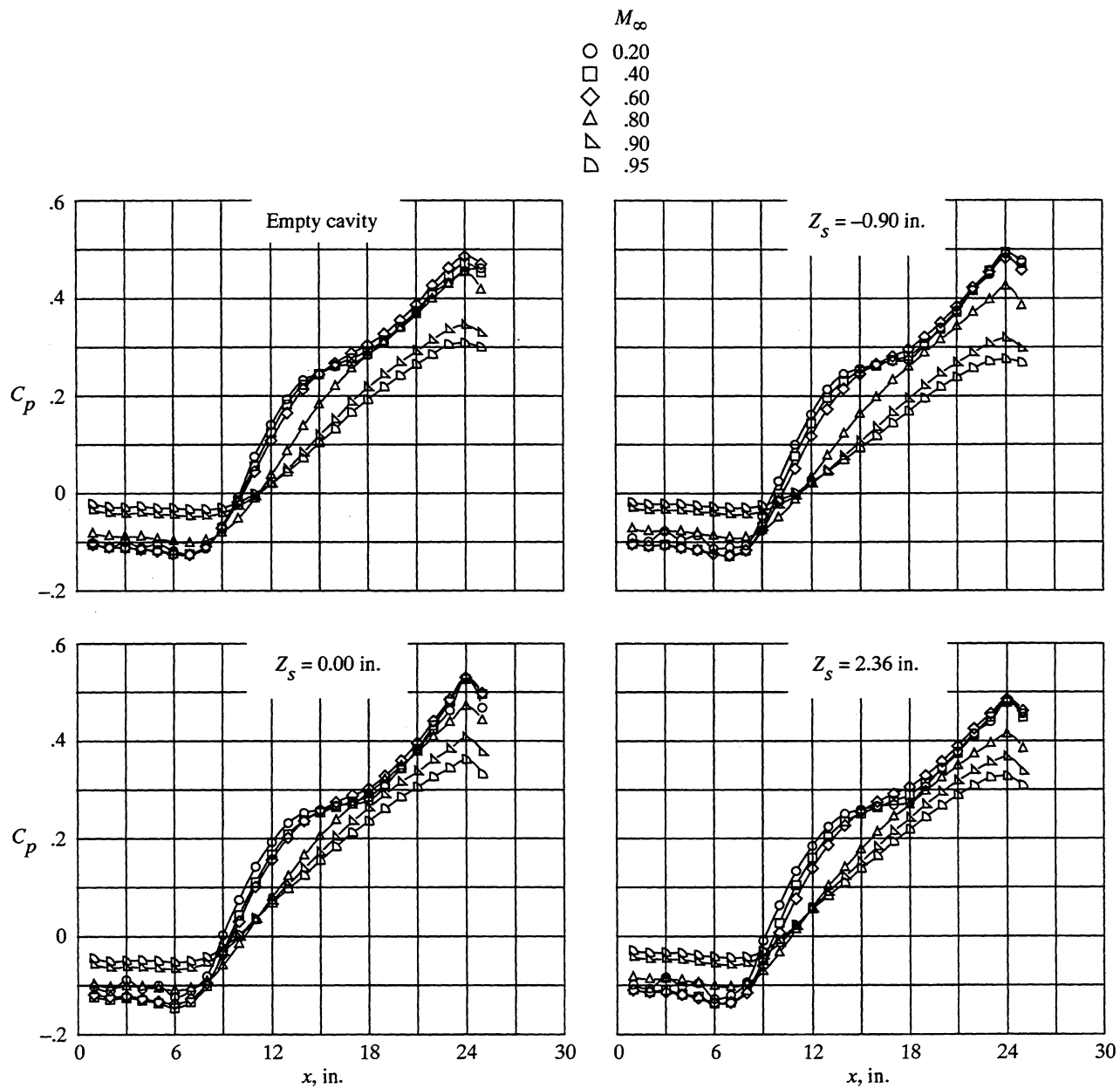


Figure 8. Boundaries of cavity flow regimes for a range of cavity variables and Mach numbers (ref. 5). Units of w and h are in inches.



(a) $l = 26.00$ in.; $l/h = 10.83$; $Y_s = 0.00$ in.

Figure 9. Effect of Mach number on cavity floor pressure distributions. $h = 2.40$ in.

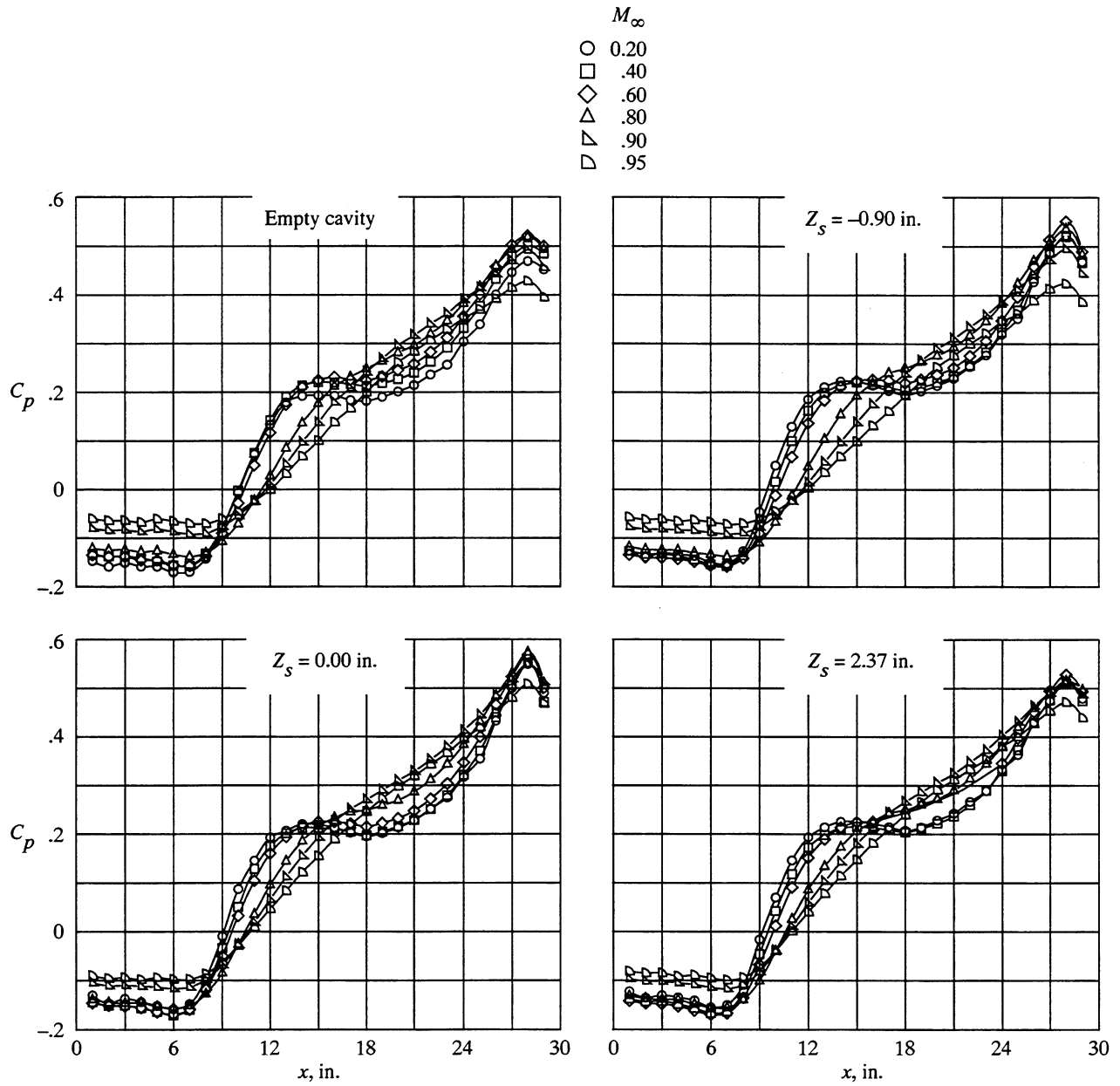


Figure 9. Continued.

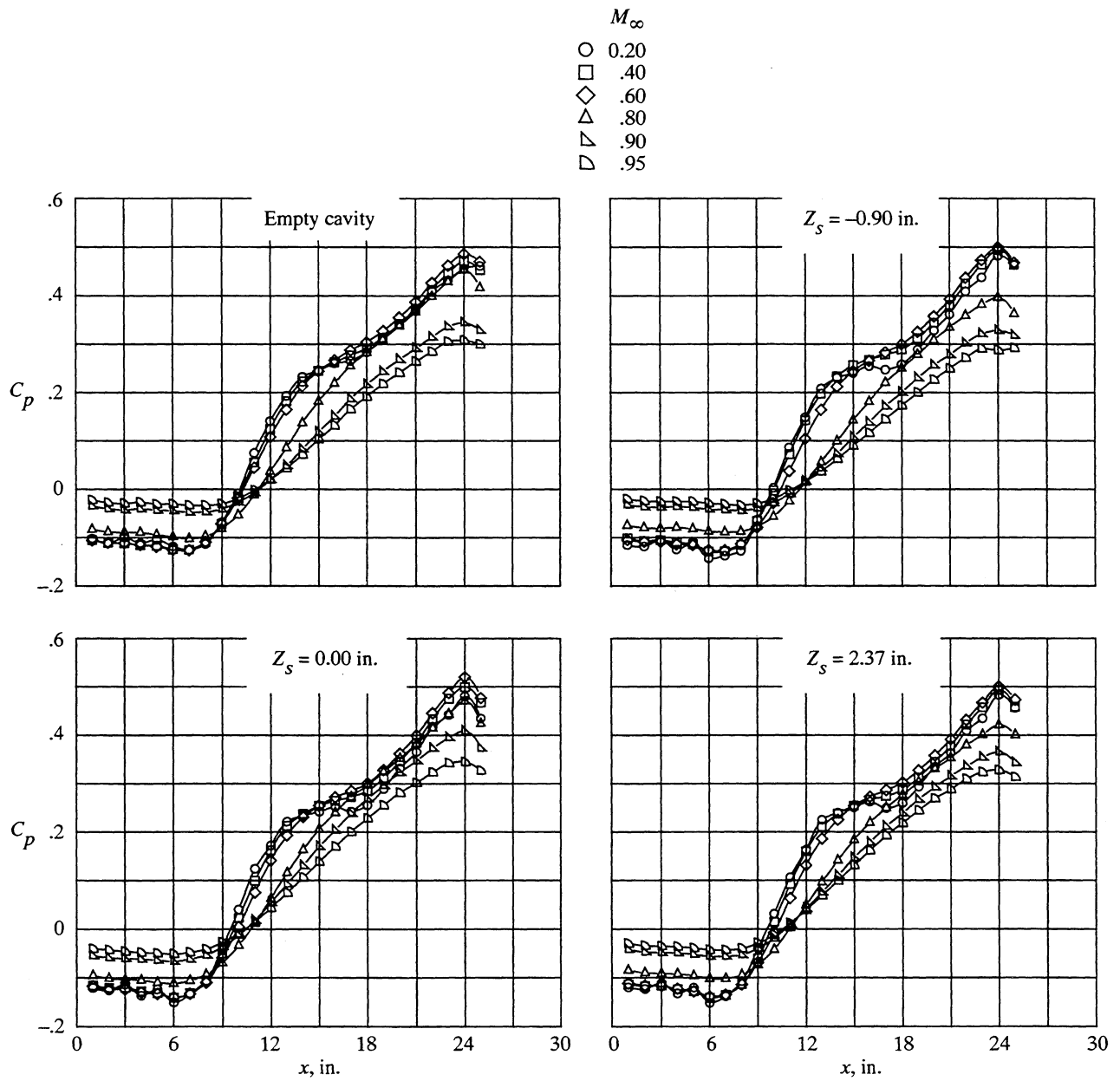
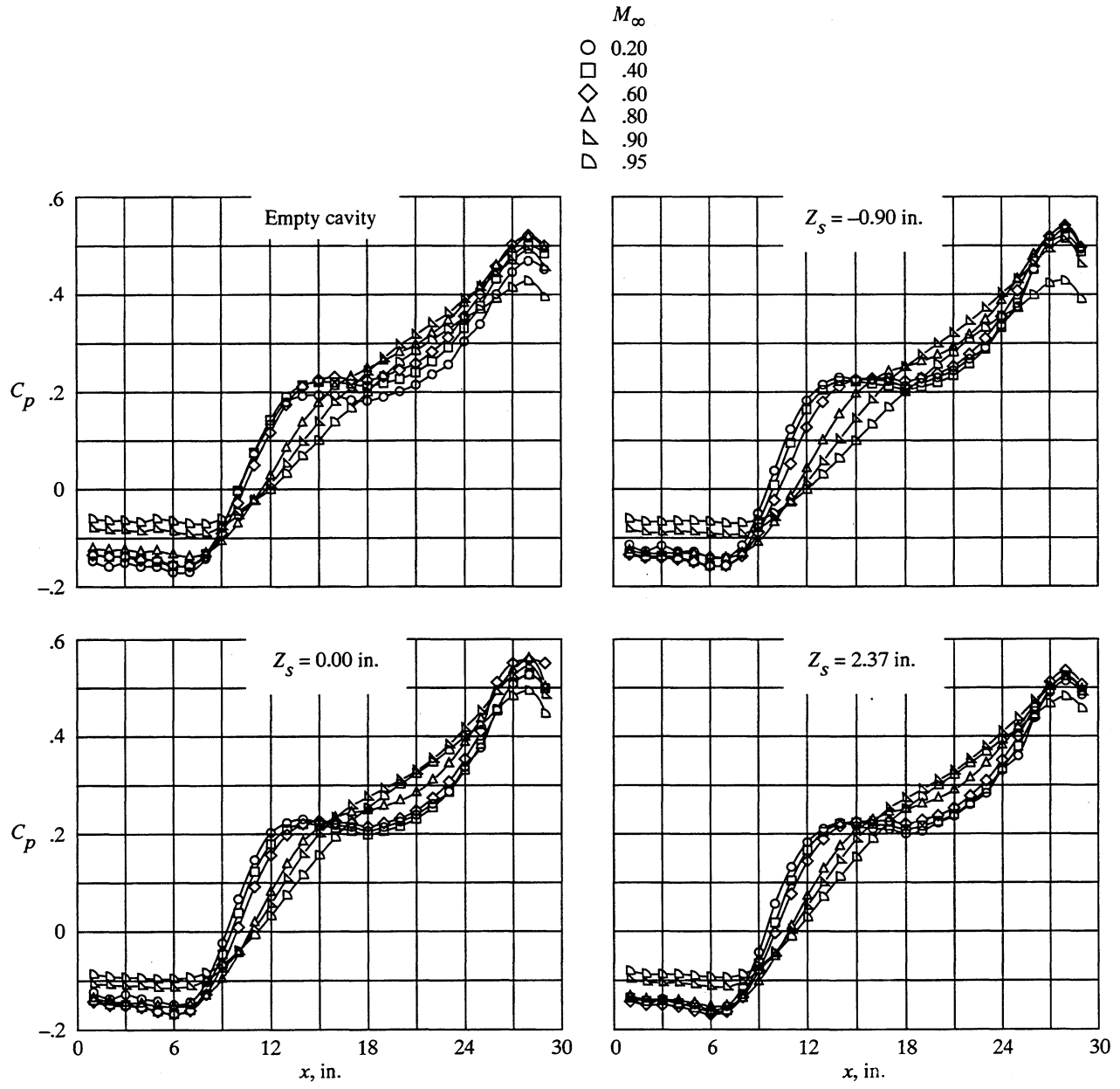
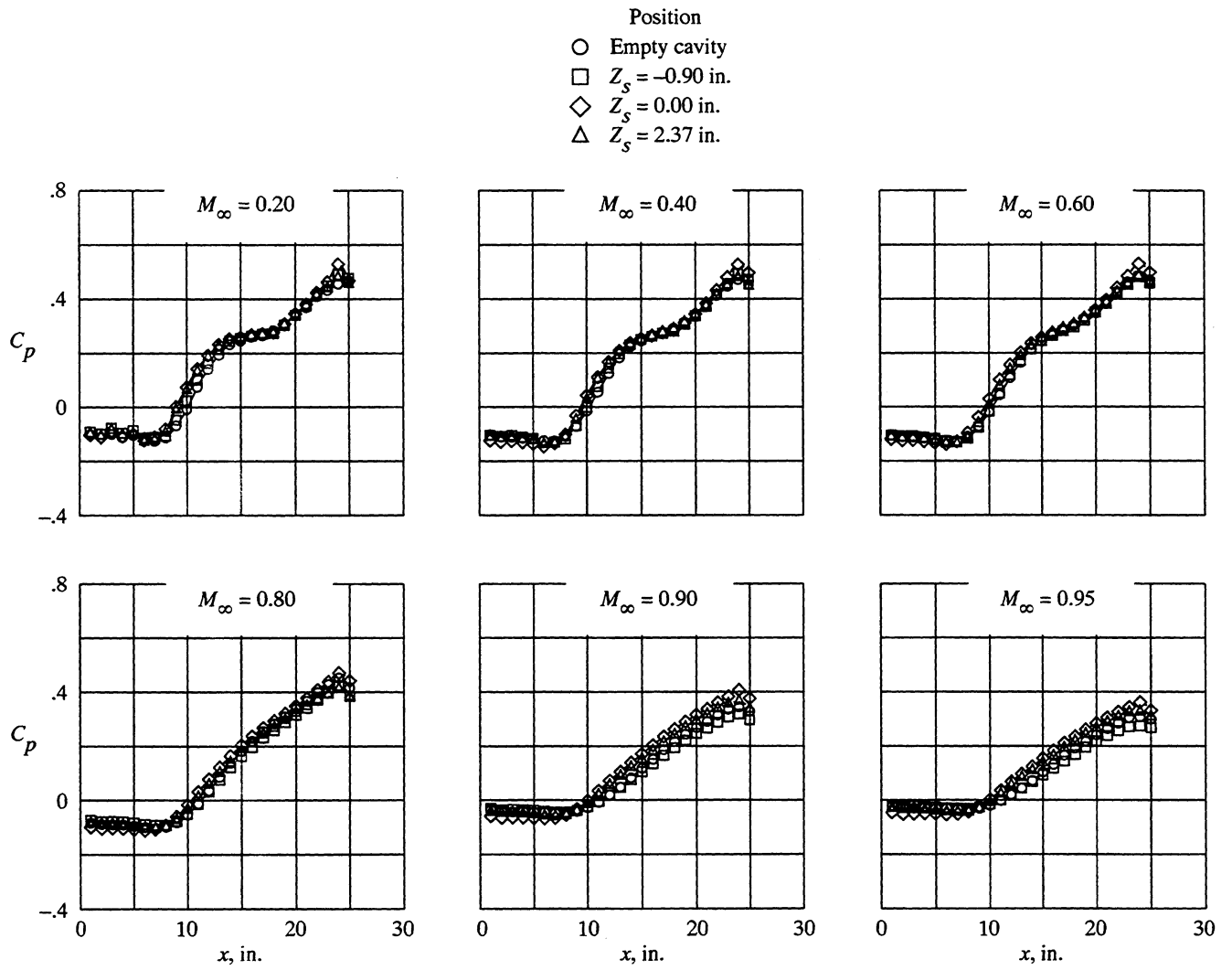


Figure 9. Continued.



(d) $l = 30.00$ in.; $l/h = 12.50$; $Y_s = 2.40$ in.

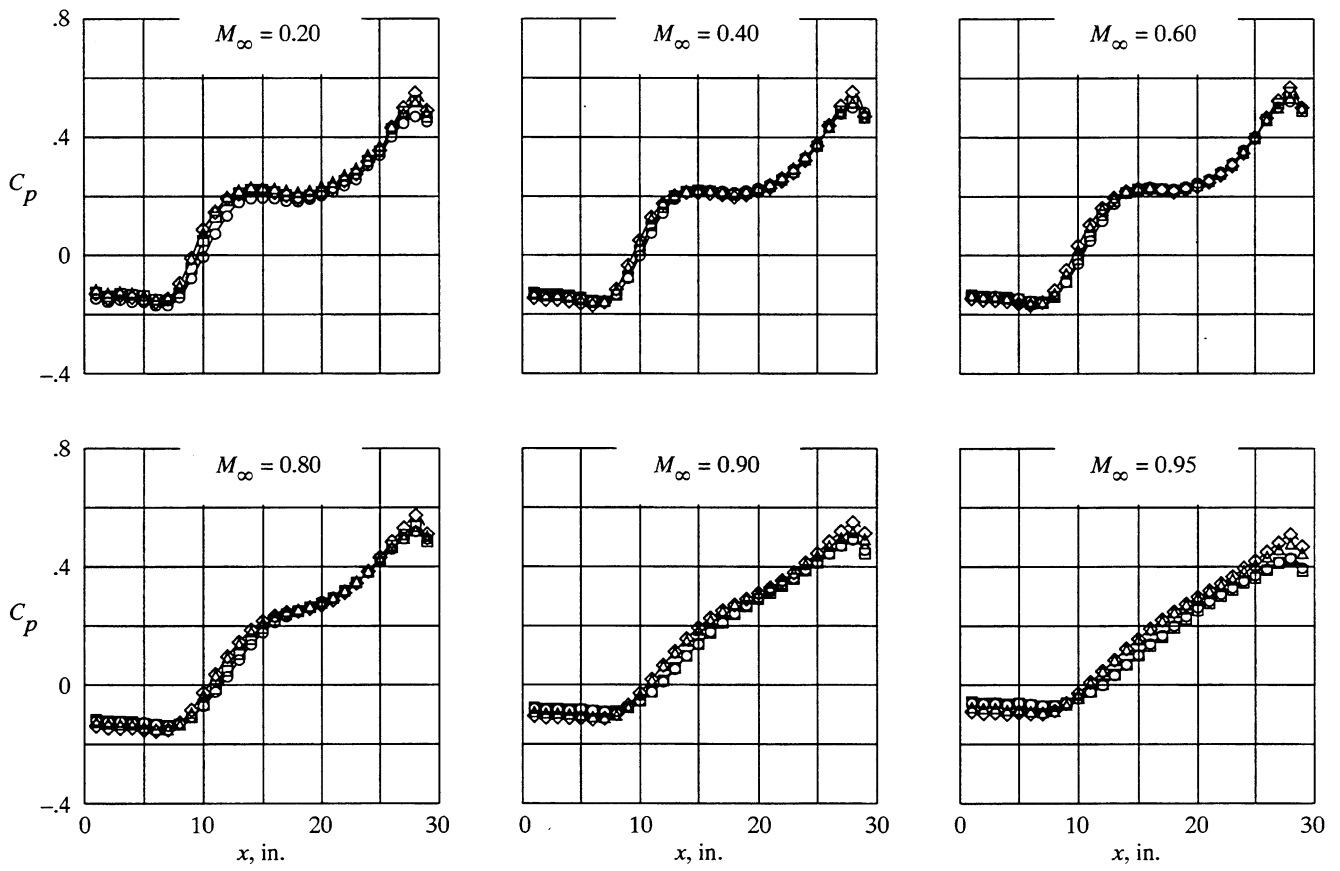
Figure 9. Concluded.



(a) $l = 26.00$ in.; $l/h = 10.83$; $Y_s = 0.00$ in.

Figure 10. Effect of store vertical position on cavity floor pressure distributions. $h = 2.40$ in.

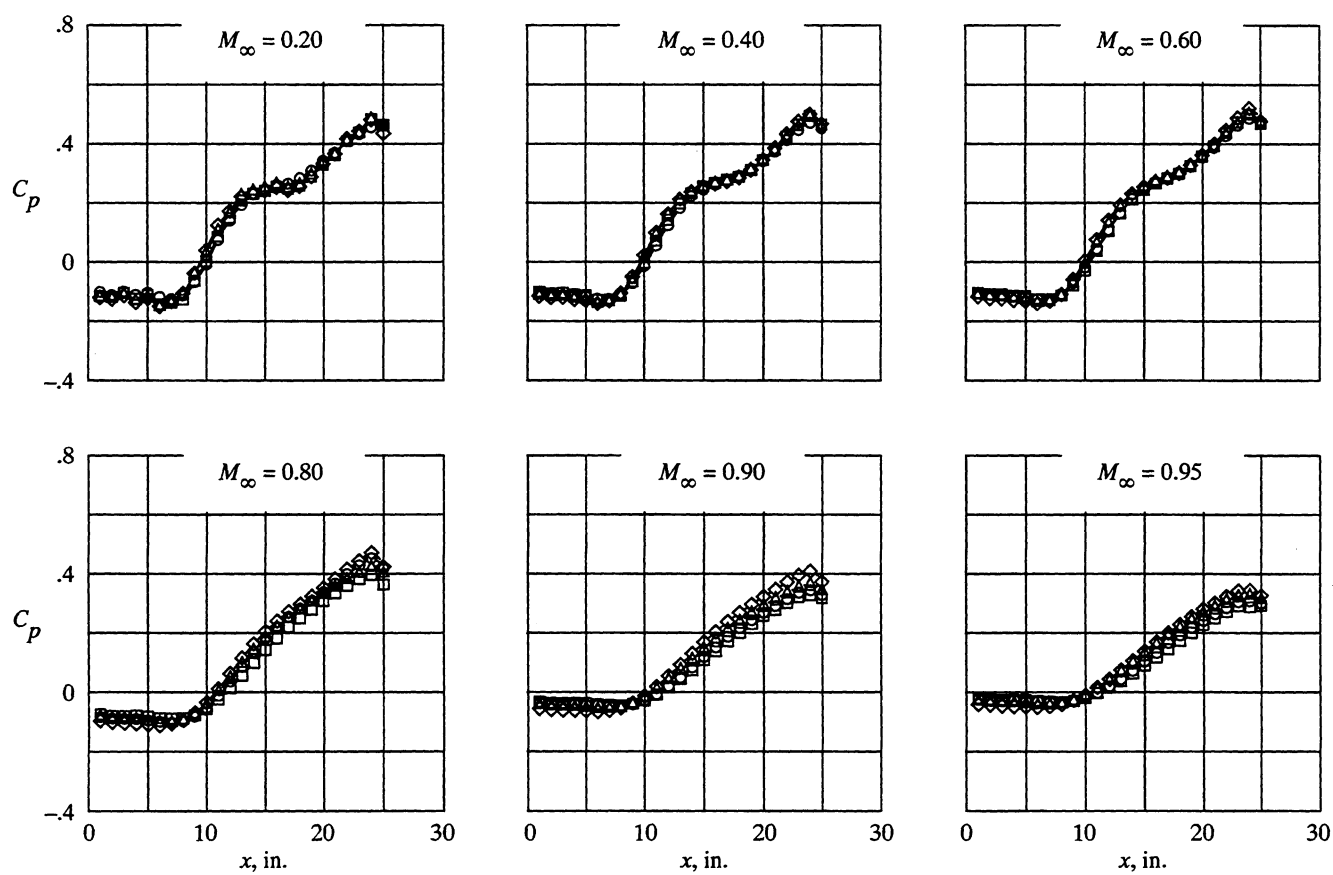
Position
 ○ Empty cavity
 □ $Z_s = -0.90$ in.
 ◇ $Z_s = 0.00$ in.
 △ $Z_s = 2.37$ in.



(b) $l = 30.00$ in.; $l/h = 12.50$; $Y_s = 0.00$ in.

Figure 10. Continued.

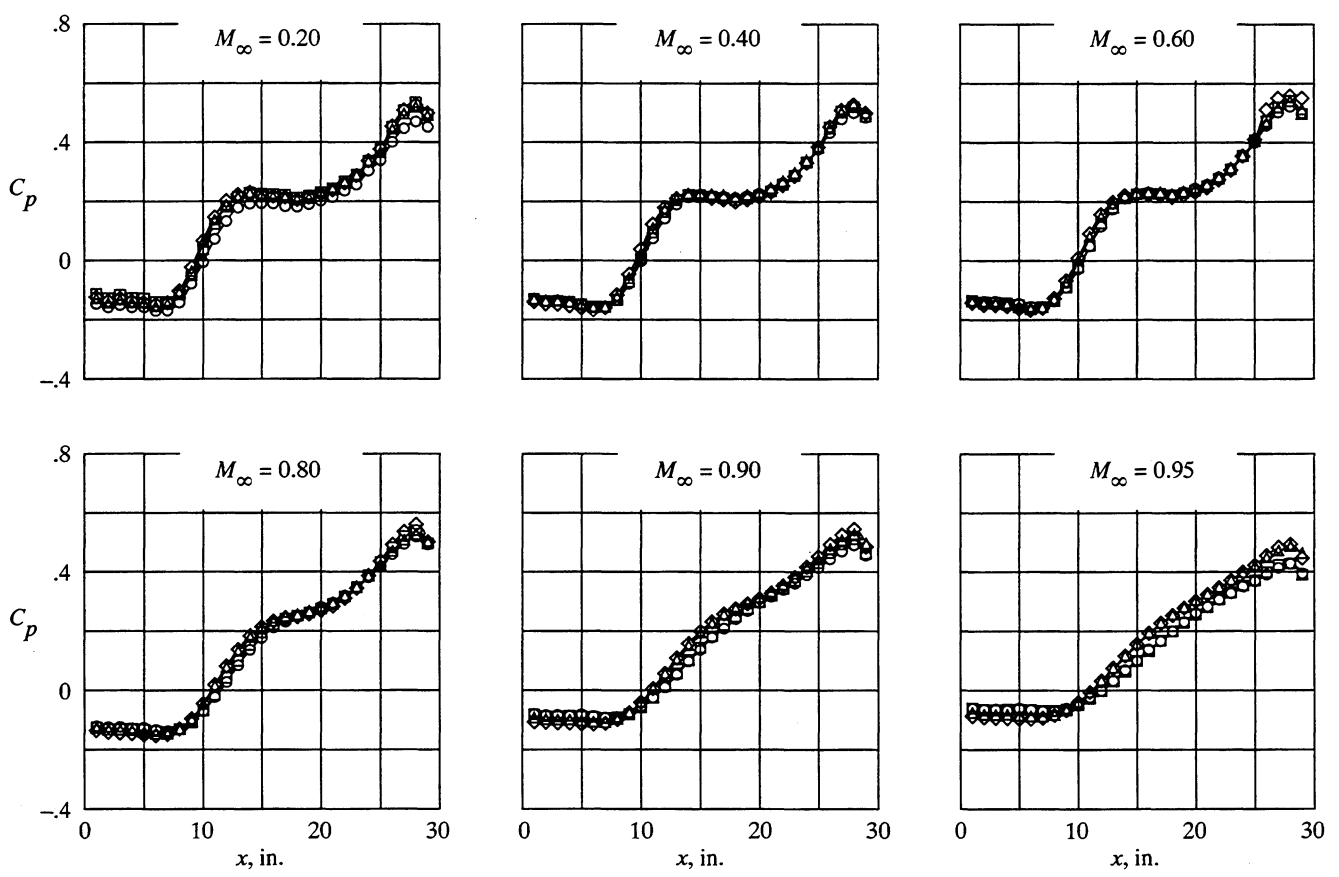
Position
 ○ Empty cavity
 □ $Z_s = -0.90$ in.
 ◇ $Z_s = 0.00$ in.
 △ $Z_s = 2.37$ in.



(c) $l = 26.00$ in.; $l/h = 10.83$; $Y_s = 2.40$ in.

Figure 10. Continued.

Position
 ○ Empty cavity
 □ $Z_s = -0.90$ in.
 ◇ $Z_s = 0.00$ in.
 △ $Z_s = 2.37$ in.



(d) $l = 30.00$ in.; $l/h = 12.50$; $Y_s = 2.40$ in.

Figure 10. Concluded.

	l , in.	l/h
○	26.00	10.83
□	30.00	12.50

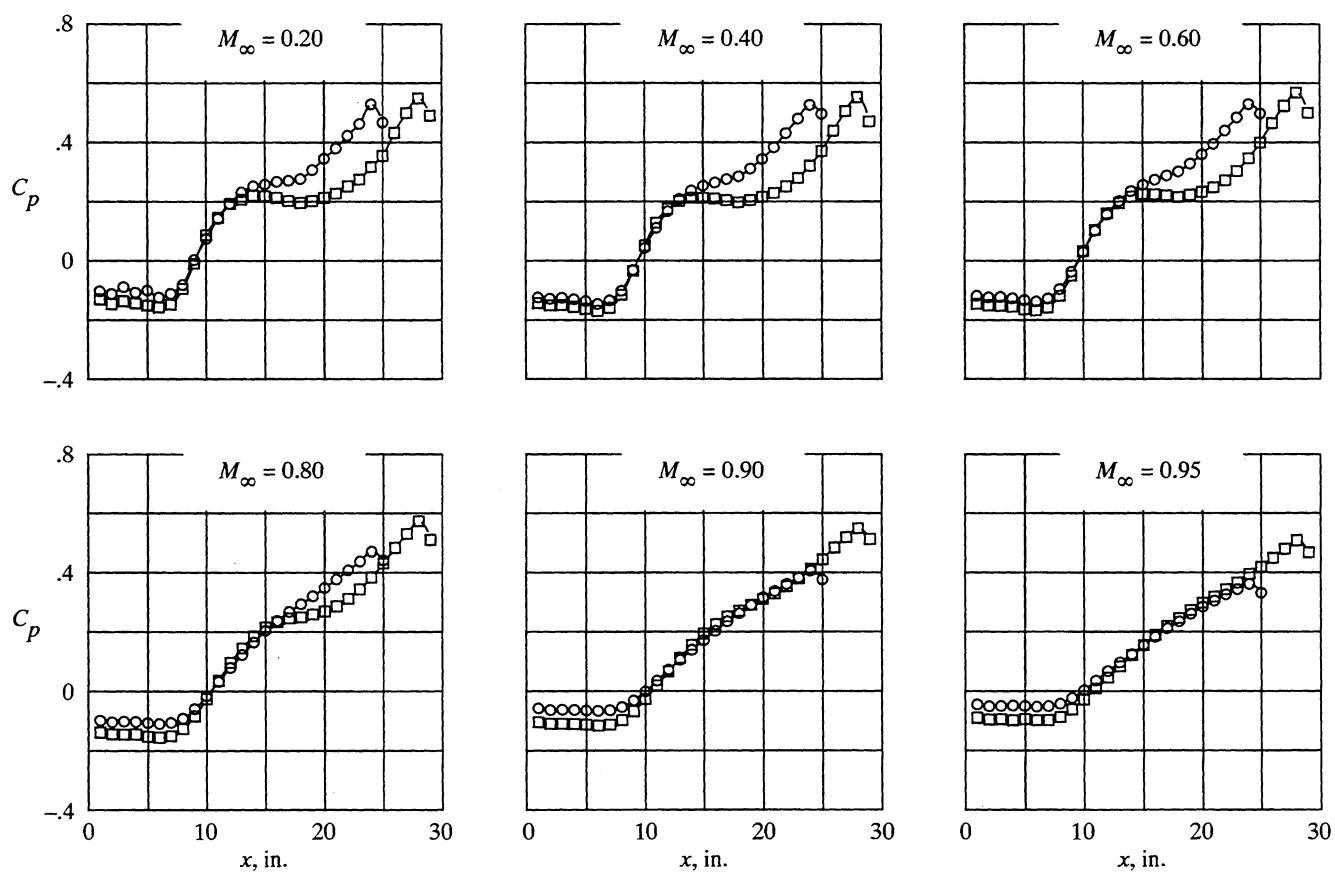
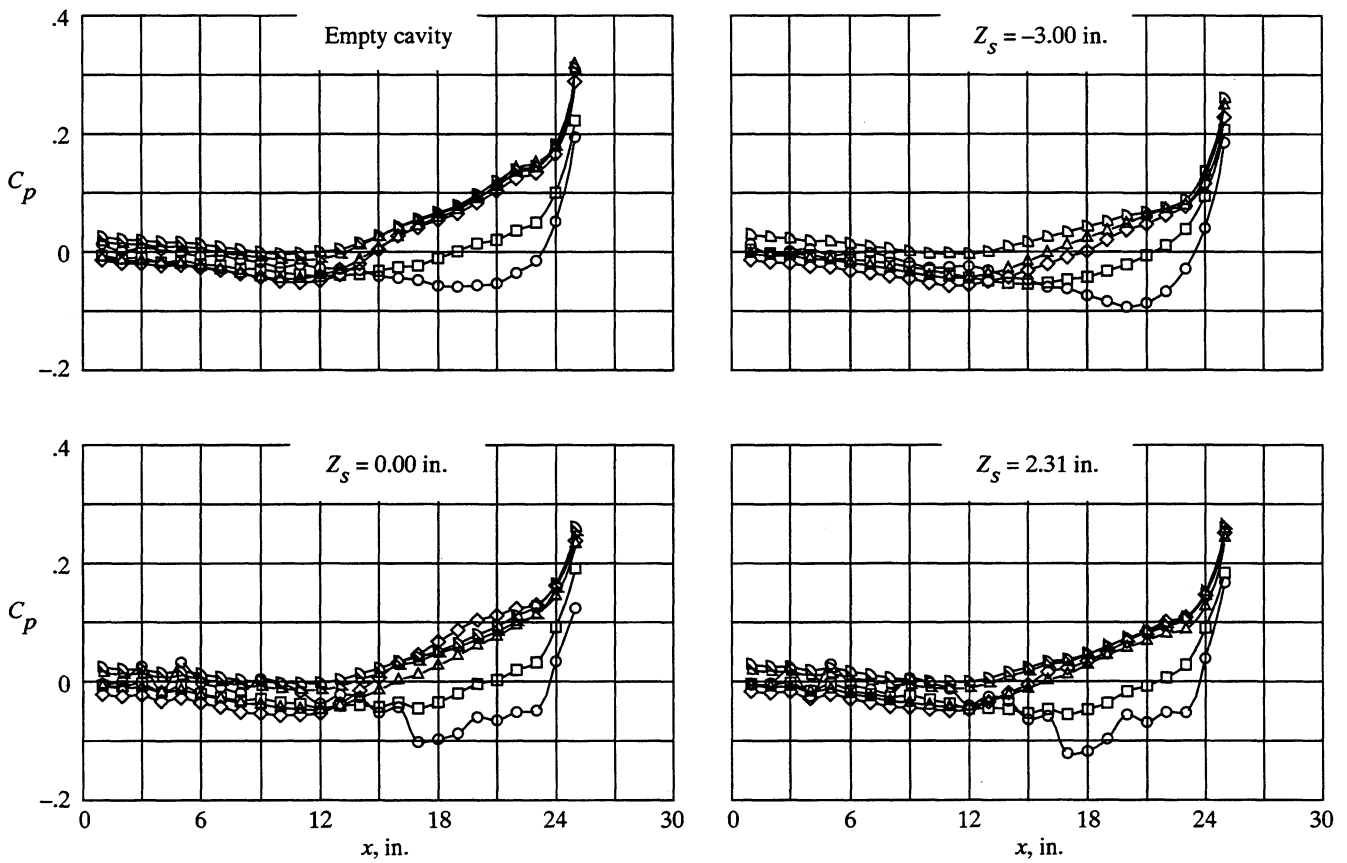


Figure 11. Effect of cavity length on cavity floor pressure distributions. $h = 2.40$ in.; $Z_s = 0.00$ in.; $Y_s = 0.00$ in.

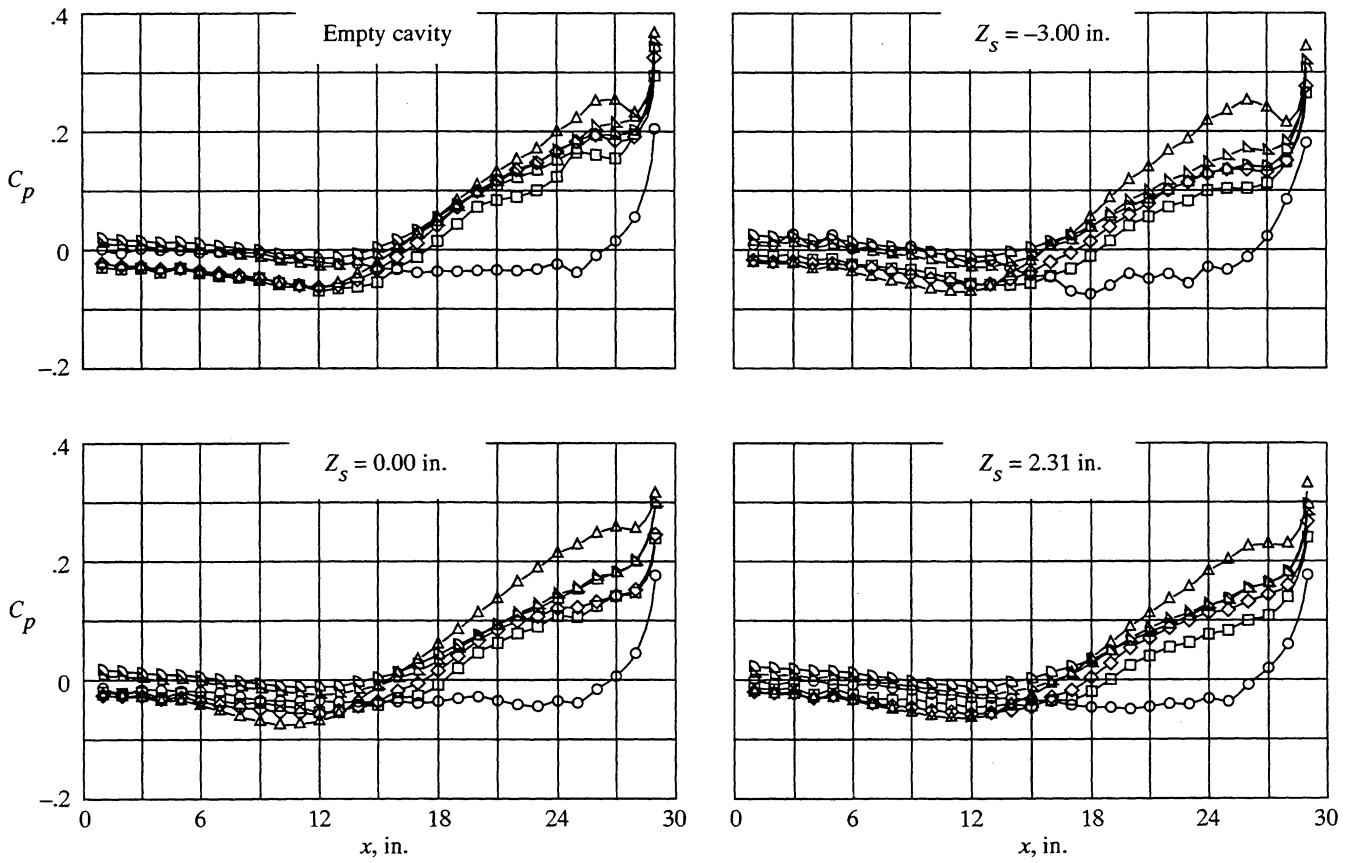
M_∞
 ○ 0.20
 □ .40
 ◇ .60
 △ .80
 ▽ .90
 ▢ .95



(a) $l = 26.00$ in.; $l/h = 5.42$; $Y_s = 0.00$ in.

Figure 12. Effect of Mach number on cavity floor pressure distributions. $h = 4.80$ in.

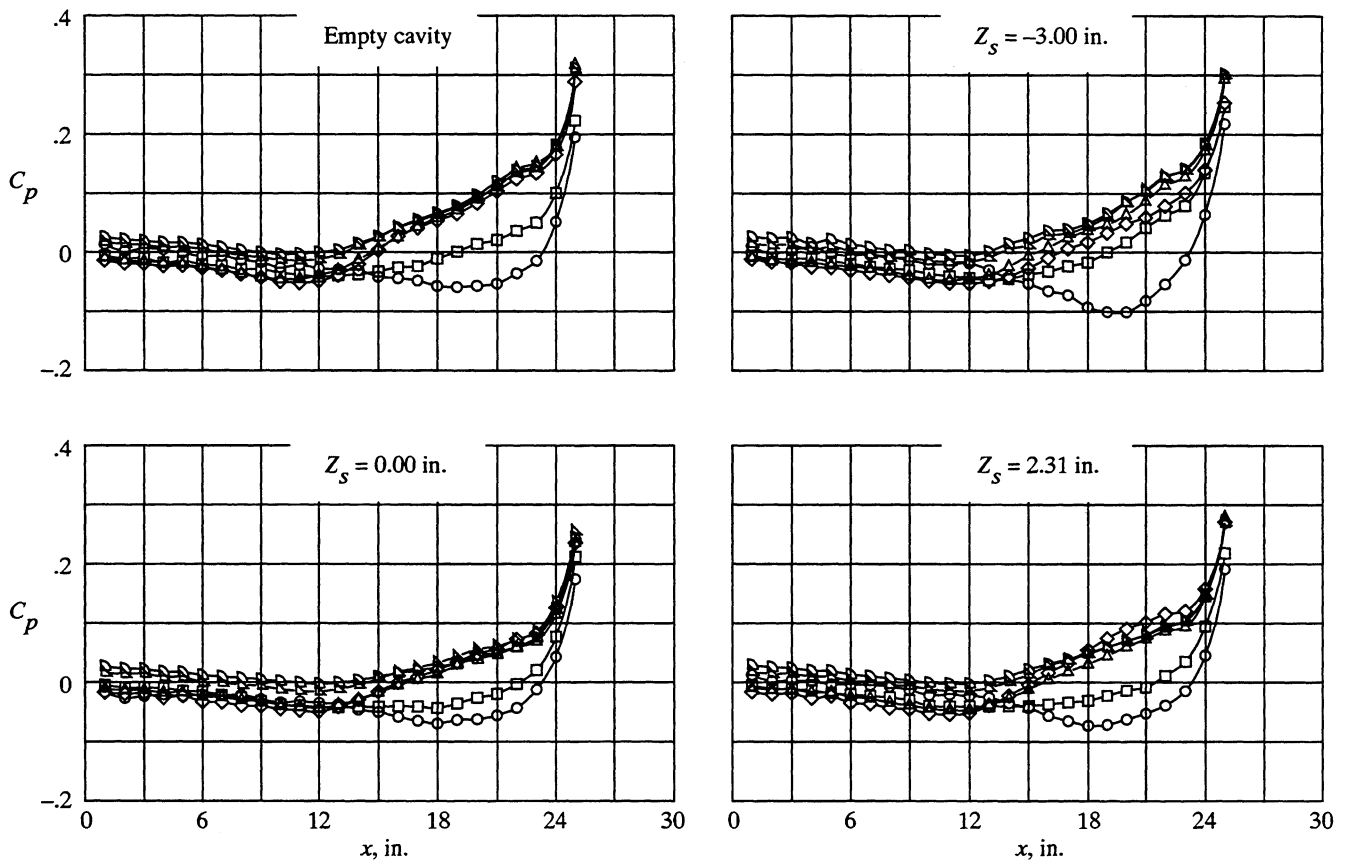
M_∞
 ○ 0.20
 □ .40
 ◇ .60
 △ .80
 ▽ .90
 ▢ .95



(b) $l = 30.00$ in.; $l/h = 6.25$; $Y_s = 0.00$ in.

Figure 12. Continued.

M_∞
 ○ 0.20
 □ .40
 ◇ .60
 △ .80
 ▽ .90
 ▢ .95



(c) $l = 26.00$ in.; $l/h = 5.42$; $Y_s = 2.40$ in.

Figure 12. Continued.

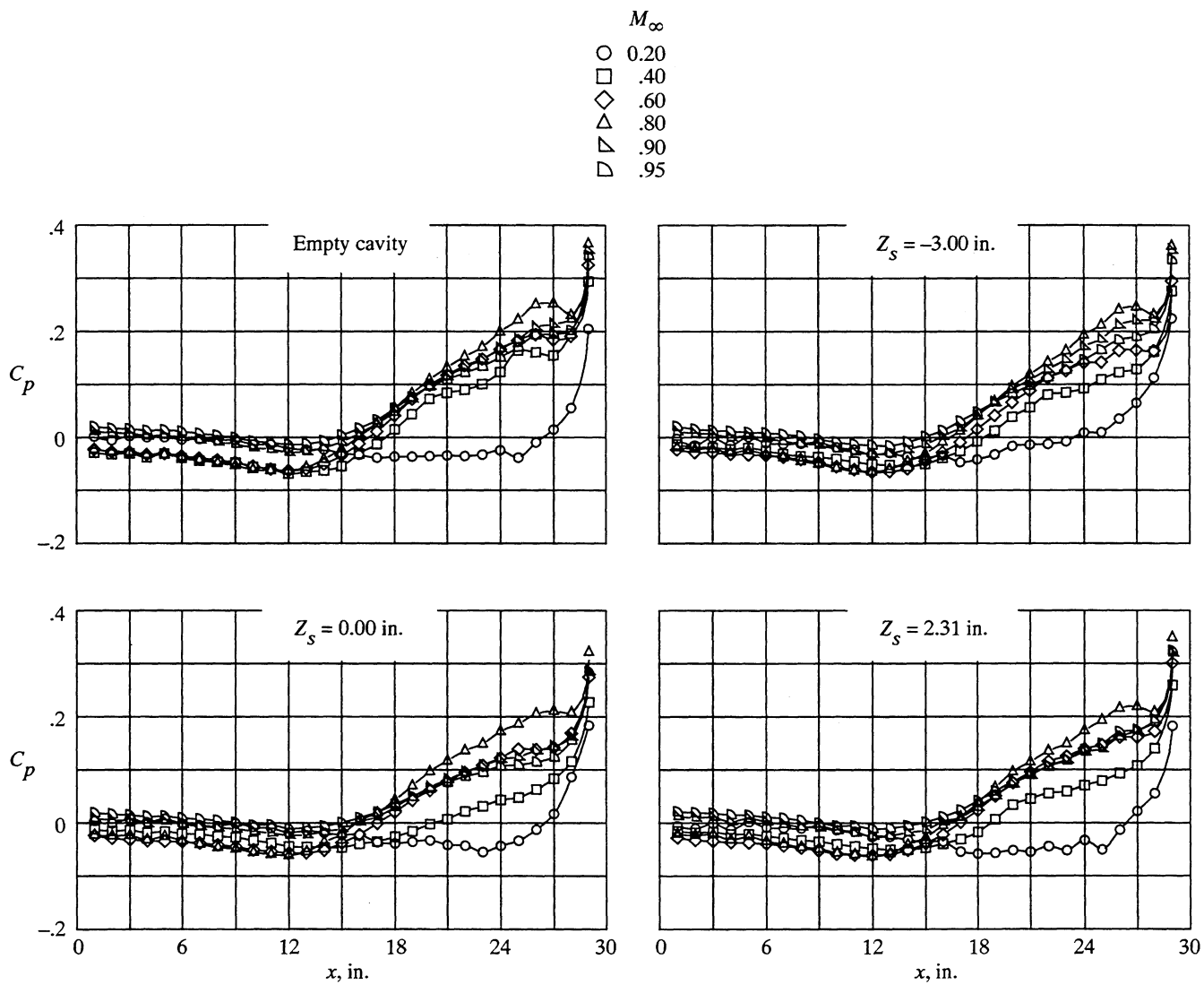
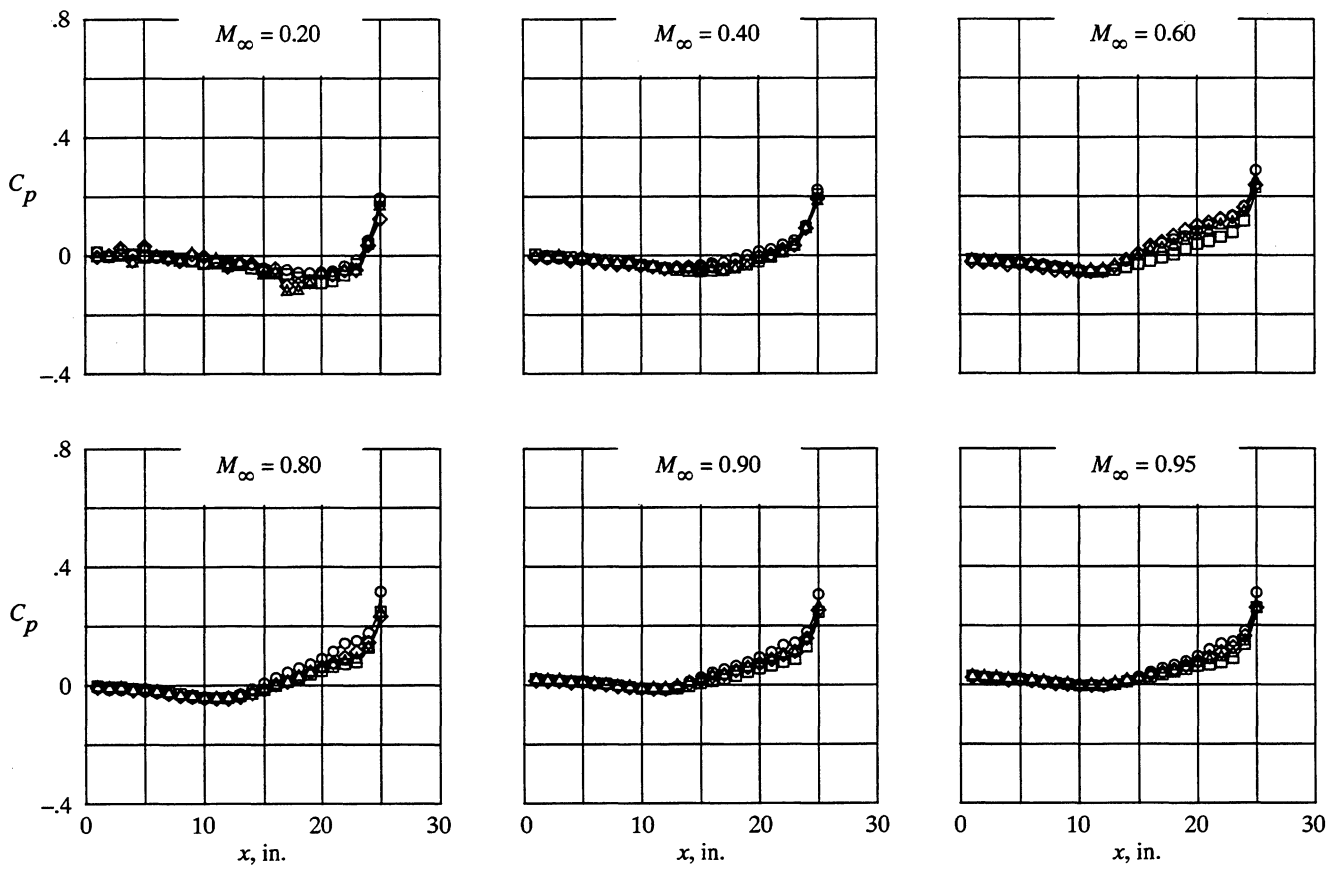


Figure 12. Concluded.

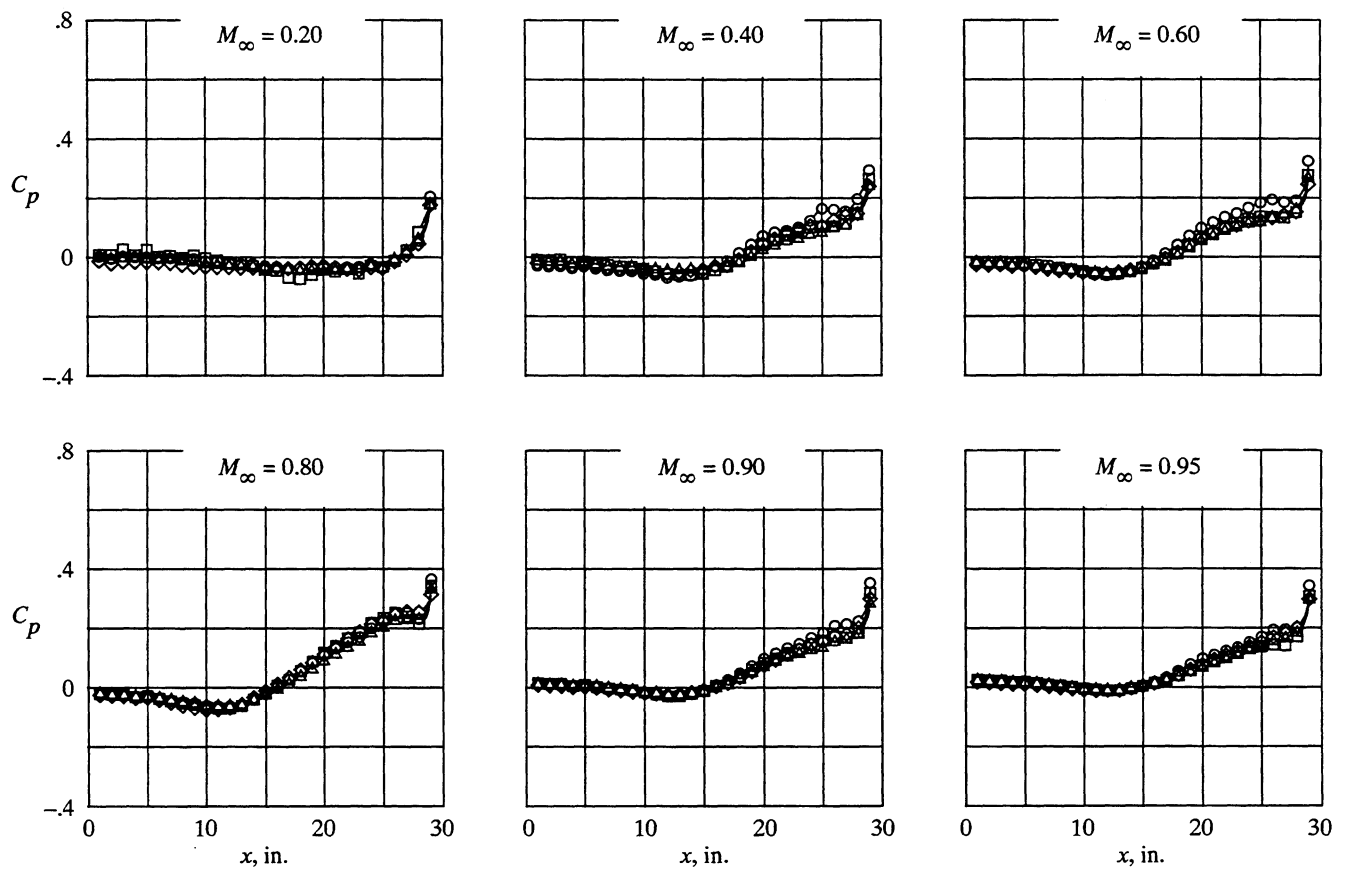
Position
 ○ Empty cavity
 □ $Z_s = -3.00$ in.
 ◇ $Z_s = 0.00$ in.
 △ $Z_s = 2.31$ in.



(a) $l = 26.00$ in.; $l/h = 5.42$; $Y_s = 0.00$ in.

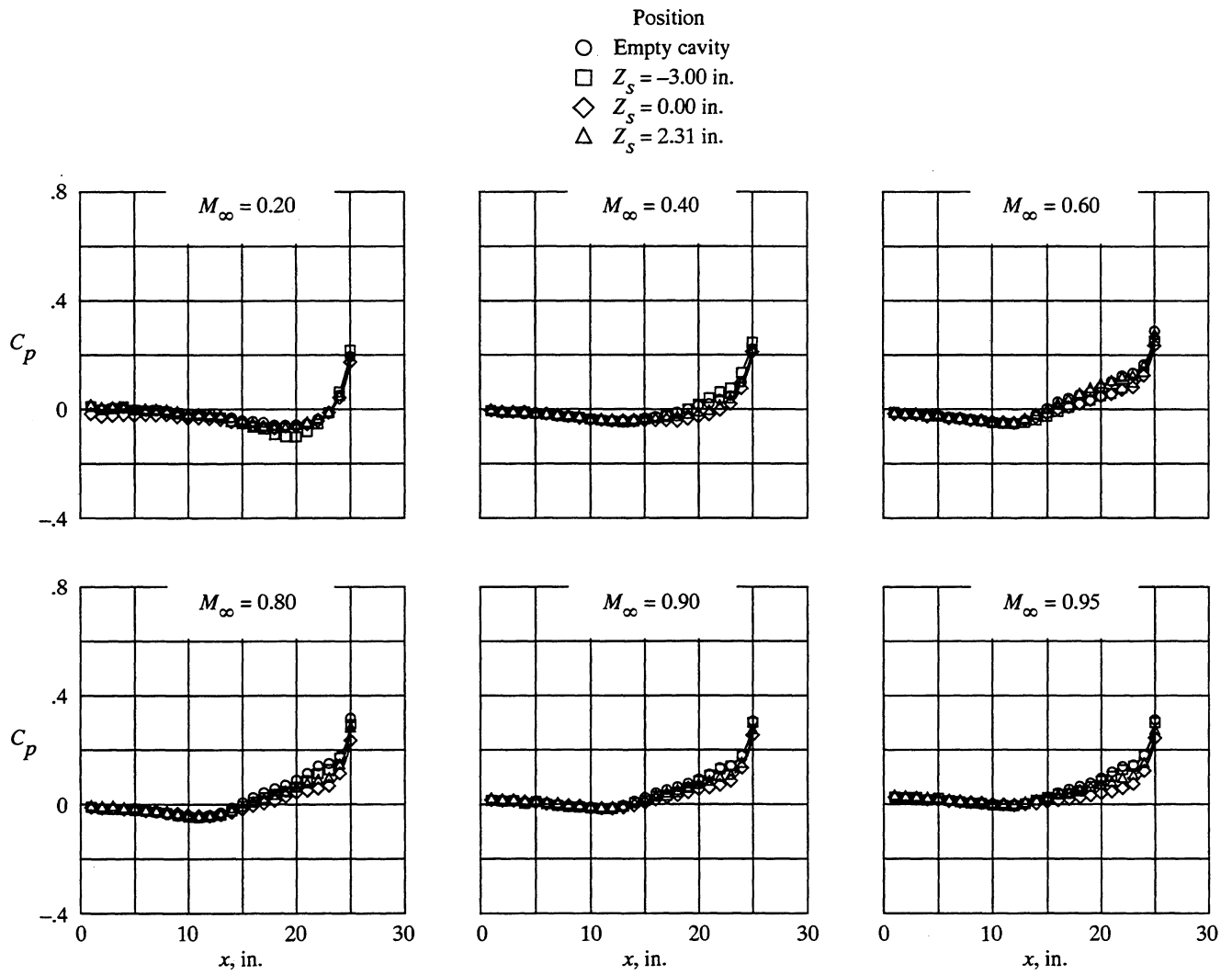
Figure 13. Effect of store vertical position on cavity floor pressure distributions. $h = 4.80$ in.

Position
 ○ Empty cavity
 □ $Z_s = -3.00$ in.
 ◇ $Z_s = 0.00$ in.
 △ $Z_s = 2.31$ in.



(b) $l = 30.00$ in.; $l/h = 6.25$; $Y_s = 0.00$ in.

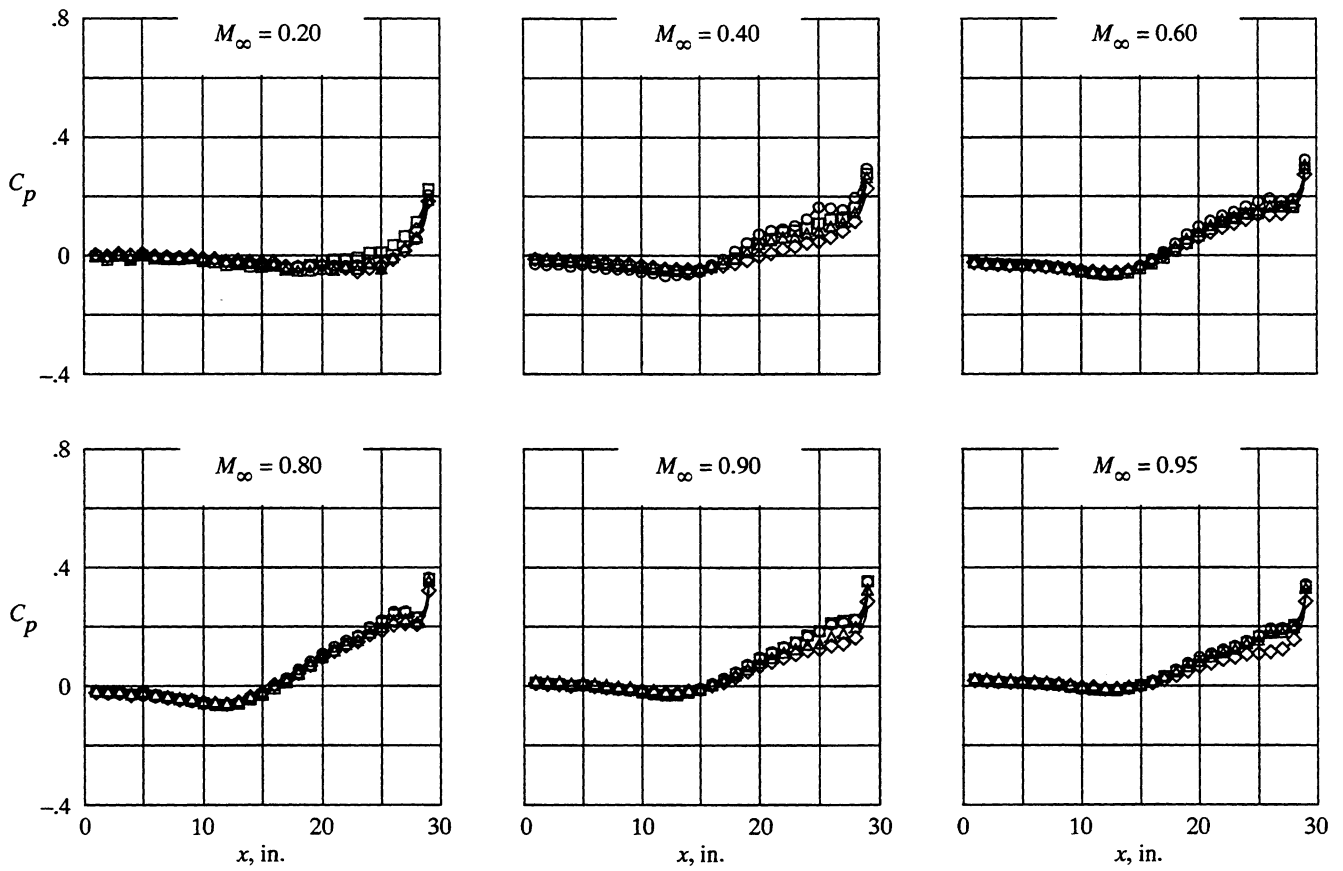
Figure 13. Continued.



(c) $l = 26.00$ in.; $l/h = 5.42$; $Y_s = 2.40$ in.

Figure 13. Continued.

Position
 ○ Empty cavity
 □ $Z_s = -3.00$ in.
 ◇ $Z_s = 0.00$ in.
 △ $Z_s = 2.31$ in.



(d) $l = 30.00$ in.; $l/h = 6.25$; $Y_s = 2.40$ in.

Figure 13. Concluded.

	l , in.	l/h
○	26.00	5.42
□	30.00	6.25

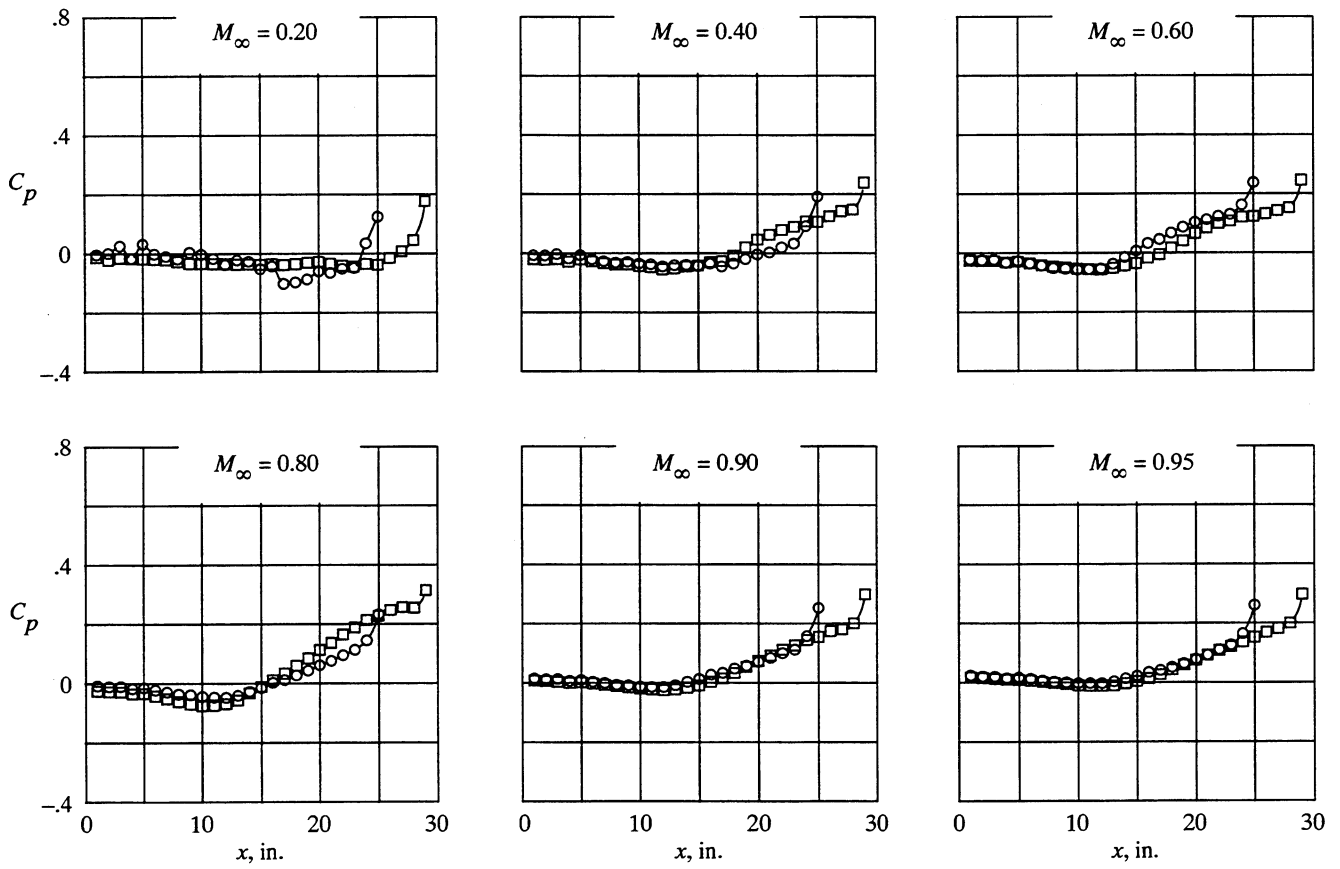


Figure 14. Effect of cavity length on cavity floor pressure distributions. $h = 4.80$ in.; $Z_s = 0.00$ in.; $Y_s = 0.00$ in.

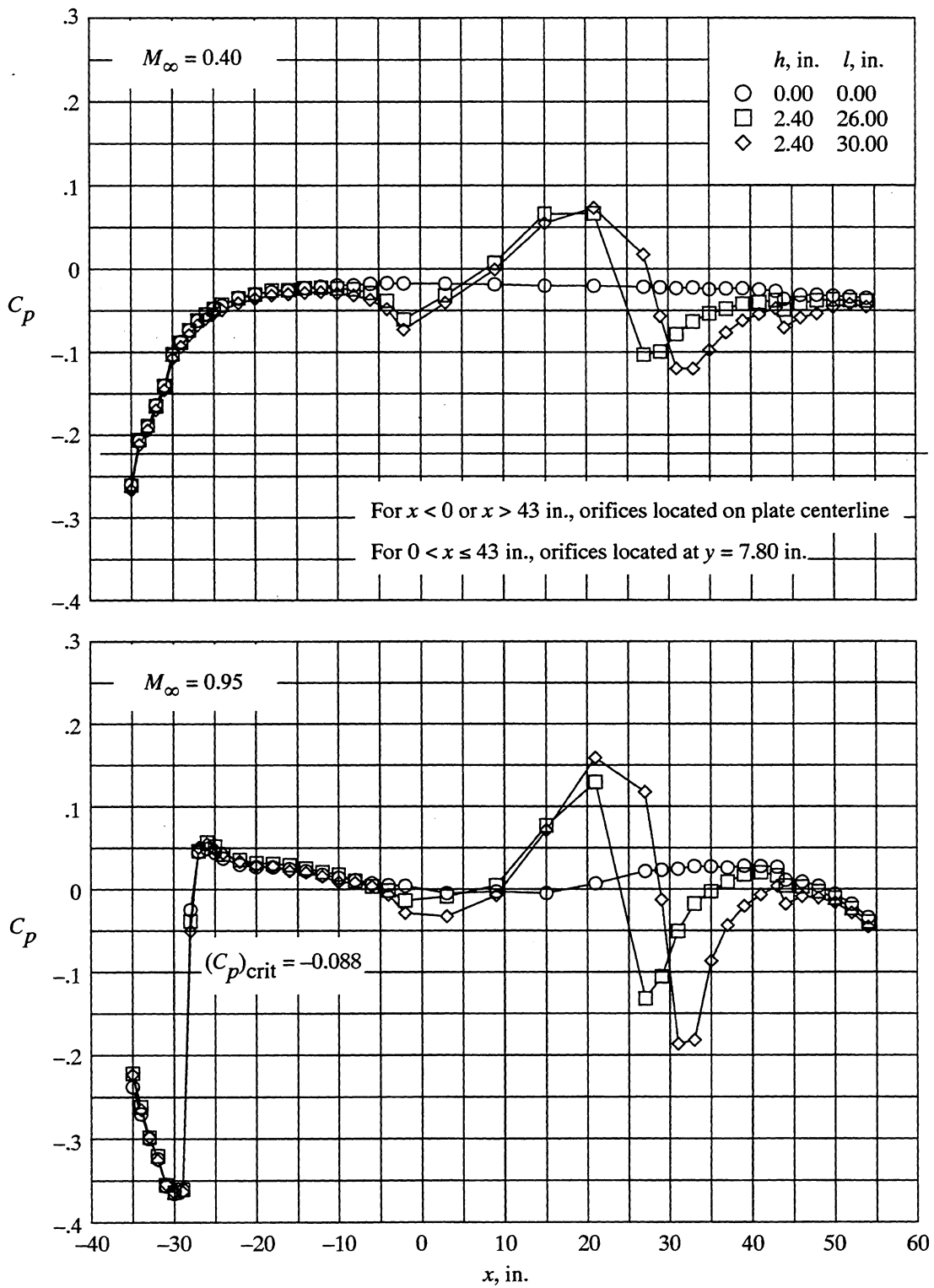
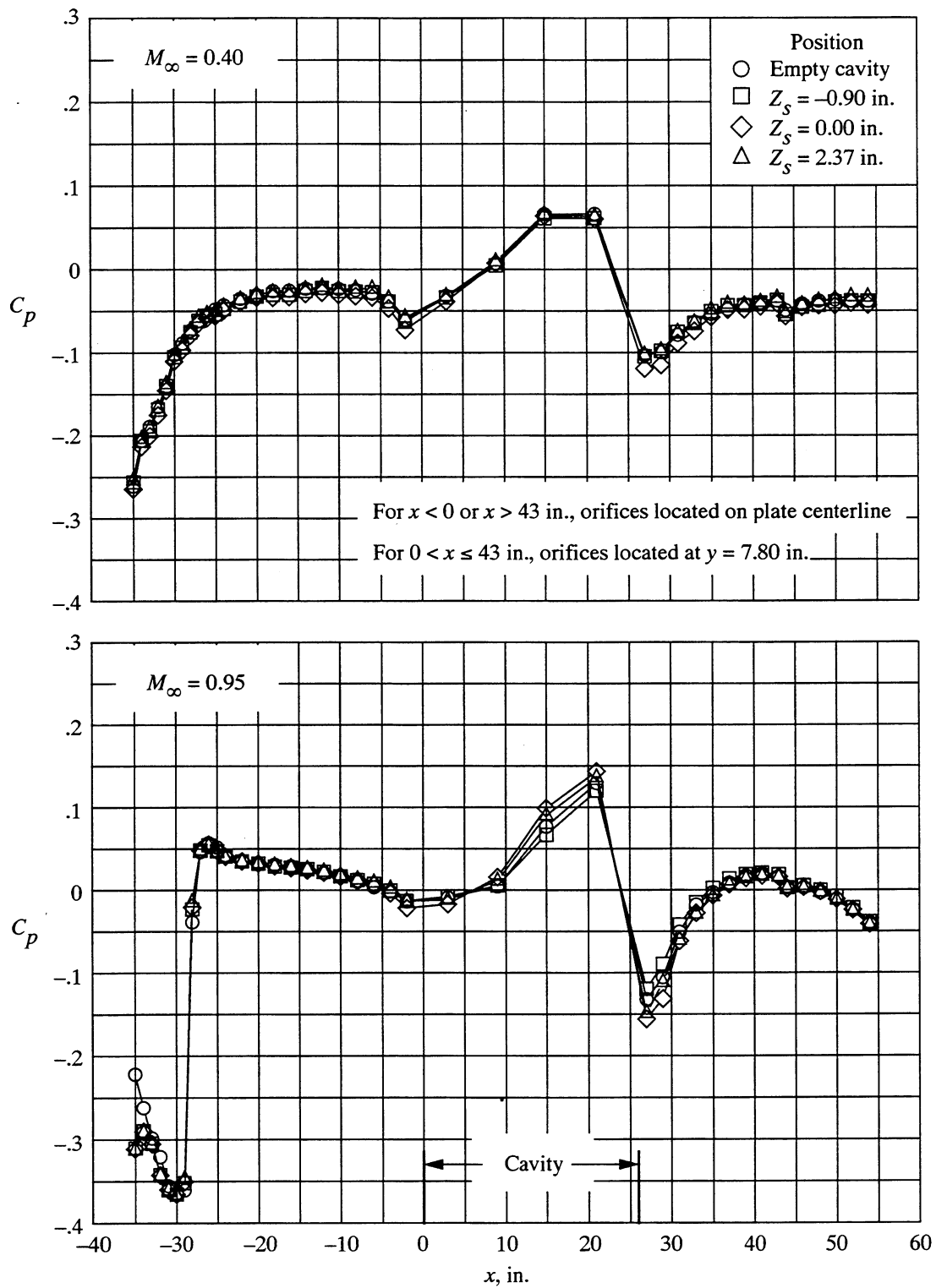
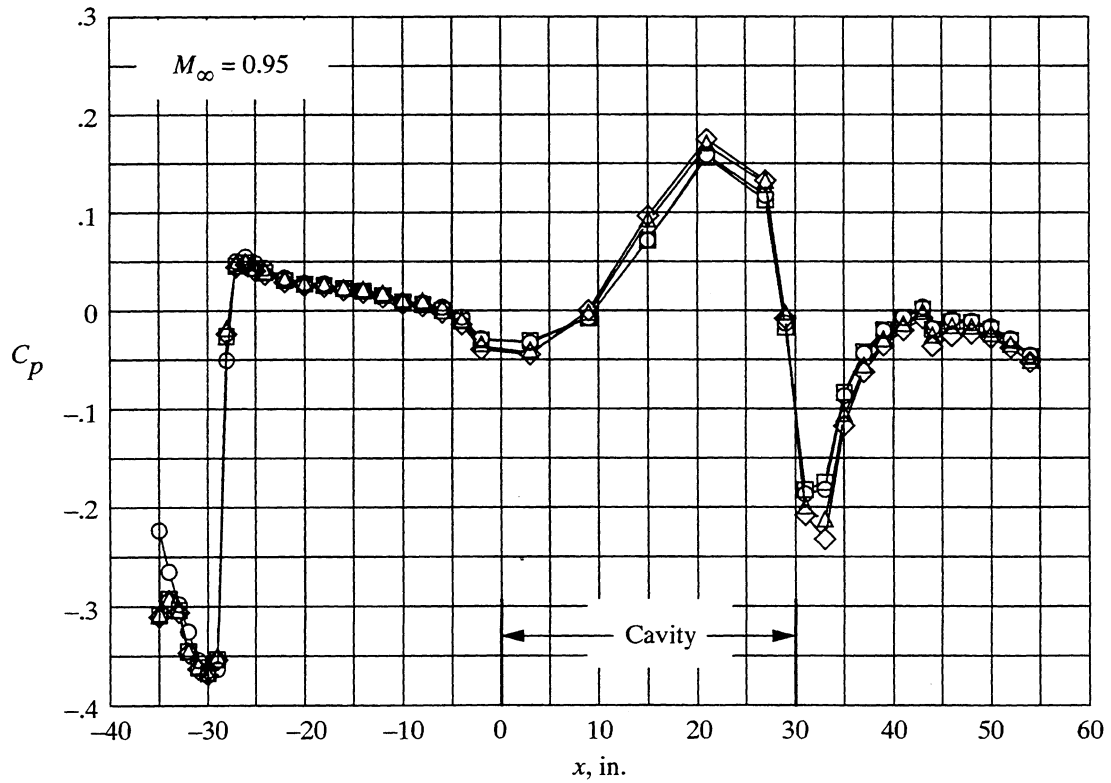
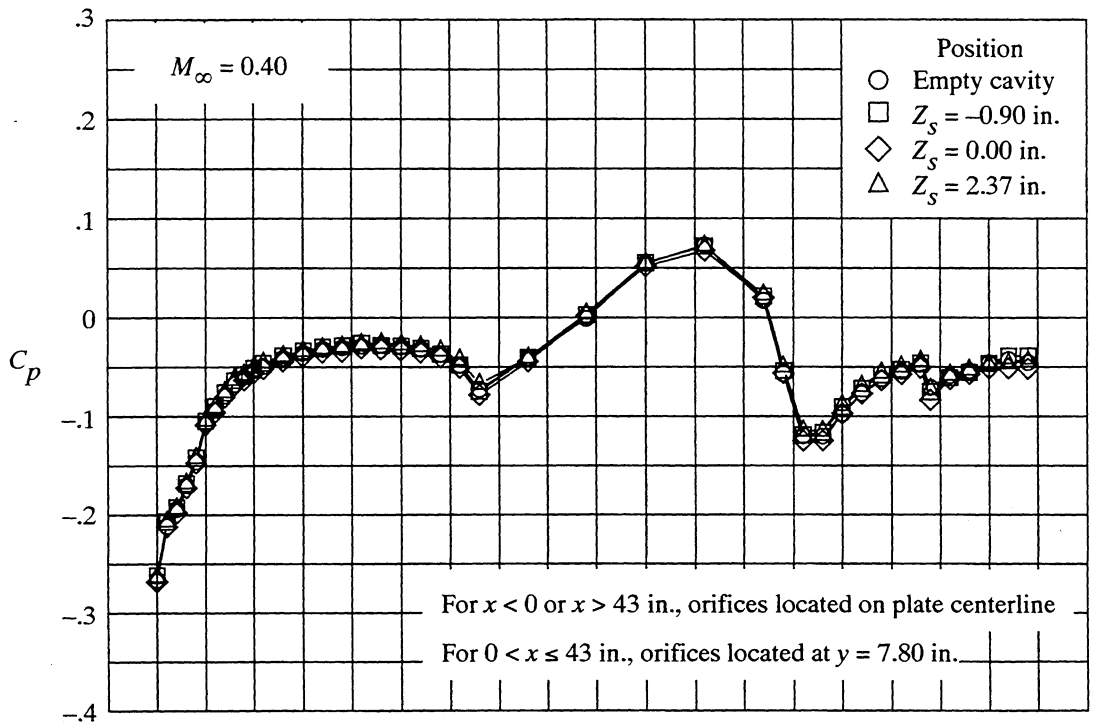


Figure 15. Effect of empty shallow cavities on flat-plate pressure distributions.



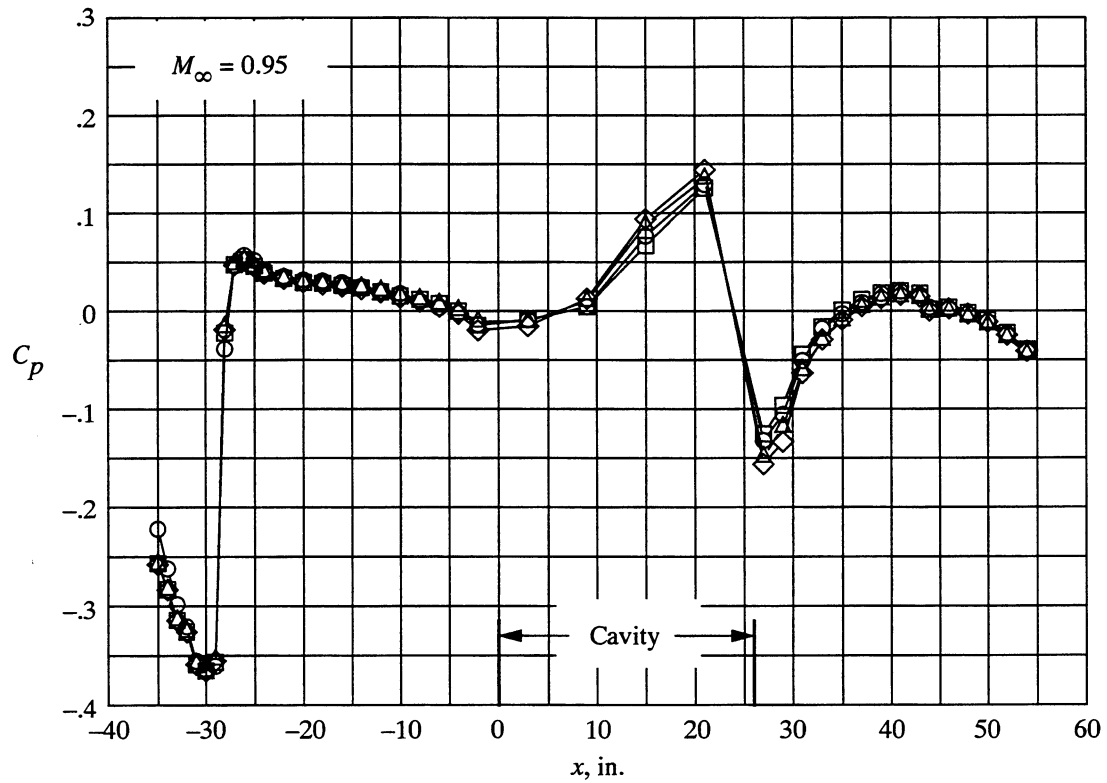
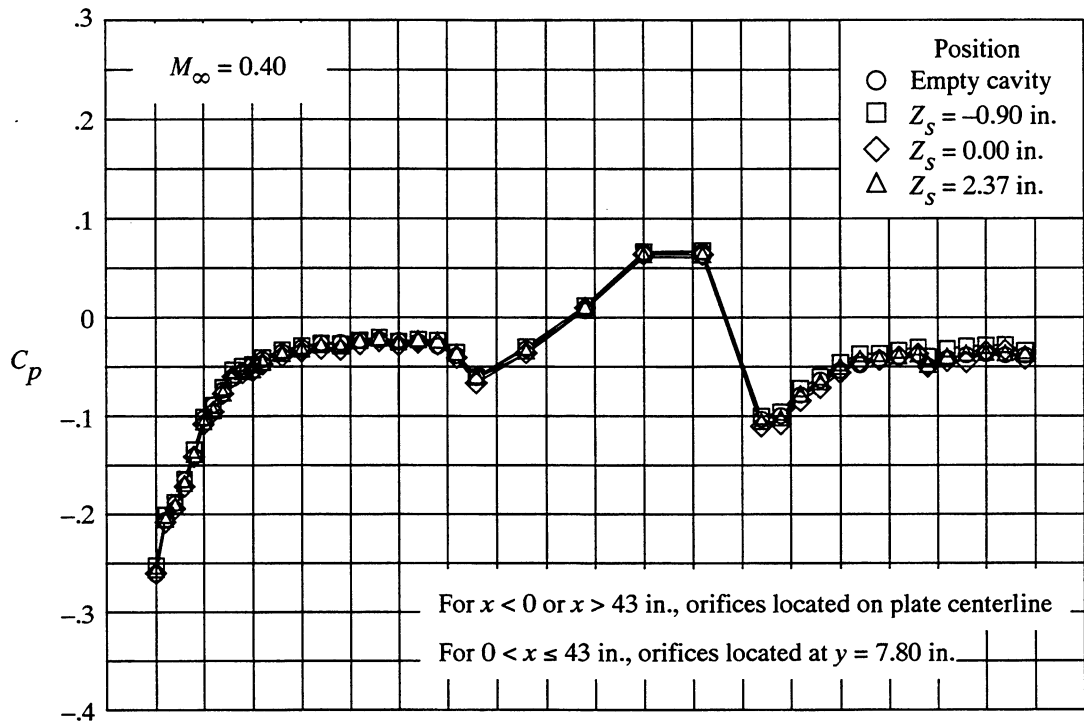
(a) $l = 26.00$ in.; $l/h = 10.83$; $Y_s = 0.00$ in.

Figure 16. Effect of store vertical position on flat-plate pressure distributions. $h = 2.40$ in.



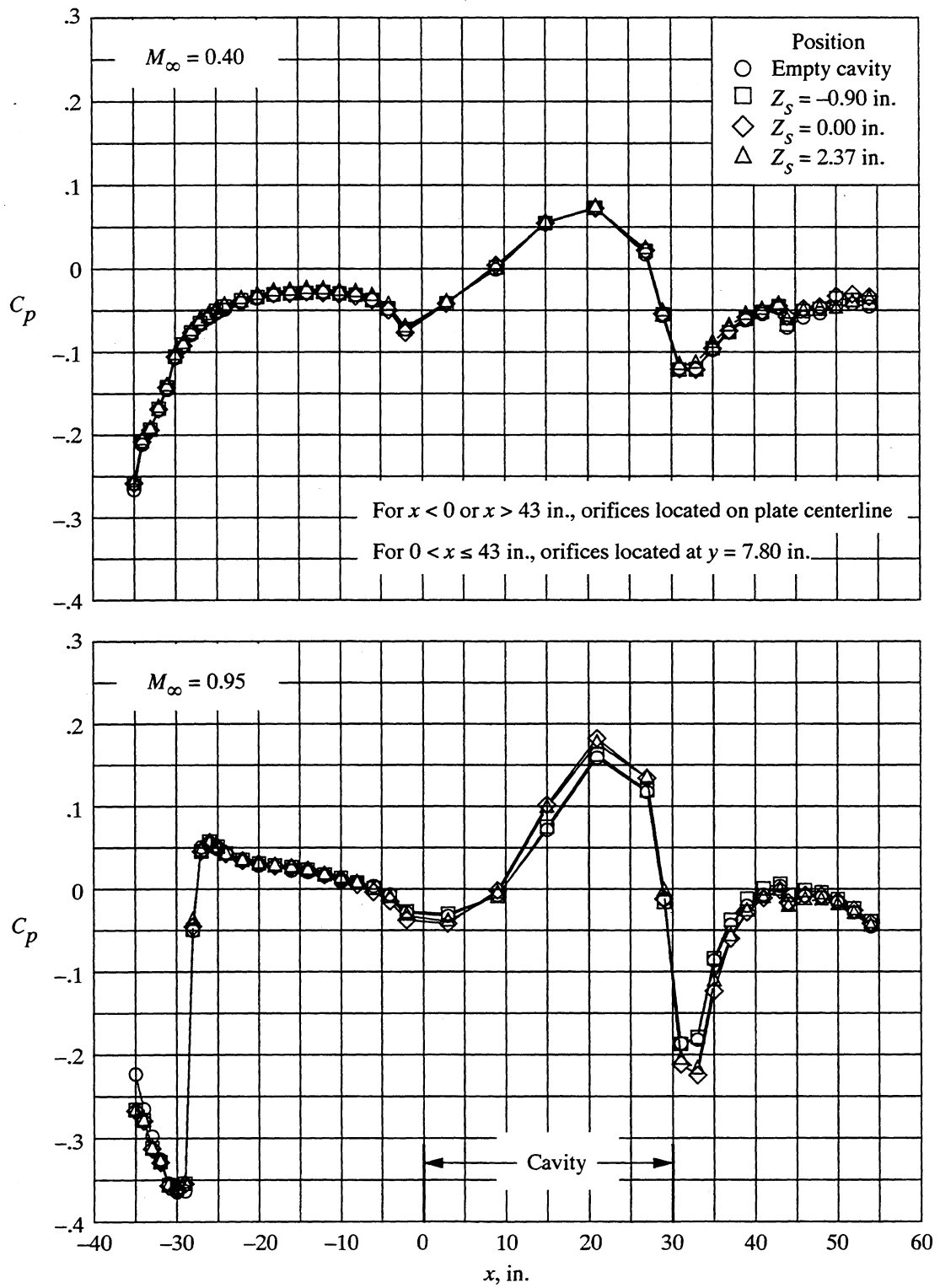
(b) $l = 30.00$ in.; $l/h = 12.50$; $Y_s = 0.00$ in.

Figure 16. Continued.



(c) $l = 26.00$ in.; $l/h = 10.83$; $Y_s = 2.40$ in.

Figure 16. Continued.



(d) $l = 30.00$ in.; $l/h = 12.50$; $Y_s = 2.40$ in.

Figure 16. Concluded.

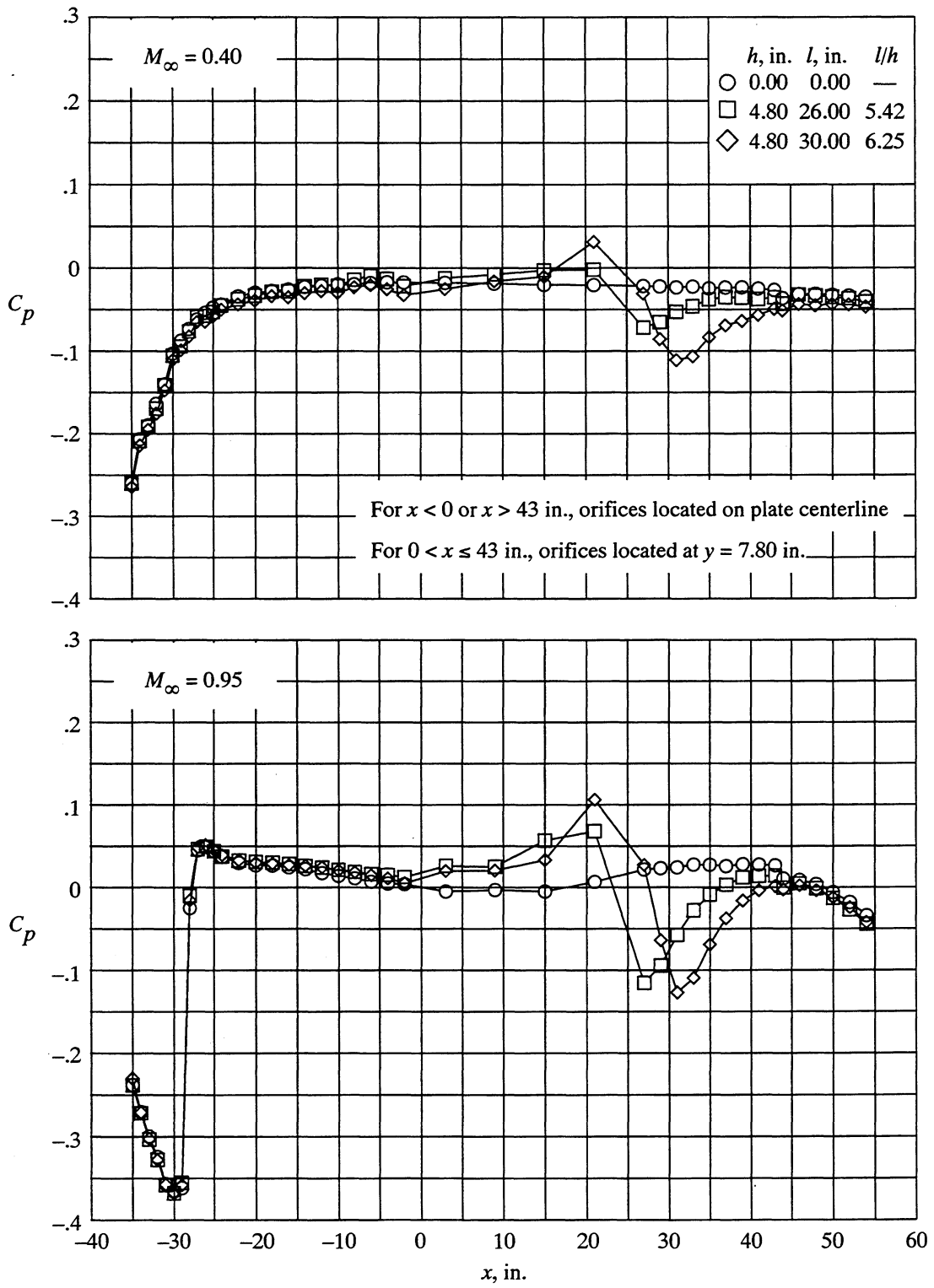
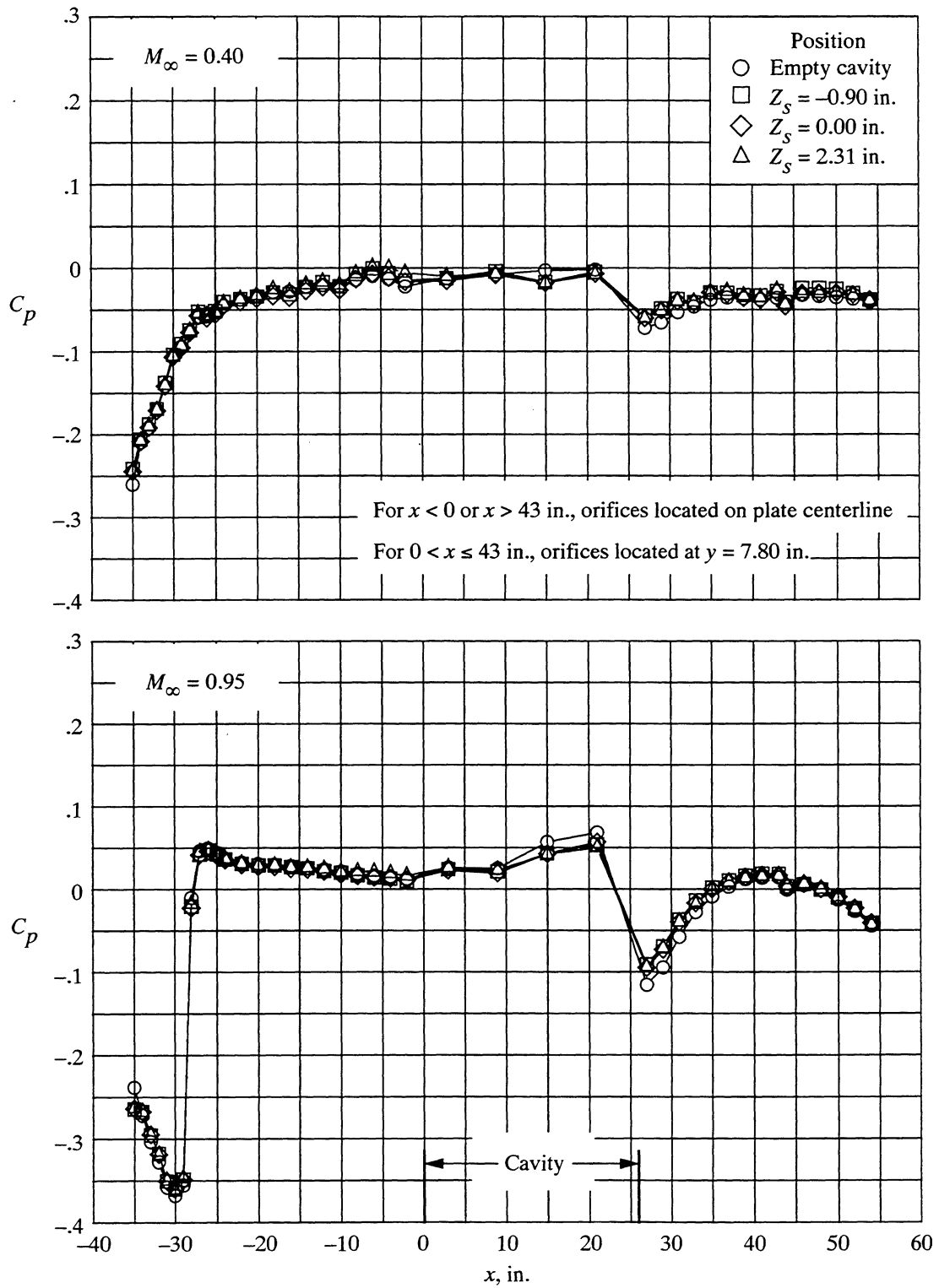
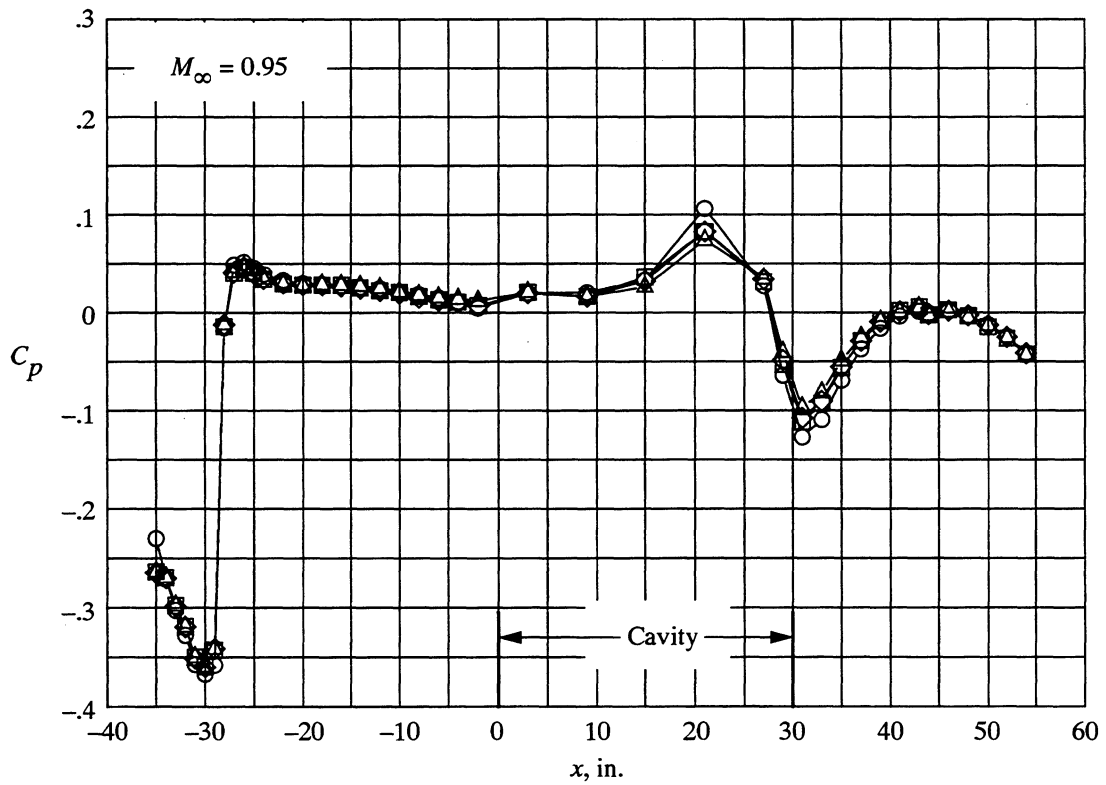
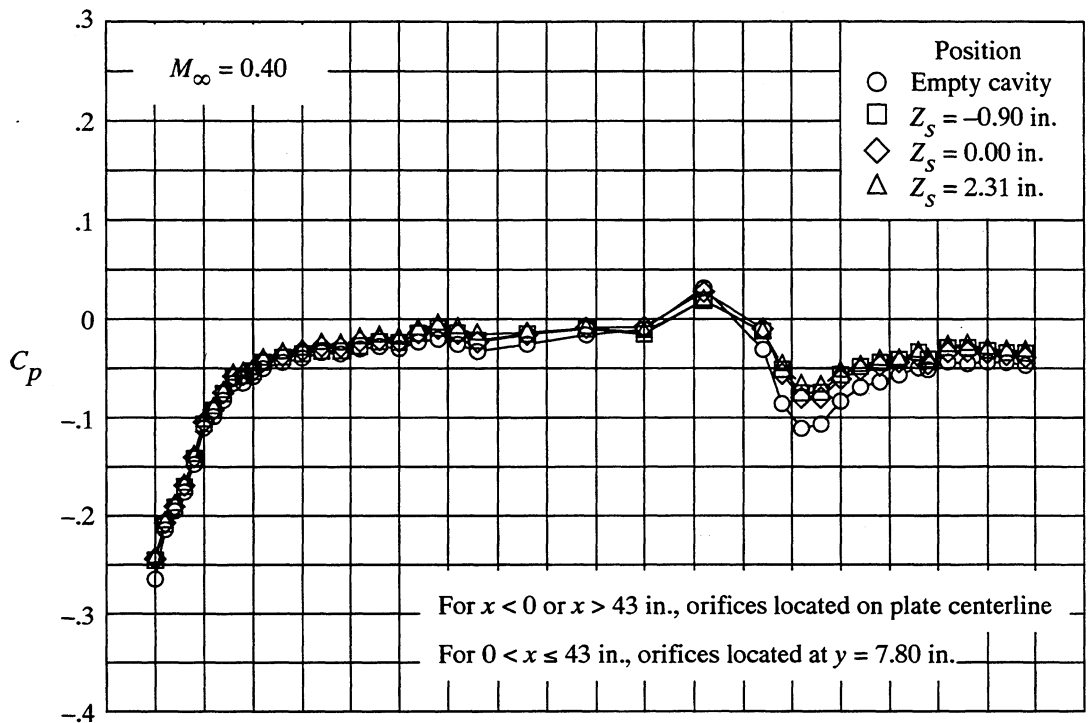


Figure 17. Effect of empty deep cavities on flat-plate pressure distributions.



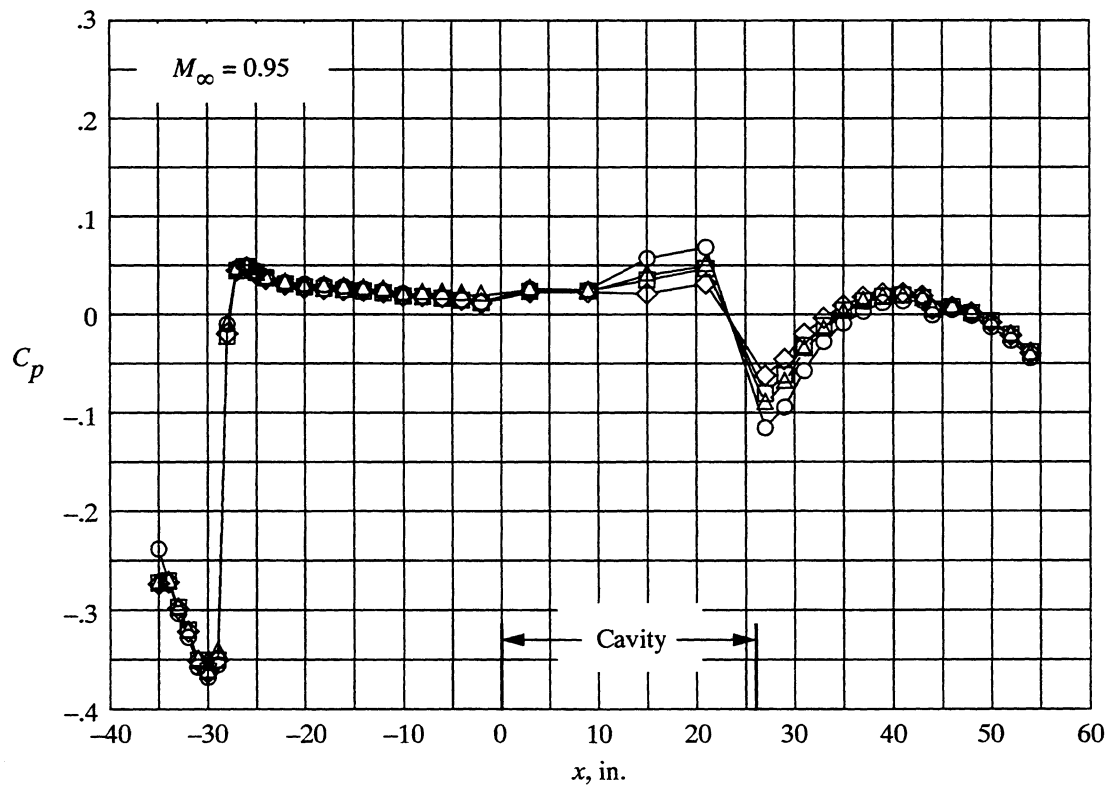
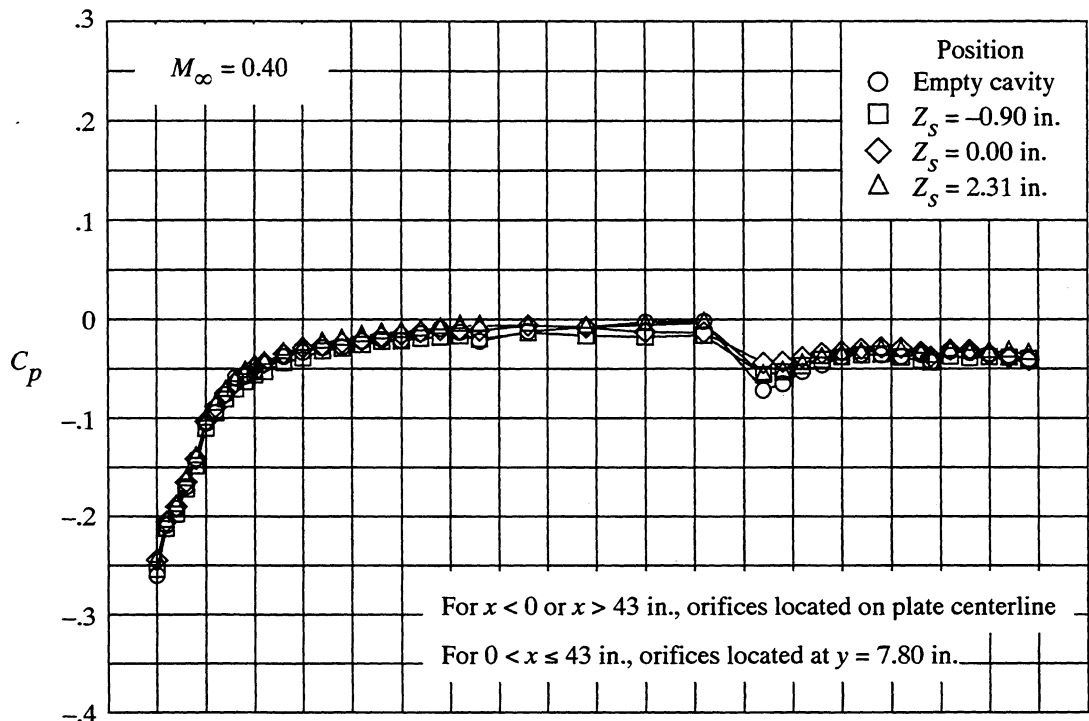
(a) $l = 26.00$ in.; $l/h = 5.42$; $Y_s = 0.00$ in.

Figure 18. Effect of store vertical position on flat-plate pressure distributions. $h = 4.80$ in.



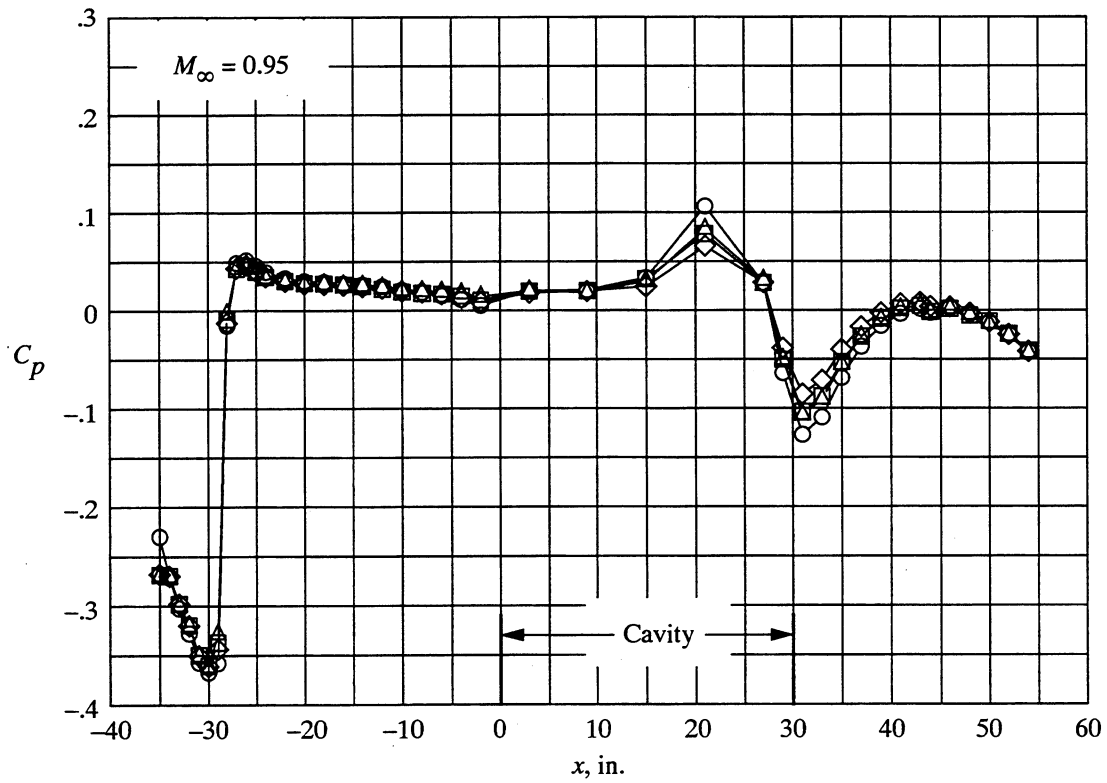
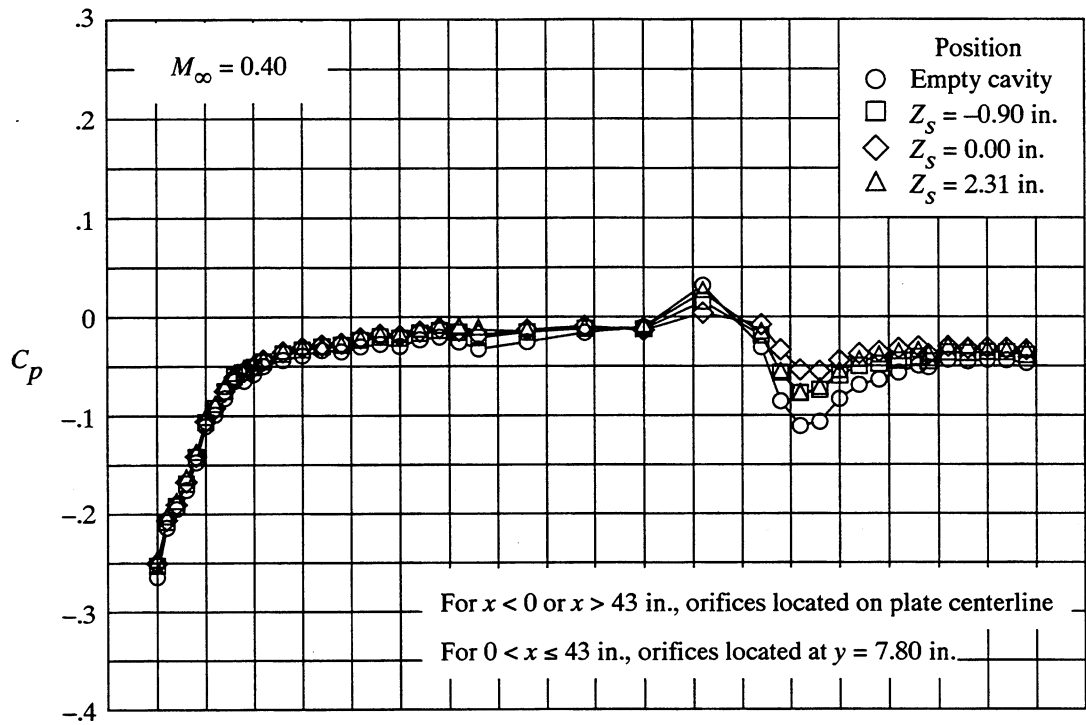
(b) $l = 30.00$ in.; $l/h = 6.25$; $Y_s = 0.00$ in.

Figure 18. Continued.



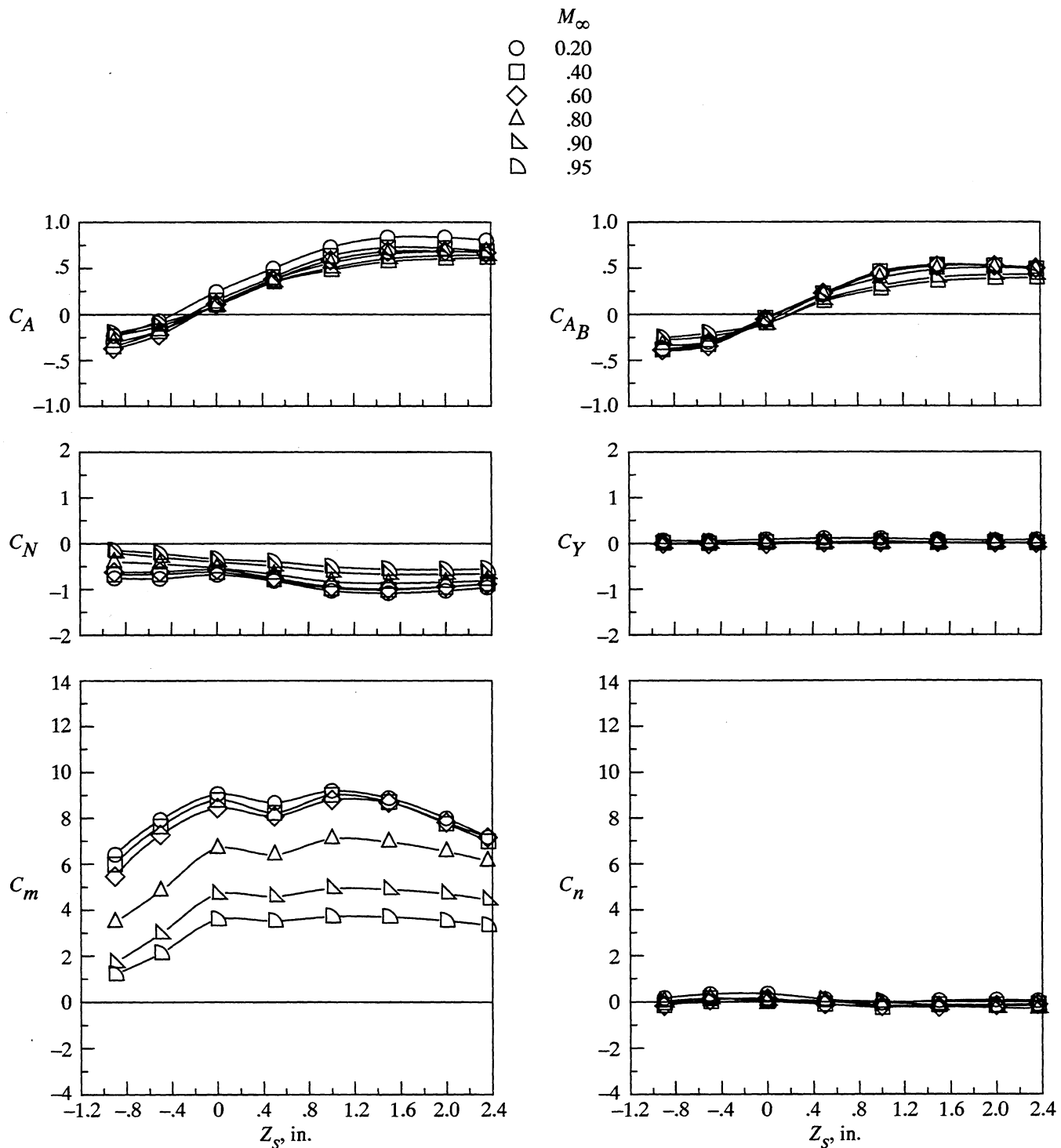
(c) $l = 26.00$ in.; $l/h = 5.42$; $Y_s = 2.40$ in.

Figure 18. Continued.



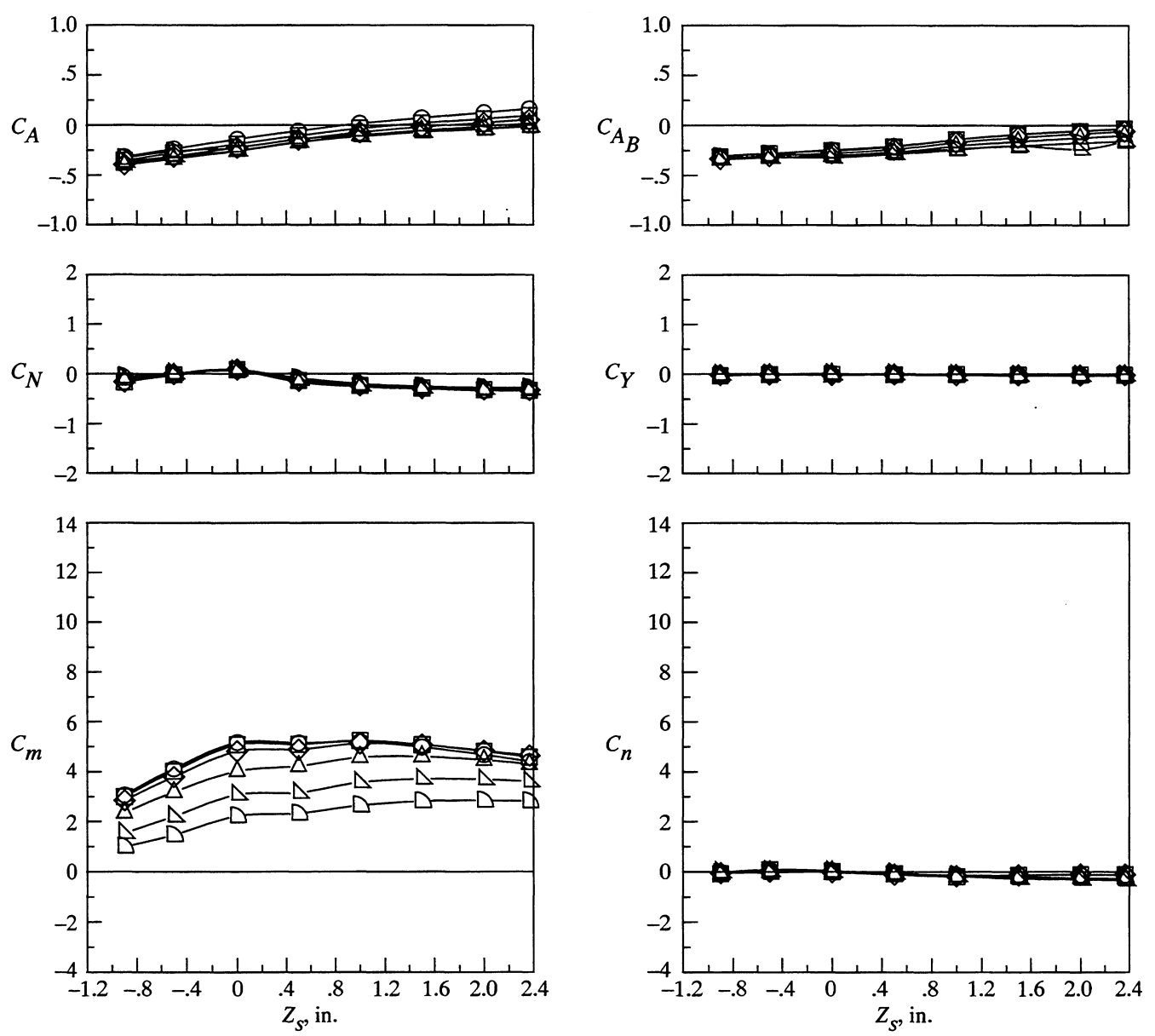
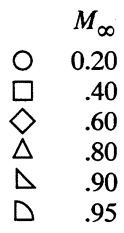
(d) $l = 30.00$ in.; $l/h = 6.25$; $Y_s = 2.40$ in.

Figure 18. Concluded.



(a) $l = 26.00$ in.; $l/h = 10.83$; $Y_s = 0.00$ in.

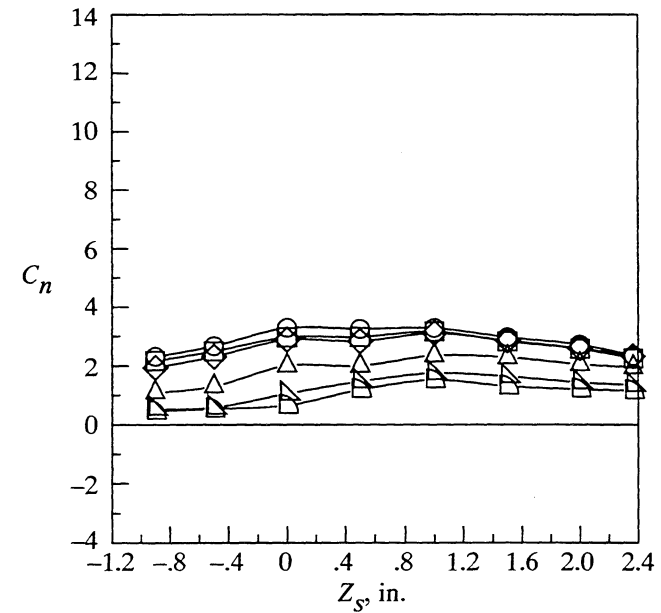
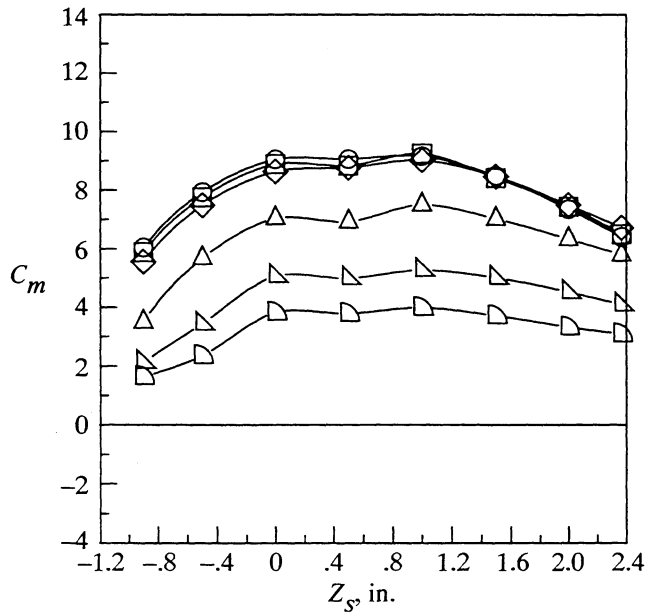
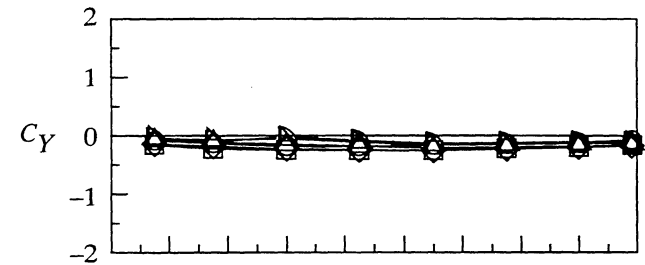
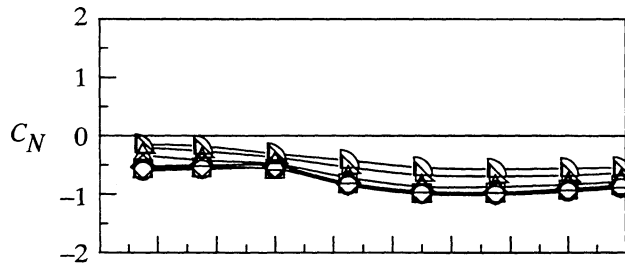
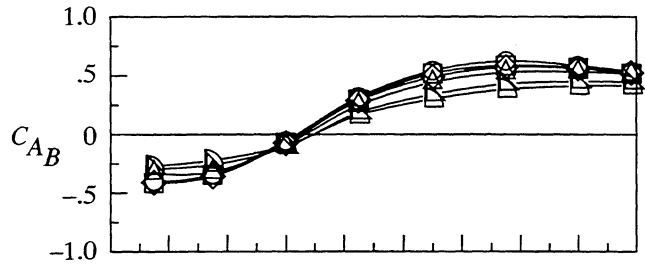
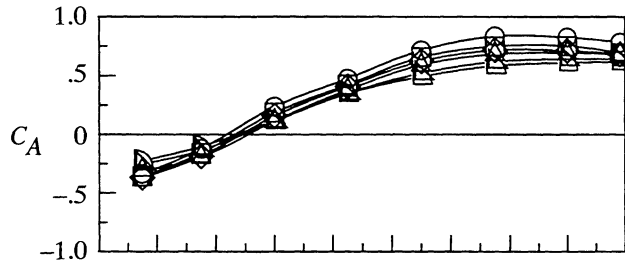
Figure 19. Effect of Mach number on store load characteristics. $h = 2.40$ in.



(b) $l = 30.00$ in.; $l/h = 12.50$; $Y_s = 0.00$ in.

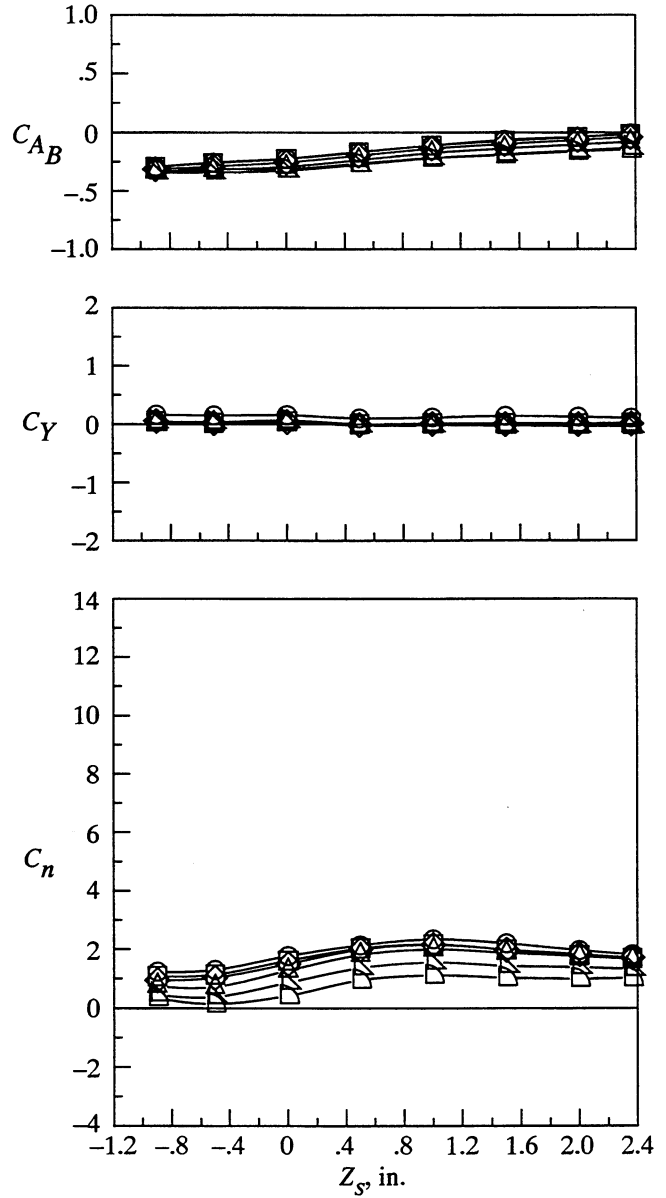
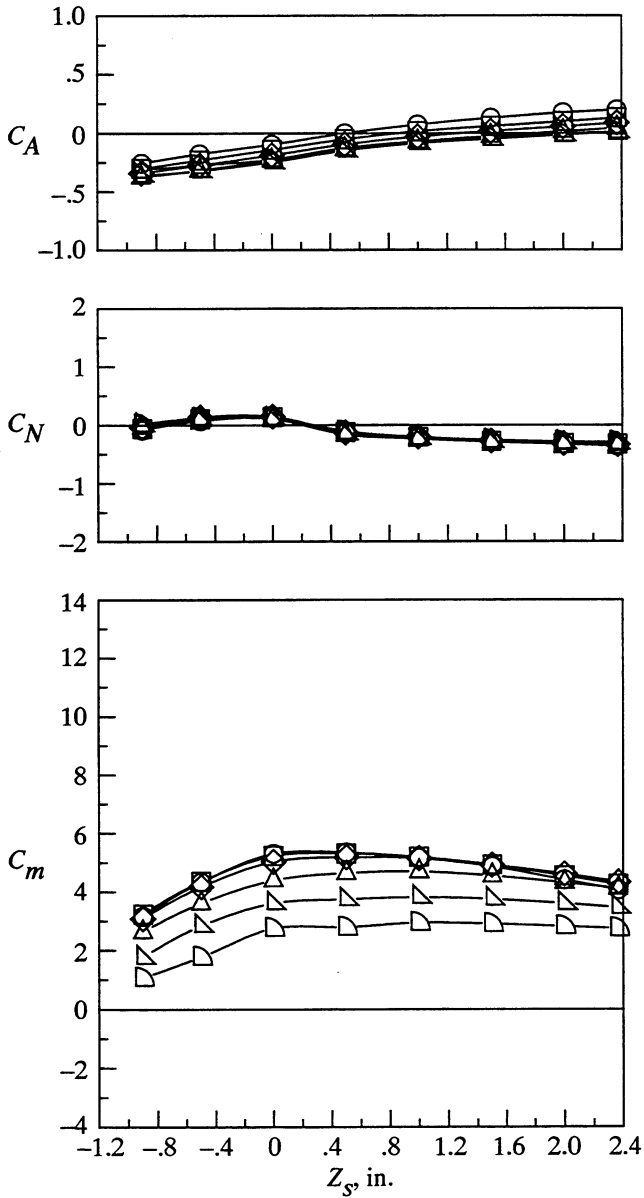
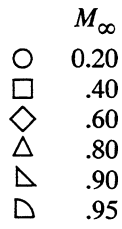
Figure 19. Continued.

M_∞
 ○ 0.20
 □ .40
 ◇ .60
 △ .80
 ▽ .90
 ▢ .95



(c) $l = 26.00$ in.; $l/h = 10.83$; $Y_s = 2.40$ in.

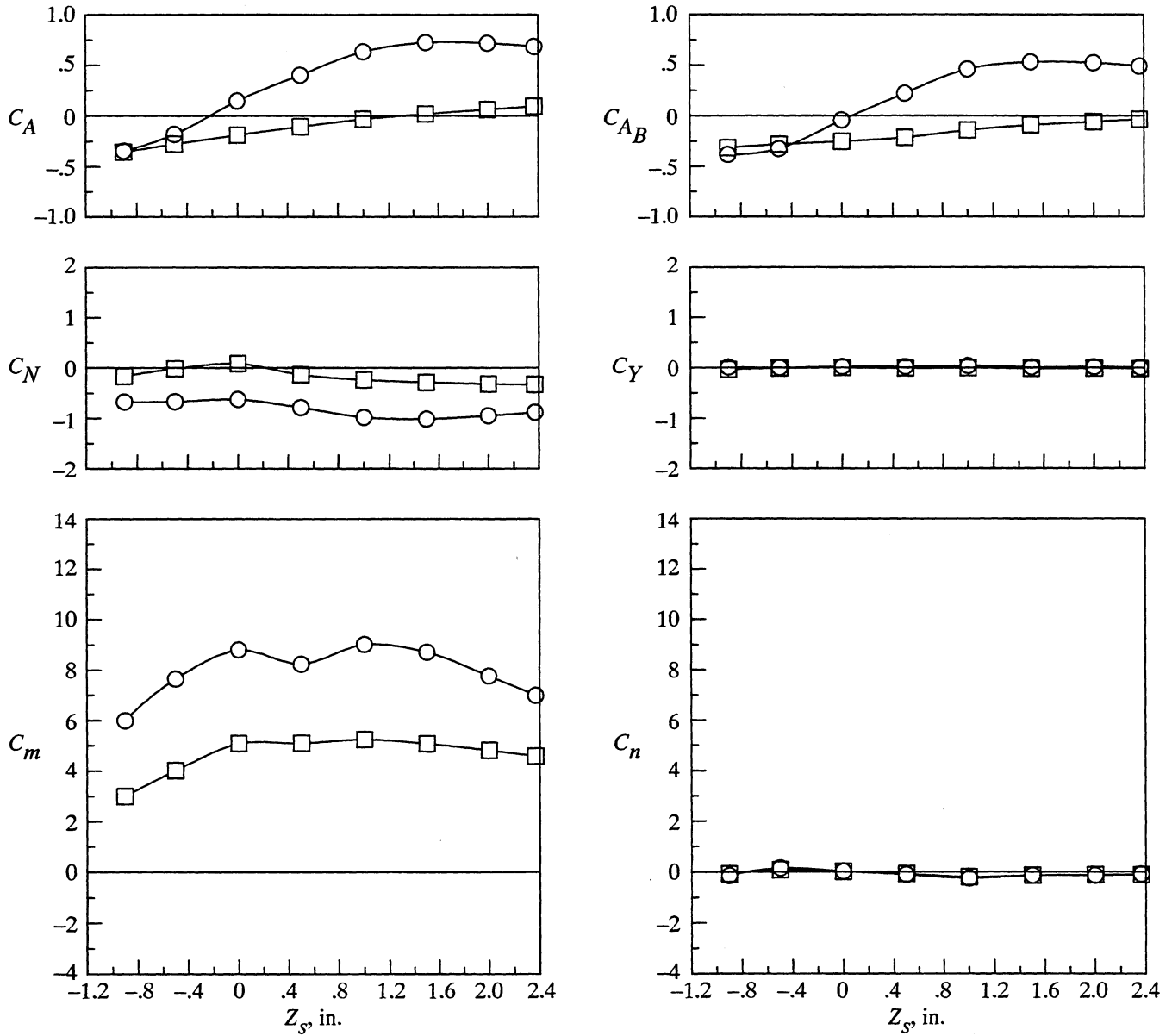
Figure 19. Continued.



(d) $l = 30.00$ in.; $l/h = 12.50$; $Y_s = 2.40$ in.

Figure 19. Concluded.

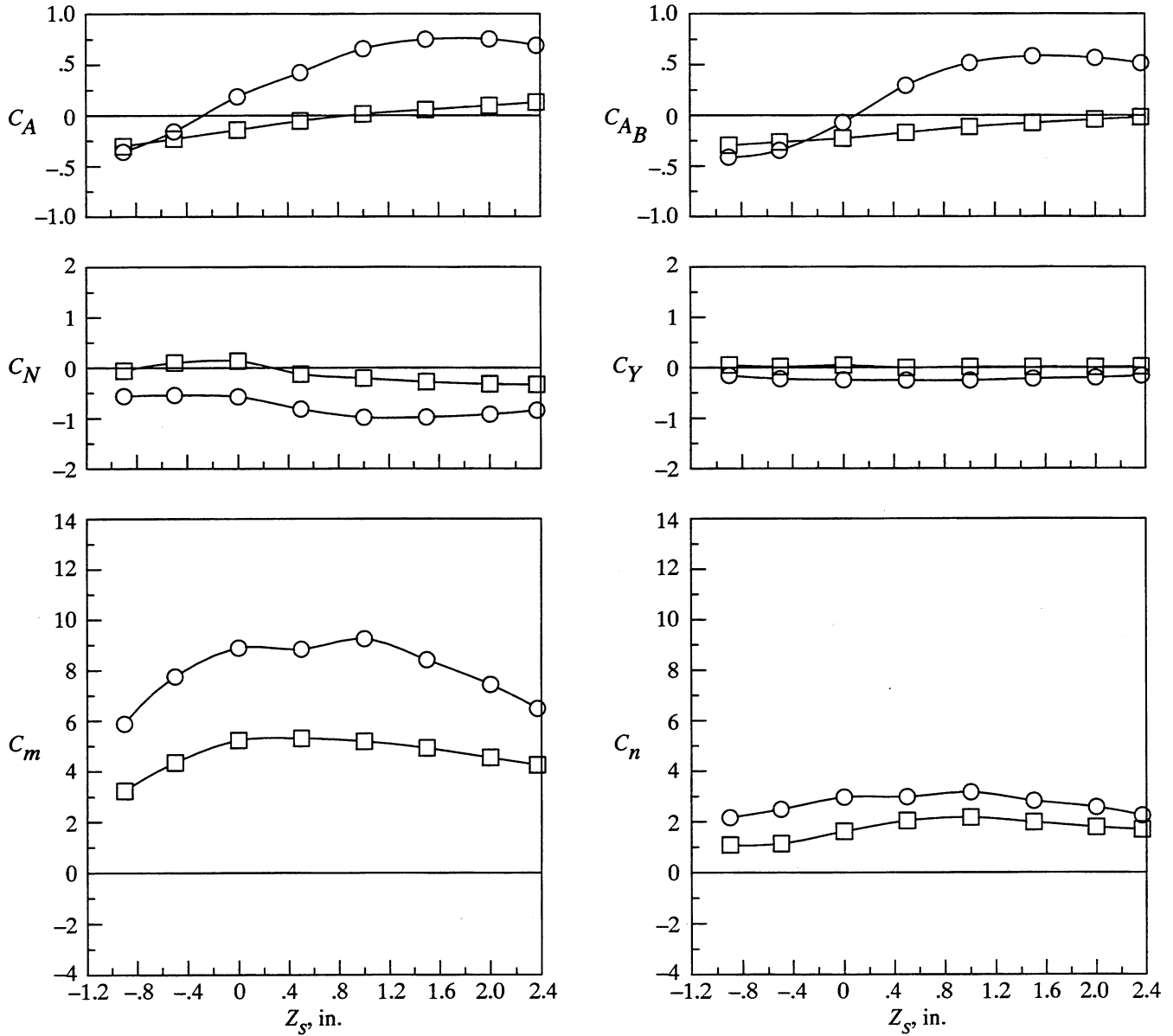
	l , in.	l/h
○	26.00	10.83
□	30.00	12.50



(a) $M_\infty = 0.40$; $Y_s = 0.00$ in.

Figure 20. Effect of cavity length on store load characteristics. $h = 2.40$ in.

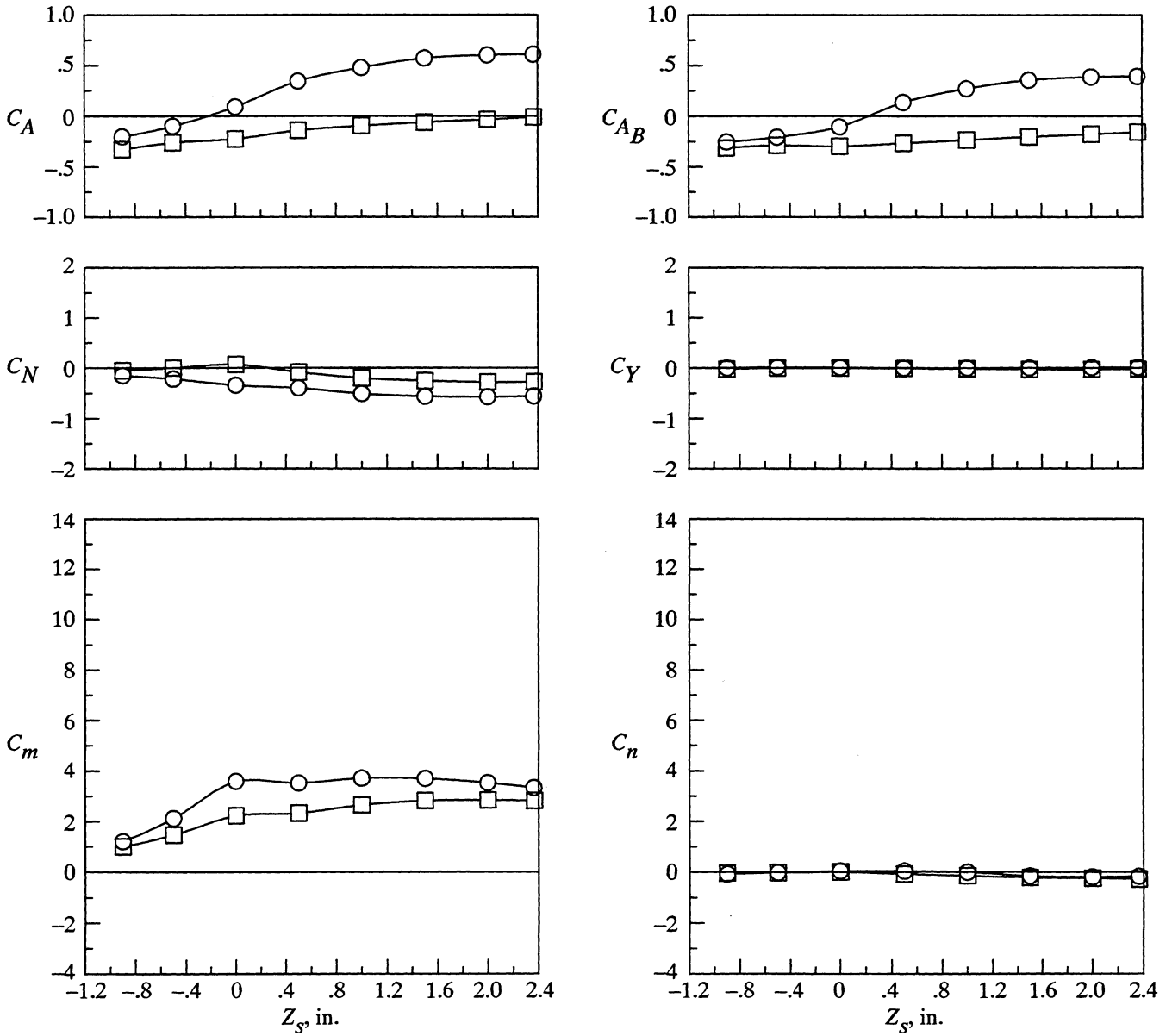
	<i>l</i> , in.	<i>l/h</i>
○	26.00	10.83
□	30.00	12.50



(b) $M_\infty = 0.40$; $Y_s = 2.40$ in.

Figure 20. Continued.

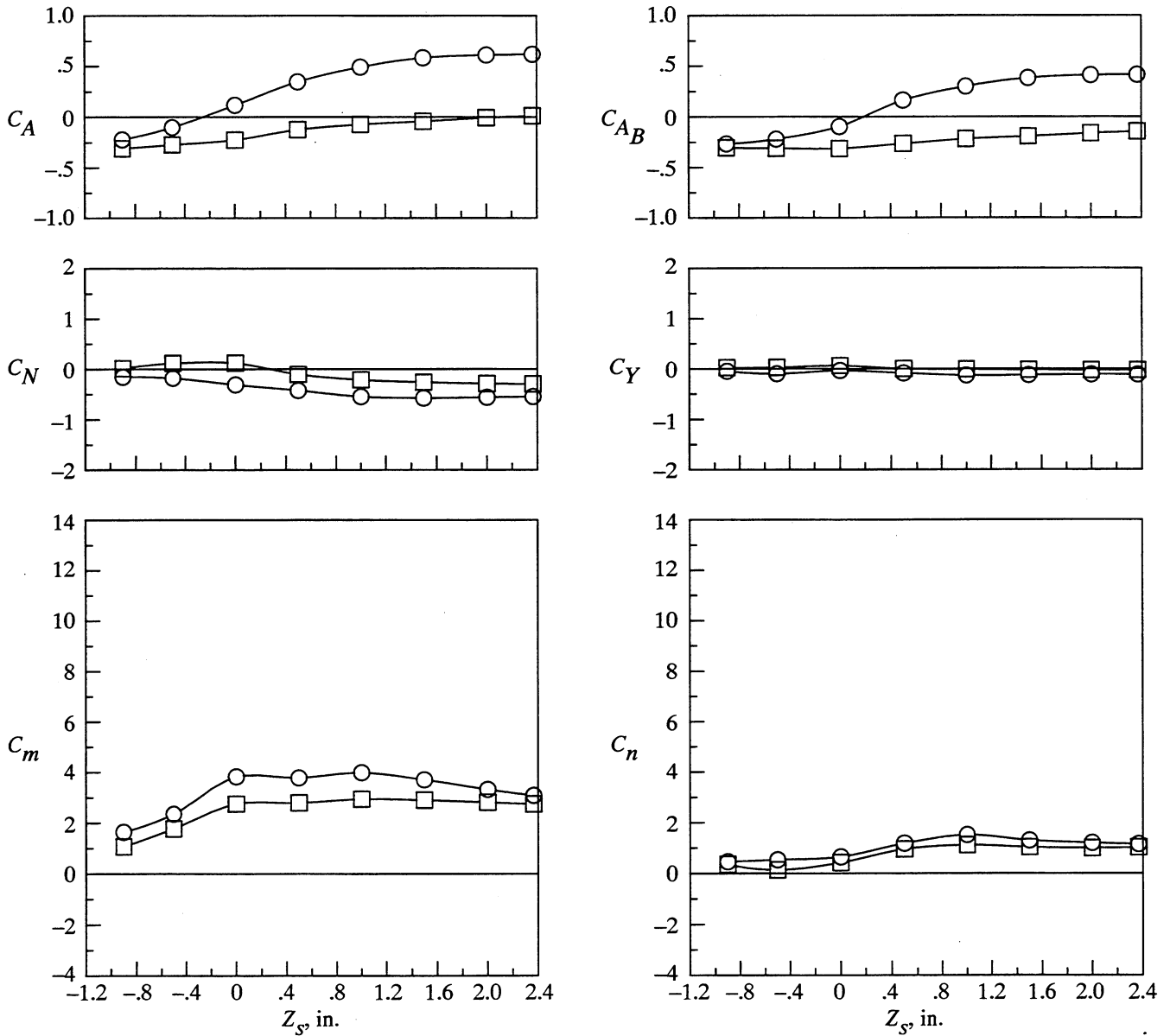
	<i>l</i> , in.	<i>l/h</i>
○	26.00	10.83
□	30.00	12.50



(c) $M_\infty = 0.95$; $Y_s = 0.00$ in.

Figure 20. Continued.

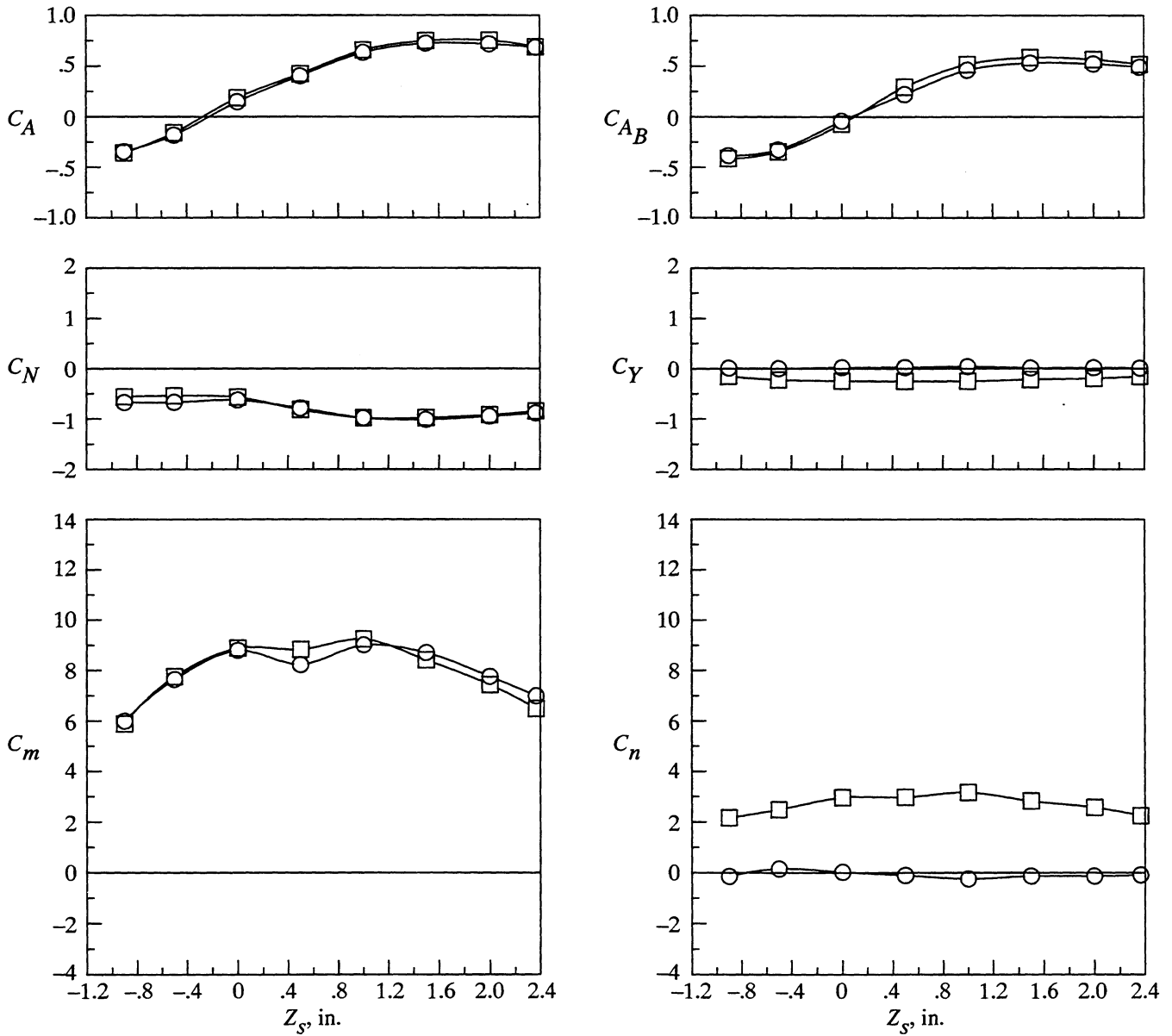
	$l, \text{ in.}$	l/h
○	26.00	10.83
□	30.00	12.50



(d) $M_\infty = 0.95; Y_s = 2.40 \text{ in.}$

Figure 20. Concluded.

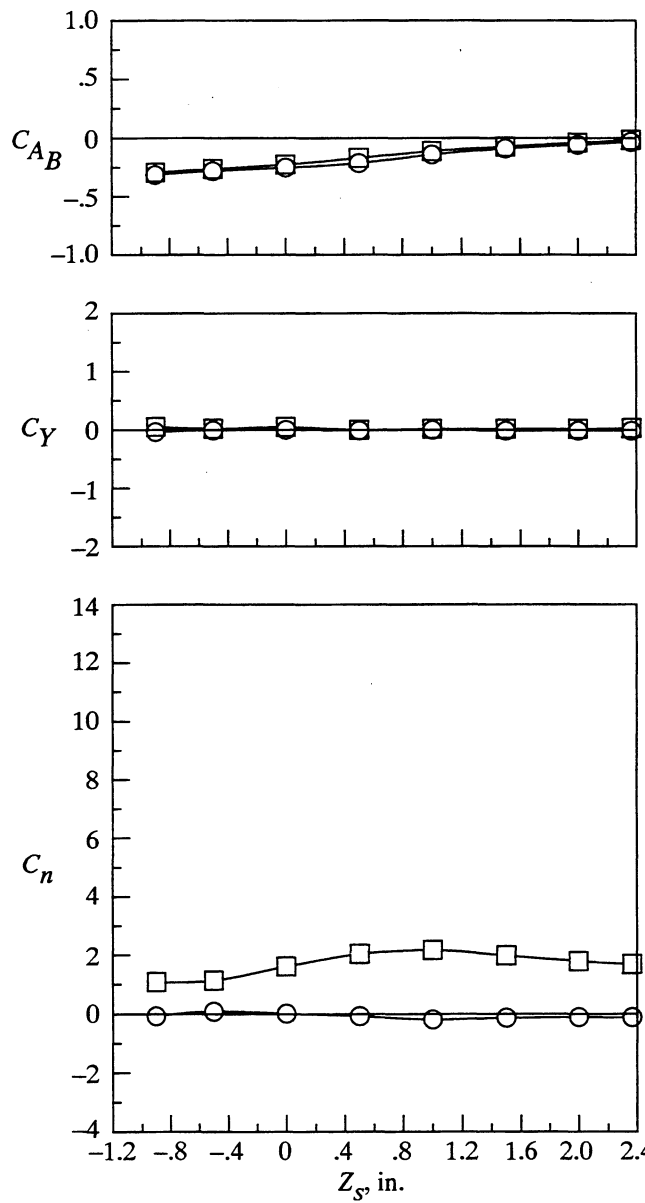
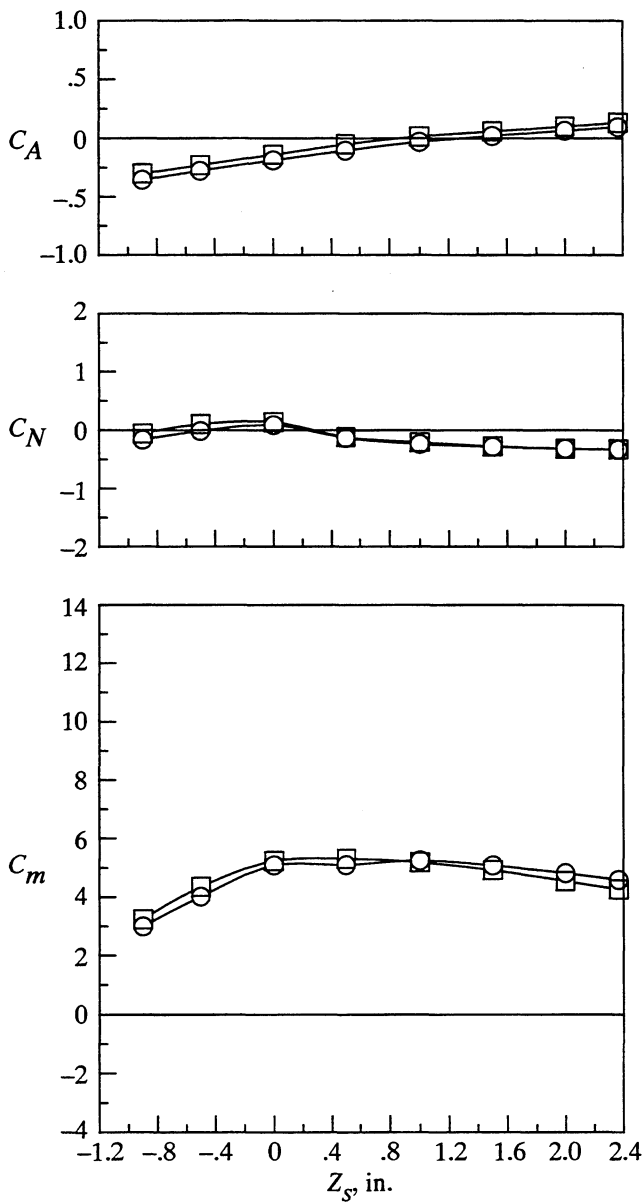
Y_S , in.
 ○ 0.00
 □ 2.40



(a) $M_\infty = 0.40$; $l = 26.00$ in.; $l/h = 10.83$.

Figure 21. Effect of lateral position on store load characteristics. $h = 2.40$ in.

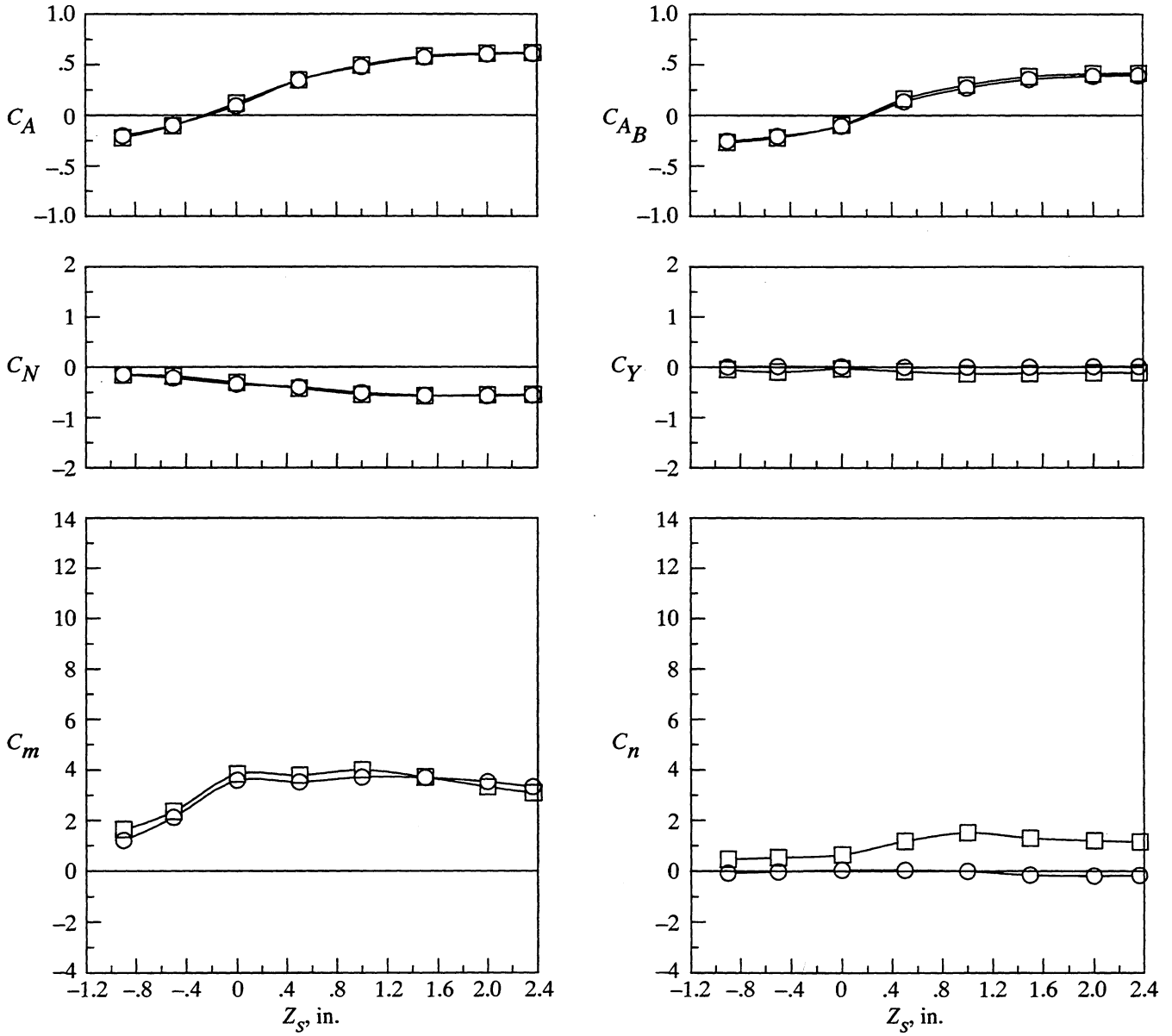
Y_s , in.
 ○ 0.00
 □ 2.40



(b) $M_\infty = 0.40$; $l = 30.00$ in.; $l/h = 12.50$.

Figure 21. Continued.

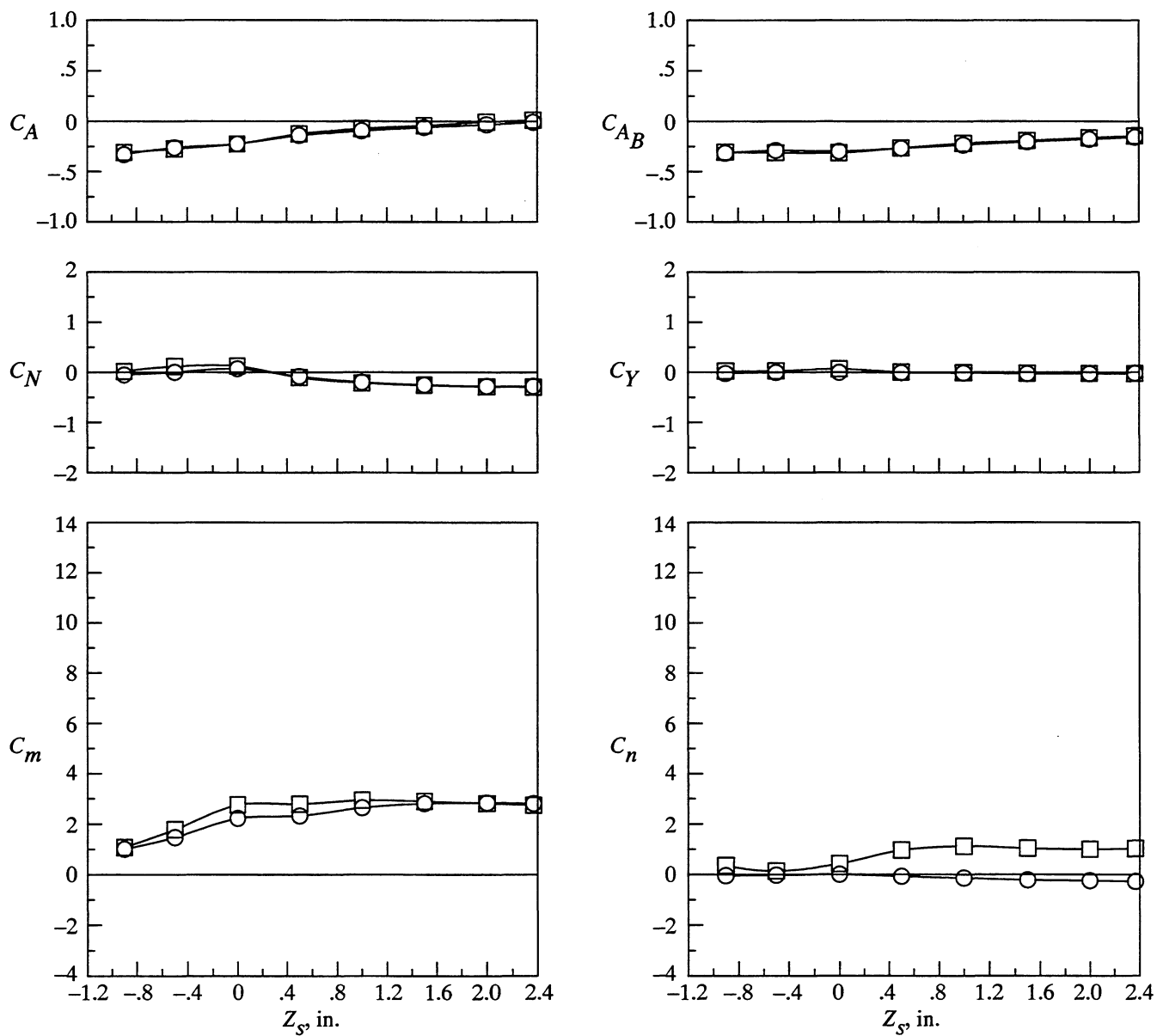
Y_s , in.
 ○ 0.00
 □ 2.40



(c) $M_\infty = 0.95$; $l = 26.00$ in.; $l/h = 10.83$.

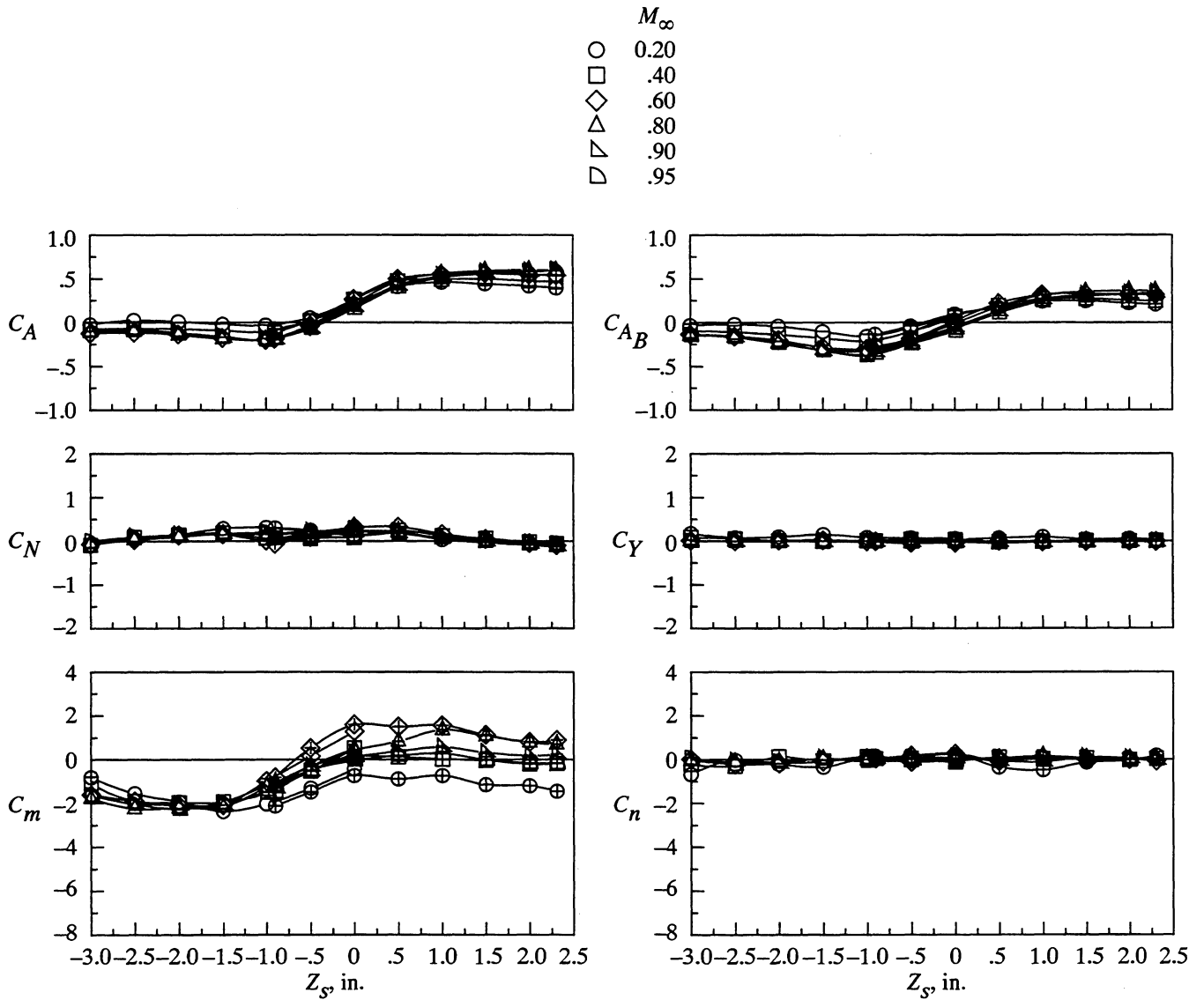
Figure 21. Continued.

Y_s , in.
 ○ 0.00
 □ 2.40



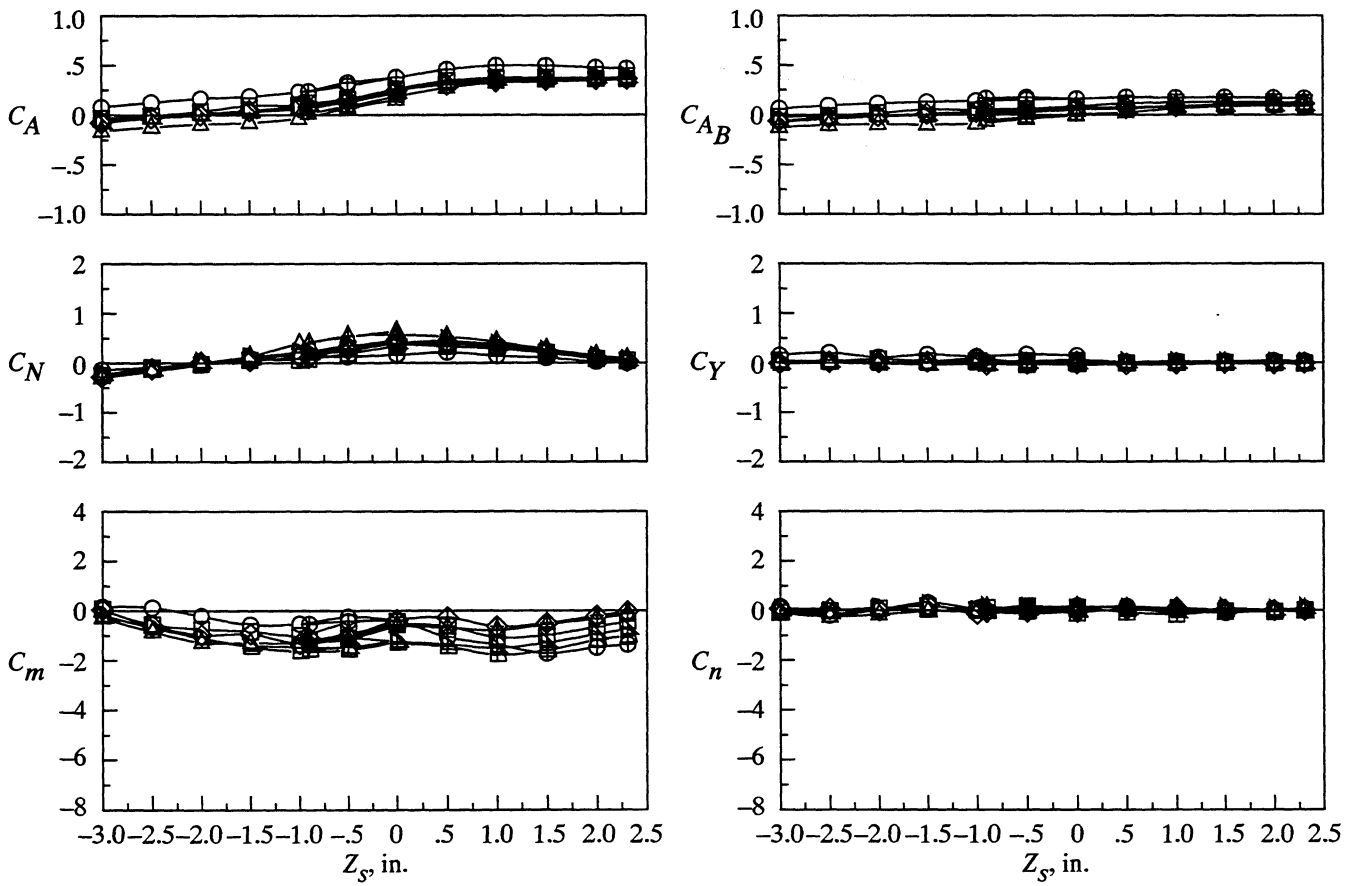
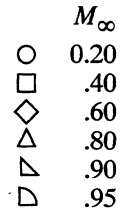
(d) $M_\infty = 0.95$; $l = 30.00$ in.; $l/h = 12.50$.

Figure 21. Concluded.



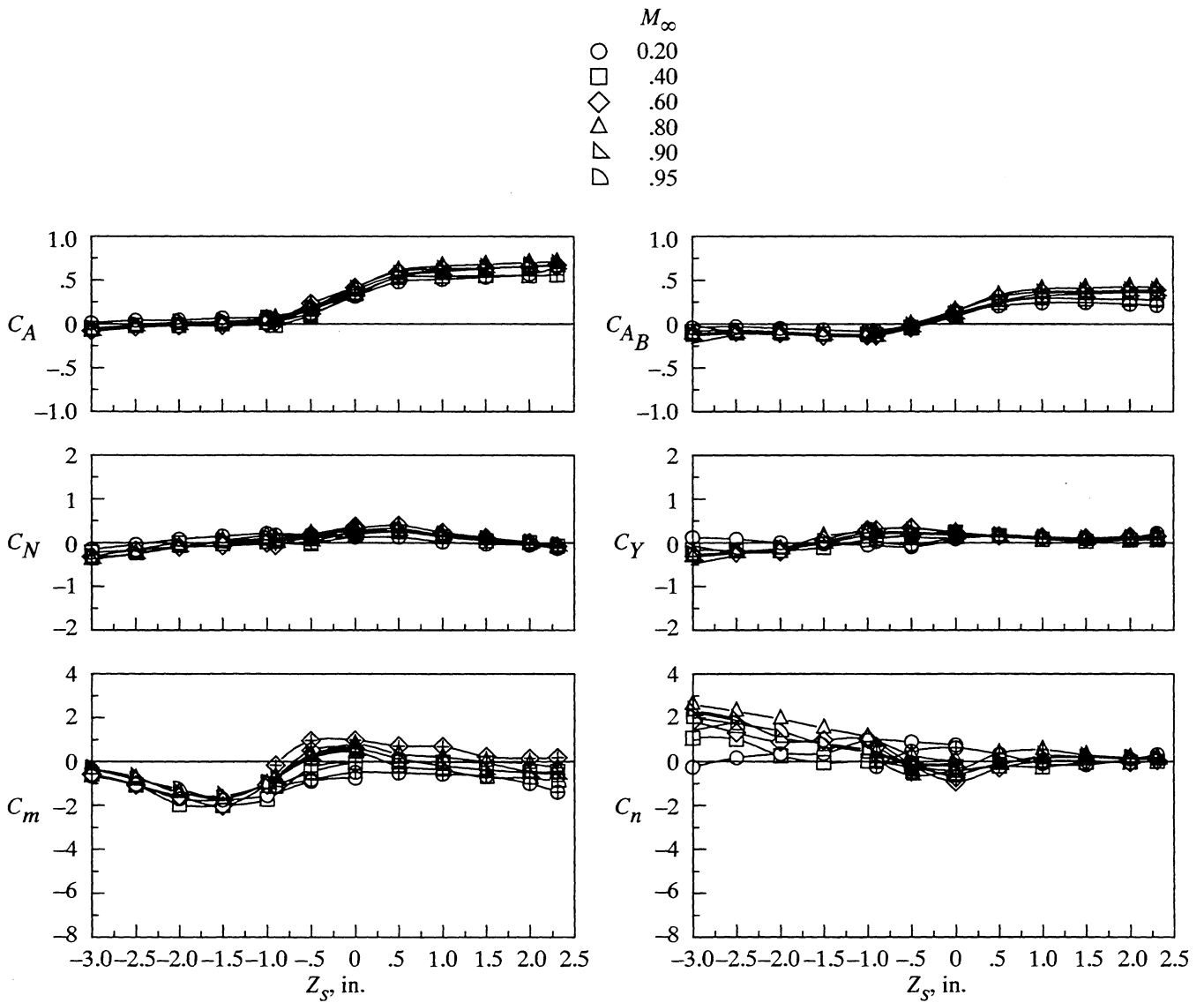
(a) $l = 26.00$ in.; $l/h = 5.42$; $Y_s = 0.00$ in.

Figure 22. Effect of Mach number on store load characteristics (open and plus-filled symbols are for strut housing extending 0.45 in. and 2.85 in., respectively, above cavity floor). $h = 4.80$ in.



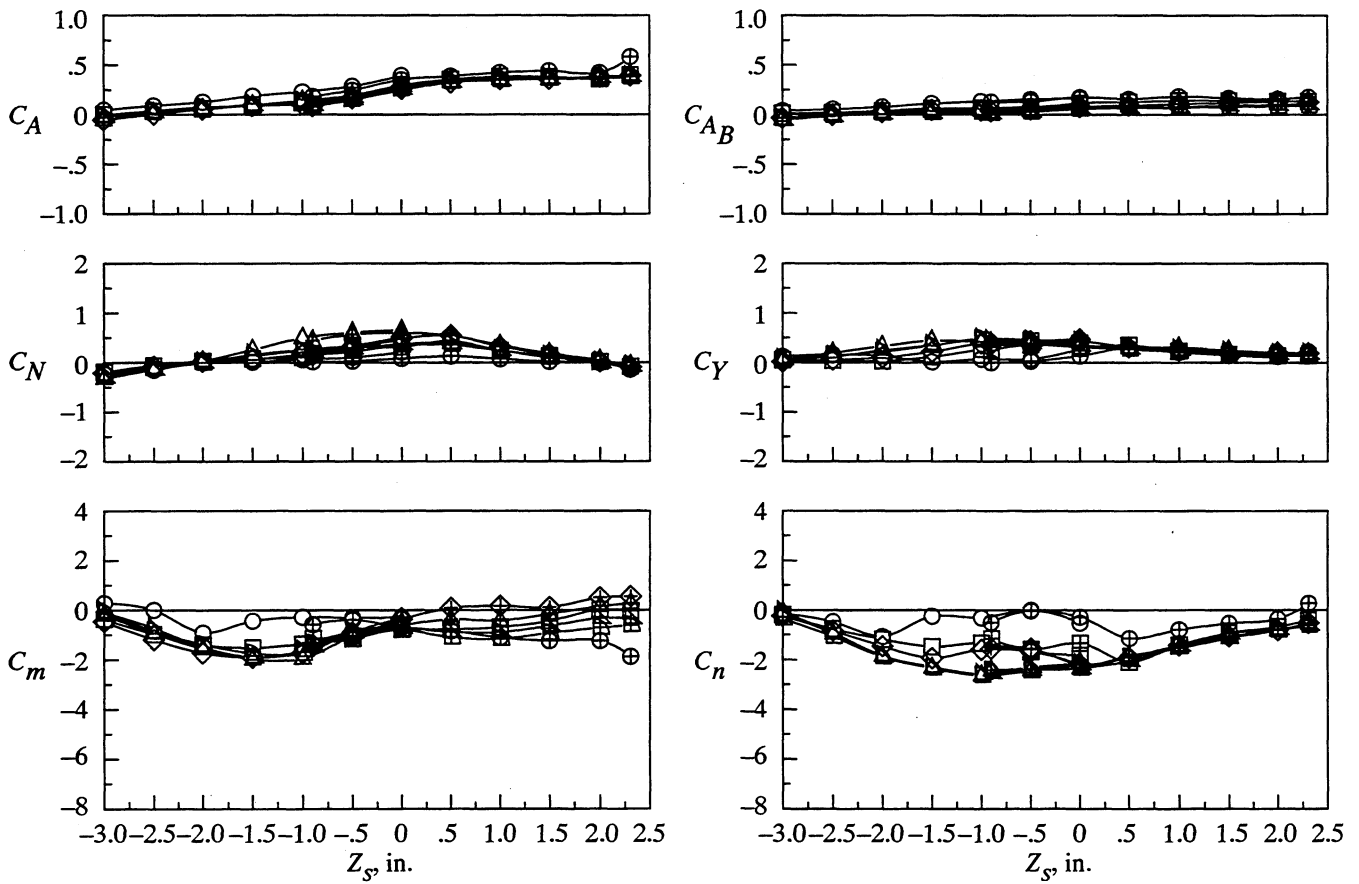
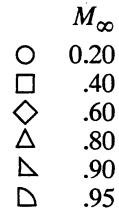
(b) $l = 30.00$ in.; $l/h = 6.25$; $Y_s = 0.00$ in.

Figure 22. Continued.



(c) $l = 26.00$ in.; $l/h = 5.42$; $Y_s = 2.40$ in.

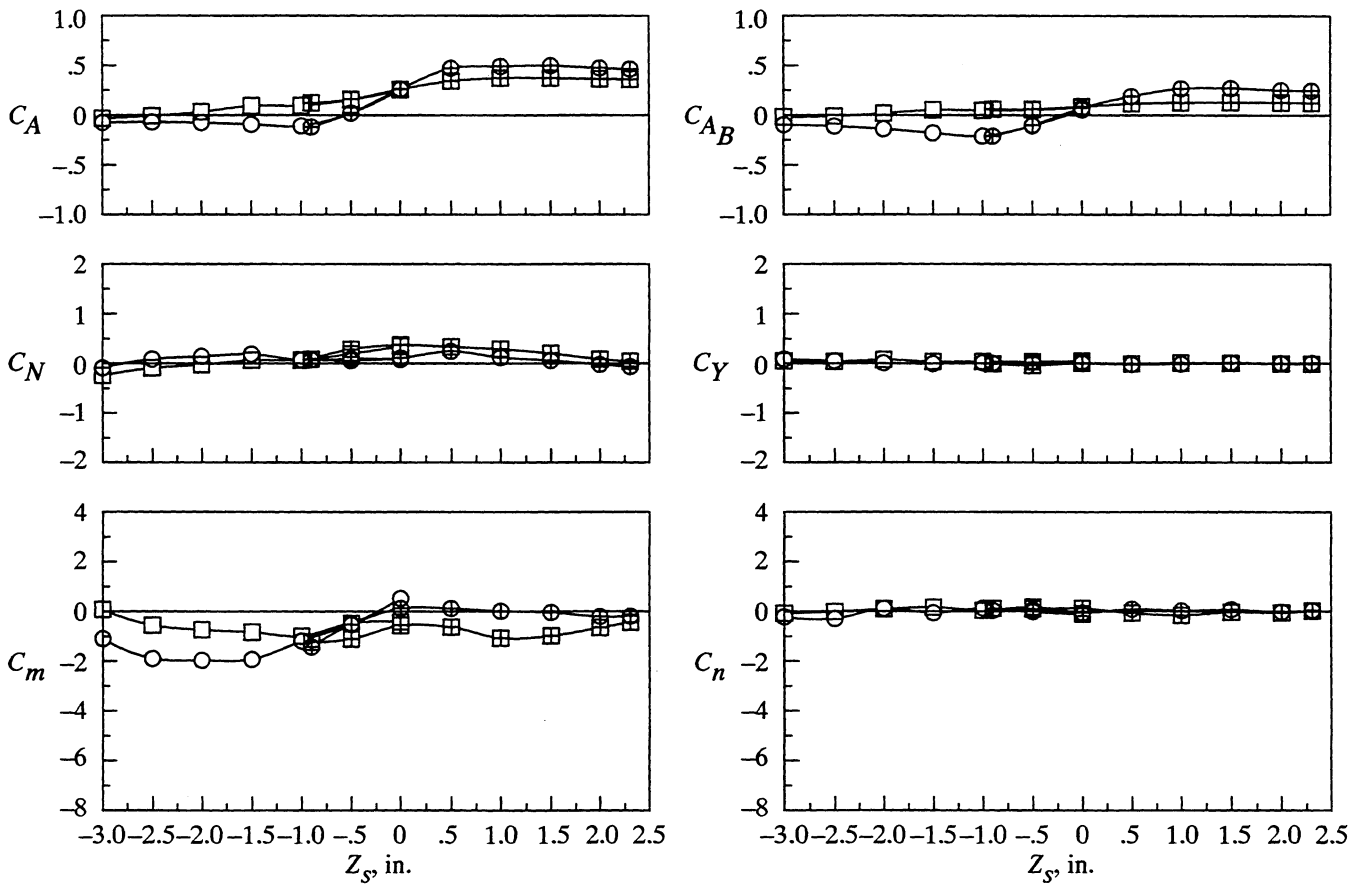
Figure 22. Continued.



(d) $l = 30.00$ in.; $l/h = 6.25$; $Y_s = 2.40$ in.

Figure 22. Concluded.

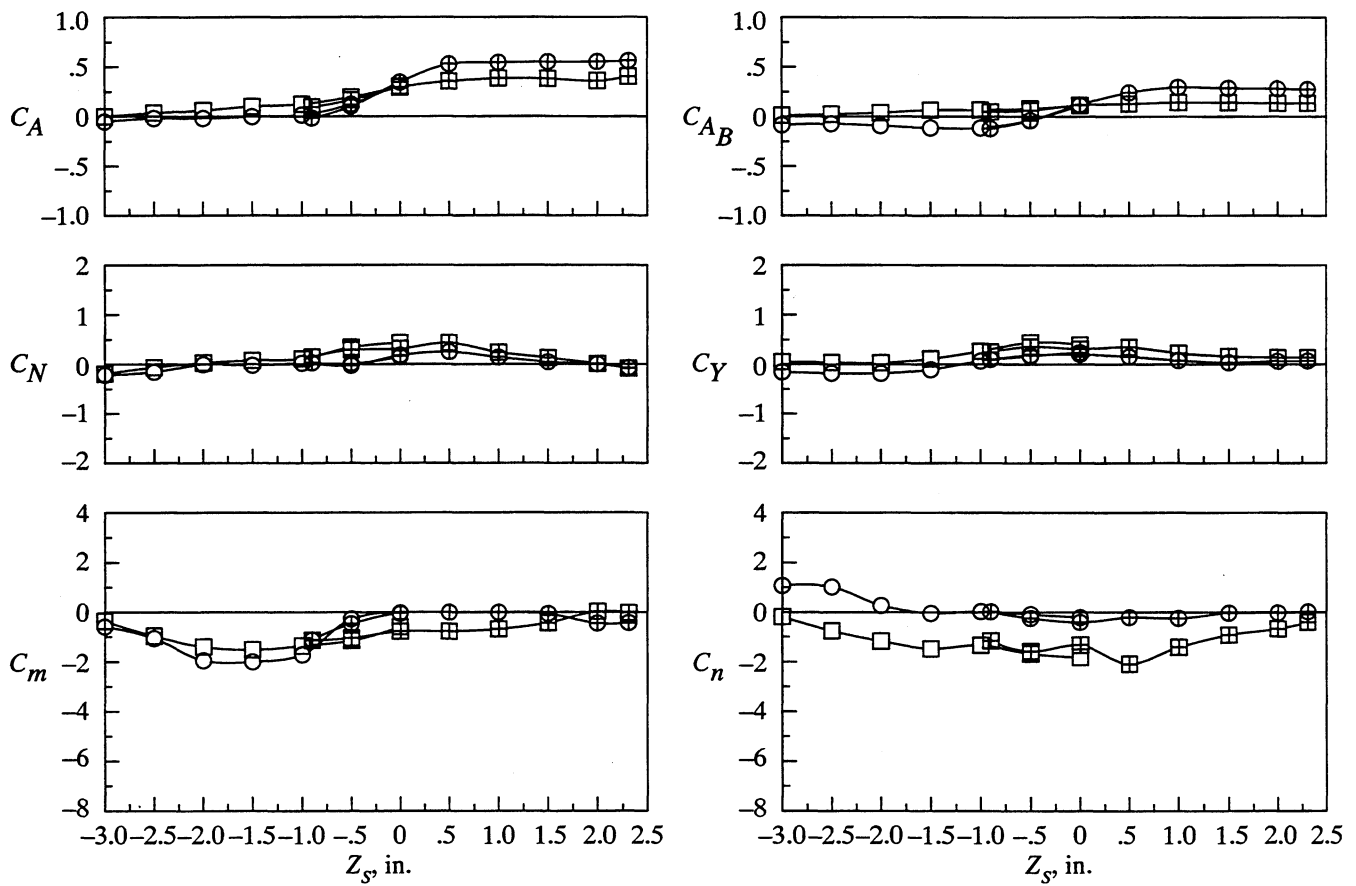
	l , in.	l/h
○	26.00	5.42
□	30.00	6.25



(a) $M_\infty = 0.40$; $Y_s = 0.00$ in.

Figure 23. Effect of cavity length on store load characteristics (open and plus-filled symbols are for strut housing extending 0.45 in. and 2.85 in., respectively, above cavity floor). $h = 4.80$ in.

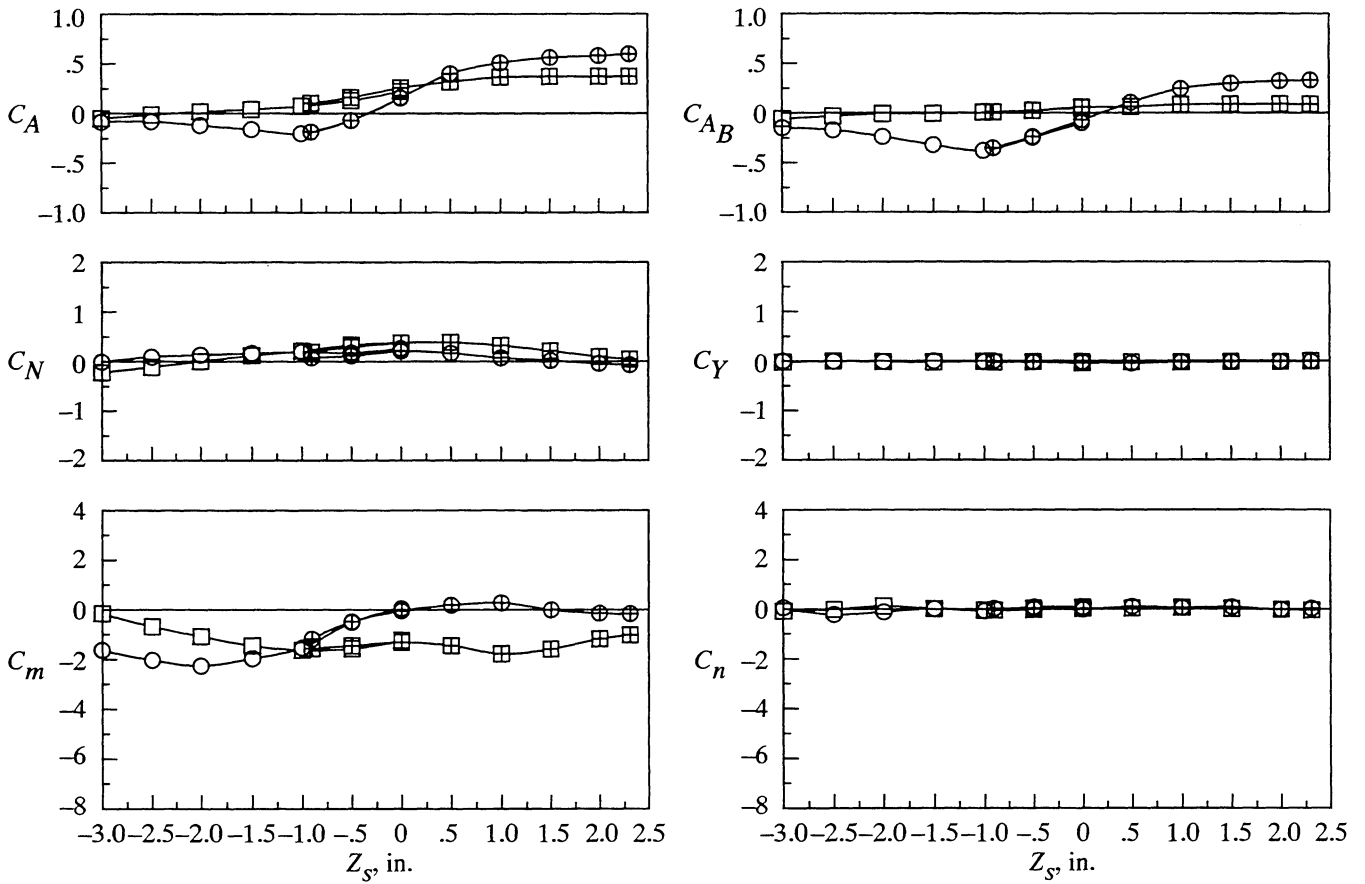
	<i>l</i> , in.	<i>l</i> / <i>h</i>
○	26.00	5.42
□	30.00	6.25



(b) $M_\infty = 0.40$; $Y_s = 2.40$ in.

Figure 23. Continued.

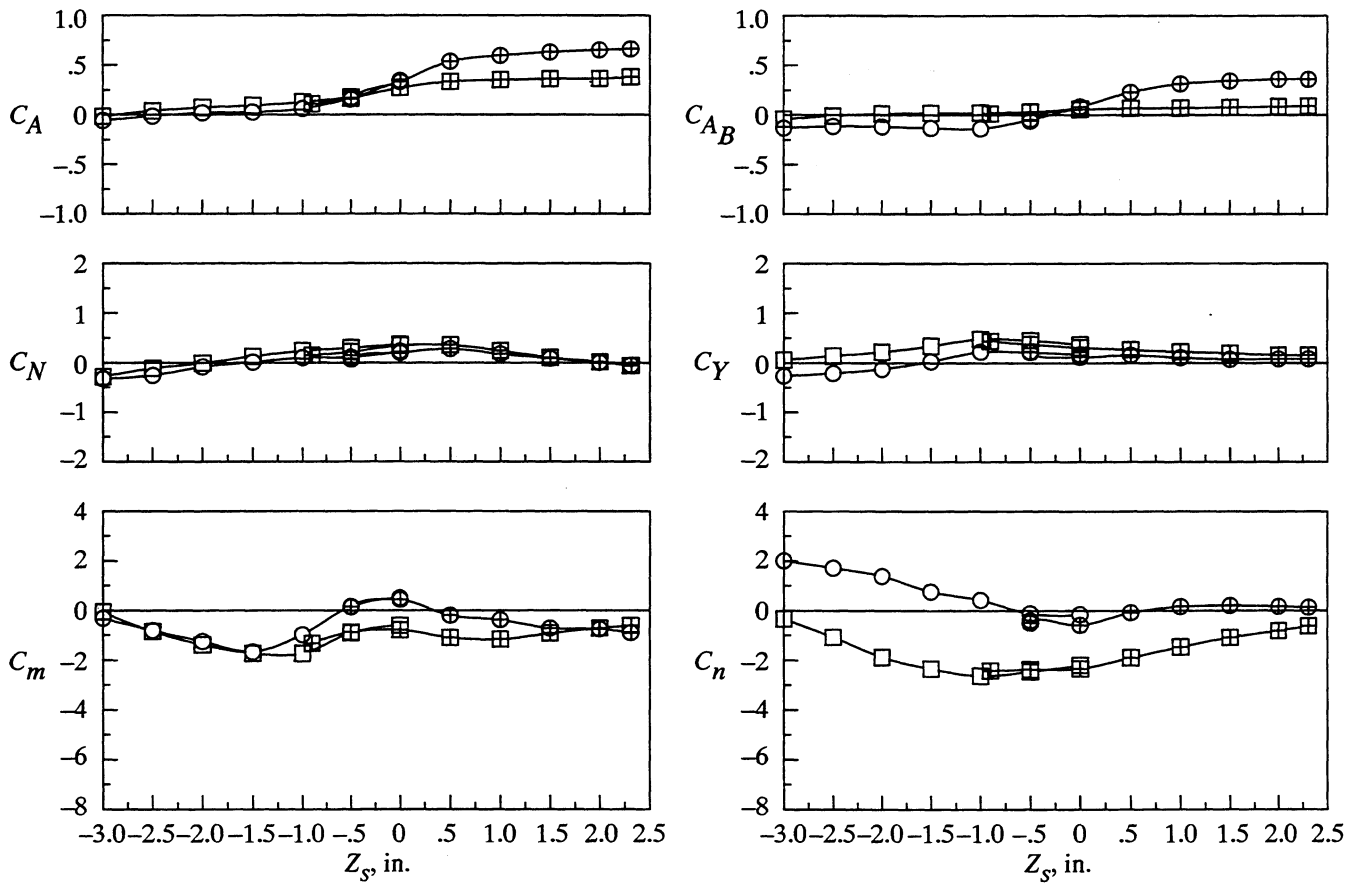
	l , in.	l/h
○	26.00	5.42
□	30.00	6.25



(c) $M_\infty = 0.95$; $Y_s = 0.00$ in.

Figure 23. Continued.

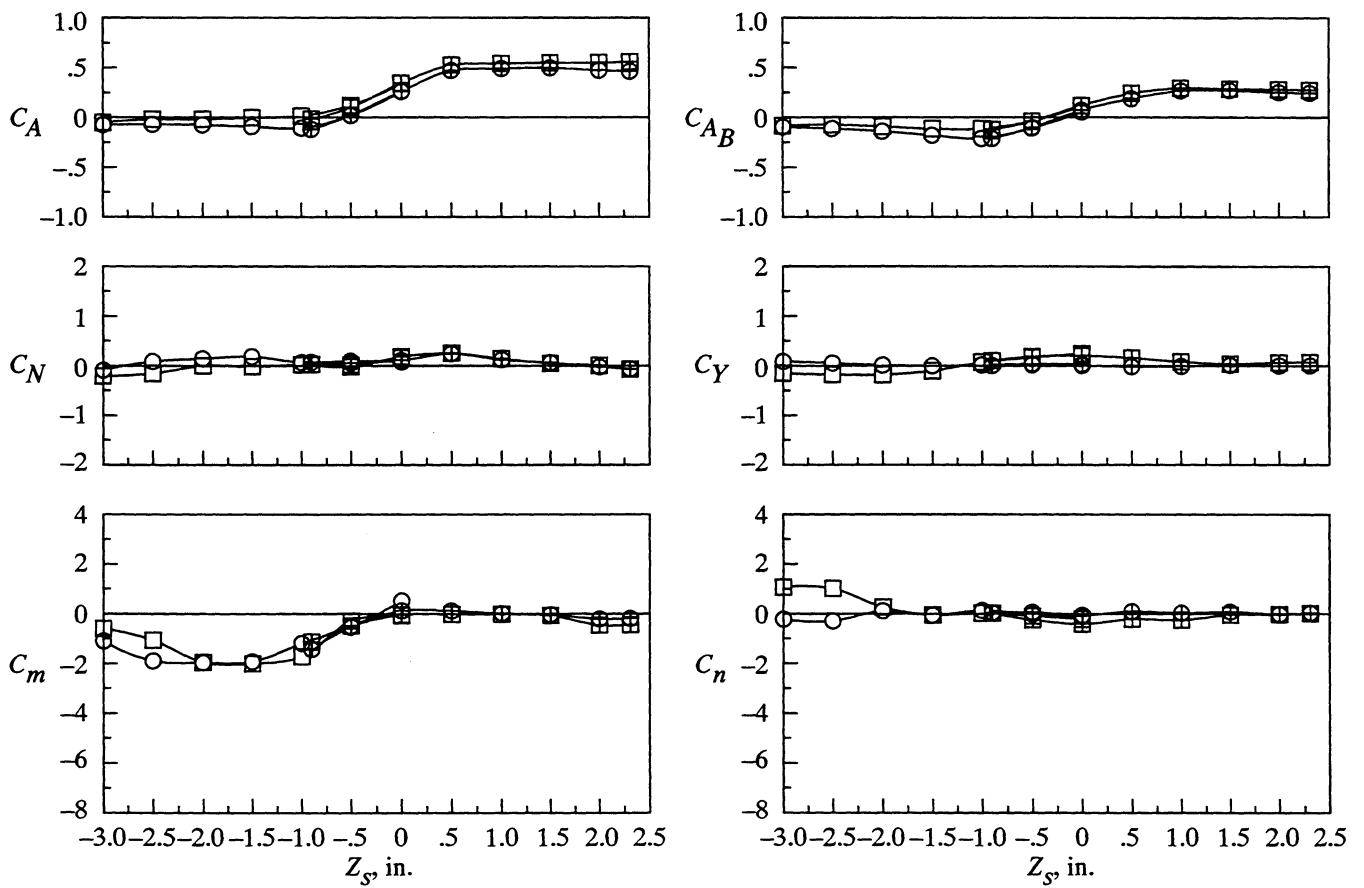
	l , in.	l/h
○	26.00	5.42
□	30.00	6.25



(d) $M_\infty = 0.95$; $Y_s = 2.40$ in.

Figure 23. Concluded.

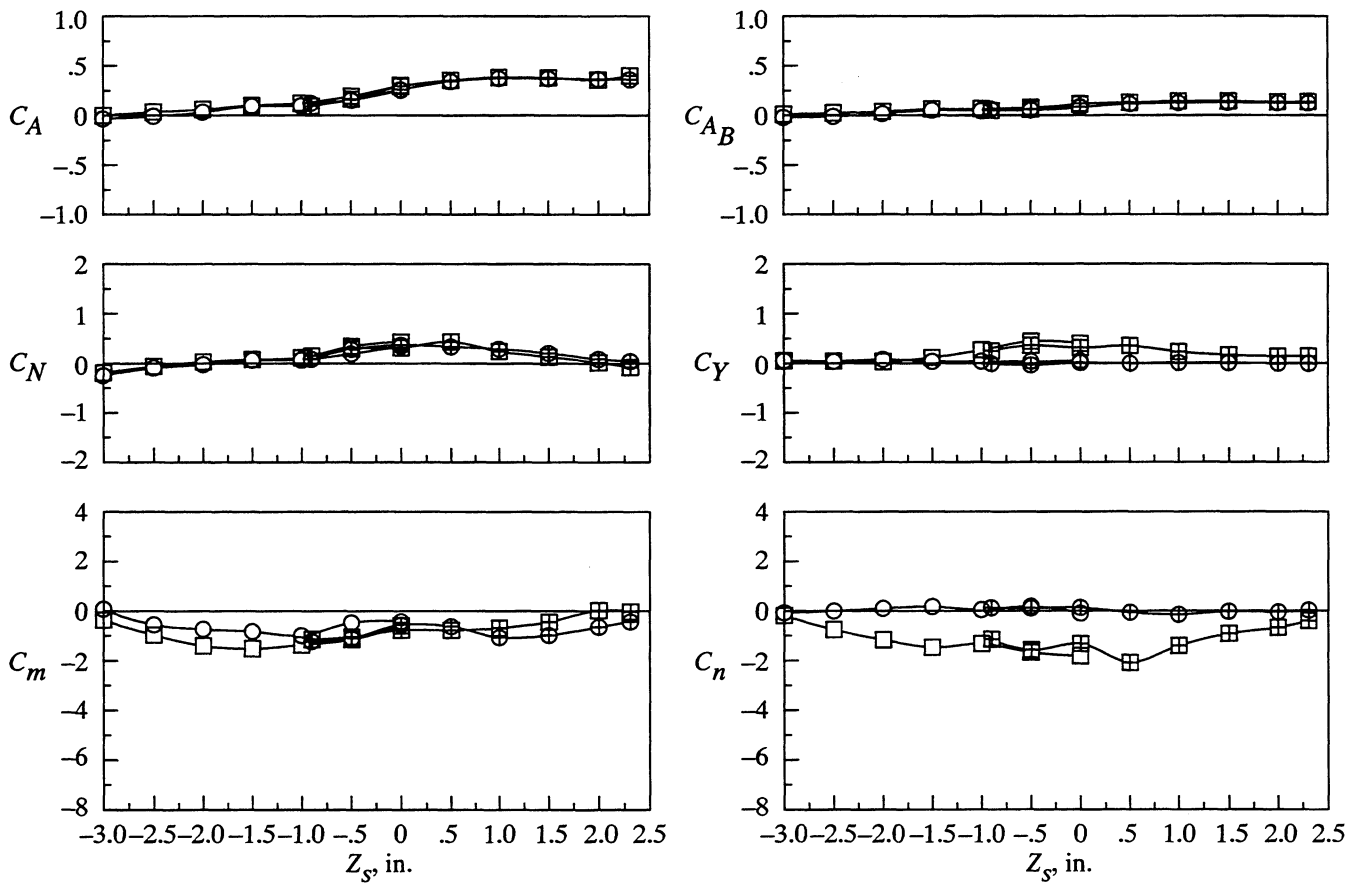
Y_s , in.
 ○ 0.00
 □ 2.40



(a) $M_\infty = 0.40$; $l = 26.00$ in.; $l/h = 5.42$.

Figure 24. Effect of lateral position on store load characteristics (open and plus-filled symbols are for strut housing extending 0.45 in. and 2.85 in., respectively, above cavity floor). $h = 4.80$ in.

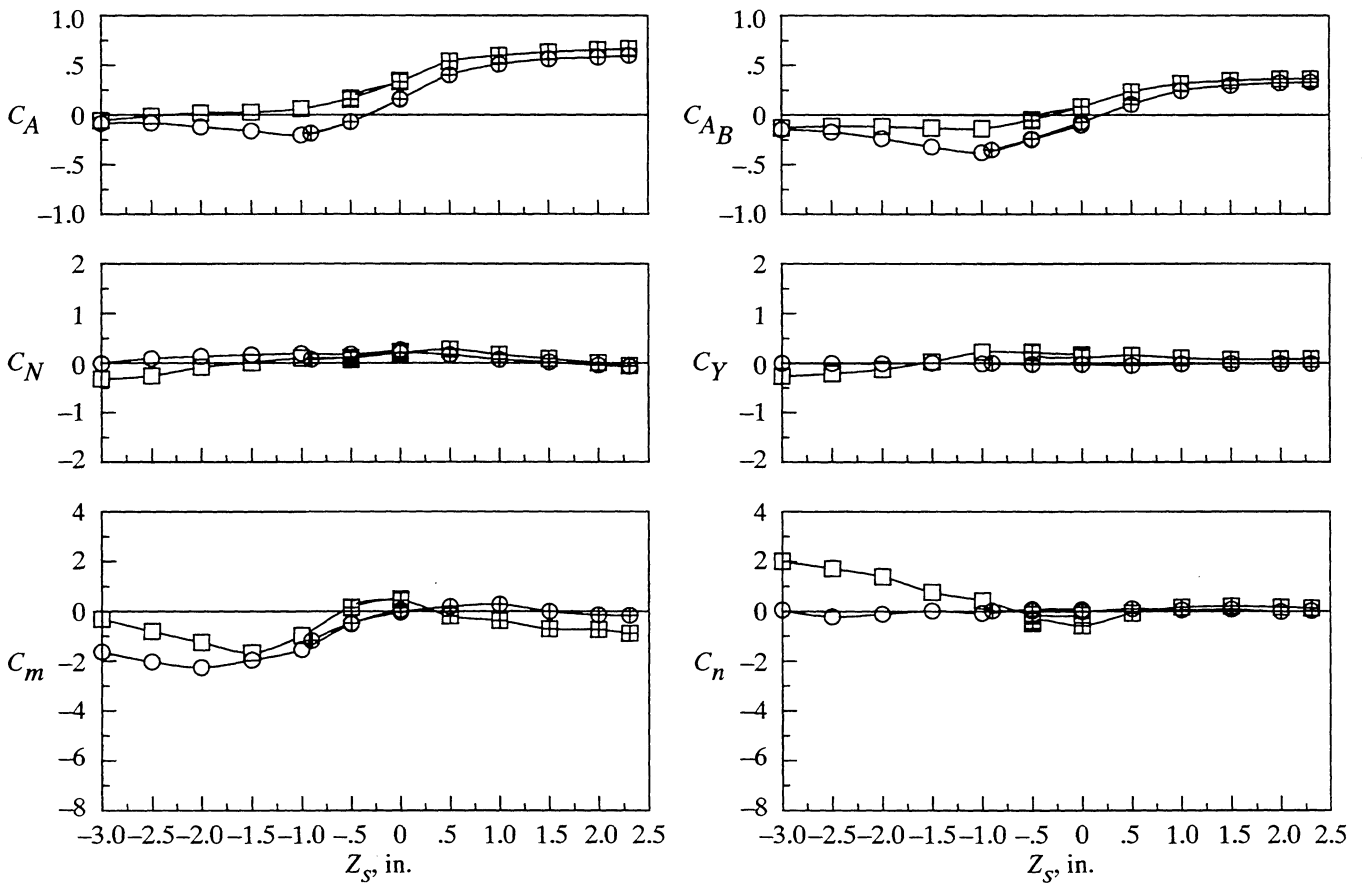
Y_s , in.
 ○ 0.00
 □ 2.40



(b) $M_\infty = 0.40$; $l = 30.00$ in.; $l/h = 6.25$.

Figure 24. Continued.

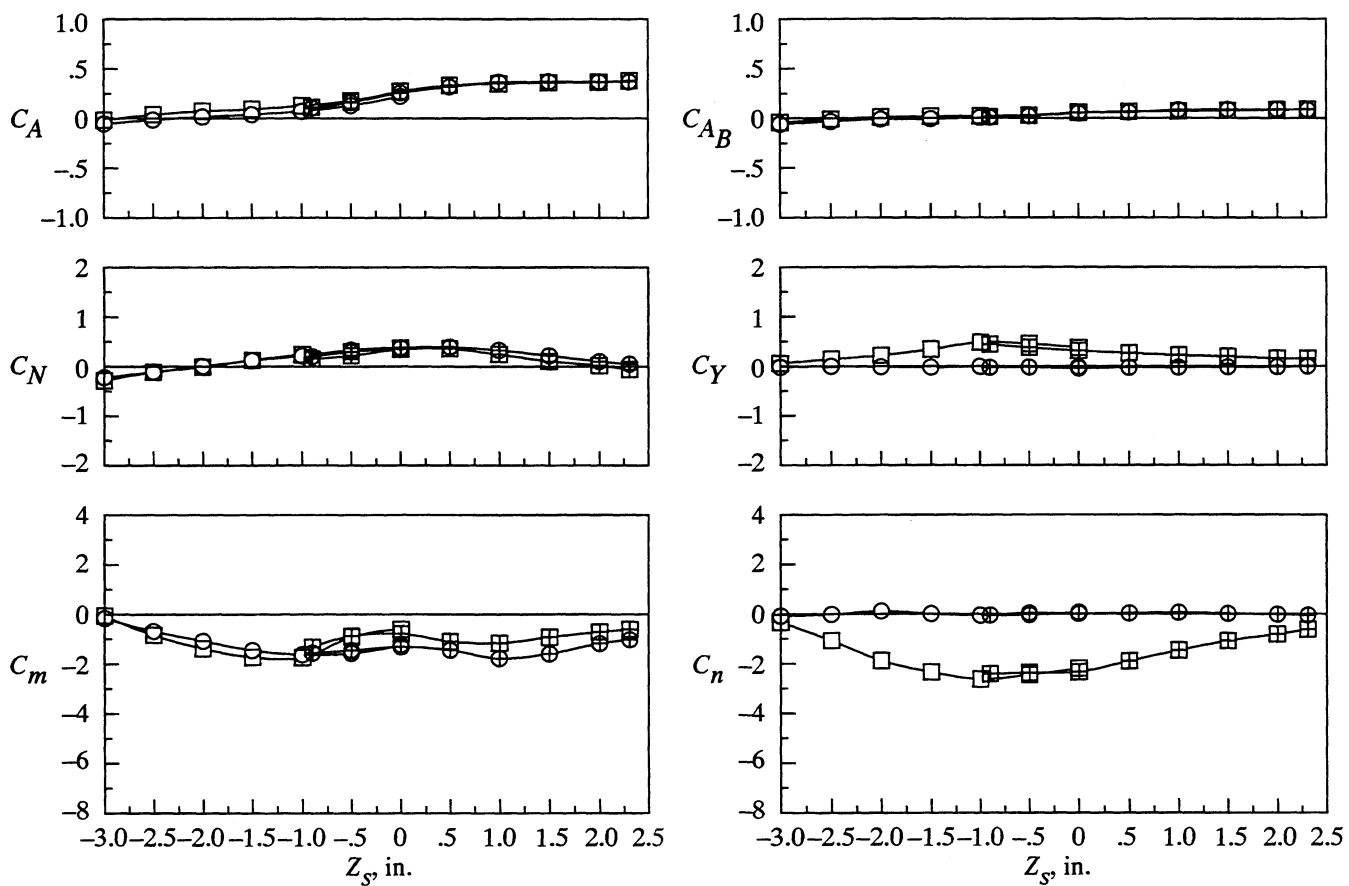
Y_S , in.
 ○ 0.00
 □ 2.40



(c) $M_\infty = 0.95$; $l = 26.00$ in.; $l/h = 5.42$.

Figure 24. Continued.

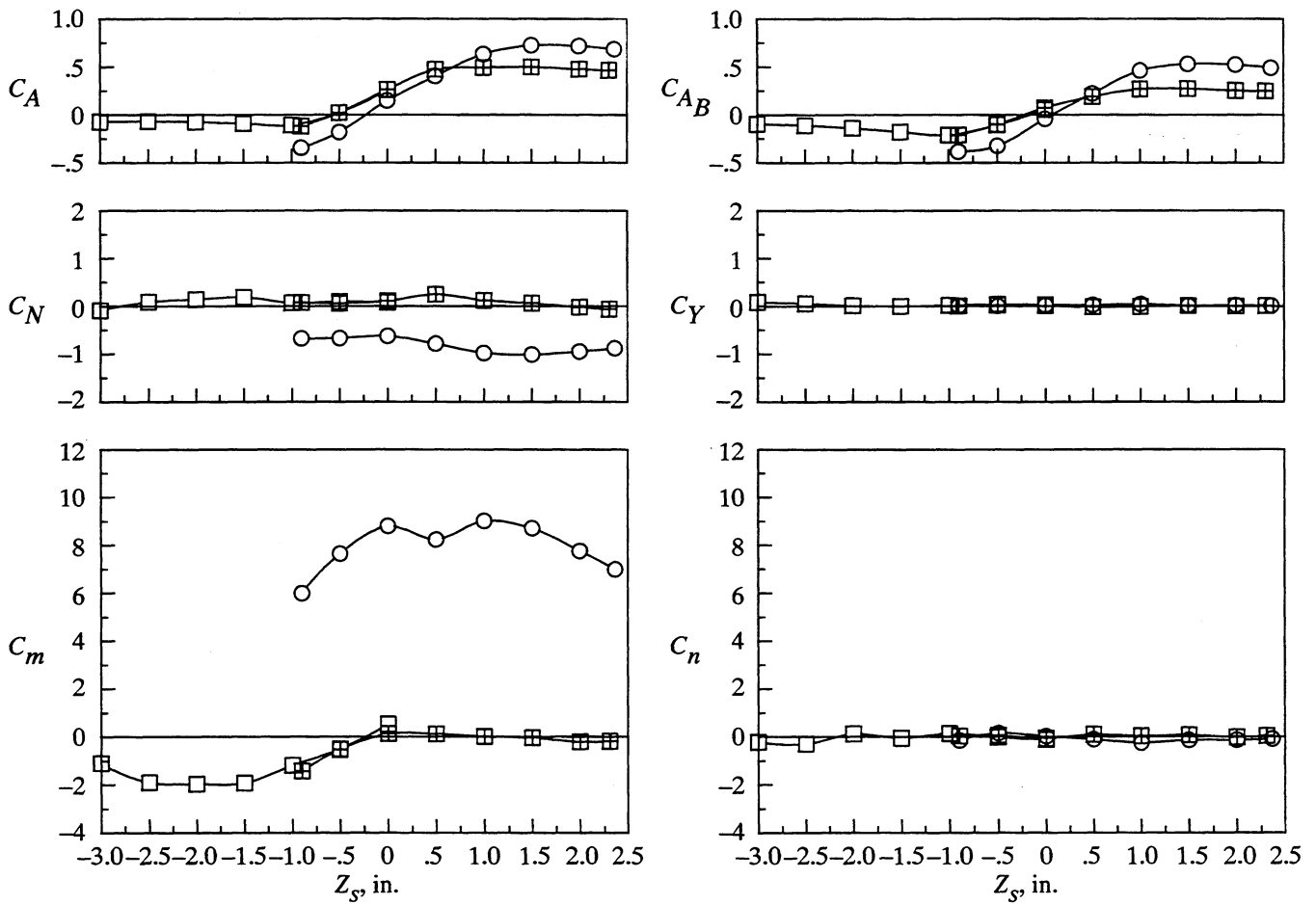
Y_s , in.
 ○ 0.00
 □ 2.40



(d) $M_\infty = 0.95$; $l = 30.00$ in.; $l/h = 6.25$.

Figure 24. Concluded.

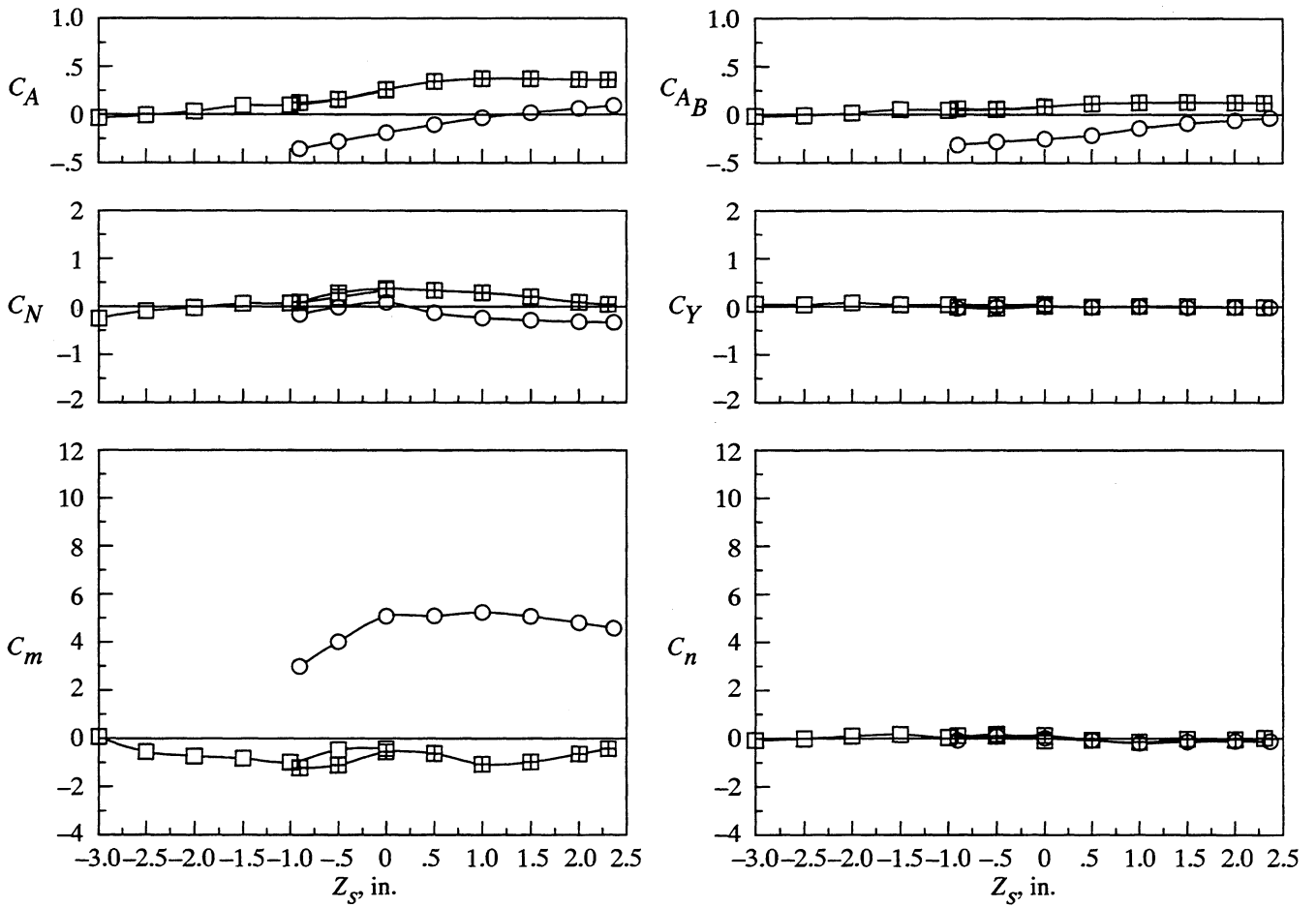
	h , in.	l/h
○	2.40	10.83
□	4.80	5.42



(a) $l = 26.00$ in.; $Y_s = 0.00$ in.

Figure 25. Effect of cavity depth on store load characteristics (open and plus-filled symbols are for strut housing extending 0.45 in. and 2.85 in., respectively, above cavity floor). $M_\infty = 0.40$.

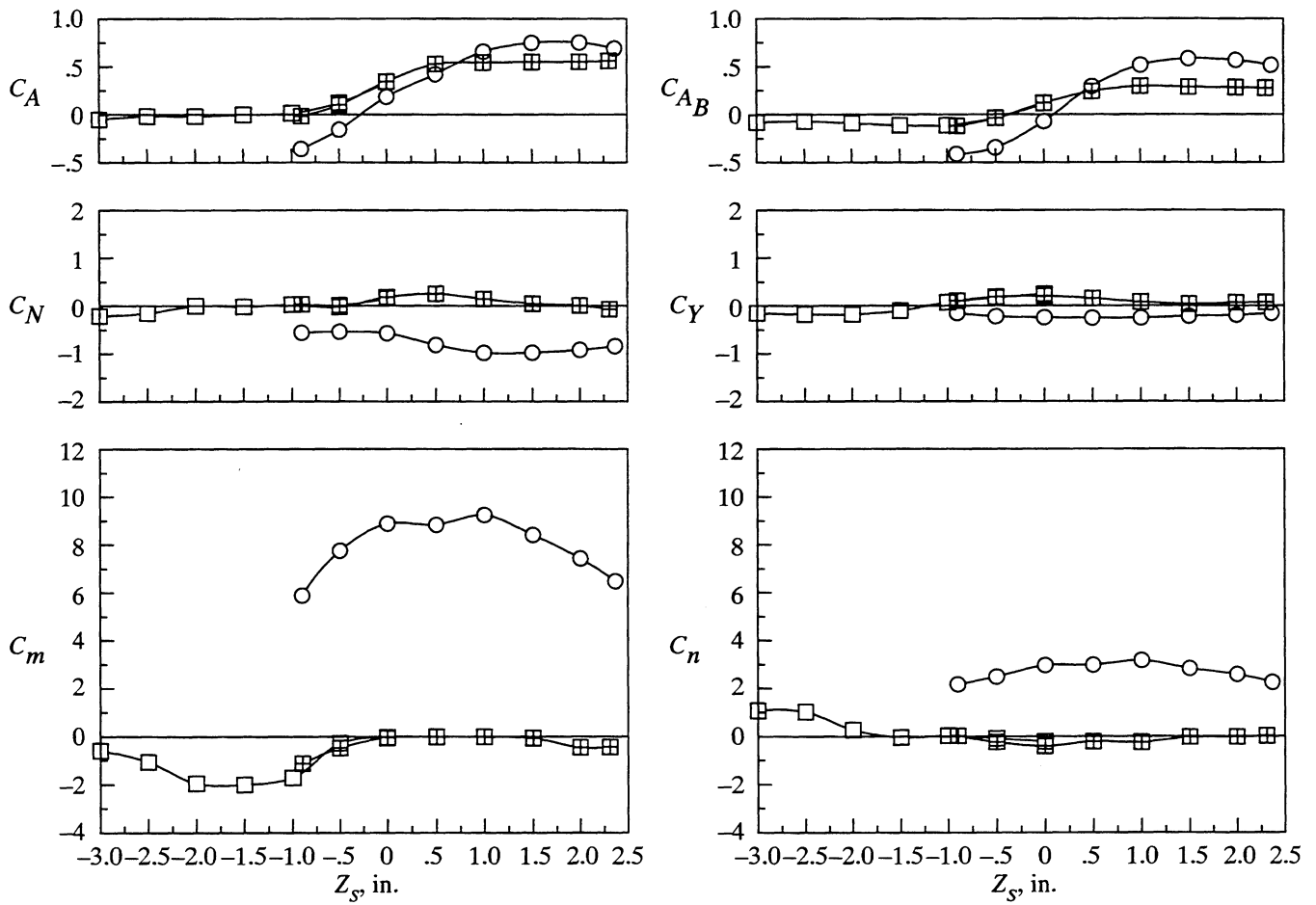
	h , in.	l/h
○	2.40	12.50
□	4.80	6.25



(b) $l = 30.00$ in.; $Y_s = 0.00$ in.

Figure 25. Continued.

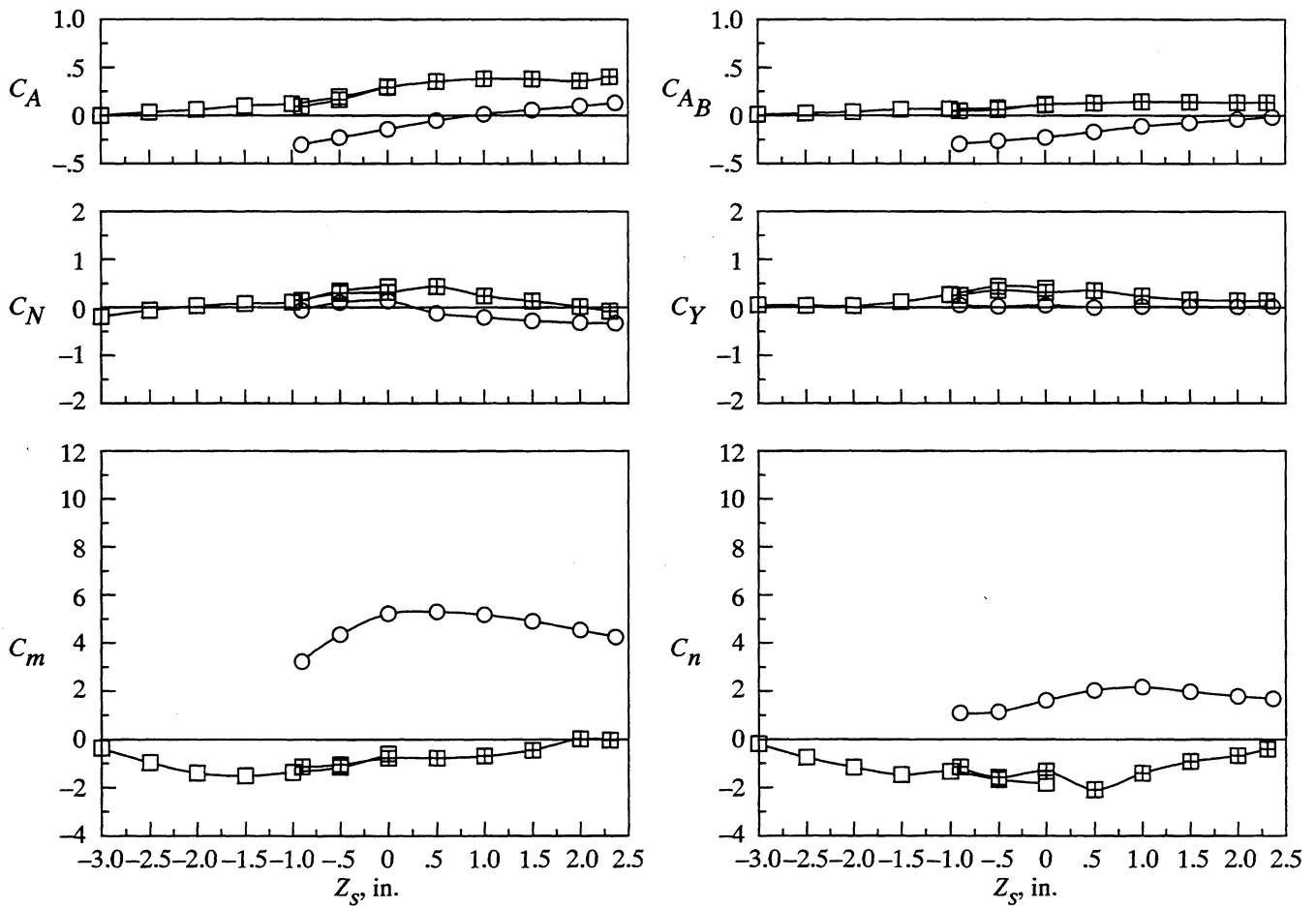
h , in.	l/h
○ 2.40	10.83
□ 4.80	5.42



(c) $l = 26.00$ in.; $Y_s = 2.40$ in.

Figure 25. Continued.

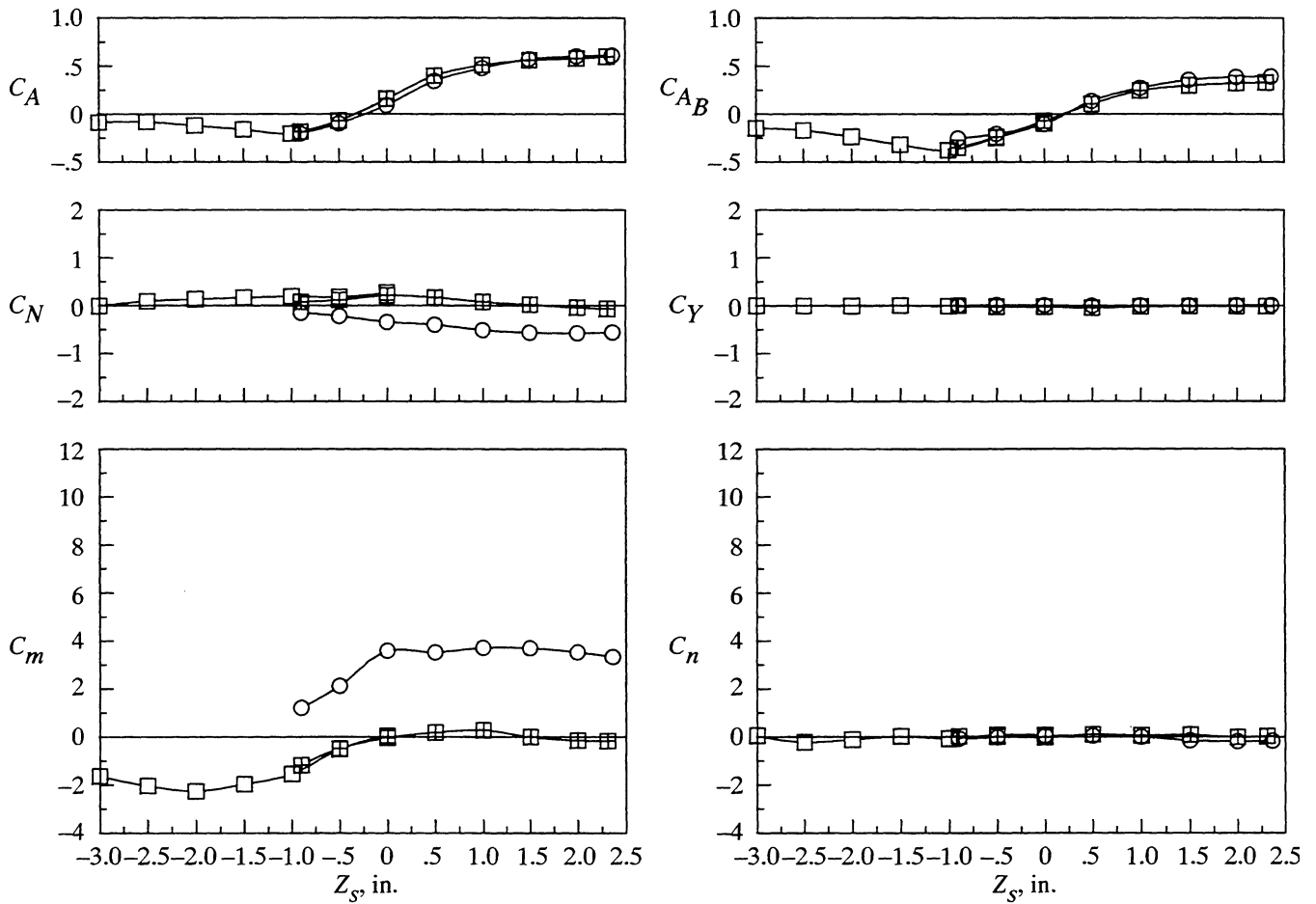
	h , in.	l/h
○	2.40	12.50
□	4.80	6.25



(d) $l = 30.00$ in.; $Y_s = 2.40$ in.

Figure 25. Concluded.

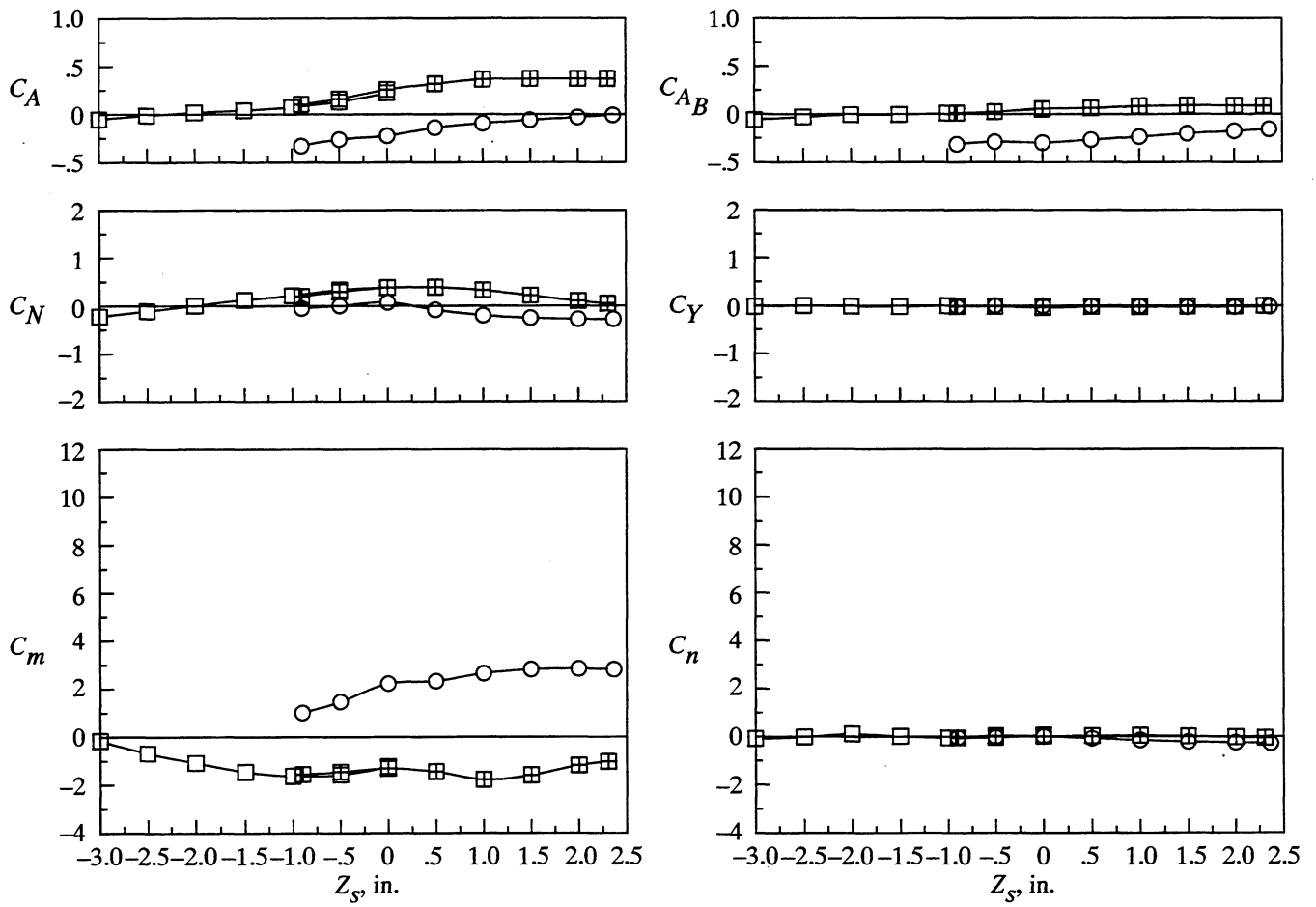
	h , in.	l/h
○	2.40	10.83
□	4.80	5.42



(a) $l = 26.00$ in.; $Y_s = 0.00$ in.

Figure 26. Effect of cavity depth on store load characteristics (open and plus-filled symbols are for strut housing extending 0.45 in. and 2.85 in., respectively, above cavity floor). $M_\infty = 0.95$.

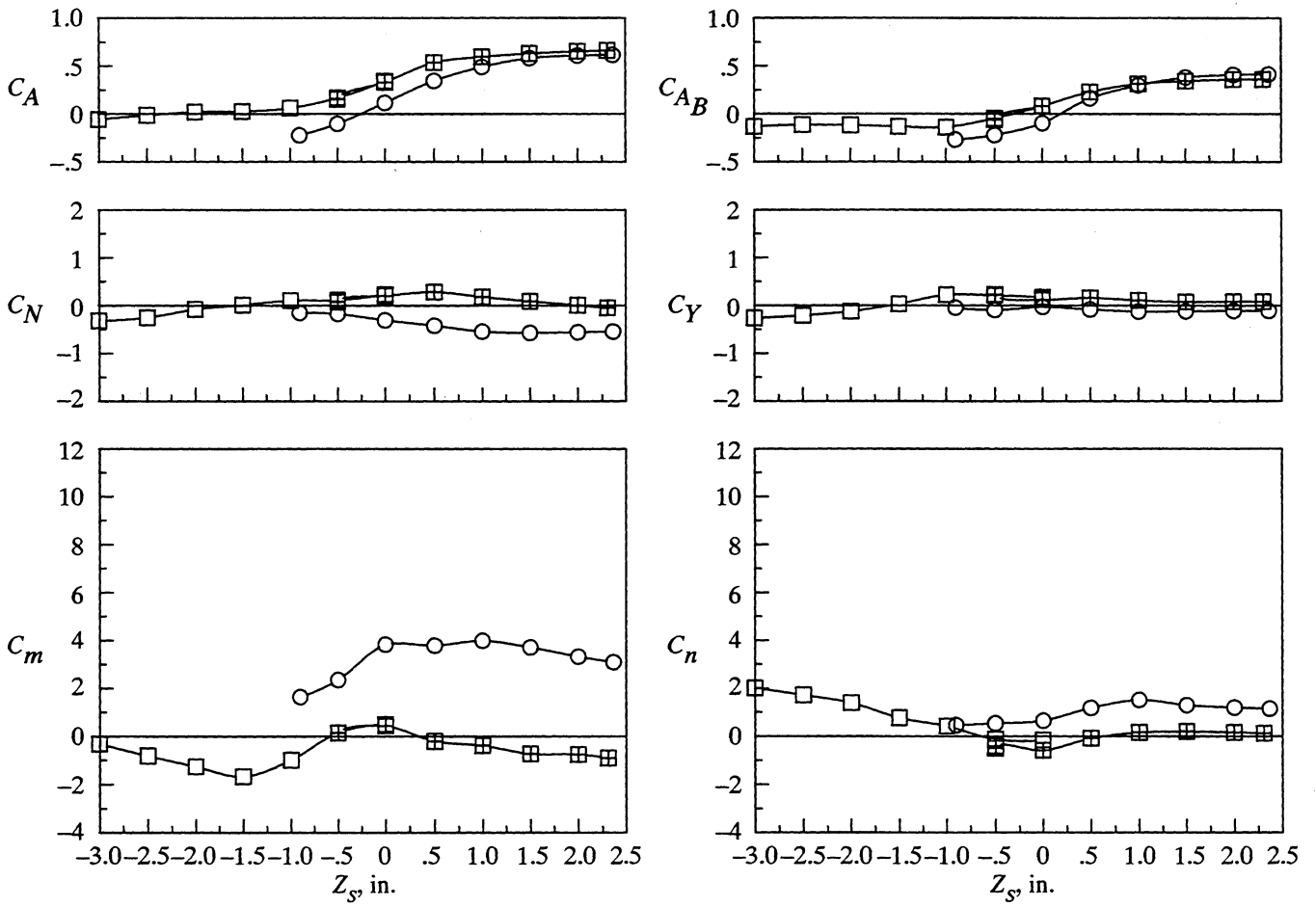
	h , in.	l/h
○	2.40	12.50
□	4.80	6.25



(b) $l = 30.00$ in.; $Y_s = 0.00$ in.

Figure 26. Continued.

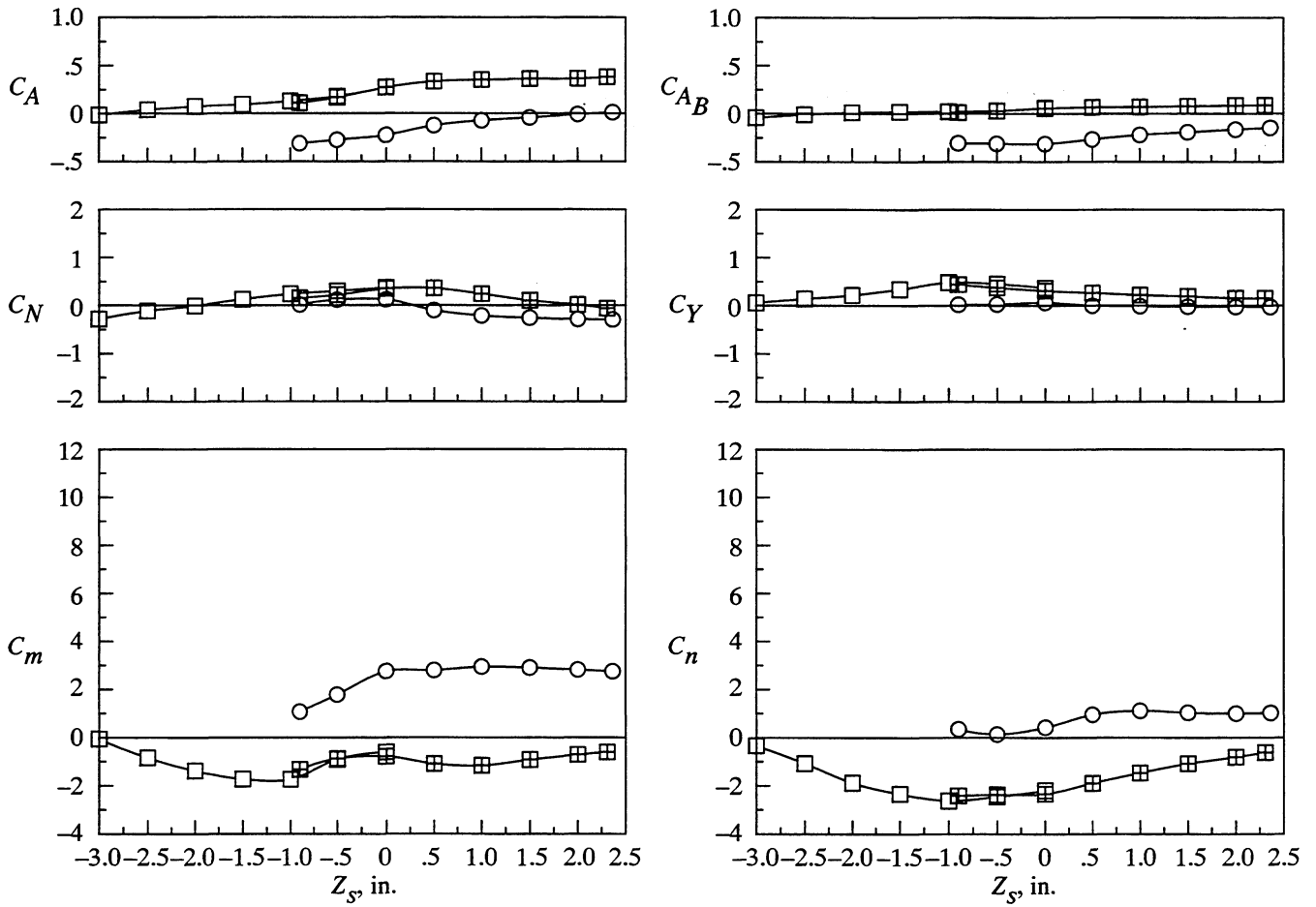
h , in.	l/h
○ 2.40	10.83
□ 4.80	5.42



(c) $l = 26.00$ in.; $Y_s = 2.40$ in.

Figure 26. Continued.

	<i>h</i> , in.	<i>l/h</i>
○	2.40	12.50
□	4.80	6.25



(d) $l = 30.00$ in.; $Y_s = 2.40$ in.

Figure 26. Concluded.

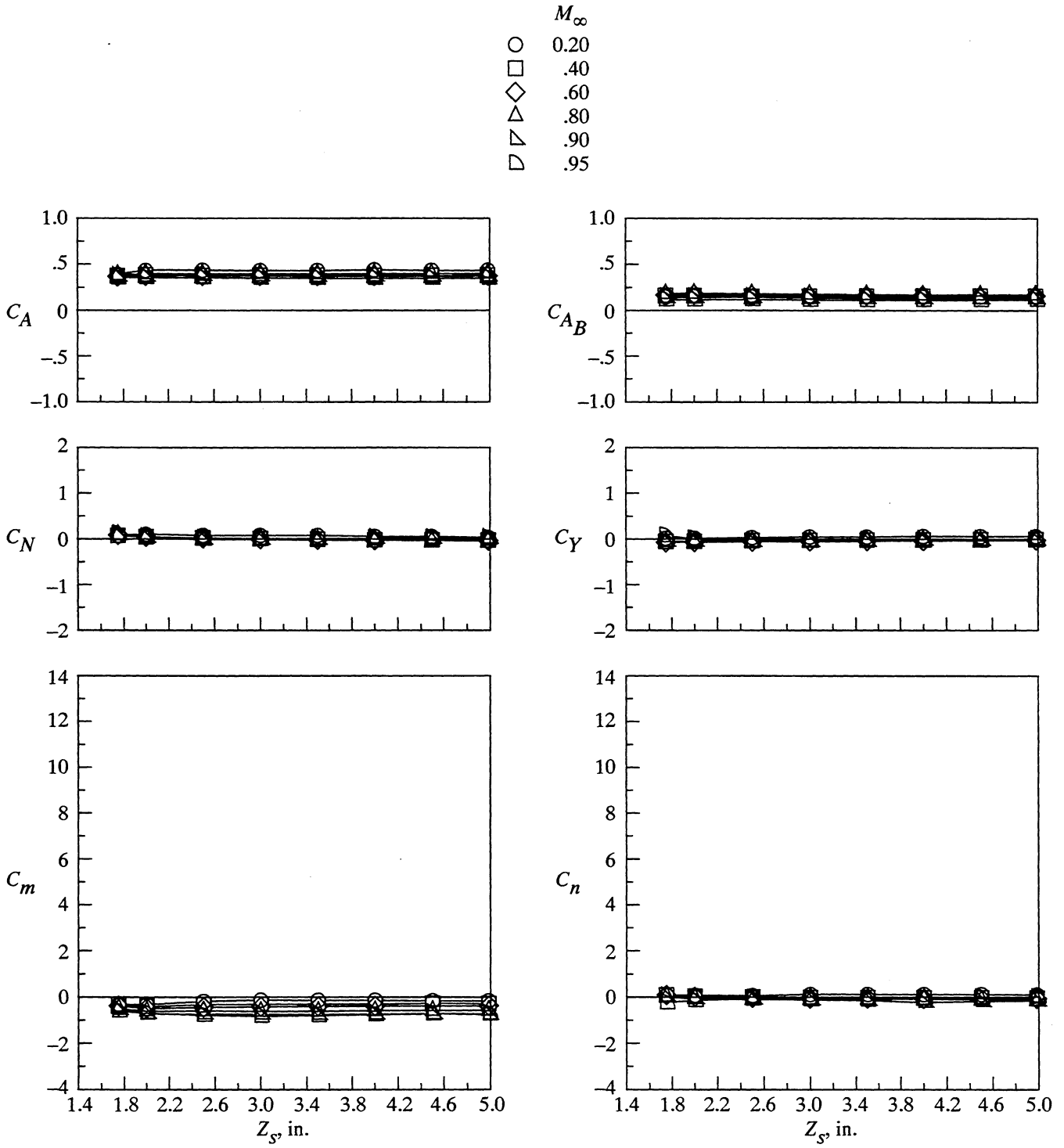


Figure 27. Effect of Mach number on store load characteristics. $h = 0.00$ in.; $Y_s = 0.00$ in.

REPORT DOCUMENTATION PAGE			Form Approved OMB No. 0704-0188	
Public reporting burden for this collection of information is estimated to average 1 hour per response, including the time for reviewing instructions, searching existing data sources, gathering and maintaining the data needed, and completing and reviewing the collection of information. Send comments regarding this burden estimate or any other aspect of this collection of information, including suggestions for reducing this burden, to Washington Headquarters Services, Directorate for Information Operations and Reports, 1215 Jefferson Davis Highway, Suite 1204, Arlington, VA 22202-4302, and to the Office of Management and Budget, Paperwork Reduction Project (0704-0188), Washington, DC 20503.				
1. AGENCY USE ONLY (Leave blank)	2. REPORT DATE May 1995	3. REPORT TYPE AND DATES COVERED Technical Memorandum		
4. TITLE AND SUBTITLE Measurements of Store Forces and Moments and Cavity Pressures for a Generic Store In and Near a Box Cavity at Subsonic and Transonic Speeds			5. FUNDING NUMBERS WU 505-68-70-09	
6. AUTHOR(S) Robert L. Stallings, Jr., E. B. Plentovich, M. B. Tracy, and Michael J. Hemsch				
7. PERFORMING ORGANIZATION NAME(S) AND ADDRESS(ES) NASA Langley Research Center Hampton, VA 23681-0001			8. PERFORMING ORGANIZATION REPORT NUMBER L-17388	
9. SPONSORING/MONITORING AGENCY NAME(S) AND ADDRESS(ES) National Aeronautics and Space Administration Washington, DC 20546-0001			10. SPONSORING/MONITORING AGENCY REPORT NUMBER NASA TM-4611	
11. SUPPLEMENTARY NOTES Stallings and Hemsch: Lockheed Engineering & Sciences Company, Hampton, VA; Plentovich and Tracy: Langley Research Center, Hampton, VA.				
12a. DISTRIBUTION/AVAILABILITY STATEMENT Unclassified-Unlimited Subject Category 02 Availability: NASA CASI (301) 621-0390			12b. DISTRIBUTION CODE	
13. ABSTRACT (Maximum 200 words) An experimental force and moment study was conducted in the Langley 8-Foot Transonic Pressure Tunnel for a generic store in and near rectangular box cavities contained in a flat-plate configuration at subsonic and transonic speeds. Surface pressures were measured inside the cavities and on the flat plate. The length-to-height ratios were 5.42, 6.25, 10.83, and 12.50. The corresponding width-to-height ratios were 2.00, 2.00, 4.00, and 4.00. The free-stream Mach number range was from 0.20 to 0.95. Surface pressure measurements inside the cavities indicated that the flow fields for the shallow cavities were either closed or transitional near the transitional/closed boundary. For the deep cavities, the flow fields were either open or near the open/transitional boundary. The presence of the store did not change the type of flow field and had only small effects on the pressure distributions. For transitional or open transitional flow fields, increasing the free-stream Mach number resulted in large reductions in pitching-moment coefficient. Values of pitching-moment coefficient were always much greater for closed flow fields than for open flow fields.				
14. SUBJECT TERMS Cavity; Cavity flow fields; Store separation; Pressure distributions; Subsonic; Transonic			15. NUMBER OF PAGES 175	
			16. PRICE CODE A08	
17. SECURITY CLASSIFICATION OF REPORT Unclassified	18. SECURITY CLASSIFICATION OF THIS PAGE Unclassified	19. SECURITY CLASSIFICATION OF ABSTRACT Unclassified	20. LIMITATION OF ABSTRACT	